A broad study of the extremophile *Chlamydomonas acidophila*, isolated from an abandoned copper mine in Parys Mountain.

A thesis submitted to The University of Manchester for the degree of Doctor of Science in the Faculty of Science and Engineering

2021

Owen A McIntosh

Department of Earth and Environmental Sciences

Contents

Abbreviations

ABA- Abscisic acid

ABC- ATP-binding cassette transporters

APX- Ascorbate peroxidase

CAT- Catalase

CAX- Cation/ proton exchanger

CCAP- Culture Collection of Algae and Protozoa

CDF- Cation Diffusion Facilitator

Clp- Class I protein

COPT/ CTR- Copper Transporter

Cys- Cysteine

EPS- Extracellular Polymeric Substances

ETR- Electron Transport Rate

FRO- Ferric Reductase Oxidase

FT-IR- Fourier Transform-InfraRed

GC-MS- Gas Chromatography Mass Spectroscopy

GR- Glutathione Reductase

GSH- Glutathione (reduced)

GSSG- Glutathione (oxidised)

HMA- Heavy Metal ATPases

HSP- Heat Shock Protein

IC- Inorganic Carbon

LC-MS- Liquid Chromatography Mass Spectroscopy

MAM- Modified Acid Media

MDA- Malondialdehyde

MTP- Metal Transport Protein

NP- Nanoparticle

NPQ- Non-Photochemical Quenching

PAM- Pulse Amplitude Modulation Fluorometry

PCS- Phytochelatin Synthase

ROS- Reactive Oxygen Species

SOD- Superoxide Dismutase

TAG- Triacylglycerol

TBARS- Thiobarbituric Reactive Substances

TP- Tris-Minimal

y-EC- y glutamylcysteine synthetase

ZIP- Zrt-, Irt-like Proteins

ZRT- Zinc Transporter Proteins

Abstract

Anthropogenic activities have caused environmental damage for thousands of years, which has been exacerbated since the industrial revolution. Mining is one such activity that has caused damage to the environment, primarily through the creation of acid-mine drainage (AMD) waters. These are created when pyrite in rocks is exposed to oxygen and water, through mining, causing the formation of sulphuric acid. As the waters become more acidic, metals disassociate from the rocks leading to acidic and metal polluted waters. One such AMD system is Parys Mountain, Wales, where our lab has isolated an acidophilic microalga, *Chlamydomonas acidophila* – strain PM01. It exhibits higher tolerance levels of copper than other strains of the same species. Whilst tolerance ranges and physiological responses of eukaryotic extremophiles have been well studied, many of their mechanisms of adaptation have yet to be elucidated. PM01 provides a fantastic model to begin to understand some of these tolerance mechanisms.

In order to tolerate the harsh conditions of AMD it is likely that *C. acidophila* has evolved differential responses to both pH differences and metal toxicity to non-adapted organisms, such as *Chlamydomonas reinhardtii* which is mesophilic in both its pH tolerance and its ability to survive metal toxicity. Firstly, in this thesis the physiological and biochemical responses of PM01 compared to the model organism *Chlamydomonas reinhardtii* (strain 11/32c) as well as other strains of *C. acidophila* (strains CCAP 11/136 and CCAP 11/137) were analysed in response to copper. Here it was found that PM01 is capable of growing at much higher copper concentrations than the other strains tested. Also, PM01 shuts down photosystem II after being exposed to copper for 3 hours, without the photosynthetic machinery appearing stressed. Additionally, a 2-stage non-photochemical quenching (NPQ) process was observed, where PM01 has different types of NPQ, depending on the actinic light intensity. The antioxidant capability of PM01 and *C. reinhardtii* was also measured. PM01 exhibited higher catalase activity, whilst the two isoforms of iron superoxide dismutase show different isoelectric points (pI). It was found that PM01 exhibits high levels of lipid oxidation in both short- and long-term copper stress, whereas *C. reinhardtii* only exhibited high lipid oxidation under a short-term copper stress. Finally, low lipid oxidation levels were shown in the other *C. acidophila* species, CCAP strains 11/136 and 11/137.

Secondly, fast, high-throughput fingerprinting techniques were used to examine the metabolic and proteomic changes of PM01 and *C. reinhardtii* in response to copper stress. FT-IR spectroscopy revealed an increase in protein content upon copper exposure in PM01, but a decrease in lipids and carbohydrates. Whilst a similar response was seen in *C. reinhardtii* it was not to the same extent as PM01. MALDI-TOF mass spectroscopy provided a rapid overview of the proteome. Here protein peaks with a high m/z arising in the long-term copper-stress treated for both PM01 and *C. reinhardtii*. These protein peaks also suggested that a protein can “switch” between a single charge and double charge and could play an important role in either metal binding or reactive oxygen species quenching. An in-depth metabolomic analysis using LC-MS techniques reveal greater insights into PM01’s adaption to copper through the identification of several key metabolic changes between PM01 and *C. reinhardtii*. Thiol groups in metabolites such as cysteine and glutathione play a central role in

copper adaptation. Additionally, amino acids such as proline, a known osmolyte, was found at elevated levels in PM01.

Finally, I conducted a transcriptomic experiment was conducted to observe the global response of PM01 and *C. reinhardtii* to a long- and short-term copper stress. A whole host of transcripts were differentially expressed under copper stress, however, we managed to find 3 main processes that were altered. Transcripts related to the antioxidant response and lipid breakdown were found to be more highly expressed in *C. reinhardtii* under a copper stress. Intracellular transport systems and reorganisation was found to be more highly expressed in PM01 under a short- and long-term copper stress. Finally, transcripts related to photosynthesis were found to be reduced in PM01 under both a short- and long-term copper stress. I also found a series of transcripts that were much more highly expressed in the PM01 cells exposed to a short-term copper stress with a wide array of biological functions. These provide an exciting source of potential biological pathways to a copper adaptation. We also investigated individual transcripts of interest, with the putative copper exporter *CTP3*, being a standout candidate to copper tolerance it was constitutively expressed in PM01 at higher levels than all other *C. reinhardtii* treatments.

This study provides an exciting insight into the copper tolerance mechanisms of PM01, an extremophile microalga that exhibits high copper tolerance levels. In this I have generated large data sets that provide a lot of further avenues for further investigation.

Declaration

I declare that no portion of the work referred to in the thesis has been submitted in support of an application for another degree or qualification of this or any other university or other institute of learning

Copyright Statement

i. The author of this thesis (including any appendices and/or schedules to this thesis) owns certain copyright or related rights in it (the “Copyright”) and he has given the University of Manchester certain rights to use such Copyright, including for administrative purposes.

ii. ii. Copies of this thesis, either in full or in extracts and whether in hard or electronic copy, may be made only in accordance with the Copyright, Designs and Patents Act 1988 (as amended) and regulations issued under it or, where appropriate, in accordance with licensing agreements which the University has from time to time. This page must form part of any such copies made.

iii. iii. The ownership of certain Copyright, patents, designs, trademarks and other intellectual property (the “Intellectual Property”) and any reproductions of copyright works in the thesis, for example graphs and tables (“Reproductions”), which may be described in this thesis, may not be owned by the author and may be owned by third parties. Such Intellectual Property and Reproductions cannot and must not be made available for use without the prior written permission of the owner(s) of the relevant Intellectual Property and/or Reproductions.

iv. iv. Further information on the conditions under which disclosure, publication and commercialisation of this thesis, the Copyright and any Intellectual Property and/or Reproductions described in it may take place is available in the University IP Policy (see http://documents.manchester.ac.uk/DocuInfo.aspx?DocID=24420), in any relevant Thesis restriction declarations deposited in the University Library, the University Library’s regulations (see http://www.library.manchester.ac.uk/about/regulations/) and in the University’s policy on Presentation of Theses

Acknowledgements

Firstly, I would like to thank all members of the Pittman lab group and the Plant Sciences Research group, past and present, who have made working there an absolute pleasure. They have allowed me to bounce ideas off them, kept my cultures alive whilst I have been away and provided a fun working environment. A special thanks goes to Javiera Ziehe, who provided fantastic support and guidance as I was starting my PhD programme continuing all the way through until she graduated.

I would also like to extend my deepest gratitude to my co-supervisor Giles Johnson whose extensive knowledge in photosynthetic processes was crucial to my data collection and analysis. His insightful suggestions allowed me to troubleshoot the many issues that arose from collecting some of my photosynthetic data. I would also like to extend my gratitude to Giles' post-doc Pablo Calza who not only gave me fantastic practical and theoretical suggestions but moral support during the long days collecting PAM data in a dark room. To both I am only disappointed there wasn't more time to delve further into some of the fascinating findings you helped me gather.

I also wish to thank my co-supervisor Roy Goodacre who provided me many opportunities to practise scientific talks in front of a large audience. Roy provided me many opportunities to collect great datasets that contributed to not only my thesis but publications I am an author on. I am also very grateful to members of the Goodacre lab group Howbeer Muhamad Ali and Nigel Gotts who were very patient with me and my many questions, and were always happy to tach me the practical side of the metabolomics world with a smile on their face.

A special thanks goes to Ivan Spasojevic who facilitated a fantastic month-long trip for me to visit the University of Belgrade to collect data. Not only did he give expert advice and insight into my research project but acted as a fantastic host showing me the many amazing sights Belgrade has to offer. I would also like to thank Jelena Bogdanovic who worked tirelessly with me to obtain enzymatic activity data of ROS quenching enzymes despite the many problems that arose. Not only Is Jelena an expert in ROS quenching enzymes but she also taught me the meaning of my name ("young warrior"). I am only sorry I did not get to reciprocate the fantastic hosting both Ivan and Jelena provided but hope that I will get the opportunity to in the future and maybe another trip out to Belgrade.

I very much appreciate all the work Leo Zeef put into helping me analyse my transcriptomic dataset. His invaluable contribution both mapping the transcripts and finding the homologues was integral to making the data set as good as it was. His computer wizardry has left me in awe, and I cannot overstate his contributions.

I would like to send my deepest gratitude to my supervisor Jon Pittman. Jon's unparalleled support has never gone unnoticed or unappreciated. Jon has always been happy to find time to help me, even when he is extremely busy himself. I would like to thank Jon for finding time to listen to my ramblings (both spoken and written). His constructive advice and extensive knowledge has helped guide me to obtain the best data I can and has always offered emotional support where needed. Jon's extensive knowledge of all things algae has proved invaluable and his input and advice has always been appreciated. He has gone above and beyond what any supervisor would be expected

to do, even including me in a grant writing process and I am extremely grateful to have been his student.

Although not strictly related to my PhD, I would like to thank Jack Fleet, James Dinsley and Armida Gjindali, my teammates at Larvita who were amazing company and collaborators for our side project of the YES 2019 competition. I learned a lot from you all and thoroughly enjoyed working with you. I will fondly remember our trips down to both Syngenta and the Royal Society.

Finally, I would like to thank my mum, Debi McIntosh, who has always been there to support me through every aspect and decision of my life and will continue to text me supportive messages even when I ignore them during the writing process of my thesis. I would also like to thank my dad Mark Hassell, sister Imogen McIntosh and my mums soon to be husband Paul Godfrey all of whom are some of the best people I know and are always there for support when needed. I would also like to thank Heledd Williams, who has taken up the unenviable task of keeping me sane throughout the writing process and I am forever grateful for her company. I would also like to thank Natalie de la Gandara for some of her artistic input into my figures and being a fantastic friend. Finally, I would like to thank the entirety of Didsbury Toc H RFC and the Manchester Mosquitos AFC all of whom provide fantastic comedic support and consist of some of my greatest friends.

1 Introduction

1.1 Life in the Extreme

1.1.1 Adaptation of microorganisms to hostile environments

There are many hostile environments that provide a wide array of challenges to life. For example, hot springs are highly acidic environments, which can reach temperatures over 80°C. Rocks more than 2 km below the Earth's surface are exposed to high pressures and no sunlight. Fuel storage ponds of nuclear power plants are highly alkaline and radioactive. Despite these highly adverse conditions, microorganisms are still able to colonise and grow in such hostile environments (Hugenholtz et al., 1998; MeGraw et al., 2018; Nixon et al., 2019). In fact, there is a whole host of organisms that can not only tolerate but thrive in extreme environments and have been classed under the broad term "extremophile". These organisms can be further classified, depending on the environment they prefer. These include; high temperatures (thermophiles), low temperatures (psychrophiles), acidic (acidophiles), alkaline (alkaliphiles), highly saline (halophiles), highly pressurised (barophiles), metal contaminated (metallophiles) and radioactive environments (radiophiles) (Raddadi et al., 2015; Stetter, 1999).

Extremophiles are found in all 3 clades of life, with, to date, a large interest being taken in prokaryotic extremophiles (Barnard et al., 2010; Oren, 2010). Some extremophiles can become so highly specialised that they can no longer grow under 'normal' physiological conditions. This is true for the acidophile, *Dunaliella acidophila* with an optimal pH requirement of 1 but cannot grow above a pH of 3. In contrast, another acidophile, a *Chlamydomonas* sp. is capable of growing over a broad pH range of 2-7, suggesting it may have a more adaptive and flexible stress response mechanism (Gimmler et al., 1989; Messerli et al., 2005). Whilst both are acidophiles, there is a clear contrast between these two organisms and their adaptive strategies are likely to be different. When we take into account the extreme environments of our planet and the biological diversity, there are likely to be many interesting adaptations can be studied for fundamental understanding and utilise for biotechnological exploitation.

1.1.2 Why are we Interested in Extremophiles?

There are numerous products that have come from extremophiles that the biotechnology industry have been able to exploit. Perhaps, some of the best-known extremophiles are species from the phylum Tardigrada, known colloquially as water bears. There has been a lot of excitement surrounding them in the media, due to their ability to survive trips into space. Their ability to survive trips into such hostile environments could provide further insights into DNA repair, long term survival and even be able to colonise different planets (Weronika and Łukasz, 2017). A DNA polymerase from the bacterium *Thermus aquaticus,* isolated from hot springs, is highly stable under high temperatures. This made it a perfect candidate for the polymerase chain reaction (PCR) assay, which is now used routinely by the scientific community. This has expanded into other fields, such as forensics, which regularly use PCR to identify suspects based on their DNA (Gurvitz et al., 1994). Other thermostable enzymes from *T. aquaticus* have also been investigated for processes such as the breakdown of lipids under high temperatures (Lopez et al., 2012). On the other end of the scale β-galactosidase enzymes from psychrophiles have been adopted for the production of lactose-free milk. The enzymes function at a cooler temperature than other variants and reduce the risk of

contamination by pathogens (Coker et al., 2003; Coker and Brenchley, 2006). Extremophiles can also directly produce valuable compounds for us. Carotenoids are used widely as food and health supplements, in 2018 the global market for one single carotenoid, astaxanthin, was $600 million USD (Ahuja and Rawat, 2019). In the halophilic microalga *Dunaliella salina* carotenoid content increases almost 10-fold under high salinity (Solovchenko et al., 2015). Another halophile, this time from the archaea clade, *Haloferax alexandrines* has also been seen to able to produce relatively large amounts of the pigment canthaxanthin under (Asker and Ohta, 2002). There are many other examples in which extremophiles have been utilised to improve processes. Isolating novel extremophiles can continue to revolutionise the biotechnology sector, through the identification of novel proteins and/or biological processes and valuable biomolecules.

1.1.3 Oxidative Stress

One shared cause of damage between different extreme environments is the production of reactive oxygen species (ROS). Understanding how these are formed and the damage they can induce to cells will help understand the experience cells undergo upon exposure to various stresses. ROS are produced in all forms of life through the metabolism of oxygen. Under normal physiological conditions ROS are present in the cell and tightly regulated, serving important roles as cell signalling molecules (Devasagayam et al., 2004). However, issues can occur when external stresses increase the amount of cellular ROS, beyond the cells capability to quench them. ROS include superoxide anions (O^{2-}) and hydrogen peroxide (H_2O_2), the oxidative power of these molecules can make them toxic as they can inactivate various enzymes and cause lipid peroxidation (Gechev et al., 2006; Moenne et al., 2016). However, these radicals are fairly selective in their reactions and can only interact with certain molecules (Halliwell, 2006). The destructive properties of hydrogen peroxide and superoxide can be exacerbated when they interact with ferric ions in what is known as the Haber-Weiss reaction (Kehrer, 2000). This interaction generates a hydroxyl radical (HO^-) which can cause significant damage to the cell as it is capable of interacting with all molecules in a cell, including DNA (Halliwell, 2006).

To counteract these dangerous radicals, cells have developed a host of defence mechanisms. This includes reactive oxygen scavenging enzymes, which include, ascorbate peroxidase (APX), superoxide dismutase (SOD), and catalase (CAT). Low molecular weight compounds, commonly known as antioxidants are also used. These include tocopherols, glutathione (GSH), carotenoids, and ascorbate (Choo et al., 2004). The radiation tolerant bacterium *Deinococcus radiodurans* was found to have constitutively high expression levels of CAT and SOD, however, content of both of the enzymes increased further upon radiation stress (Basu and Apte, 2012). Furthermore, mutants generated for both of these enzymes in *D. radiodurans* were found to increase its sensitivity to ionising radiation (Markillie et al., 1999). The extremophile microalga *Euglena gracilis* also saw an increase in SOD expression under several metal stresses. Additionally, there was also an increase in expression of glutathione transferases which are involved in the detoxification of proteins/ substrates affected by oxidative stress (Khatiwada et al., 2020). Excessive ROS can be highly damaging to cells and a series of abiotic and biotic factors can lead to elevated ROS

Many metals undergo oxidation and reduction processes, most notably copper and iron. Iron can occur as Fe2+, Fe3+ and in less common instances Fe4+ (Jomova et al., 2012). In warm, well oxygenated waters Fe2+ has a short half life and is readily oxidised into Fe3+, reducing its solubility and potentially bioavailability. However, under more anoxic conditions and cooler temperatures the

half-life of Fe2+ is increased and is less readily oxidised to Fe3+ (Behnke and LaRoche, 2020). Copper is most prevalent in the Cu2+ form in well oxygenated neutral pH freshwaters. However, when organic matter/ ligands are present in the waters Cu can complex with these biomolecules and is the most dominant form within the waterbody (Martin and Goldblatt, 2007). Copper can be highly damaging to cells through the generation of ROS, but also through their ability to undergo the Haber-Weiss reaction (Angelé-Martínez et al., 2017). We will explore how metals such as copper can cause ROS stress later.

1.1.4 Glutathione

Glutathione transferases rely on the metabolite glutathione (GSH) to function. GSH has a wide variety of functions within cells to help deal with stress through the interaction of other co-factors and proteins. However, GSH can also directly quench ROS as it acts as a reductant, leaving it in its oxidised form (GSSG) (Mallick and Mohn, 2000). γ-glutamylcysteine (γ-EC) synthesis is the first step in glutathione synthesis. γ-glutamylcysteine synthetase (γ-ECS) catalyses the formation of γ-EC from L-Glu and L-Cys (May et al., 1998). γ-ECS activity appears to be controlled by cellular GSH concentrations, this has been extensively reviewed by Mendoza-Cózatl et al. (2006). When GSH is depleted or consumed γ-ECS activity increases, however Mendoza-Cózatl et al. (2006) also suggest that GSSG is still able to prevent an increase in γ-ECS activity suggesting that cells do not detect GSSG as a depletion of cellular GSH. Having readily available GSH is crucial for an adaptive stress response. A salt-tolerant wild relative of the cultivated tomato plant, *Solanum pennellii*, was able increase glutathione synthesis and GSH/GSSG ratios within 2 weeks of salt-stress. On the other hand, its domesticated relative *Solanum esculentum,* had no such increase (Mittova et al., 2003). Over expression of three genes involved in glutathione metabolism *GSH1*, *CYS3* and *GLR1* in *Saccharomyces cerevisiae* lead to the formation of a more robust strain when compared to the wild type (Ask et al., 2013). Another way organisms can modify their glutathione metabolism to adapt to stress is by increasing glutathione reductase (GR) activity. A review conducted by Harshavardhan et al. (2017) found 16 instances of either down-regulation or over-expression of GR in multiple species of plants in response to stress conditions. In the case of over expression, most lines saw an increase in tolerance to stresses such as oxidative, heat, cold, paraquat, ozone, methyl-viologen and salt stress. In the cases of GR being down-regulated, the organisms involved exhibited a higher sensitivity to such stress. Glutathione can also play an integral role in metal detoxification by binding and sequestering it within thiol groups of GSH, utilising the high metal affinity amino acid, cysteine (Jozefczak et al., 2012). Additionally, glutathione molecules can be synthesised into larger oligomers called phytochelatins, and can chelate metals using the cysteine residues (Pérez-Rama et al., 2001). Phytochelatins will be discussed further in section 1.2.5.

Although glutathione clearly plays an important role within eukaryotes, prokaryotic organisms do not seem to rely on it as much. A study of multiple species of both gram-positive and gram-negative bacteria has shown that most species, especially of gram-positive bacteria have very low concentrations of GSH and GSSG with the exception of a few species such as *Escherichia coli* and *Alcaligenes faecalis* (Fahey et al., 1978). This is also seen in extremophile prokaryotic organisms. Multiple halobacteria were studied for their glutathione content and whilst little detectable GSH content was found within the cells, the precursor γ-EC, was found at high concentrations (Newton and Javor, 1985).

1.1.5 Cell Membrane and Cell Wall Adaptations

For many microorganisms the cell wall and the outer cell membrane is the first boundary to harsh external factors. For extremophiles cell membrane and/or cell wall adaptions prove crucial to their ability to tolerate such extreme conditions. Acidophiles have been found to have a positive membrane potential. This helps to minimise the influx of protons inside thus cell, causing further cellular acidity (Gimmler et al., 1989). It is also possible that these positive charges on the cell surface can help repel metal cations, usually prevalent in acidic waters (Gimmler et al., 1991). Two other acidic species of green algae, *Euastrum binale* and *Staurastrum hirsutum*, were found to change both their cell shape and size to reduce the surface area to volume ratio (Černá and Neustupa, 2010). Thermophillic bacteria contain ether lipids to aid in membrane stability under high temperatures. A new lipid has been found in *Thermotoga maritima*, 15,16-Dimethyl-30-glyceryloxytriacontanoic acid, which is thought to stabilise the membrane and allow the bacteria to grow in temperatures of 90 °C and above (De Rosa et al., 1988). Interestingly, archaea are also found to contain ether lipids in their membrane, regardless as to whether they are found in a high temperature environment (Koga, 2012). Cell walls are often composed of complex polymers and contain many different functional groups such as carboxy, hydroxy, sulphate and phosphate groups providing various binding sites for metal cations (Kaplan, 2013). Cadmium, copper, lead and zinc were found to be mainly bound externally of the moss *Scorpiurum circinatum* with the authors suggesting most likely to the binding sites in the cell wall, preventing the metals reaching the cytoplasm (Basile et al., 2012). A great example of cell walls acting as a barrier to metal toxicity is seen in the comparison of cadmium toxicity between pea and maize plants. Pea plants were found to be more susceptible to cadmium toxicity whilst also showing the highest cadmium concentrations within the cytoplasm. Conversely, maize showed much higher concentrations of cadmium associated to the cell wall, thus blocking cadmium transport into the cytoplasm and conferring a higher tolerance (Lozano-Rodríguez et al., 1997). Additionally, *Chlorella sorokiniana* changes it cell wall structure and releases a host of polyphosphates in mucilage excretions in response to copper stress (Vojvodić et al., 2020b). Interestingly, the capacity of Cu^{2+} binding capability of *C. sorkiniana* was found to increase after UV radiation (Vojvodić et al., 2020a). The authors highlighted that the cell wall is a dynamic structure capable of quickly adapting to new environments and stresses in an effort to increase an organism's survivability.

1.1.6 Heat Shock Proteins (HSP)

HSPs are a family of molecular chaperone proteins typically associated with stress. These were initially discovered in response to heat shock, so earning their name but have been found to be associated with and upregulated in response to a whole host of different stresses. The major classes of HSPs are categorised by their molecular size, which are as follows; HSP100 (100-104 kDa), HSP90 (82-90 kDa), HSP70 (68-75 kDa), HSP40 (35-54 kDa) sHSP (15-30 kDa) (Park and Seo, 2015). 3 HSPs (HSP101, HSP70 and HSP60) were found to be more highly, constitutively expressed in the psychrophile *Eutrema salsuginea* when compared to *Arabidopsis thaliana* (Gamburg et al., 2014). HSP101 is part of the HSP100 family, these are typically associated with the disaggregation of denatured protein clusters. These solubilised proteins can then be refolded with the HSP70 system, which are mainly involved in protein refolding, preventing protein aggregation and protein import and synthesis (Wang et al., 2004). In prokaryotic organisms HSPs are also prevalent and play similar roles to those in eukaryotes. However, they are not typically coined HSPs in prokaryotes, for

example the HSP100 are normally prefaced as class I proteins (CIp) whilst the HSP70 class are referred to as DnaK; Henderson et al. (2006) provide an extensive review and comparison of the two classes. Mutants of the HtpG heatshock protein (part of the HSP90 family) in the cyanobacteria, *Synechococcus* sp*.* led to an increased sensitivity to heat to the extent that the organisms could no longer live above 42 °C (Tanaka and Nakamoto, 1999). Interestingly, ectopic expression of DnaK from *Synechocystis* spp*.* in *A. thaliana* conferred a greater salt tolerance whilst also providing a reduction in H_2O_2 (Kim et al., 2014). A previous study has found that ascorbate peroxidase and catalase activities both increase in transgenic rice and tobacco containing an overexpressed DnaK from the cyanobacteria *Aphanothece halophytica* (Uchida et al., 2008). It is possible that DnaK plays an important role in sustaining crucial antioxidative enzymes that may get damaged during their roles under stress conditions rather than playing a direct role in the reduction of H_2O_2.

1.1.7 Protein Adaptations

For extremophiles to survive in harsh conditions, their proteins must maintain their functionality. For this reason, many extremophile species show differential protein adaptations corresponding to their natural environment. For example, thermophiles have been shown to have increased salt bridges in their proteins providing higher stability at greater temperatures, while these features are almost absent from mesophile-derived proteins (Karshikoff and Ladenstein, 2001). Conversely psychrophilic proteins are much less stable to allow them more flexibility in a lower energy system. This can be done by increasing the number of glycine residues or having them located close to functional regions such as active sites or binding sites, whilst having reduced number of proline and arginine (capable of forming salt bridges) residues (Feller, 2010). Codon usage and amino acid usage has been seen to play an important role in adaptation of extremophile organisms. Eukaryotic acidophiles have been shown to have an enrichment of serine and cysteine residues, whilst both eukaryotic, prokaryotic and archaeal acidophiles have been shown to have a depletion of glutamine and aspartate residues (Goodarzi et al., 2008; Puente-Sánchez et al., 2018).

1.1.8 Lipid and Pigment Accumulation

Non-extremophile microorganisms are well known to accumulate lipids under certain stress conditions such as nutrient starvation and salt stress (Driver et al., 2017; Li et al., 2020), to allow the cells to go into a more dormant state until better conditions arise. The acidophile *Coccomyxa onubensis* was able to accumulate around 13% of fatty acids as a percentage of the dry biomass, whilst the total lipid fraction accounted for about 30% of the dry biomass (Ruiz-Domínguez et al., 2015). The authors stated this was on-par with non-extremophile organisms, however, organisms such as *Botryococcus braunii* were able to accumulate up to 75% of lipids as a percentage of dry biomass (Mata et al., 2010). Lipid roles are not always clear in stress responses and can vary from organism to organism and from treatment to treatment. The extremophile actinobacteria, *Rodococcus,* had a varied lipid accumulation profile to two contrasting oxidative stresses. Addition of methyl-viologen (which creates the superoxide radical) led to a reduction of triacylglycerol (TAG) accumulation within cells. In the same study inhibition of TAG synthesis did not alter the susceptibility of cells exposed to both H_2O_2 or methyl-viologen, although cells exposed to H_2O_2 did exhibit a lower tolerance when lipolysis was blocked under carbon starvation (Urbano et al., 2014). Other strains of *Rhodococcus*, found at high altitudes were found to accumulate TAGs under nutrient stress. However, when exposed to other abiotic stresses such as osmotic stress, UV, desiccation and

organic carbon starvation the TAG stores were depleted to aid cell survivability. When TAG mobilisation was inhibited cell survival was reduced with little or no cells remaining upon abiotic stresses (Bequer Urbano et al., 2013). Identification of lipids by Fourier Transform- infrared (FT-IR) spectroscopy showed a decrease in lipid content when multiple algal species were exposed to a copper stress in a time-dependent manner (Dean et al., 2019). Lipid bodies were also found to increase in response to phosphate limitation in the acidophile *Chlamydomonas acidophila* (Spijkerman et al., 2007). Additionally, another acidophilic *Chalmydomonas* sp. was found to accumulate lipids and have a much higher fatty acid content than its non-extremophile counterpart, *Chlamydomonas reinhardtii* (Tatsuzawa et al., 1996). It is unclear as to why an increase in lipids may help extremophiles survive adverse conditions, when they may be exposed to them for long periods of time. Lipids are known to be a target of ROS, it could be that cells accumulate them as targets for ROS, protecting more important cellular machinery however, this claim is currently unsupported.

Carotenoids are an essential component of the photosynthetic machinery in photosynthetic organisms. They are lipid soluble and tend to be located in the chloroplast or chromoplasts (Bartley and Scolnik, 1995). Carotenoids provide essential protection against photooxidative damage by preventing chlorophylls reaching excited triplet states, quenching ROS and also enhance light capture in light harvesting complexes (Koyama, 1991). They are also precursors to abscisic acid (ABA), a stress indicator in cells (Bartley and Scolnik, 1995). Various stresses are known to increase carotenoid synthesis including metal exposure, various oxidative stresses and even recently UV-C stress have all been shown to stimulate carotenoid biosynthesis (Kobayashi et al., 1991; Shaish et al., 1993; Sharma et al., 2015). Carotenoids are well known for their ability to quench reactive oxygen and reactive nitrogen species especially singlet oxygen species (Mandelli et al., 2012). Their antioxidant properties are dependent upon their structure. Greater numbers of conjugated double bonds and specific structural end groups have been shown to increase the antioxidant properties of carotenoids (Albrecht et al., 2000). Aerial microalgae typically show greater stress tolerance than their aquatic counterparts as they are exposed to high light, drought and susceptible to large temperature fluctuations. The aerial microalgae *Scenedesmus* sp. and *Coelastrella* sp. were found to accumulate carotenoids under high light stresses which likely leads to their increased tolerance under stress conditions (Aburai et al., 2013).

From here on in I will focus on one specific extreme environment, acid mine drainage (AMD) contaminated environments. As the name suggests these are highly acidic environments, but also typically have high concentrations of metal contaminants. My thesis will focus on an alga adapted to an AMD environment in an abandoned copper mine, therefore, showing more elevated copper concentrations than other AMD environments. We will look at how organisms have adapted to survive such an environment, before focussing on specific more specific copper stresses and adaptations.

1.2 A Blueprint to Surviving ArMageDdon, AMD (Acid Mine Drainage)

1.2.1 Acid Mine Drainage (AMD)

Most acidic waters arise from the oxidation of pyrite, one of the most abundant sulphide minerals in the Earth's crust, leading to the release of ferric iron and sulphuric acid (Sánchez-Andrea et al., 2011). This effect can be exacerbated by chemolithic bacteria that oxidise iron and sulphide minerals

as an energy source (Johnson and Hallberg, 2008). These waters can occur naturally and in many environments worldwide (Runnells et al., 1992). These acidic waters can be further contaminated, or even new ones created, by anthropogenic activities, such as mining (Nordstrom, 2000). The Rio Tinto is such an environment, at over 90 km long the river is an extremely acidic and metal contaminated environment in which iron oxidising bacteria are thought to have existed 300,000 years ago. However, 5000 years of mining activity will have magnified these effects (Zettler et al., 2002). Acidic waters increase the solubility of metal ions, allowing their release from minerals in rocks and causing a higher concentration of trace metals in the waters (Aguilera et al., 2006). As a result of these toxic conditions it is unsurprising that biodiversity is much lower than non-contaminated, more neutral waters. The general consensus is that bacteria and archaea are the most predominant forms of life in AMD systems (Méndez-García et al., 2015). Due to proteobacteria such as *Acidithiobacillus ferrooxidans* ability to utilise Fe^{2+} and sulphur compounds as an energy source, it is unsurprising that bacteria can thrive in these conditions, especially considering that chemolithic metabolism is not unique to this clade (Fabisch et al., 2013; Valdés et al., 2008). Similar properties are also seen in the predominant archaea, *Ferroplasma*, found in the Iron Mountain, California which constituted up to 85% of the microbial diversity (Edwards et al., 2000). Most studies on extremophile organisms tend to focus on prokaryotes or archaea, as there is a general consensus that they are most prevalent in harsh environments. However, this is not always the case, algae were found to account for 65% of the total biomass in the Rio Tinto, contributing a significant proportion to the primary production of the ecosystem (López-Archilla et al., 2001). Indeed, algae tend to be some of the most dominant form of eukaryotes present in AMD ponds and can outnumber bacteria and archaea. Dean et al. (2019) found a high diversity of species in acidic ponds ranging from pH 1.6 - 5.6. Microalgae were found to be present in all ponds equalling species richness of fungi. AMD presents a harsh environment and as such organisms must adopt novel adaptations to survive, we will explore some of the ways in which they can do so.

Copper commonly occurs in sulphide based minerals such as bornite (Cu_5FeS_4), chalcopyrite ($CuFeS_2$), covellite (CuS) and chalcocite (Cu_2S) (Martin and Goldblatt, 2007). Oxidation of these sulphide minerals can contribute to the acidity of AMD as has previously discussed, but also cause the immediate dissolution of copper into free copper ions (Duczmal-Czernikiewicz et al., 2021). This process can be exacerbated by acidophilic bacteria such as *Acidithiobacillus ferrooxidans*, which metabolises the iron in such minerals as an energy source, through a process known as bioleaching (Bevilaqua et al., 2010). Copper can also be present in carbonate and oxide minerals such as azurite ($(Cu_3CO_3)_2(OH_2)$), malachite ($Cu_2CO_3(OH)_2$) and cuprite (Cu_2O), which can present other sources of copper ions which can dissociate under acidic conditions (Duczmal-Czernikiewicz et al., 2021; Martin and Goldblatt, 2007).

1.2.2 Adapting to a Low pH

Living at a low pH imposes challenges to life and we have to consider how organisms living in AMD have adapted to acidic conditions. In nature, acidic conditions are used to break down and denature large macromolecules for example, in the stomachs of large multicellular organisms or in acidic lysosomes. As such they can create hostile conditions and make survival difficult. pH and total acidity are not synonymous. The capability of a solution of donating protons is known as the total acidity. This takes into account three factors: the pH, concentration of metals (can generate mineral acidity)

and the organic compound concentration which produces organic acidity (Olaveson and Nalewajko, 2000). Acidity provides challenge to non-adapted organisms here we will explore how extremophiles have managed to overcome some of these challenges.

Acidophiles appear to have varying adpatation mechanisms to a low pH environment. When grown over a range of pH's most organisms, such as *D. salina*, *C. acidophila* and *Cyanidium caldarium*, maintain a near neutral cytosolic pH (Enami et al., 1986; Gimmler et al., 1988; Messerli et al., 2005). In contrast, *Euglena mutabilis* have been shown to have internal pH of 5 when grown within a similar acidity range, although there is variation and some individual replicates have a cytosolic pH near 7 (Lane and Burris, 1981). In addition, the methods tested by Lane and Burris (1981) measured total cellular acidity in comparison to pH. As such acidic enzymes may make the cytosolic pH seem more acidic (Messerli et al., 2005). However, some prokaryotes have certainly been found to have below circumneutral cytosolic pH also. For example, *Sarcina ventriculi* was found to have a cytosolic pH of 4.25 (Messerli et al., 2005). There are two main ways organisms can maintain a neutral cytosolic pH under acidic environmental conditions. Firstly, they can make their membranes more impermeable as seen in *Acidothiobacillus* ferrooxidans, which decreased membrane fluidity under acidic conditions preventing an influx of protons (Mykytczuk et al., 2010). Secondly, proton export using ATPases can efflux protons from the cell to maintain a neutral pH (Gross, 2000). However, this can have a large energy burden on the cell. Higher dark respiration rates were seen in both D. acidophila and C. acidophila grown at its their optimal pH (Gerloff-Elias et al., 2005; Gimmler, 2001). This has been attributed the energy costs of excreting protons that had gathered intracellularly (Gimmler, 2001). However, growth rates between C. acidophila and C. reinhardtii were found to be very similar when grown at their optimum pH's (pH 3-5 and pH 7 respectively). This was due to an increase in the photosynthetic rates of C. acidophila to compensate for the higher dark respiration rates seen (Gerloff-Elias et al., 2005). Under neutral cytosolic pH conditions, other bioprocesses, such as photosynthesis, would not be affected, therefore these adaptations, although costly would have great benefit to organisms.

If acidophiles do have a lower than neutral pH it could be likely that different extremophiles have different mechanisms to tolerate varying acidities. Organisms with a more cellular acidic pH are likely to have acid-tolerant enzymes, whilst extremophiles with circumneutral pHs may have more efficient proton efflux mechanisms. Thermophilic and acidophilic strains of fungi were found to have high activities of certain carboxymethyl cellulase (CMCase) activities. These were shown to have higher activities at pH 3 than at pH 5 or 7 (Thanh et al., 2019). This has fantastic biotechnological applications as we continue to search for more efficient ways of cell wall break down as a renewable biofuel source. Additionally, another isoform of an industrially relevant enzyme L-arabinose isomerase, has been found in *Shewanella* sp. This was found to have an optimum pH of 5.5-6.5 and produced more of the desired product at lower temperatures than other isoforms (Rhimi et al., 2011).

Not only does acidity have direct negative effects but it can also cause indirect stresses to organisms. It has already been described how acidity can cause metals to be released into the environment more easily. These soluble metals have are significantly more toxic to organisms, as they can move through the environment more easily and be transferred into the cell. This has lead to many studies to research into biomolecules, such as organic acids, clay colloids and hydroxides, that can bind

and insolubilise heavy metals, thus reducing their ability to interact with cells (An et al., 2015; Boechat et al., 2016). In addition, acidity can also affect the inorganic carbon (IC) availability for aquatic organisms. CO_2 diffuses easily through the air, therefore, for land plants uptake of IC is simple. In aquatic systems CO_2 diffuses much more slowly and IC can be found in other forms such as Bicarbonate (HCO_3^-) or Carbonate (CO_3^{2-}). The solubility of CO_2 in freshwater, at 18 °C, is 10-15 µM. When CO_2 is depleted, such as being consumed for photosynthesis this is rapidly replenished from a large pool of HCO_3^- in neutral or alkaline waters. However, in acidic waters (pH<4) the HCO_3^- pool is virtually non-existent, so CO_2 concentrations are rapidly depleted. This can, in part, be made up for the rapid dissolution of CO_2 from the atmosphere in acidic waters. At pH 2 it takes 0.42s for CO_2 to reach 99.9% equilibrium, whilst at pH 7 this takes 3.5 mins (Gross, 2000). In some environments photosynthesis has been shown to be limited due to low IC levels (Stepien et al., 2016). In acidic mining lakes, the pH can be as low as 1 but usually varies between 2.3 - 3.3 in areas such as the Rio Tinto or Parys Mountain mine, and in these waters HCO_3^- is virtually non-existent and the only form of carbon is CO_2 (Dean et al., 2019; Spijkerman, 2008). This has led to suggestions that IC is a rate limiting factor for aquatic acidophilic organisms. It has been well documented that acidophilic green algae are capable of maintaining a neutral pH , such that they use the proton gradient between the cell and the external environment to allow diffusion of IC into the cell (Balkos and Colman, 2007; El-Ansari and Colman, 2015; Spijkerman, 2005; Verma et al., 2009). It has been found that in *Chlamydomonas* sp. the diffusion is sufficient due to a low Km value for CO_2 of Rubisco (Balkos and Colman, 2007; Spijkerman, 2005).

1.2.3 Restricting Metals from Entering the Cell

Metal stress tolerance is a complicated process, we will focus on some of the many adaptation's extremophile cells can use to provide tolerance to excess metal stress, and the responses in non-extremophile species to help tolerate such conditions. Some metals are absolutely necessary for life, they play central roles in many physiological and biochemical processes, such as acting as enzyme co-factors. Essential metals include copper, manganese, iron, zinc, magnesium, cobalt, molybdenum, nickel, and chromium (Tchounwou et al., 2012). Whilst necessary for cell growth, some metals, such as copper, have a very limited window between concentrations where they are needed and concentrations that are too toxic (Mehta et al., 2006). However, some metals are not involved in any cellular processes, and when they enter the cell can be extremely harmful, these include but not limited to: cadmium, gold, silver, lithium, mercury and tin (Tchounwou et al., 2012). The first and most obvious step to adapting to metal stress is to restrict metal uptake. Restricting metals from entering the cell can be done in multiple ways, but the umbrella term for this process is primarily known as metal adsorption. It has already been described how functional groups on the cell surface can bind metals (section 1.1.5). To enhance this protection cells can secrete extracellular polymeric substances (EPS). EPS are composed of many substances including polysaccharides, humic acids, phospholipids, glycoproteins and nucleic acids, they are also the major component in biofilms (McSwain et al., 2005). A biofilm from a mine tailings reservoir was found to increase EPS production in a concentration dependent matter to both copper and zinc metal toxicity. Although individual contributions to biofilm production was not clarified both a green alga (*Chlorococcum* sp.) and a cyanobacteria (*Phormidium* sp.) were identified in the biofilm (García-Meza et al., 2005). *Bacillus* sp. S3, a soil bacterium, was found to be tolerant to heavy metals such as chromium, cadmium and

copper. In response to these metal stresses EPS was found to increase to sequester these metals, with the EPS consisting predominantly of proteins (Zeng et al., 2020). This method of immobilising metal ions, thus making them less bioavailable, can occur through different chemical interactions such as ion exchange, complexation and precipitation (De Philippis et al., 2011; Gupta and Diwan, 2017; Wang et al., 2010).

1.2.4 The Transport of Metals into and within the Cell

Although a large majority of metals are adsorbed on the cell surface, it has been shown that organisms found in AMD environments can accumulate metals to high concentrations (Dean et al., 2019; Martínez-Macias et al., 2019). The main route of entry into the cell will be through metal transporters, whether this be intentionally or not. However, once metals are inside the cells, metal transporters still play an important role in delivering metals to organelles where they can utilised. If metals are in excess, they can also be sequestered and portioned into organelles where they will not cause as much harm. We will look at some of these processes over the next section, however, for many extremophile microalgae, a lot of these processes are yet to be understood. We will focus on seven main metal transport families that have been identified in plants and well characterised, these include:

1) Zinc regulated transporter, iron regulated transporter-like proteins (ZIP)

The ZIP family of proteins mediate the influx of metal cations into the cytoplasm from either the external environment or from subcellular compartments. They are a diverse family of proteins with 14 genes being identified for them in *C. reinhardtii*, most of these have been found to be expressed in either the vacuolar or plasma membrane (Hanikenne et al., 2005). ZIPs have mainly been found to involved in the uptake of metals such as iron, manganese, zinc and copper (Grotz et al., 1998; Guerinot, 2000; Krämer et al., 2007). Many ZIPs have been found to be upregulated in response to zinc deficiency in A. *thaliana.* Additionally, ZIPs have been found to be constitutively expressed in hyper-accumulators such as *Arabidopsis halleri* aiding zinc import into the cell (Krämer et al., 2007). However, a ZIP1 protein isolated from *Oryza sativa* L. was found to function as an efflux protein, and has the potential to act as a efflux transporter for metals such as zinc copper and cadmium (Liu et al., 2019).

2) Copper transporters (COPT)

Represent a family of copper transporters that can transport copper into the cell in only a Cu^{+} form. In *A. thaliana* they have been shown to be crucial for copper uptake, heterologous expression of COPT genes in a yeast mutant was able to restore copper uptake (Sancenón et al., 2003). COPT transporters can be reliant on two associated proteins expressed in copper deficiency ferric reductase oxidase (FRO) enables the reduction of copper from its most common form Cu^{2+} to Cu^{+} to overcome copper deficiency (Bernal et al., 2012). COPT are also known as copper transporters (CTRs). When exposed to copper deficiency *C. reinhardtii CTR1*, *CTR2* and *CTR3* showed an increase in expression in response to copper deficiency and are thought to be under the control of the copper response regulator (CRR1) (Page et al., 2009).

3) Cation diffusion facilitators (CDF)

CDFs are referred to as metal transport proteins (MTP) in plants and are thought to be ubiquitous across algae. A screen of 33 taxonomically diverse alga found at least one CDF gene within each species tested. This recent study also identified two functionally undefined groups, suggesting that there are still many potentially exciting metal transporters to be studied (Ibuot et al., 2020). These are involved in the efflux of metal cations from the cytoplasm into the extracellular space or intracellular compartments such as vacuoles (Paulsen and Saier Jr., 1997). They facilitate the efflux of metal cations, such as Zn^{2+}, Mn^{2+}, Cd^{2+}, Co^{2+}, with the counter-exchange of Na^{+} or H^{+} ions (Gupta et al., 2016). An Arabidopsis metal transporter, MTP3 was shown to be important in Zinc tolerance. Arrivault et al. (2006) found MTP3 could sequester Zinc into the vacuole whilst Jiang & Wang (2008) found that most of the cellular Zinc was stored in the vacuole. Complementation experiments of a *Thlaspi goesingense* metal transporter found that MTP1 was able to confer an array of metal resistance to a metal sensitive yeast strain (Persans et al., 2001). Overexpression of a *C. reinhardtii* MTP4, conferred a greater cadmium tolerance and accumulation. Despite this success, waste-water tolerant strains still outperformed this transgenic organism, suggesting metal tolerance and accumulation is not a simple process (Ibuot et al., 2017).

4) Cation exchangers (CAX)

This family of proteins are antiporters facilitating the exchange of cations and protons. They facilitate the transport of cations such as Zn^{2+}, Cd^{2+} and Mn^{2+} into vacuoles or subcellular vesicles. This has been shown to confer a level of metal tolerance to both plants and algae (Pittman and Hirschi, 2016). Some CAX transporters have been shown to be more selective in their cation transportation showing a high selectivity of cations such as Cd^{2+} (Koren'kov et al., 2007). Further CAX have also shown to increase tolerance to salt stress. Higher expression of CAX genes were found in salt tolerant strains of *O. sativa* than less tolerant strains (Yamada et al., 2014). It is not yet fully understood if CAX directly confer metal tolerance, as there is some evidence to suggest calcium signalling, which may induce other tolerance mechanisms accordingly (Pittman and Hirschi, 2016)

5) Heavy-metal type ATPases (HMA)

HMAs are a subfamily of P-type ATPases involved in heavy metal transport across. They are ubiquitous in nature and have diverse functions and tissue localisations, however they share the same characteristic 6-8 transmembrane domains that flank the large ATP binding cytoplasmic loop (Argüello et al., 2007). This subfamily can then be further divided depending on their preferred substrate. Some transport monovalent cations including Cu^{+} and Ag^{+} or divalent cations including Zn^{2+}, Co^{2+}, Pb^{2+}, and Cd^{2+} (Cobbett et al., 2003). The function of the HMA transporters varies from providing copper to proteins in the Golgi network (Cobbett et al., 2003) to Cd^{2+} transport in the hyper accumulator *Arabidopsis halleri* providing a higher tolerance (Bernard et al., 2004). A HMA from *Silene vulgaris,* SvHMA5II, was found to associate with the endoplasmic reticulum, however, when exposed to copper it relocalises to the plasma membrane where it could act as a copper efflux mechanism (Li et al., 2017). Copper transport proteins (CTP) are a type of HMA P-type ATPase, that as the name suggest, transport copper across membranes. Of special interest is CTP3 which has shown similarity to *A. thaliana* HMA3, which is involved in copper efflux out of cells (Blaby-Haas and Merchant, 2012; Pedersen et al., 2012).

6) ATP binding cassette (ABC) transporters

The ABC transporter family is one of the larger family of transport proteins and are involved in a number of physiological processes. As such they have been split into smaller sub-families of which only two, MRP and ATM/ HMT are thought to be involved in metal transport (Hanikenne et al., 2005). Both subfamilies utilise ATP as the energy source for transportation across the membrane. MRP proteins can bind only glutathione-S conjugates with metals. This is vital as it sequesters chelated metals into compartments, such as the vacuoles, where they are less likely to do damage (Rea et al., 1998). ATM/ HMT transporters are known as half size transporters located on the mitochondrial or vacuolar membranes but work in a similar manner to MRPs in that they bind glutathione or glutathione derived products such as phytochelatins (Hanikenne et al., 2005).

ABC transporters can also be involved in detoxifying the cells. Two stress-detoxification ABC transporter transcripts were found to be upregulated in response to copper stress in the brown alga *Ectocarpus siliculosus* (Ritter et al., 2014). A proteomic analysis of copper stressed *Scytosiphon gracilis* saw three ABC transporters increase in expression (Contreras et al., 2010). An ABC transporter, MRP1, in *C. reinhardtii* has shown to be important in the cellular accumulation of Cadmium through the binding of most likely glutathione although they could still be bound to phytochelatins (Wang and Wu, 2006). The authors identified a vacuole targeting sequence in the protein suggesting that CrMRP2 would be located on the vacuolar membrane. This infers that the Cadmium -glutathione complexes could be sequestered into the vacuole. Although this has not yet been fully confirmed, plants are well known to sequester heavy metals into their vacuoles. Given that metals transporters appear to play an important role in metal stress resistance it is odd that Olsson et al. (2015) did not identify any upregulated transporters in their transcriptomics study in an extremophile adapted to high metal stress environments. However, as they did not compare the extremophile to a non-adapted organism it is possible that they may have missed any constitutively expressed genes to confer this resistance.

7) Natural resistance-associated macrophage proteins (NRAMP)

NRAMPs are involved in metal homeostasis by re-releasing metal cations from the vacuoles into the cytoplasm. They have been shown to mobilise metals such as iron and manganese when limited to prevent loss of photosynthesis or seed germination (Lanquar et al., 2010, 2005). There is also evidence to suggest that NRAMPS can be localised to the plasma membrane and are involved in metal uptake into the cell. A divalent metal transporter (DMT1) was identified in *C. reinhardtii* which shows high similarity to prokaryotic NRAMPS. Functional complementation of DMT1 in yeast with diminished metal transport capability revealed it could transport manganese, iron and copper into the cell, as well as the non-essential metal cadmium (Rosakis and Köster, 2005). Additionally, *C. reinhardtii nramp3nramp4* mutants were found to be highly sensitive to copper deficient environments and growth is severely inhibited (Carrió-Seguí et al., 2019).

1.2.5 Metal Sequestration

Once metals are inside the cell they can be utilised for specific functions, such as key co-factors for enzymes, or if the metals accumulate inside the cell at elevated concentrations, they can cause toxicity. Sequestration can also refer to metals being compartmentalised into subcellular compartments, such as vacuoles, or even specific tissues in multicellular organisms, such as the pith cells in plants (Tian et al., 2011; Wang & Wu, 2006). Speciation of metals is an important factor when

considering their toxicity. The effect of metal chelation can be shown when observing the growth rate of *Chlorella pyrenoidosa* in a media spiked with copper and additional added chelators. The growth was inhibited in a copper spiked minimal media, but was increased copper spiked high nutrient media containing metal chelators such as EDTA and silicate. The minimal media contained more free metal ions that are highly reactive, and therefore, more toxic (Stauber and Florence, 1989). Metal chelators have been well documented in higher plants, microalgae, fungi and prokaryotes and come in a wide array of forms depending on the species producing the chelator and the different metals they have an affinity for (Hastrup et al., 2014; Parker et al., 2004; Stauber and Florence, 1989; Yoneyama et al., 2015).

Phytochelatins (PCs) were first described by Grill et al. (1985) in *Rauvolfia serpentina* and were found to be able to bind cadmium. They found that 90% of intracellular cadmium was bound to these polypeptides through their cysteine (Cys) thiol groups. At the time, Grill et al. (1985) described them as having a completely different structure to previously known metal-binding polypeptides, such as metallothioneins. However, in 1985 metallothionein classification was revised to include polypeptides which share several of the following properties: “low molecular mass, high metal content, high Cys content with the absence of aromatic amino acids and histidine. An abundance of Cys-X-Cys sequences where X is an amino acid other than Cys, spectroscopic features characteristic of metal thiolates, and metal thiolate clusters” (Rauser, 1990). As such phytochelatins were later classified as class III metallothioneins and are commonly referred to in the literature by either name. Class I and II metallothioneins function in a similar manner to class III metallothioneins in that they bind heavy metals. However, these are gene-encoded proteins (Perales-Vela et al., 2006). Other amino acids have also been shown to chelate metals. Using Fourier Transform infrared (FT-IR) spectroscopy, a method which utilises molecular stretching at different wavelengths under an IR light, Gerbino et al. (2011) found that protein could change their secondary structure to accommodate metal ions with most of the metal/protein interactions working through Asp and Glut residues. FT-IR spectroscopy has been used in arrange of other metal binding studies, through which metals have been found to bind to cell surfaces and EPS (Giotta et al., 2011; Kalita and Joshi, 2017).

Phytochelatins are formed from glutathione metabolism rather than direct protein synthesis (Rauser, 1990), however, not all species of microalgae produce phytochelatins. They sequester metals using the sulphhydryl groups in their cysteine residues to chelate metals (Pérez-Rama et al., 2001). Phytochelatin synthesis has been shown to be induced with differing amounts by Cd^{2+}, Ag^{+}, Bi^{3+}, Pb^{2+}, Zn^{2+}, Cu^{2+}, Hg^{2+}, As anions, Au^{2+} and Fe^{3+} through the activation of phytochelatin synthase (PCS), an enzyme which catalyses the production of phytochelatins (Grill et al., 1989; Rea et al., 2004; Schmöger et al., 2000). PCS binds to glutathione molecules together to form short chain phytochelatin. It can then increase the chain length of phytochelatin by the addition of further glutathione molecules (García-García et al., 2014). One study comparing an *A. thaliana* PCS to a marine diatom *Thalassiosira pseudonana* PCS suggests properties of PCS may be species specific as the TpPCS showed a higher affinity for cadmium whilst also being much more sensitive to oxidation (Gupton-Campolongo et al., 2013). As such PCS may be an adaptable protein which can help organisms tolerate specific environments. García-García et al. (2014) proved this in *Euglena gracilis*, a cadmium hyperaccumulating green alga. In this study they described a novel characteristic

in the enzymatic core. In addition, the expression of EgPCS was found to be constitutively expressed, which differs with the situation in *C. reinhardtii* (Bräutigam et al., 2011), *A. thaliana* (Lee and Korban, 2002), and *Brassica juncea* (Heiss et al., 2003) in which PCS activity was seen to increase in response to cadmium exposure. Finally, the study also showed that the heterologous expression of EgPCS in a Cadmium sensitive *S. cerevisiae* strain was able to confer resistance to cadmium. Clemens et al. (1999) also highlighted the effects of PCS through heterologous expression of a wheat, *A. thaliana* and *Schizosaccharomyces pombe* PCS genes in *S. cerevisiae*. They were able to significantly increase transgenic *S. cerevisiae* growth rates in the presence of cadmium. However, overexpression of an *A. thaliana* PCS has conferred cadmium sensitivity to the transgenic plants (Li et al., 2004; Wojas et al., 2008). It is thought that high amounts of cadmium-PC complexes in the cytosol may still be toxic if the downstream processing step of these complexes are not upregulated to deal with these extra complexes. Interestingly, a high cadmium accumulating strain of *C. acidophila* showed similar levels of PCS activity and PC levels as a non-accumulating strain of *C. acidophila*. Regardless, the high accumulating strain was still able to accumulate up to 170 times more cadmium than the non-accumulating strain (Nishikawa et al., 2006). Even though we have seen the importance of PCs in metal detoxification there is mounting evidence to suggest that the quantity of PC may not be as important. γ-ECS is thought to be the rate limiting enzyme in glutathione synthesis (May et al., 1998). A transcriptomics study found an increase in γ-ECS activity in *D. acidophila* under metal stress, this was in addition to a whole array of other enzymes involved in glutathione synthesis. However, they also did find an increase in PCS transcripts, although, it was only a minor increase and there is no data on the activity or abundance of the protein in downstream processes (Puente-Sánchez et al., 2016). It is clear that different organisms use different strategies to adapt to these extreme environments. Although PCs are important in detoxifying metals, they may not be the most important factor in adapting to metal stress. It seems the cycling of GSH may play a bigger part. However, due to the diversity of extreme environments and the organisms that inhabit in them it seems unlikely that there will be a one glove fits all rule and PCs could still play an important role in other extremophiles.

1.3 *Effects of Copper on Green Microalgae and Their Adaptations*

1.3.1 Copper - An Essential Nutrient but Highly Damaging in Excess

Copper is an essential metal that acts as an important co-factor in proteins and involved in several metabolic processes (Pätsikkä et al., 2002). For example, the ability of copper to switch between its oxidised state (Cu^{2+}) to its reduced form (Cu^{+}) by accepting or donating electrons, makes it a very attractive metal for electron transport processes such as photosynthesis. Plastocyanin is the most prevalent copper-associated protein in photosynthetic organisms and facilitates the transfer of electrons from cytochrome f to $P700^{+}$ due to these characteristics (Printz et al., 2016). However, this useful characteristic in electron transport chains can also make copper highly toxic as it is a very redox active metal. Excess copper is a well known inhibitor of photosynthesis with photosystem II (PSII) having been shown to be particularly sensitive to excess copper concentrations (Caspi et al., 1999). Copper complexes have even been created as novel herbicide - shown to induce reduced GSR activity, PSII carbonic anhydrase and PSII (Rodionova et al., 2017). Excess copper seems to have similar negative effects across microalgal species. The freshwater alga *Closterium ehrenbergii*

exhibited a decrease in pigment levels and photosynthetic efficiency whilst simultaneously increasing ROS generation and lipid peroxidation (Wang et al., 2018). A decrease in the maximum photochemical efficiency of PSII as well as pigment levels also decreased upon copper exposure in *C. reinhardtii*. The authors ascribed the decrease in photosynthetic efficiency and cell growth due to an increase in lipid oxidation, suggesting a breakdown in membrane lipids (Jiang et al., 2016). An overview of copper specific stress targets and adaptation mechanisms can be seen in Figure 1.1, and which will be discussed in further detail below.

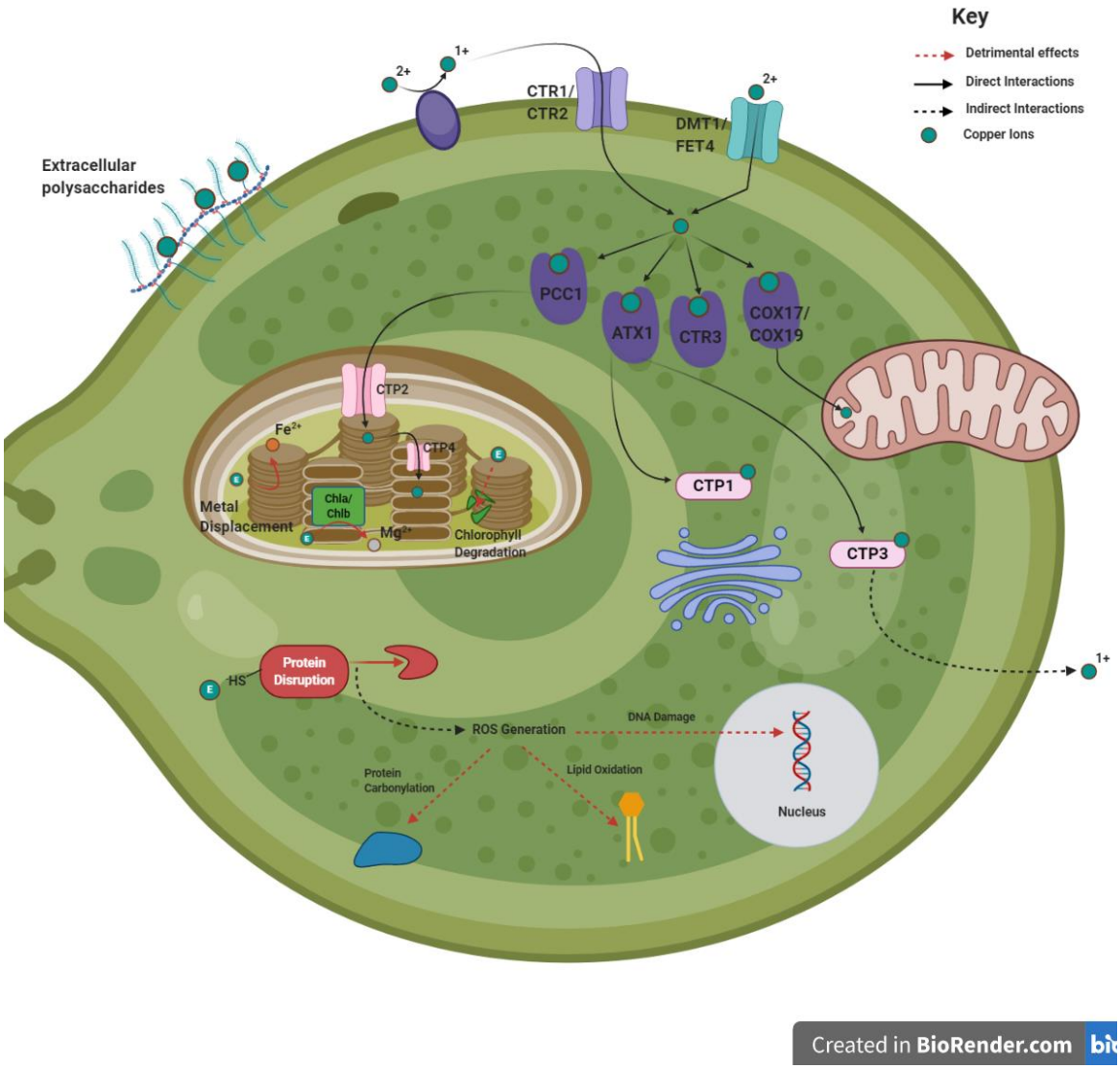

Figure 1.1 Overview of Excess Copper on Microalgal Cells. Copper is imported into the cell through specific copper transporters or more broad divalent cation transporters. They are met by chaperone proteins once inside the cell which help deliver copper to functional protein inside other compartments of the cell. Excess copper can have detrimental effects which are also seen in the overview.

1.3.2 Copper Transport and Availability in Algal Cells

Copper has been found to accumulate inside vacuoles of extremophile microalgae such as *E. gracilis* and *Chlamydomonas* sp. (Aguilera and Amils, 2005; Einicker-Lamas et al., 2002). This would suggest that these organisms have a sophisticated copper transport system to help them survive a high copper environment. As previously mentioned in sections 1.1.5 and 1.2.3 the first and foremost way of easing abiotic stresses such as excess metals is by preventing them from entering the cells. The fresh water green alga *Chlorella pyrenoidosa* was exposed to solid CuO nanoparticles, which induced a 4-fold increase in the EPS layer. There was no indication to the amount of metals adsorbed by this EPS however CuO nanoparticles were still taken up into the cells (Zhao et al., 2016). It has also been shown that the affinity of amino acid side chains for Cu^{+} is dependent on pH. The amino acids Cys and Met were shown to be preferred at more acidic pHs (~4.5) whilst Cys and His are preferred at a more neutral pH (7.4) in yeast (Rubino et al., 2011). There is a lot of confusion in the literature with regards to the naming system of copper transporters in microalgae, with many proteins being individually named multiple times. For simplicity I will be following the naming system used in the review by Blaby-Haas and Merchant (2012), but as protein function seems to be less controversial I will still draw from other sources.

Copper is primarily taken up in the Cu^{+} form through the family of CTR copper transport proteins. CTR1 and CTR2 are localised to the plasma membrane and work in conjunction with a cupric reductase which reduces Cu^{2+} to Cu^{+} and allows for a very high affinity uptake of copper (Page et al., 2009). As previously mentioned copper, when unregulated, can be highly damaging to cell components. For this reason, upon entering the cell copper is met with metallochaperones which facilitate the safe transfer of copper to storage compartments or sites of cupric protein synthesis. CTR1, CTR2 and COPT1 (another member of the CTR family) all show cysteine and histidine domains on the C terminus that are able to transfer copper ions to a chaperone (Page et al., 2009). Once copper is bound to the chaperones, intracellular copper concentrations are low and it is this concentration gradient that drives the transfer of copper into the cells. It is also possible that Cu^{2+} could enter the cell through other low affinity metal transporters. Cu^{2+} can enter the cell through FET4, a low affinity iron transporter in yeast iron deficiency (Hassett et al., 2000). Additionally, the broad range divalent metal transporter from the NRAMP family, DMT1, has been shown to facilitate the uptake of various metal ions such as manganese, copper, cadmium and iron. Interestingly, zinc was found to not be transported by this broad range transporter (Rosakis and Köster, 2005). Sánchez-Marín, Fortin and Campbell, (2014) observed that copper and lead share a common uptake mechanism in *C. reinhardtii*, although this has not been characterised to molecular detail, but it further proves that there are multiple common uptake mechanisms into algal cells. Different copper chaperones have been detected in microalgae depending on the site of delivery, in plants three groups of copper chaperones have been identified CCH, CCS and COX17 (Yruela, 2005). The algal copper chaperone ATX1, which shows high homology to CCH chaperones, is involved in delivering copper to ferroxidase at the plasma membrane, (La Fontaine et al., 2002). CTR3 is also thought to act as a copper chaperone as it is found in the soluble proteome and the CTR family show sequence similarity to ATX1 (Blaby-Haas and Merchant, 2012). Whilst copper chaperones COX17 and COX19 have been identified in *C. reinhardtii* which are required for the delivery of Copper to cytochrome oxidase in the mitochondria (Merchant et al., 2006). Finally, PCC1 is thought to be a copper

chaperone that facilitates the transport of copper to the chloroplasts (Castruita et al., 2011). To the best of my knowledge there is no evidence for CCS copper chaperones in microalgae. CCS chaperones are involved in the transfer of copper to Cu/Zn SOD (Yruela, 2005). As green microalgae such as *C. reinhardtii* are known to not have Cu/Zn isoforms of SOD, this could explain the lack of evidence for CCS in microalgae (Dudley Page et al., 2012).

Once copper is safely bound to chaperones and directed towards its intracellular targets, they need to be transported across membranes into their respective vacuoles, mitochondria or chloroplasts. This requires specific metal transporters. P_{1B}-type ATPases are capable of transporting copper, as well as other heavy metals, through phosphorylation using ATP to drive the metals across membranes and are divided into three classes (Pedersen et al., 2012).The genome of *C. reinhardtii* encodes five P_{1B}-type ATPases of which four can be found in one class, P_{1B-1}-type. The other, can be found in the P_{1B-4}-type ATPase cluster, both clusters have been found to be capable of transporting copper (Pedersen et al., 2012). P_{1B-1}-type ATPases can be classed into two further subgroups Cu-A and Cu-B, the first include proteins such as CTP2 and CTP4 which are involved in the transport of copper to plastocyanin in the thylakoids. They are located in the chloroplast membrane and thylakoid inner membrane respectively and show homology to PAA1 and PAA2, which are involved delivering copper to the chloroplast in *A. thaliana* (Blaby-Haas and Merchant, 2012; Pilon et al., 2006). PAA1 and PAA2 specifically deliver copper to plastocyanin in the thylakoids, located in the chloroplast envelope inner membrane and thylakoids respectively (Pilon et al., 2006). The second cluster, Cu-B, play more varied roles. CTP1 is a Cu-B P_{1B-1}-type ATPase that is predicted to accept copper off of the chaperone ATX1 and deliver it to FOX1, a multicopper ferroxidase, in the Golgi apparatus where it is matured before delivery to the plasma membrane (Blaby-Haas and Merchant, 2012). The other Cu-B P_{1B-1}-type ATPase is CTP3, Blaby-Haas and Merchant, (2012) found CTP3 to show a similar sequence similarity to AtHMA5 and have so proposed that it is involved in detoxifying copper through the secretory pathway.

1.3.3 Excess Copper Can Have Detrimental Effects on Photosynthesis

Photosynthesis is a highly balanced and regulated process due to the high rate of electron transfer and free radicals created. Therefore, any perturbance to this system can apply great stress to photosynthetic organisms and have many negative downstream effects. Heavy metals in general have been shown to have deleterious effects on photosynthesis, with chlorophyll fluorescence yields found to decrease under metal stresses such as copper, zinc, chromium and cadmium (Baumann et al., 2009). Copper plays an important metabolic role in organisms, serving as a carrier in electron transport chains and vital cofactor of important enzyme systems such as amine oxidase and cytochrome c oxidase (Suresh Kumar et al., 2014). It even works as a cofactor for the important antioxidant enzyme Cu/Zn SOD, although these isoforms are not present in chlorophyte microalgae (Dudley Page et al., 2012). However, at elevated concentrations Copper is highly toxic to plants and algae, as it is a potent inhibitor of photosynthesis. When *Chlorella pyrenoidosa* was exposed to copper just 0.1 mg L^{-1} of Cu^{2+} exposure was enough to cause a decrease in photosynthesis whilst 0.5 mg L^{-1} led to a complete inhibition of photosynthesis. Cu^{2+} had a much more profound effect than any of the other metals tested (chromium and nickel) in which both treatments were unable to completely inhibit photosynthesis (Wong and Chang, 1991). One way in which Cu^{2+} can inhibit photosynthesis is by directly displacing Mg^{2+} in chlorophyll. Cu^{2+} can readily displace Mg^{2+} in

chlorophyll *a*, whilst at elevated concentrations Cu^{2+} can also displace Mg^{2+} in the more stable chlorophyll *b* molecules (Küpper et al., 2002). The authors suggest that Cu-chlorophylls are not able to bind axial ligands required to assimilate and maintain chlorophyll properly within the light harvesting complex II (LHC II) and could lead to the breakdown if chlorophyll into phaeophytin by a process known as phaeophytisation. In the extremophile *E. gracilis* photosynthetic quantum efficiency was found to decrease after 48 hours of copper exposure. The main cause of this was due to damage of the PSII reaction centre, the damaged photosynthesis apparatus led to an enhanced production of ROS (Rocchetta and Küpper, 2009). Free Cu^{2+} ions have been shown to negatively affect both the acceptor and donor sides of PSII. Cu^{2+} ions can inhibit fast reduction of the primary electron donor of PSII ($P680^{+}$) from a redox active tyrosine residue during the water splitting process (Jegerschold et al., 1995; Schroder et al., 1994). Che *et al.* (2018) also noted that the oxygen evolving complex (also known as the water splitting complex) was the most susceptible CuO nanoparticle (NP) stress through the dissociation of manganese by copper. As previously mentioned, copper can also negatively affect photosynthesis on the acceptor side, Cu^{2+} has also been shown to irreversibly decouple Fe^{2+} ions from Q_A, a quinone acceptor involved in electron transport from PSII to PSI (Jegerschold et al., 1995). Cu^{2+} can also negatively affect photosynthesis on a more structural level. Copper, either in its ionic form or as nanoparticles, has also been shown to disrupt the cell membrane of chloroplasts. This altering and disrupting of their structure is thought to be caused primarily through ROS generation and can further inhibit and reduce photosynthetic efficiency (Che et al., 2018; Einicker-Lamas et al., 2002).

1.3.4 Copper Sequestration

Phytochelatins are synthesised through the combination of two GSH molecules (see section 1.2.4 and 2.2.5). Smith et al. (2014) found a similar decrease in reduced GSH with it reaching 19% of the total cellular GSH content a concurrent increase in phytochelatin concentration when *Ceratoneis closterium* was exposed to copper after 72 hours. This was also matched with a marked increase in GSSG, as such, it is likely that the reduction of reduced GSH is due to GSH quenching dangerous free radicals and thus indicates there is a high oxidative burden on the cells. In contrast, *Phaeodactylum tricornutum* was able to maintain its reduced GSH between 58-80% of the total cellular GSH content. *P. tricornutum* was able to maintain a much higher cellular GSH and phytochelatin content, this would suggest that it dealt better with the copper stress than *C. closterium.* The study by Smith et al. (2014) highlights the importance of observing the molecules of interest in all states when considering metal toxicity as they inevitably affect the redox state to the cells. This provides a much better picture of the cellular response and can help further characterise the state of the cells and the tolerance process.

1.4 A Brief Introduction to Parys Mountain

This thesis focuses on an extremophile microalga *Chlamydomonas acidophila* isolated from a pond in Parys Mountain, Anglesey, Wales. Parys Mountain is an abandoned open cast copper mine, that was continuously active from the mid-18^{th} century. Mining ceased in 1911 and since then the discharges from Parys Mountain are the largest contributors of copper and zinc to the Irish Sea (Dean et al., 2013). It is also the single largest source of iron release in the UK (Mayes et al., 2010). A full overview of the composition of all the ponds found in Parys Mountain can be found in Dean et al. (2019). But in brief pond 1, where PM01 was isolated from contains high quantities of copper and

zinc (Figure 1.2 (A and B)). Pond 1 is located on the spoil outcrop of the site at an elevated position (Dean et al., 2019). Parys mountain is an interesting site that has been studied for alternate metal remediation methods, such as wetland remediation. Parys Mountain discharges come from both the southern Afon Goch and northern Afon Goch which drain into the Irish Sea. The southern Afon Goch runs through a natural wetlands system offering, a method of natural bioremediation (Dean et al., 2019). Parys Mountain drainage enters the northern Afon Goch through an adit approximately half way down the river, and gives a good comparison to test the effectiveness of natural wetlands system in the bioremediation of AMD (Dean et al., 2019). This site has also provided an excellent system to monitor microbial community change in response to varying amounts of AMD (Aguinaga et al., 2019, 2018).

A

Pond 1

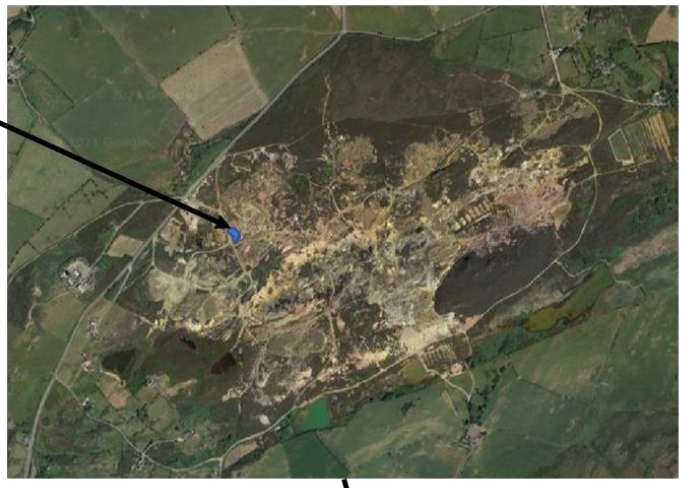

B

Metal	Free Ionic Metal (mg L^{-1})
Cadmium	0.16
Copper	36.59
Zinc	28.69

Figure 1.2 (A) Satellite image of Parys mountain taken from Google Maps, highlighted to it's location within the UK, pond 1 is highlighted and is the pond the strain of C. acidophila , PM01 was isolated from. (B) A snapshot of the metal composition of pond 1

1.5 *Aims and objectives*

Our lab has previously isolated a highly copper tolerant strain of *C. acidophila* (PM01), that exhibits a much higher copper tolerance levels than other strains (Dean et al., 2019). I wanted to understand some of these adaptation mechanisms to 1) Gain a better understanding of copper tolerance in extremophile eukaryotic organisms and 2) Identify any possible bioremediation or biotechnological applications. I examined the cellular responses of up to four organisms, these were PM01, two less copper tolerant strains of *C. acidophila* (CCAP 11/136 and CCAP 11/137), and the model organism *C. reinhardtii*. To discriminate between any short-term adaptation and long-term adaptations, I exposed the samples to 3-hour copper stresses and cultures grown in the presence of copper for two weeks. First, Chapter 2 looks at the physiological and biochemical responses of the four species of microalgae. I aimed to observe the impact of copper on photosynthetic parameters as well as other key indicators of stress and stress responses such as lipid oxidation and the antioxidative response. Secondly, Chapter 3 explores the metabolic response of *C. reinhardt*ii and PM01 to a short and long-term copper stress, utilising techniques such as FT-IR, MALDI-TOF and LC-MS. Finally, in Chapter 4 I aim to identify key gene expression changes PM01 has undergone to adapt to a high copper contaminated environment. This was be done by sequencing the transcriptome of PM01 and *C. reinhardtii* under a short-term and long-term copper stress. By comparing PM01 to a non-extremophile I identified unique responses to PM01 that could be of interest for further biotechnological or bioremediation applications.

1.6 References

Aburai, N., Ohkubo, S., Miyashita, H., Abe, K., 2013. Composition of carotenoids and identification of aerial microalgae isolated from the surface of rocks in mountainous districts of Japan. Algal Res. 2, 237–243. https://doi.org/10.1016/j.algal.2013.03.001

Aguilera, A., Amils, R., 2005. Tolerance to cadmium in *Chlamydomonas* sp. (Chlorophyta) strains isolated from an extreme acidic environment, the Tinto River (SW, Spain). Aquat. Toxicol. 75, 316–329. https://doi.org/10.1016/j.aquatox.2005.09.002

Aguilera, A., Manrubia, S.C., Gómez, F., Rodríguez, N., Amils, R., 2006. Eukaryotic community distribution and its relationship to water physicochemical parameters in an extreme acidic environment, Río Tinto (Southwestern Spain). Appl. Environ. Microbiol. 72, 5325–5330. https://doi.org/10.1128/AEM.00513-06

Aguinaga, O.E., McMahon, A., White, K.N., Dean, A.P., Pittman, J.K., 2018. Microbial Community Shifts in Response to Acid Mine Drainage Pollution Within a Natural Wetland Ecosystem. Front. Microbiol. 9, 1445. https://doi.org/10.3389/fmicb.2018.01445

Aguinaga, O.E., Wakelin, J.F.T., White, K.N., Dean, A.P., Pittman, J.K., 2019. The association of microbial activity with Fe, S and trace element distribution in sediment cores within a natural wetland polluted by acid mine drainage. Chemosphere 231, 432–441. https://doi.org/10.1016/j.chemosphere.2019.05.157

Ahuja, K., Rawat, A., 2019. Astaxanthin Market Growth Projections Statistics 2019-2026 [WWW Document]. Glob. Mark. Insights. URL https://www.gminsights.com/industry-analysis/astaxanthin-market (accessed 1.22.20).

Albrecht, M., Shinichi, T., Steiger, S., Wang, Z.-Y., Sandmann, G., 2000. Novel hydroxycarotenoids with improved antioxidative properties produced by gene combination in Escherichia coli. Nat. Biotechnol. 18, 843–846.

An, J., Jho, E.H., Nam, K., 2015. Effect of dissolved humic acid on the Pb bioavailability in soil solution and its consequence on ecological risk. J. Hazard. Mater. 286, 236–241. https://doi.org/10.1016/J.JHAZMAT.2014.12.016

Angelé-Martínez, C., Nguyen, K.V.T., Ameer, F.S., Anker, J.N., Brumaghim, J.L., 2017. Reactive Oxygen Species Generation by Copper(II) Oxide Nanoparticles Determined by DNA Damage Assays and EPR Spectroscopy. Nanotoxicology 11, 278. https://doi.org/10.1080/17435390.2017.1293750

Argüello, J.M., Eren, E., González-Guerrero, M., 2007. The structure and function of heavy metal transport P1B-ATPases. BioMetals 20, 233–248. https://doi.org/10.1007/s10534-006-9055-6

Arrivault, S., Senger, T., Kramer, U., 2006. The Arabidopsis metal tolerance protein AtMTP3 maintains metal homeostasis by mediating Zn exclusion from the shoot under Fe deficiency and Zn oversupply. Plant J. 46, 861–879. https://doi.org/10.1111/j.1365-313X.2006.02746.x

Ask, M., Mapelli, V., Höck, H., Olsson, L., Bettiga, M., 2013. Engineering glutathione biosynthesis of Saccharomyces cerevisiae increases robustness to inhibitors in pretreated lignocellulosic materials. Microb. Cell Fact. 12, 87. https://doi.org/10.1186/1475-2859-12-87

Asker, D., Ohta, Y., 2002. Production of canthaxanthin by Haloferax alexandrinus under non-aseptic conditions and a simple, rapid method for its extraction. Appl. Microbiol. Biotechnol. 58, 743–750. https://doi.org/10.1007/s00253-002-0967-y

Balkos, K.D., Colman, B., 2007. Mechanism of CO2 acquisition in an acid-tolerant Chlamydomonas. Plant, Cell Environ. 30, 745–752. https://doi.org/10.1111/j.1365-3040.2007.001662.x

Barnard, D., Casanueva, A., Tuffin, M., Cowan, D., 2010. Extremophiles in biofuel synthesis. Environ. Technol. 31, 871-888. https://doi.org/10.1080/09593331003710236

Bartley, G.E., Scolnik, P. a, 1995. Plant carotenoids: pigments for photoprotection, visual attraction, and human health. Plant Cell 7, 1027–1038. https://doi.org/10.1105/tpc.7.7.1027

Basile, A., Sorbo, S., Pisani, T., Paoli, L., Munzi, S., Loppi, S., 2012. Bioacumulation and ultrastructural effects of Cd, Cu, Pb and Zn in the moss Scorpiurum circinatum (Brid.) Fleisch.

& Loeske. Environ. Pollut. 166, 208–211. https://doi.org/10.1016/j.envpol.2012.03.018

Basu, B., Apte, S.K., 2012. Gamma radiation-induced proteome of Deinococcus radiodurans primarily targets DNA repair and oxidative stress alleviation. Mol. Cell. Proteomics 11. https://doi.org/10.1074/mcp.M111.011734

Baumann, H.A., Morrison, L., Stengel, D.B., 2009. Metal accumulation and toxicity measured by PAM-Chlorophyll fluorescence in seven species of marine macroalgae. Ecotoxicol. Environ. Saf. 72, 1063–1075. https://doi.org/10.1016/j.ecoenv.2008.10.010

Behnke, J., LaRoche, J., 2020. Iron uptake proteins in algae and the role of Iron Starvation-Induced Proteins (ISIPs). https://doi.org/10.1080/09670262.2020.1744039 55, 339–360. https://doi.org/10.1080/09670262.2020.1744039

Bequer Urbano, S., Albarracín, V.H., Ordoñez, O.F., Farías, M.E., Alvarez, H.M., 2013. Lipid storage in high-altitude Andean Lakes extremophiles and its mobilization under stress conditions in Rhodococcus sp. A5, a UV-resistant actinobacterium. Extremophiles 17, 217–227. https://doi.org/10.1007/s00792-012-0508-2

Bernal, M., Casero, D., Singh, V., Wilson, G.T., Grande, A., Yang, H., Dodani, S.C., Pellegrini, M., Huijser, P., Connolly, E.L., Merchant, S.S., Krämer, U., 2012. Transcriptome sequencing identifies SPL7-regulated copper acquisition genes FRO4/FRO5 and the copper dependence of iron homeostasis in Arabidopsis. Plant Cell 24, 738–61. https://doi.org/10.1105/tpc.111.090431

Bernard, C., Roosens, N., Czernic, P., Lebrun, M., Verbruggen, N., 2004. A novel CPx-ATPase from the cadmium hyperaccumulator Thlaspi caerulescens. FEBS Lett. 569, 140–148. https://doi.org/10.1016/j.febslet.2004.05.036

Bevilaqua, D., Garcia, O., Tuovinen, O.H., 2010. Oxidative dissolution of bornite by Acidithiobacillus ferrooxidans. Process Biochem. 45, 101–106. https://doi.org/10.1016/J.PROCBIO.2009.08.013

Blaby-Haas, C.E., Merchant, S.S., 2012. The ins and outs of algal metal transport. Biochim. Biophys. Acta 1823, 1531–1552. https://doi.org/10.1016/j.bbamcr.2012.04.010

Bräutigam, A., Schaumlöffel, D., Preud'Homme, H., Thondorf, I., Wesenberg, D., 2011. Physiological characterization of cadmium-exposed Chlamydomonas reinhardtii. Plant, Cell Environ. 34, 2071–2082. https://doi.org/10.1111/j.1365-3040.2011.02404.x

Carrió-Seguí, À., Romero, P., Curie, C., Mari, S., Peñarrubia, L., 2019. Copper transporter COPT5 participates in the crosstalk between vacuolar copper and iron pools mobilisation. Sci. Rep. 9. https://doi.org/10.1038/s41598-018-38005-4

Caspi, V., Droppa, M., Horváth, G., Malkin, S., Marder, J.B., Raskin, V.I., 1999. The effect of copper on chlorophyll organization during greening of barley leaves. Photosynth. Res. 62, 165–174. https://doi.org/10.1023/a:1006397714430

Castruita, M., Casero, D., Karpowicz, S.J., Kropat, J., Vieler, A., Hsieh, S.I., Yan, W., Cokus, S., Loo, J.A., Benning, C., Pellegrini, M., Merchant, S.S., 2011. Systems biology approach in Chlamydomonas reveals connections between copper nutrition and multiple metabolic steps. Plant Cell 23, 1273–1292. https://doi.org/10.1105/tpc.111.084400

Černá, K., Neustupa, J., 2010. The pH-related morphological variations of two acidophilic species of Desmidiales (Viridiplantae) isolated from a lowland peat bog, Czech Republic. Aquat. Ecol. 44, 409–419. https://doi.org/10.1007/s10452-009-9296-x

Che, X., Ding, R., Li, Y., Zhang, Z., Gao, H., Wang, W., 2018. Mechanism of long-term toxicity of CuO NPs to microalgae. Nanotoxicology 12, 923–939. https://doi.org/10.1080/17435390.2018.1498928

Choo, K.S., Snoeijs, P., Pedersén, M., 2004. Oxidative stress tolerance in the filamentous green algae Cladophora glomerata and Enteromorpha ahlneriana. J. Exp. Mar. Bio. Ecol. 298, 111–123. https://doi.org/10.1016/j.jembe.2003.08.007

Clemens, S., Kim, E.J., Neumann, D., Schroeder, J.I., 1999. Tolerance to toxic metals by a gene

family of phytochelatin synthases from plants and yeast. EMBO J. 18, 3325–3333. https://doi.org/10.1093/emboj/18.12.3325

Cobbett, C.S., Hussain, D., Haydon, M.J., 2003. Structural and functional relationships between type 1B heavy metal-transporting P-type ATPases in Arabidopsis. New Phytol. 159, 315–321. https://doi.org/10.1046/j.1469-8137.2003.00785.x

Coker, J.A., Brenchley, J.E., 2006. Protein engineering of a cold-active β-galactosidase from Arthrobacter sp. SB to increase lactose hydrolysis reveals new sites affecting low temperature activity. Extremophiles 10, 515–524. https://doi.org/10.1007/s00792-006-0526-z

Coker, J.A., Sheridan, P.P., Loveland-Curtze, J., Gutshall, K.R., Auman, A.J., Brenchley, J.E., 2003. Biochemical characterization of a β-galactosidase with a low temperature optimum obtained from an Antarctic Arthrobacter isolate. J. Bacteriol. 185, 5473–5482. https://doi.org/10.1128/JB.185.18.5473-5482.2003

Contreras, L., Moenne, A., Gaillard, F., Potin, P., Correa, J.A., 2010. Proteomic analysis and identification of copper stress-regulated proteins in the marine alga Scytosiphon gracilis (Phaeophyceae). Aquat. Toxicol. 96, 85–89. https://doi.org/10.1016/j.aquatox.2009.10.007

De Philippis, R., Colica, G., Micheletti, E., 2011. Exopolysaccharide-producing cyanobacteria in heavy metal removal from water: molecular basis and practical applicability of the biosorption process. Appl. Microbiol. Biotechnol. 2011 924 92, 697–708. https://doi.org/10.1007/S00253-011-3601-Z

De Rosa, M., Gambacorta, A., Huber, R., Lanzotti, V., Nicolaus, B., Stetter, K.O., Trincone, A., 1988. A new 15,16-dimethyl-30-glyceryloxytriacontanoic acid from lipids of Thermotoga maritima. J. Chem. Soc. Chem. Commun. 1300–1301. https://doi.org/10.1039/C39880001300

Dean, A.P., Hartley, A., McIntosh, O.A., Smith, A., Feord, H.K., Holmberg, N.H., King, T., Yardley, E., White, K.N., Pittman, J.K., 2019. Metabolic adaptation of a Chlamydomonas acidophila strain isolated from acid mine drainage ponds with low eukaryotic diversity. Sci. Total Environ. 647, 75–87. https://doi.org/10.1016/j.scitotenv.2018.07.445

Dean, A.P., Lynch, S., Rowland, P., Toft, B.D., Pittman, J.K., White, K.N., 2013. Natural wetlands are efficient at providing long-term metal remediation of freshwater systems polluted by acid mine drainage. Environ. Sci. Technol. 47, 12029–12036. https://doi.org/10.1021/es4025904

Devasagayam, T.P.A., Tilak, J., Boloor, K.K., Sane, K.S., Ghaskadbi, S.S., Lele, R.D., 2004. Free radicals and antioxidants in human health: current status and future prospects. J Assoc Physicians India 52, 794–804. https://doi.org/10.1016/S0300-483X(03)00149-5

Driver, T., Trivedi, D.K., McIntosh, O.A., Dean, A.P., Goodacre, R., Pittman, J.K., 2017. Two glycerol-3-phosphate dehydrogenases from Chlamydomonas have distinct roles in lipid metabolism. Plant Physiol. 174, 2083–2097. https://doi.org/10.1104/pp.17.00491

Duczmal-Czernikiewicz, A., Baibatsha, A., Bekbotayeva, A., Omarova, G., Baisalova, A., 2021. Ore Minerals and Metal Distribution in Tailings of Sediment-Hosted Stratiform Copper Deposits from Poland and Kazakhstan. Miner. 2021, Vol. 11, Page 752 11, 752. https://doi.org/10.3390/MIN11070752

Dudley Page, M., Allen, M.D., Kropat, J., Urzica, E.I., Karpowicz, S.J., Hsieh, S.I., Loo, J.A., Merchant, S.S., 2012. Fe sparing and Fe recycling contribute to increased superoxide dismutase capacity in iron-starved Chlamydomonas reinhardtii. Plant Cell 24, 2649–2665. https://doi.org/10.1105/tpc.112.098962

Edwards, K.J., Bond, P.L., Gihring, T.M., Banfield, J.F., 2000. An Archaeal iron-oxidizing extreme acidophile important in acid mine drainage. Science (80-.). 287, 1796–1799. https://doi.org/10.1126/science.287.5459.1796

Einicker-Lamas, M., Antunes Mezian, G., Benevides Fernandes, T., Silva, F.L.S., Guerra, F., Miranda, K., Attias, M., Oliveira, M.M., 2002. Euglena gracilis as a model for the study of Cu2+ and Zn2+ toxicity and accumulation in eukaryotic cells. Environ. Pollut. 120, 779–786. https://doi.org/10.1016/S0269-7491(02)00170-7

El-Ansari, O., Colman, B., 2015. Inorganic carbon acquisition in the acid-tolerant alga Chlorella

kessleri. Physiol. Plant. 153, 175–182. https://doi.org/10.1111/ppl.12228

Enami, I., Akutsu, H., Kyogoku, Y., 1986. Intracellular ph regulation in an acidophilic unicellular alga cyanidium-caldarium phosphorus-31 nmr determination of intracellular ph. Plant Cell Physiol 27, 1351–1360. https://doi.org/10.1093/OXFORDJOURNALS.PCP.A077233

Fabisch, M., Beulig, F., Akob, D.M., Küsel, K., 2013. Surprising abundance of Gallionella-related iron oxidizers in creek sediments at pH 4.4 or at high heavy metal concentrations. Front. Microbiol. 4, 390. https://doi.org/10.3389/fmicb.2013.00390

Fahey, R.C., Brown, W.C., Adams, W.B., Worsham, M.B., 1978. Occurrence of glutathione in bacteria. J. Bacteriol. 133, 1126–1129. https://doi.org/10.1128/jb.133.3.1126-1129.1978

Feller, G., 2010. Protein stability and enzyme activity at extreme biological temperatures. J. Phys. Condens. Matter. 22, 323101.https://doi.org/10.1088/0953-8984/22/32/323101

Gamburg, K.Z., Korotaeva, N.E., Baduev, B.K., Borovsky, G.B., Voinikov, V.K., 2014. The relationship between the differences in frost resistance of Arabidopsis and Thellungiella and heat shock proteins and dehydrins. Russ. J. Plant Physiol. 61, 318–323. https://doi.org/10.1134/S1021443714030054

García-García, J.D., Girard, L., Hernández, G., Saavedra, E., Pardo, J.P., Rodríguez-Zavala, J.S., Encalada, R., Reyes-Prieto, A., Mendoza-Cózatl, D.G., Moreno-Sánchez, R., 2014. Zn-bis-glutathionate is the best co-substrate of the monomeric phytochelatin synthase from the photosynthetic heavy metal-hyperaccumulator Euglena gracilis. Metallomics 6, 604–16. https://doi.org/10.1039/c3mt00313b

García-Meza, J.V., Barrangue, C., Admiraal, W., 2005. Biofilm formation by algae as a mechanism for surviving on mine tailings. Environ. Toxicol. Chem. 24, 573–581. https://doi.org/10.1897/04-064R.1

Gechev, T.S., Van Breusegem, F., Stone, J.M., Denev, I., Laloi, C., 2006. Reactive oxygen species as signals that modulate plant stress responses and programmed cell death. BioEssays 28, 1091–1101. https://doi.org/10.1002/bies.20493

Gerbino, E., Mobili, P., Tymczyszyn, E., Fausto, R., Gómez-Zavaglia, A., 2011. FTIR spectroscopy structural analysis of the interaction between Lactobacillus kefir S-layers and metal ions. J. Mol. Struct. 987, 186–192. https://doi.org/10.1016/j.molstruc.2010.12.012

Gerloff-Elias, A., Spijkerman, E., Pröschold, T., 2005. Effect of external pH on the growth, photosynthesis and photosynthetic electron transport of Chlamydomonas acidophila Negoro, isolated from an extremely acidic lake (pH 2.6). Plant, Cell Environ. 28, 1218–1229. https://doi.org/10.1111/j.1365-3040.2005.01357.

Gimmler, H., 2001. Acidophilic and Acidotolerant Algae, in: Algal Adaptation to Environmental Stresses. Springer, Berlin, Heidelberg, pp. 259–290. https://doi.org/10.1007/978-3-642-59491-5_9

Gimmler, H., Kugel, H., Leibfritz, D., Mayer, A., 1988. Cytoplasmic pH of *Dunaliella parva* and Dunaliella acidophila as monitored by in vivo P-NMR spectroscopy and the DMO method. Physiol. Plant. 74, 521–530. https://doi.org/10.1111/j.1399-3054.1988.tb02013.x

Gimmler, H., Schieder, M., Kowalski, M., Zimmermann, U., Pick, U., 1991. Dunaliella acidophila: an algae with a positive zeta potential at its optimal pH for growth. Plant. Cell Environ. 14, 261–269. https://doi.org/10.1111/j.1365-3040.1991.tb01500.x

Gimmler, H., Weis, U., Weiss, C., Kugel, H., Treffny, B., 1989. Dunaliella acidophila (Kalina) Masyuk an alga with a positive membrane potential. New Phytol. 113, 175–184. https://doi.org/10.1111/j.1469-8137.1989.tb04704.x

Giotta, L., Mastrogiacomo, D., Italiano, F., Milano, F., Agostiano, A., Nagy, K., Valli, L., Trotta, M., 2011. Reversible binding of metal ions onto bacterial layers revealed by protonation-induced ATR-FTIR difference spectroscopy. Langmuir 27, 3762–3773. https://doi.org/10.1021/la104868m

Goodarzi, H., Torabi, N., Najafabadi, H.S., Archetti, M., 2008. Amino acid and codon usage profiles:

Adaptive changes in the frequency of amino acids and codons. Gene 407, 30–41. https://doi.org/10.1016/j.gene.2007.09.020

Grill, E., Löffler, S., Winnacker, E.L., Zenk, M.H., 1989. Phytochelatins, the heavy-metal-binding peptides of plants, are synthesized from glutathione by a specific gamma-glutamylcysteine dipeptidyl transpeptidase (phytochelatin synthase). Proc. Natl. Acad. Sci. U. S. A. 86, 6838–6842. https://doi.org/10.1073/pnas.86.18.6838

Grill, E., Winnacker, E.L., Zenk, M.H., 1985. Phytochelatins : The Principal Heavy-Metal Complexing Peptides of Higher Plants Author (s): Erwin Grill , Ernst-L . Winnacker and Meinhart H . Zenk Published by : American Association for the Advancement of Science Stable URL : http://www.jstor.org/stab. Science (80-.). 230, 674–676.

Gross, W., 2000. Ecophysiology of algae living in highly acidic environments. Hydrobiologia 433, 31–37. https://doi.org/10.1023/A:1004054317446

Grotz, N., Fox, T., Connolly, E., Park, W., Guerinot, M. Lou, Eide, D., 1998. Identification of a family of zinc transporter genes from Arabidopsis that respond to zinc deficiency. Proc. Natl. Acad. Sci. U. S. A. 95, 7220–7224. https://doi.org/10.1073/pnas.95.12.7220

Guerinot, M. Lou, 2000. The ZIP family of metal transporters. Biochim. Biophys. Acta - Biomembr. 1465, 190-198. https://doi.org/10.1016/S0005-2736(00)00138-3

Gupta, P., Diwan, B., 2017. Bacterial Exopolysaccharide mediated heavy metal removal: A Review on biosynthesis, mechanism and remediation strategies. Biotechnol. Reports. https://doi.org/10.1016/j.btre.2016.12.006

Gupta, N., Ram, H., Kumar, B., 2016. Mechanism of Zinc absorption in plants: uptake, transport, translocation and accumulation. Rev. Environ. Sci. Biotechnol. 15, 89-109 https://doi.org/10.1007/s11157-016-9390-1

Gupton-Campolongo, T., Damasceno, L.M., Hay, A.G., Ahner, B.A., 2013. Characterization of a High Affinity Phytochelatin Synthase From The Cd-Utilizing Marine Diatom Thalassiosira pseudonana. J. Phycol. 49, 32–40. https://doi.org/10.1111/jpy.12022

Gurvitz, A., Lai, L.Y., Neilan, B.A., 1994. Exploiting biological materials in forensic science. Australas. Biotechnol. 4, 88-91.

Halliwell, B., 2006. Reactive species and antioxidants. Redox biology is a fundamental theme of aerobic life. Plant Physiol. 141, 312–322. https://doi.org/10.1104/pp.106.077073

Hanikenne, M., Krämer, U., Demoulin, V., Baurain, D., 2005. A comparative inventory of metal transporters in the green alga Chlamydomonas reinhardtii and the red alga Cyanidioschizon merolae. Plant Physiol. 137, 428–446. https://doi.org/10.1104/pp.104.054189

Harshavardhan, V.T., Wu, T.M., Hong, C.Y., 2017. Glutathione reductase and abiotic stress tolerance in plants, in: Glutathione in Plant Growth, Development, and Stress Tolerance. Springer International Publishing, pp. 265–286. https://doi.org/10.1007/978-3-319-66682-2_12

Hassett, R., Dix, D.R., Eide, D.J., Kosman, D.J., 2000. The Fe(II) permease Fet4p functions as a low affinity copper transporter and supports normal copper trafficking in Saccharomyces cerevisiae. Biochem. J. 351, 477–484. https://doi.org/10.1042/0264-6021:3510477

Hastrup, A.C.S., Jensen, B., Jellison, J., 2014. Fungal accumulation of metals from building materials during brown rot wood decay. Arch. Microbiol. 196, 565–574. https://doi.org/10.1007/s00203-014-0993-z

Heiss, S., Wachter, A., Bogs, J., Cobbett, C., Rausch, T., 2003. Phytochelatin synthase (PCS) protein is induced in Brassica juncea leaves after prolonged Cd exposure. J. Exp. Bot. 54, 1833–1839. https://doi.org/10.1093/jxb/erg205

Henderson, B., Allan, E., Coates, A.R.M., 2006. Stress wars: The direct role of host and bacterial molecular chaperones in bacterial infection. Infect. Immun. 74, 3693- 3706. https://doi.org/10.1128/IAI.01882-05

Hugenholtz, P., Pitulle, C., Hershberger, K.L., Pace, N.R., 1998. Novel division level bacterial

diversity in a Yellowstone hot spring. J. Bacteriol. 180, 366–376.

Ibuot, A., Dean, A.P., McIntosh, O.A., Pittman, J.K., 2017. Metal bioremediation by CrMTP4 over-expressing Chlamydomonas reinhardtii in comparison to natural wastewater-tolerant microalgae strains. Algal Res. 24, 89–96. https://doi.org/10.1016/j.algal.2017.03.002

Ibuot, A., Dean, A.P., Pittman, J.K., 2020. Multi-genomic analysis of the cation diffusion facilitator transporters from algae †. Metallomics 12, 617. https://doi.org/10.1039/d0mt00009d

Jegerschold, C., Arellano, J.B., Schroder, W.P., van Kan, P.J.M., Barón, M., Styring, S., 1995. Copper(II) Inhibition of Electron Transfer through Photosystem II Studied by EPR Spectroscopy. Biochemistry 34, 12747–12754. https://doi.org/10.1021/bi00039a034

Jiang, X., Wang, C., 2008. Zinc distribution and zinc-binding forms in Phragmites australis under zinc pollution. J. Plant Physiol. 165, 697–704. https://doi.org/10.1016/j.jplph.2007.05.011

Jiang, Y., Zhu, Y., Hu, Z., Lei, A., Wang, J., 2016. Towards elucidation of the toxic mechanism of copper on the model green alga Chlamydomonas reinhardtii. Ecotoxicology 25, 1417–1425. https://doi.org/10.1007/s10646-016-1692-0

Johnson, D.B., Hallberg, K.B., 2008. Carbon, Iron and Sulfur Metabolism in Acidophilic Micro-Organisms. Adv. Microb. Physiol. 54, 201-255 https://doi.org/10.1016/S0065-2911(08)00003-9

Jomova, K., Baros, S., Valko, M., 2012. Redox active metal-induced oxidative stress in biological systems. Transit. Met. Chem. 37, 127–134. https://doi.org/10.1007/s11243-012-9583-6

Jozefczak, M., Remans, T., Vangronsveld, J., Cuypers, A., 2012. Glutathione is a key player in metal-induced oxidative stress defenses. Int. J. Mol. Sci. 3, 3145- 3175. https://doi.org/10.3390/ijms13033145

Kalita, D., Joshi, S.R., 2017. Study on bioremediation of Lead by exopolysaccharide producing metallophilic bacterium isolated from extreme habitat. Biotechnol. Reports 16, 48–57. https://doi.org/10.1016/j.btre.2017.11.003

Kaplan, D., 2013. Absorption and Adsorption of Heavy Metals by Microalgae, in: Handbook of Microalgal Culture: Applied Phycology and Biotechnology: Second Edition. pp. 602–611. https://doi.org/10.1002/9781118567166.ch32

Karshikoff, A., Ladenstein, R., 2001. Ion pairs and the thermotolerance of proteins from hyperthermophiles: A “traffic rule” for hot roads. Trends Biochem. Sci. 9, 550-557. https://doi.org/10.1016/S0968-0004(01)01918-1

Kehrer, J.P., 2000. The Haber–Weiss reaction and mechanisms of toxicity. Toxicology 149, 43–50. https://doi.org/10.1016/S0300-483X(00)00231-6

Khatiwada, B., Hasan, M.T., Sun, A., Kamath, K.S., Mirzaei, M., Sunna, A., Nevalainen, H., 2020. Proteomic response of Euglena gracilis to heavy metal exposure – Identification of key proteins involved in heavy metal tolerance and accumulation. Algal Res. 45, 101764. https://doi.org/10.1016/j.algal.2019.101764

Kim, J., Ahn, M.S., Park, Y.M., Kim, S.W., Min, S.R., Jeong, W.J., Liu, J.R., 2014. Synechocystis PCC6803 and PCC6906 dnaK2 expression confers salt and oxidative stress tolerance in Arabidopsis via reduction of hydrogen peroxide accumulation. Mol. Biol. Rep. 41, 1091–1101. https://doi.org/10.1007/s11033-013-2955-y

Kobayashi, M., Kakizono, T., Nagai, S., 1991. Astaxanthin production by a green alga, Haematococcus pluvialis accompanied with morphological changes in acetate media. J. Ferment. Bioeng. 71, 335–339. https://doi.org/10.1016/0922-338X(91)90346-I

Koga, Y., 2012. Thermal adaptation of the archaeal and bacterial lipid membranes. Archaea. 2012, 789652. https://doi.org/10.1155/2012/789652

Koren’kov, V., Park, S., Cheng, N.H., Sreevidya, C., Lachmansingh, J., Morris, J., Hirschi, K., Wagner, G.J., 2007. Enhanced Cd2+-selective root-tonoplast-transport in tobaccos expressing Arabidopsis cation exchangers. Planta 225, 403–411. https://doi.org/10.1007/s00425-006-

0352-7

Koyama, Y., 1991. New trends in photobiology. Structures and functions of carotenoids in photosynthetic systems. J. Photochem. Photobiol. B Biol. 9, 265–280. https://doi.org/10.1016/1011-1344(91)80165-E

Krämer, U., Talke, I.N., Hanikenne, M., 2007. Transition metal transport. FEBS Lett. 581, 2263–2272. https://doi.org/10.1016/j.febslet.2007.04.010

Küpper, H., Šetlík, I., Spiller, M., Küpper, F.C., Prášil, O., 2002. Heavy metal-induced inhibition of photosynthesis: Targets of in vivo heavy metal chlorophyll formation. J. Phycol. 38, 429–441. https://doi.org/10.1046/j.1529-8817.2002.t01-1-01148.x

La Fontaine, S., Quinn, J.M., Nakamoto, S.S., Dudley Page, M., Göhre, V., Moseley, J.L., Kropat, J., Merchant, S., 2002. Copper-dependent iron assimilation pathway in the model photosynthetic eukaryote Chlamydomonas reinhardtii. Eukaryot. Cell 1, 736–757. https://doi.org/10.1128/EC.1.5.736-757.2002

Lane, A.E., Burris, J.E., 1981. Effects of Environmental pH on the Internal pH of Chlorella pyrenoidosa, Scenedesmus quadricauda, and Euglena mutabilis. Plant Physiol. 68, 439–442. https://doi.org/10.1104/pp.68.2.439

Lanquar, V., Lelièvre, F., Bolte, S., Hamès, C., Alcon, C., Neumann, D., Vansuyt, G., Curie, C., Schröder, A., Krämer, U., Barbier-Brygoo, H., Thomine, S., 2005. Mobilization of vacuolar iron by AtNRAMP3 and AtNRAMP4 is essential for seed germination on low iron. EMBO J. 24, 4041–4051. https://doi.org/10.1038/sj.emboj.7600864

Lanquar, V., Ramos, M.S., Lelièvre, F., Barbier-Brygoo, H., Krieger-Liszkay, A., Krämer, U., Thomine, S., 2010. Export of vacuolar manganese by AtNRAMP3 and AtNRAMP4 is required for optimal photosynthesis and growth under manganese deficiency. Plant Physiol. 152, 1986–99. https://doi.org/10.1104/pp.109.150946

Lee, S., Korban, S.S., 2002. Transcriptional regulation of Arabidopsis thaliana phytochelatin synthase (AtPCS1) by cadmium during early stages of plant development. Planta 215, 689–693. https://doi.org/10.1007/s00425-002-0821-6

Li, X., Zhang, X., Zhao, Y., Yu, X., 2020. Cross-talk between gama-aminobutyric acid and calcium ion regulates lipid biosynthesis in Monoraphidium sp. QLY-1 in response to combined treatment of fulvic acid and salinity stress. Bioresour. Technol. 315, 123833. https://doi.org/10.1016/j.biortech.2020.123833

Li, Y., Dhankher, O.., Carreira, L., Lee, D., Chen, A., Schroeder, J.I., Balish, R.S., Meagher, R.B., 2004. Overexpression of Phytochelatin Synthase in Arabidopsis Leads to Enhanced Arsenic Tolerance and Cadmium Hypersensitivity. Plant Cell Physiol. 45, 1787–1797. https://doi.org/10.1093/pcp/pch202

Li, Y., Iqbal, M., Zhang, Q., Spelt, C., Bliek, M., Hakvoort, H.W.J., Quattrocchio, F.M., Koes, R., Schat, H., 2017. Two *Silene vulgaris* copper transporters residing in different cellular compartments confer copper hypertolerance by distinct mechanisms when expressed in *Arabidopsis thaliana*. New Phytol. 215, 1102–1114. https://doi.org/10.1111/nph.14647

Liu, X.S., Feng, S.J., Zhang, B.Q., Wang, M.Q., Cao, H.W., Rono, J.K., Chen, X., Yang, Z.M., 2019. OsZIP1 functions as a metal efflux transporter limiting excess zinc, copper and cadmium accumulation in rice. BMC Plant Biol. 19, 283. https://doi.org/10.1186/s12870-019-1899-3

López-Archilla, A.I., Marin, I., Amils, R., 2001. Microbial community composition and ecology of an acidic aquatic environment: The Tinto River, Spain. Microb. Ecol. 41, 20–35. https://doi.org/10.1007/s002480000044

Lopez, E., Dominguez, B., Deive, F.J., Sanroman, M.A., Longo, M.A., 2012. Scaling-up the production of thermostable lipolytic enzymes from Thermus aquaticus YT1. Bioprocess Biosyst. Eng. 35, 1011–1022. https://doi.org/10.1007/s00449-012-0686-4

Lozano-Rodríguez, E., Hernández, L.E., Bonay, P., Carpena-Ruiz, R.O., 1997. Distribution of cadmium in shoot and root tissues of maize and pea plants: Physiological disturbances. J. Exp. Bot. 48, 123–128. https://doi.org/10.1093/jxb/48.1.123

Mallick, N., Mohn, F.H., 2000. Reactive oxygen species: response of algal cells. J. Plant Physiol. 157, 183–193. https://doi.org/10.1016/S0176-1617(00)80189-3

Mandelli, F., Miranda, V.S., Rodrigues, E., Mercadante, A.Z., 2012. Identification of carotenoids with high antioxidant capacity produced by extremophile microorganisms. World J. Microbiol. Biotechnol. 28, 1781–1790. https://doi.org/10.1007/s11274-011-0993-y

Markillie, L.M., Varnum, S.M., Hradecky, P., Wong, K.K., 1999. Targeted mutagenesis by duplication insertion in the radioresistant bacterium Deinococcus radiodurans: Radiation sensitivities of catalase (katA) and superoxide dismutase (sodA) mutants. J. Bacteriol. 181, 666–669. https://doi.org/10.1128/jb.181.2.666-669.1999

Martin, A.J., Goldblatt, R., 2007. Speciation, behavior, and bioavailability of copper downstream of a mine-impacted lake. Environ. Toxicol. Chem. 26, 2594–2603. https://doi.org/10.1897/07-038.1

Martínez-Macias, M. del R., Correa-Murrieta, M.A., Villegas-Peralta, Y., Dévora-Isiordia, G.E., Álvarez-Sánchez, J., Saldivar-Cabrales, J., Sánchez-Duarte, R.G., 2019. Uptake of copper from acid mine drainage by the microalgae Nannochloropsis oculata. Environ. Sci. Pollut. Res. 26, 6311–6318. https://doi.org/10.1007/s11356-018-3963-1

Mata, T.M., Martins, A.A., Caetano, N.S., 2010. Microalgae for biodiesel production and other applications: A review. Renew. Sustain. Energy Rev. 14, 317-232. https://doi.org/10.1016/j.rser.2009.07.020

May, M.J., Vernoux, T., Leaver, C., Montagu, M. Van, Inze, D., 1998. Glutathione homeostasis in plants : implications for environmental sensing and plant development. J. Exp. Bot. 49, 649–667. https://doi.org/10.1093/jxb/49.321.649

Mayes, W.M., Potter, H.A.B., Jarvis, A.P., 2010. Inventory of aquatic contaminant flux arising from historical metal mining in England and Wales. Sci. Total Environ. 408, 3576–3583. https://doi.org/10.1016/j.scitotenv.2010.04.021

McSwain, B.., Irvine, R.., Hausner, M., Wilderer, P.A., 2005. Composition and Distribution of Extracellular Polymeric Substances in Aerobic Flocs and Granular Sludge. Appl. Environ. Microbiol. 71, 1051–1057. https://doi.org/10.1128/AEM.71.2.1051

MeGraw, V.E., Brown, A.R., Boothman, C., Goodacre, R., Morris, K., Sigee, D., Anderson, L., Lloyd, J.R., 2018. A novel adaptation mechanism underpinning algal colonization of a nuclear fuel storage pond. MBio 9. https://doi.org/10.1128/mBio.02395-17

Mehta, R., Templeton, D.M., O'Brien, P.J., 2006. Mitochondrial involvement in genetically determined transition metal toxicity. II. Copper toxicity. Chem. Biol. Interact. 163, 77–85. https://doi.org/10.1016/j.cbi.2006.05.011

Méndez-García, C., Peláez, A.I., Mesa, V., Sánchez, J., Golyshina, O. V., Ferrer, M., 2015. Microbial diversity and metabolic networks in acid mine drainage habitats. Front. Microbiol. 6, 1–17. https://doi.org/10.3389/fmicb.2015.00475

Mendoza-Cózatl, D.G., Rodríguez-Zavala, J.S., Rodríguez-Enríquez, S., Mendoza-Hernandez, G., Briones-Gallardo, R., Moreno-Sánchez, R., 2006. Phytochelatin-cadmium-sulfide high-molecular-mass complexes of Euglena gracilis. FEBS J. 273, 5703–5713. https://doi.org/10.1111/j.1742-4658.2006.05558.x

Merchant, S.S., Allen, M.D., Kropat, J., Moseley, J.L., Long, J.C., Tottey, S., Terauchi, A.M., 2006. Between a rock and a hard place: Trace element nutrition in Chlamydomonas. Biochim. Biophys. Acta - Mol. Cell Res. 1763, 578-594. https://doi.org/10.1016/j.bbamcr.2006.04.007

Messerli, M.A., Amaral-Zettler, L.A., Zettler, E., Jung, S.-K., Smith, P.J.S., Sogin, M.L., 2005. Life at acidic pH imposes an increased energetic cost for a eukaryotic acidophile. J. Exp. Biol. 208, 2569–79. https://doi.org/10.1242/jeb.01660

Mittova, V., Theodoulou, F.L., Kiddle, G., Gómez, L., Volokita, M., Tal, M., Foyer, C.H., Guy, M., 2003. Coordinate induction of glutathione biosynthesis and glutathione-metabolizing enzymes is correlated with salt tolerance in tomato. FEBS Lett. 554, 417–421. https://doi.org/10.1016/S0014-5793(03)01214-6

Moenne, A., González, A., Sáez, C.A., 2016. Mechanisms of metal tolerance in marine macroalgae, with emphasis on copper tolerance in Chlorophyta and Rhodophyta. Aquat. Toxicol. 176, 30-37. https://doi.org/10.1016/j.aquatox.2016.04.015

Newton, G.L., Javor, B., 1985. γ-Glutamylcysteine and thiosulfate are the major low-molecular-weight thiols in halobacteria. J. Bacteriol. 161, 438–441. https://doi.org/10.1128/jb.161.1.438-441.1985

Nishikawa, K., Onodera, A., Tominaga, N., 2006. Phytochelatins do not correlate with the level of Cd accumulation in Chlamydomonas spp. Chemosphere 63, 1553–1559. https://doi.org/10.1016/j.chemosphere.2005.09.056

Nixon, S.L., Daly, R.A., Borton, M.A., Solden, L.M., Welch, S.A., Cole, D.R., Mouser, P.J., Wilkins, M.J., Wrighton, K.C., 2019. Genome-Resolved Metagenomics Extends the Environmental Distribution of the Verrucomicrobia Phylum to the Deep Terrestrial Subsurface. mSphere 4. https://doi.org/10.1128/mSphere.00613-19

Nordstrom, D.K., 2000. Advances in the Hydrogeochemistry and Microbiology of Acid Mine Waters. Int. Geol. Rev. 42, 499–515. https://doi.org/10.1080/00206810009465095

Olaveson, M.M., Nalewajko, C., 2000. Effects of acidity on the growth of two Euglena species. Hydrobiologia 433, 39–56. https://doi.org/10.1023/A:1004006401516

Oren, A., 2010. Industrial and environmental applications of halophilic microorganisms. Environ. Technol. 31, 825-834. https://doi.org/10.1080/09593330903370026

Page, M.D., Kropat, J., Hamel, P.P., Merchant, S.S., 2009. Two Chlamydomonas CTR copper transporters with a novel cys-met motif are localized to the plasma membrane and function in copper assimilation. Plant Cell 21, 928–943. https://doi.org/10.1105/tpc.108.064907

Park, C.J., Seo, Y.S., 2015. Heat shock proteins: A review of the molecular chaperones for plant immunity. Plant Pathol. J. 31, 323-333. https://doi.org/10.5423/PPJ.RW.08.2015.0150

Parker, D.L., Sposito, G., Tebo, B.M., 2004. Manganese(III) binding to a pyoverdine siderophore produced by a manganese(II)-oxidizing bacterium. Geochim. Cosmochim. Acta 68, 4809–4820. https://doi.org/10.1016/j.gca.2004.05.038

Pätsikkä, E., Kairavuo, M., Šeršen, F., Aro, E.M., Tyystjärvi, E., 2002. Excess copper predisposes photosystem II to photoinhibition in vivo by outcompeting iron and causing decrease in leaf chlorophyll. Plant Physiol. 129, 1359–1367. https://doi.org/10.1104/pp.004788

Paulsen, I.T., Saier Jr., M.H., 1997. A novel family of ubiquitous heavy metal ion transport proteins. J Membr Biol 156, 99–103.

Pedersen, C.N.S., Axelsen, K.B., Harper, J.F., Palmgren, M.G., 2012. Evolution of plant P-type ATPases. Front. Plant Sci. 3, 31. https://doi.org/10.3389/fpls.2012.00031

Perales-Vela, H.V., Peña-Castro, J.M., Cañizares-Villanueva, R.O., 2006. Heavy metal detoxification in eukaryotic microalgae. Chemosphere. 64, 1-10. https://doi.org/10.1016/j.chemosphere.2005.11.024

Pérez-Rama, M., Herrero López, C., Abalde Alonso, J., Torres Vaamonde, E., 2001. Class III metallothioneins in response to cadmium toxicity in the marine microalga Tetraselmis suecica (Kylin) Butch. Environ. Toxicol. Chem. 20, 2061–6.

Persans, M.W., Nieman, K., Salt, D.E., 2001. Functional Activity and Role of Cation-Efflux Family Members in Ni Hyperaccumulation Linked references are available on JSTOR for this article : Functional activity and role c f cation-efflux family members in Ni hyperaccumul ation in Thlaspi goesingense. Proc. Natl. Acad. Sci. U. S. A. 98, 9995–10000.

Pilon, M., Abdel-Ghany, S.E., Cohu, C.M., Gogolin, K.A., Ye, H., 2006. Copper cofactor delivery in plant cells. Curr. Opin. Plant Biol. 9, 256- 263. https://doi.org/10.1016/j.pbi.2006.03.007

Pittman, J.K., Hirschi, K.D., 2016. CAX-ing a wide net: Cation/H $^{+}$ transporters in metal remediation and abiotic stress signalling. Plant Biol. 18, 741–749. https://doi.org/10.1111/plb.12460

Printz, B., Lutts, S., Hausman, J.F., Sergeant, K., 2016. Copper trafficking in plants and its implication on cell wall dynamics. Front. Plant Sci. 7, 601. https://doi.org/10.3389/fpls.2016.00601

Puente-Sánchez, F., Díaz, S., Penacho, V., Aguilera, A., Olsson, S., 2018. Basis of genetic adaptation to heavy metal stress in the acidophilic green alga Chlamydomonas acidophila. Aquat. Toxicol. 200, 62–72. https://doi.org/10.1016/j.aquatox.2018.04.020

Raddadi, N., Cherif, A., Daffonchio, D., Neifar, M., Fava, F., 2015. Biotechnological applications of extremophiles, extremozymes and extremolytes. Appl. Microbiol. Biotechnol. 99, 7907-7913. https://doi.org/10.1007/s00253-015-6874-9

Rauser, W.E., 1990. Phytochelatins. Annu. Rev. Biochem. 59, 61–86.

Rea, P.A., Li, Z.-S., Lu, Y.-P., Drozdowicz, Y.M., Martinoia, E., 1998. From Vacuolar Gs-X Pumps To Multispecific ABC Transporters. Annu. Rev. Plant Physiol. Plant Mol. Biol. 49, 727–760. https://doi.org/10.1146/annurev.arplant.49.1.727

Rea, P.A., Vatamaniuk, O.K., Rigden, D.J., 2004. Weeds, worms, and more: papain's long-lost cousin. Plant Physiol. 136, 2463–2474. https://doi.org/10.1104/pp.104.048579.LONG-CHAIN

Rhimi, M., Bajic, G., Ilhammami, R., Boudebbouze, S., Maguin, E., Haser, R., Aghajari, N., 2011. The acid-tolerant L-arabinose isomerase from the mesophilic Shewanella sp. ANA-3 is highly active at low temperatures. Microb. Cell Fact. 10, 1–11. https://doi.org/10.1186/1475-2859-10-96

Ritter, A., Dittami, S.M., Goulitquer, S., Correa, J.A., Boyen, C., Potin, P., Tonon, T., 2014. Transcriptomic and metabolomic analysis of copper stress acclimation in Ectocarpus siliculosus highlights signaling and tolerance mechanisms in brown algae. BMC Plant Biol. 14, 116.https://doi.org/10.1016/j.cub.2011.05.006

Rocchetta, I., Küpper, H., 2009. Chromium- and copper-induced inhibition of photosynthesis in *Euglena gracilis* analysed on the single-cell level by fluorescence kinetic microscopy. New Phytol. 182, 405–420. https://doi.org/10.1111/j.1469-8137.2009.02768.x

Rodionova, M. V., Zharmukhamedov, S.K., Karacan, M.S., Venedik, K.B., Shitov, A. V., Tunç, T., Mamaş, S., Kreslavski, V.D., Karacan, N., Klimov, V. V., Allakhverdiev, S.I., 2017. Evaluation of new Cu(II) complexes as a novel class of inhibitors against plant carbonic anhydrase, glutathione reductase, and photosynthetic activity in photosystem II. Photosynth. Res. 133, 139–153. https://doi.org/10.1007/s11120-017-0392-9

Rosakis, A., Köster, W., 2005. Divalent metal transport in the green microalga Chlamydomonas reinhardtii is mediated by a protein similar to prokaryotic Nramp homologues. BioMetals 18, 107–120. https://doi.org/10.1007/s10534-004-2481-4

Rubino, J.T., Chenkin, M.P., Keller, M., Riggs-Gelasco, P., Franz, K.J., 2011. A comparison of methionine, histidine and cysteine in copper(i)-binding peptides reveals differences relevant to copper uptake by organisms in diverse environments. Metallomics 3, 61–73. https://doi.org/10.1039/c0mt00044b

Ruiz-Domínguez, M.C., Vaquero, I., Obregón, V., de la Morena, B., Vílchez, C., Vega, J.M., 2015. Lipid accumulation and antioxidant activity in the eukaryotic acidophilic microalga Coccomyxa sp. (strain onubensis) under nutrient starvation. J. Appl. Phycol. 27, 1099–1108. https://doi.org/10.1007/s10811-014-0403-6

Runnells, D.D., Shepherd, T.A., Angino, E.E., 1992. Metals in Water. Determining Natural Background Concentrations in Mineralized Areas. Environ. Sci. Technol. 26, 2316–2323. https://doi.org/10.1021/es00036a001

Sancenón, V., Puig, S., Mira, H., Thiele, D.J., Peñarrubia, L., 2003. Identification of a copper transporter family in Arabidopsis thaliana. Plant Mol. Biol. 51, 577–587. https://doi.org/10.1023/A:1022345507112

Sánchez-Andrea, I., Rodríguez, N., Amils, R., Sanz, J.L., 2011. Microbial diversity in anaerobic sediments at Río Tinto, a naturally acidic environment with a high heavy metal content. Appl. Environ. Microbiol. 77, 6085–6093. https://doi.org/10.1128/AEM.00654-11

Sánchez-Marín, P., Fortin, C., Campbell, P.G.C.C., 2014. Lead (Pb) and copper (Cu) share a common uptake transporter in the unicellular alga Chlamydomonas reinhardtii. BioMetals 27, 173–181. https://doi.org/10.1007/s10534-013-9699-y

Schmöger, M.E., Oven, M., Grill, E., 2000. Detoxification of arsenic by phytochelatins in plants. Plant Physiol. 122, 793–801. https://doi.org/10.1104/pp.122.3.793

Schroder, W.P., Arellano, J.B., Bittner, T., Baron, M., Eckert, H.J., Renger, G., 1994. Flash-induced absorption spectroscopy studies of copper interaction with photosystem II in higher plants. J. Biol. Chem. 269, 32865–32870. https://doi.org/10.1016/S0021-9258(20)30071-5

Shaish, A., Avron, M., Pick, U., Ben-Amotz, A., 1993. Are active oxygen species involved in induction of B-carotene in Dunaliella bardawil? Planta 190, 363–368. https://doi.org/10.1007/BF00196965

Sharma, K.K., Ahmed, F., Schenk, P.M., Li, Y., 2015. UV-C mediated rapid carotenoid induction and settling performance of Dunaliellasalina and Haematococcus pluvialis. Biotechnol. Bioeng. 112, 2106–2114. https://doi.org/10.1002/bit.25621

Solovchenko, A.E., Selivanova, E.A., Chekanov, K.A., Sidorov, R.A., Nemtseva, N. V., Lobakova, E.S., 2015. Induction of Secondary Carotenogenesis in New Halophile Microalgae from the Genus Dunaliella (Chlorophyceae). Biochemistry. (Mosc). 80, 1508–1513. https://doi.org/10.1134/S0006297915110139

Spijkerman, E., 2008. What physiological acclimation supports increased growth at high CO 2 conditions? Physiol. Plant. 133, 41–48. https://doi.org/10.1111/j.1399-3054.2008.01062.x

Spijkerman, E., 2005. Inorganic carbon acquisition by Chlamydomonas acidophila across a pH range. Can. J. Bot. 83, 872–878. https://doi.org/10.1139/b05-073

Spijkerman, E., Barua, D., Gerloff-Elias, A., Kern, J., Gaedke, U., Heckathorn, S.A., 2007. Stress responses and metal tolerance of Chlamydomonas acidophila in metal-enriched lake water and artificial medium. Extremophiles 11, 551–562. https://doi.org/10.1007/s00792-007-0067-0

Stauber, J.L., Florence, T.M., 1989. The effect of culture medium on metal toxicity to the marine diatom Nitzschia closterium and the freshwater green alga Chlorella pyrenoidosa. Water Res. 23, 907–911. https://doi.org/10.1016/0043-1354(89)90016-X

Stepien, C.C., Pfister, C.A., Wootton, J.T., 2016. Functional Traits for Carbon Access in Macrophytes. PLoS One 11, e0159062. https://doi.org/10.1371/journal.pone.0159062

Stetter, K.O., 1999. Extremophiles and their adaptation to hot environments. FEBS Lett. 452, 22-25. https://doi.org/10.1016/S0014-5793(99)00663-8

Suresh Kumar, K., Dahms, H.-U.U., Lee, J.-S.S., Kim, H.C., Lee, W.C., Shin, K.-H.H., 2014. Algal photosynthetic responses to toxic metals and herbicides assessed by chlorophyll a fluorescence. Ecotoxicol. Environ. Saf. 104, 51–71. https://doi.org/10.1016/j.ecoenv.2014.01.042

Tanaka, N., Nakamoto, H., 1999. HtpG is essential for the thermal stress management in cyanobacteria. FEBS Lett. 458, 117–123. https://doi.org/10.1016/S0014-5793(99)01134-5

Tatsuzawa, H., Takizawa, E., Wada, M., Yamamoto, Y., 1996. Fatty acid and lipid composition of the acidophilic green alga Chlamydomonas sp. J. Phycol. 32, 598–601. https://doi.org/10.1111/j.0022-3646.1996.00598.x

Tchounwou, P.B., Yedjou, C.G., Patlolla, A.K., Sutton, D.J., 2012. Heavy Metals Toxicity and the Environment, in: Molecular, Clinical and Environmental Toxicology. NIH Public Access, pp. 133–164. https://doi.org/10.1007/978-3-7643-8340-4_6

Thanh, V.N., Thuy, N.T., Huong, H.T.T., Hien, D.D., Hang, D.T.M., Anh, D.T.K., Hüttner, S., Larsbrink, J., Olsson, L., 2019. Surveying of acid-tolerant thermophilic lignocellulolytic fungi in Vietnam reveals surprisingly high genetic diversity. Sci. Rep. 9, 1–12. https://doi.org/10.1038/s41598-019-40213-5

Tian, S., Lu, L., Labavitch, J., Yang, X., He, Z., Hu, H., Sarangi, R., Newville, M., Commisso, J.,

Brown, P., 2011. Cellular sequestration of cadmium in the hyperaccumulator plant species Sedum alfredii. Plant Physiol. 157, 1914–1925. https://doi.org/10.1104/pp.111.183947

Uchida, A., Hibino, T., Shimada, T., Saigusa, M., Takabe, Tetsuko, Araki, E., Kajita, H., Takabe, Teruhiro, 2008. Overexpression of DnaK chaperone from a halotolerant cyanobacterium Aphanothece halophytica increases seed yield in rice and tobacco. Plant Biotechnol. 25, 141–150. https://doi.org/10.5511/plantbiotechnology.25.141

Urbano, S.B., Di Capua, C., Cortez, N., Farías, M.E., Alvarez, H.M., 2014. Triacylglycerol accumulation and oxidative stress in Rhodococcus species: Differential effects of pro-oxidants on lipid metabolism. Extremophiles 18, 375–384. https://doi.org/10.1007/s00792-013-0623-8

Valdés, J., Pedroso, I., Quatrini, R., Dodson, R.J., Tettelin, H., Blake, R., Eisen, J.A., Holmes, D.S., 2008. Acidithiobacillus ferrooxidans metabolism: From genome sequence to industrial applications. BMC Genomics 9, 1–24. https://doi.org/10.1186/1471-2164-9-597

Verma, V., Bhatti, S., Huss, V.A.R., Colman, B., 2009. Photosynthetic inorganic carbon acquisition in an acid-tolerant, free-living species of coccomyxa (Chlorophyta). J. Phycol. 45, 847–854. https://doi.org/10.1111/j.1529-8817.2009.00718.x

Vojvodić, S., Luković, J.D., Zechmann, B., Jevtović, M., Pristov, J.B., Stanić, M., Lizzul, A.M., Pittman, J.K., Spasojević, I., 2020a. The effects of ionizing radiation on the structure and antioxidative and metal-binding capacity of the cell wall of microalga Chlorella sorokiniana. Chemosphere 260, 127553. https://doi.org/10.1016/j.chemosphere.2020.127553

Vojvodić, S., Stanic, M., Zechmann, B., Ducic, T., Žižic, M., Dimitrijevic, M., Lukovic, J.D., Milenkovic, M.R., Pittman, J.K., Spasojevic, I., 2020b. Mechanisms of detoxification of high copper concentrations by the microalga Chlorella sorokiniana. Biochem. J. 477, 3729–3741. https://doi.org/10.1042/BCJ20200600

Wang, H., Ebenezer, V., Ki, J.S., 2018. Photosynthetic and biochemical responses of the freshwater green algae Closterium ehrenbergii Meneghini (Conjugatophyceae) exposed to the metal coppers and its implication for toxicity testing. J. Microbiol. 56, 426–434. https://doi.org/10.1007/s12275-018-8081-8

Wang, S., Teng, S., F, M., 2010. Interaction between Heavy Metals and Aerobic Granules. Environ. Manage. https://doi.org/10.5772/10106

Wang, T., Wu, M., 2006. An ATP-binding cassette transporter related to yeast vacuolar ScYCF1 is important for Cd sequestration in Chlamydomonas reinhardtii. Plant, Cell Environ. 29, 1901–1912. https://doi.org/10.1111/j.1365-3040.2006.01566.x

Wang, W., Vinocur, B., Shoseyov, O., Altman, A., 2004. Role of plant heat-shock proteins and molecular chaperones in the abiotic stress response. Trends Plant Sci. 9, 244-252. https://doi.org/10.1016/j.tplants.2004.03.006

Weronika, E., Łukasz, K., 2017. Tardigrades in Space Research - Past and Future. Orig. Life Evol. Biosph. 47, 545–553. https://doi.org/10.1007/s11084-016-9522-1

Wojas, S., Clemens, S., Hennig, J., Skłodowska, A., Kopera, E., Schat, H., Bal, W., Antosiewicz, D.M., 2008. Overexpression of phytochelatin synthase in tobacco: Distinctive effects of AtPCS1 and CePCS genes on plant response to cadmium. J. Exp. Bot. 59, 2205–2219. https://doi.org/10.1093/jxb/ern092

Wong, P.K., Chang, L., 1991. Effects of copper, chromium and nickel on growth, photosynthesis and chlorophyll a synthesis of Chlorella pyrenoidosa 251. Environ. Pollut. 72, 127–139. https://doi.org/10.1016/0269-7491(91)90063-3

Yamada, N., Theerawitaya, C., Cha-um, S., Kirdmanee, C., Takabe, T., 2014. Expression and functional analysis of putative vacuolar Ca2+-transporters (CAXs and ACAs) in roots of salt tolerant and sensitive rice cultivars. Protoplasma 251, 1067–1075. https://doi.org/10.1007/s00709-014-0615-2

Yoneyama, T., Ishikawa, S., Fujimaki, S., 2015. Route and regulation of zinc, cadmium, and iron transport in rice plants (Oryza sativa L.) during vegetative growth and grain filling: Metal transporters, metal speciation, grain Cd reduction and Zn and Fe biofortification. Int. J. Mol. Sci.

16, 19111- 19129. https://doi.org/10.3390/ijms160819111

Yruela, I., 2005. Copper in plants. Brazilian J. Plant Physiol. 17, 145-156. https://doi.org/10.1590/s1677-04202005000100012

Zeng, W., Li, F., Wu, C., Yu, R., Wu, X., Shen, L., Liu, Y., Qiu, G., Li, J., 2020. Role of extracellular polymeric substance (EPS) in toxicity response of soil bacteria Bacillus sp. S3 to multiple heavy metals. Bioprocess Biosyst. Eng. 43, 153–167. https://doi.org/10.1007/s00449-019-02213-7

Zettler, L.A.A., Gómez, F., Zettler, E., Keenan, B.G., Amils, R., Sogin, M.L., 2002. Eukaryotic diversity in Spain's River of Fire: This ancient and hostile ecosystem hosts a surprising variety of microbial organisms. Nature 417, 137. https://doi.org/10.1038/417137a

2 Biochemical and Physiological Responses of an Extremophile Microalga *Chlamydomonas acidophila* and the Model Organism *Chlamydomonas reinhardtii* in Response to Copper

2.1 Abstract

PM01 is an extremophile strain of the *Chlamydomonas acidophila* species that shows high tolerance to both acidic and metal contaminated environments. Our lab has previously isolated PM01 from Parys Mountain, an abandoned copper mine in Wales. Whilst the tolerance ranges of PM01 are well understood, the mechanisms of this adaptation are were not known. In this study I present of the growth characteristics of PM01 in response to both a short-term and long-term copper stress and in comparison to the model organism *Chlamydomonas reinhardtii.* Additionally, I also assessed the physiological and biochemical responses copper stress induces on these organisms, including lipid oxidation, photosynthetic parameters and attempting to quantify reactive oxygen species. I show, that PM01 completely reduces the efficiency of photosystem II in response to a short-term copper stress to negligible levels. In contrast, *C. reinhardtii* still exhibits photosystem II activity under a short-term copper stress. I believe this shut down of photosystem II activity could be a crucial adaptation for PM01 to adapt to a high copper stress under a short-term adaptation. Additionally, high levels of lipid oxidation in both a short-term and long-term copper stress were found in PM01, whilst *C. reinhardtii* only exhibits high levels of lipid oxidation under a short-term copper stress. Interestingly, other strains of *C. acidophila* show no increase in lipid oxidation levels under both a short and long-term copper stress. Finally, it was found that PM01 has higher antioxidative capacities under control conditions and, interestingly, this lowers under a long-term copper stress.

2.2 Introduction

Acid mine drainage (AMD) systems are highly toxic to the environment and provide an extreme environment that only adapted organisms can populate. No AMD environment is the same and the properties they exhibit can depend on their source and geochemical properties (Gross, 2000), for example the Los Peces Creek within the Iberian Pyrite Belt was found to contain up to 736 mg L^{-1} of Zn and 291 mg L^{-1} of Al (Galván et al., 2021). Whilst, another river within the Iberian Pyrite Belt, the Rio Tinto, exhibits very high level of metals such as Fe (139 mg L^{-1}) and Cu (20 mg L^{-1}) whilst metals such as Al and Zn were comparatively lower (71 mg L^{-1} and 18 mg L^{-1} respectively). *Chlamydomonas acidophila* PM01 is a previously isolated strain of *C. acidophila* from an abandoned copper mine, Parys Mountain, in Wales. Initial experimental characterisation found that the strain has a very high copper tolerance alongside an ability to accumulate copper (Dean et al., 2019). *C. acidophila* CCAP11/136 (referred to as 11/136 from here on in) is a strain of *C. acidophila* isolated from a peat marsh in the Czech Republic (Fott and Mccarthy, 1964), while *C. acidophila* CCAP11/137 (referred to as 11/137 from here on in) is another strain of *C. acidophila* isolated from a lignite mine in Germany (Gerloff-Elias et al., 2005). Both 11/136 and 11/137 were found to have a much lower copper tolerance to PM01, despite being the same species (Dean et al., 2019). Another strain, *C. acidophila* RT-46 isolated from Spain's "River of Fire" the Rio Tinto, has been identified with high copper tolerance (Olsson et al., 2015). Despite being an interesting model to study, there has been very little research to understand the physiological adaptations of PM01 or RT-46 to a high copper environment.

Copper has been found to be highly damaging to the photosynthetic apparatus, from the displacement of Mg^{2+} in the core of the light harvesting complexes attached to chlorophylls, rendering them inactive (Küpper et al., 1996), or even causing direct damage to the photosystem II (PSII) reaction centre itself (Küpper et al., 2002). Additionally, Sandmann & Böger, (1980) found that excess copper induced the formation of the superoxide radical, leading the formation of hydrogen peroxide (H_2O_2) and noted an increase in lipid oxidation. Copper was found to stimulate photosynthetic activity in *Chlorella vulgaris* as determined by parameters such as the maximal quantum yield of PSII (F_v/F_m), the photochemical yield of photosystem II (ΦPSII), photochemical quenching efficiency, the non-photochemical quenching efficiency (NPQ) and electron transport rate. However, under excessive copper conditions (>3 μM) all of these parameters were completely depleted. Disruption of the photosynthetic electron transport chain can lead to the formation of reactive oxygen species (ROS) such as oxygen ($^1O_2{}^*$) and superoxide ($O_2{}^{\bullet-}$) (Fernandes and Henriques, 1991). Plenty of studies have looked at the effect of copper (ranging from 20 μM to 160 μM) on photosynthesis between tolerant and less tolerant species of microalgae (Bazihizina et al., 2015; Nalewajko et al., 1997; Nalewajko and Olaveson, 1995; Ouzounidou et al., 1994). However, none of these tolerant species were examined under the high copper conditions both PM01 and RT-46 have been able to grow in (Puente-Sánchez et al., 2016). Olsson et al. (2015) studied some minor photosynthetic parameters of RT-46, in which they looked at the relative maximum electron transport rate (rETR) and the maximum potential quantum efficiency of Photosystem II (F_v/F_m). There were minimal differences in F_v/F_m when RT-46 was exposed to 0.5 mM copper, and it appeared that the rETR increased under the copper stress. Although this provides some insight into the physiological copper response in a tolerant microalga and the mechanisms of copper tolerance, there are a lot more in-depth

photosynthetic parameters that would give us a deeper insight into how these extremophiles can adapt to a high copper environment.

In addition to damaging photosynthesis, Cu^{2+} is well known to induce the formation of ROS. It can exacerbate the so-called Fenton reaction which produce extremely damaging hydroxyl radicals (OH^-) (Mehta et al., 2006), whilst also directly inhibiting abscisic acid catabolism and catalase activity (Ye et al., 2014). These radicals can then cause further damage to the cell such as inducing lipid oxidation and, in the case of the hydroxyl radical, even DNA damage (Halliwell, 2006). There is contrasting evidence to the severity of copper induction of ROS formation. Whilst Stoiber et al. (2013) found copper induced the most amount of ROS out of the heavy metals they tested, including Cd, Szivák et al. (2009) determined that Cd induced higher cellular ROS over copper. Whilst there may be debates to the severity of different heavy metals in regards to ROS formation, there is no doubt that chronic exposure to heavy metals can induce high levels of ROS, which, in some cases, can be too much for organisms to handle. As mentioned in chapter 1, cells can combat excessive ROS through the use of ROS scavenging enzymes such as catalase (CAT), superoxide dismutase (SOD), and ascorbate peroxidase (Choo et al., 2004). Copper has been shown to induce an antioxidative response in a variety of microalgae such as *C. reinhardtii*, *Scenedesmus bijugatus* and *Pavlova viridis* which seemingly increased in a dose-dependent manner (Jiang et al., 2016; Li et al., 2006; Sabatini et al., 2009).

The aim of this study was to further examine the physiological and biochemical changes of the highly copper tolerant extremophile, PM01. This provides the opportunity to compare this strain to different strains of *C. acidophila* with varied copper tolerance, and to the related copper sensitive, model organism *C. reinhardtii*. I hypothesised that PM01 must have adaptive mechanisms to cope with the various stresses excess copper can cause, such as altered photosynthetic capabilities and enhanced ROS production. This has the potential to uncover more robust strategies of dealing with copper stress as many previous eukaryotic organisms studied do not have the capability to grow in the high concentrations of copper (up to 2 mM Cu) as PM01.

2.3 *Materials and Methods*

2.3.1 Growth Conditions

Chlamydomonas acidophila strains PM01 (isolated as described previously by Dean et al. (2019)), CCAP11/136 (11/136) and CCAP11/137 (11/137) (both obtained from the Culture Collection of Algae and Protozoa (CCAP) stock centre) were grown without the presence of an organic carbon source (photoautotrophically) in a modified acid medium (MAM) pH 3, as described by (Olaveson and Stokes, 1989). Whilst *Chlamydomonas reinhardtii* CCAP11/32C (obtained from CCAP) was grown photoautotrophically in a Tris-minimal phosphate (TP) medium at pH 7 as described by Harris, (2009), except for lacking acetate. Cultures were grown with 3 – 5 biological replicates at 24 °C and 16 h:8 h light: dark cycle at 150µmol m^{-2} s^{-1} light intensity on an orbital shaker (120 rpm). Two sets of samples were grown in control conditions (with no additional copper) and one set grown in copper stressed conditions (2 mM $CuCl_2$ for PM01, 300 or 350 µM $CuCl_2$ for 11/136 and 11/137 and 75 µM $CuCl_2$ for 11/32c – referred to as long-term copper exposure. After two weeks growth one of the control sets was spiked with 4 times the original copper stress (8 mM for PM01 and 300 µM for 11/32C) for 3 hours – referred to as short-term copper exposure. Copper spiking experiments were

not performed with the 11/136 and 11/137 strains. Cells were harvested by centrifuging at 10,000 g for 5 mins. The supernatant was removed, then the cells were washed with 1 ml of ddH_2O, then centrifuged again at 10,000 g for 5 min and the supernatant removed.

2.3.2 Cell Density Measurement

Cell cultures were grown in 50 ml tissue culture flasks containing 30 ml of respective media. Cultures were grown for 30 days in total and samples were measured every 3 days to monitor the growth of the cultures. Cell growth was measured using optical density (OD) at a wavelength of 750 nm using a Jenway 7315 UV-visible spectrophotometer. Cell growth was also measured by cell counting. All of the *C. acidophila* culture cell counts were measured using a haemocytometer (manufacturer name). Briefly, 20 µl of Lugol's iodine was added to 1 ml of cell culture and mixed. A 20 µl aliquot was then added to a haemocytometer and cell counts were measured following manufacturer's instructions. The *C. reinhardtii* cultures were measured using a cellometer (Nexcelom) according to manufactures instructions.

2.3.3 Determining Cell Viability

To assess cell viability under a copper stress in comparison to control conditions, Evans Blue staining was used. Cultures were normalised to an OD_{750nm} value of 2 and pellets were collected by centrifuging at 14,000 g for 5 min. The supernatant was removed, and the pellets were then resuspended in 1 ml of 0.1% Evans Blue dye (Sigma). Cell counts were then taken using a haemocytometer where both the dead, blue cells and normal, viable cells were counted. Dead cells were calculated as a percentage, of the dead cells to total cells counted.

2.3.4 Determining Chlorophyll Content

Cell cultures were grown for 14 days as described in section 2.3.1. 5 ml of cell culture was aliquoted, and a cell pellet was obtained by centrifuging at 16000 g for 5 min. The supernatant was removed, and the cell pellet was resuspended in 5 ml of 96% ethanol and left at room temperature for 5 mins, allowing ample time for cell disruption. After 5 mins samples were centrifuged at 16000 g for 5 mins to remove the cell debris and 1 ml of the supernatant was transferred into a cuvette. Light absorbance was measured at 649 nm and 665 nm and chlorophyll content was measured using the following equations taken from Lichtenthaler and Wellburn, (1983).

$$Chlorophyll\ a\ (\mu g\ ml^{-1}) = (13.95\ \times\ A665nm) - (6.88\ \times A649nm)$$

$$Chlorophyll\ b\ (\mu g\ ml^{-1}) = (24.96\ \times\ A649nm) - (7.32\ \times A665nm)$$

2.3.5 Photosynthetic Response to Copper

To determine how photosynthesis is affected in response to copper, the efficiency of photosystem II (PS II) and levels of non-photochemical quenching (NPQ) were measured using pulse-amplitude modulation (PAM) fluorimetry. Cultures were grown for 2 weeks and cells were then harvested and normalised to an OD_{750nm}. For measurements of the photosynthetic parameters, a 1 ml of sample of cell culture was pipetted into a Walz KS-101 suspension cuvette, a magnetic stirrer was used for the duration of the measurement to prevent cells from settling. To prevent carbon-limited photosynthesis, bicarbonate was added to the sample to a final concentration of 1 µM. Samples were left in the dark for 30 min prior to taking a measurement to allow relaxation of any photoprotective mechanisms. For

spiked short-term copper stress cultures, 1 ml aliquots were taken 3 h before measuring and spiked with their respective amounts of copper. They were left in the dark for 30 min prior to measuring. The strains were tested at an array of actinic lights including 90, 150, 200, 250, 350, 500, 1000 and 1500 µmol m^{-2} s^{-1} with a LED ENGIN LZ9 warm white light. Saturating light flashes were provided every 60 s for 0.6 s at 4200 µmol m^{-2} s^{-1}. The initial fluorescence (F_0), maximal fluorescence (F_m) and variable fluorescence (F_v) values were measured using PAM101, Walz (Germany) and recorded using Laboratory written software, written using LabView (National Instruments). Non-photochemical quenching (NPQ) and the efficiency of photosystem II (ΦPSII) were determined after saturating light flashes as described by Maxwell and Johnson (2000) as seen below. Each sample ran for 15 min, with the average of the last 3 saturating light flashes being used for analysis.

$$\Phi\mathrm{PSII} = (\mathrm{F'm} - \mathrm{Ft})/\mathrm{F'm}$$

$$\mathrm{NPQ} = (\mathrm{F}\frac{o}{m} - \mathrm{F'm})/\mathrm{F'm}$$

F'm= Maximum fluorescence in the light

Ft= Fluorescence immediately before flash

$\mathrm{F}\frac{o}{m}$= Maximal fluorescence level

2.3.6 Quantifying ROS

Cell cultures were normalised to an OD_{750nm} value of 2 prior to measurements, cultures were then spiked with either 8 mM $CuCl_2$ (PM01), 1.2 mM $CuCl_2$ (11/136 and 11/137) or 300 µM $CuCl_2$ (11/32c). A 1 ml volume of culture was aliquoted into a fresh 2 ml Eppendorf tube at 30 min, 1 h, 3 h, 8 h and 24 h time points. The cultures in the Eppendorf tubes were centrifuged at 10,000 g for 5 min to obtain a cell pellet, the supernatant was removed, then flash frozen in liquid nitrogen until measurements could be taken. To determine the level of ROS in algal samples the "Total reactive oxygen species (ROS) assay kit 520 nm" from Invitrogen was used according to manufacturer's instructions. In brief the 500x ROS assay stain stock solution was diluted to 1x using the ROS assay buffer. Cell pellets were then resuspended in 100 µl of the 1x ROS stain solution and left to incubate at 37°C for 1 h. The samples were then loaded into a 96-wel Ganttt plate and read on a BMG CLARIOStar Multi-mode microplate reader with the excitation at 490 nm and reading the emission at 520 nm.

2.3.7 Measuring ROS Enzyme Activity and Identifying SOD Isoforms

Biomass flash frozen in liquid nitrogen and stored at -80 °C was homogenized with the extraction buffer (50 mM phosphate buffer pH 7.0 containing 1 mM EDTA, 0.1% (v/v) Triton X-100, 1 mM dithiothreitol (DTT) and 2% (w/v) polyvinylpyrrolidone (PVP) with protease inhibitor cocktail for plant cell and tissue extracts (Sigma). The homogenates were stirred on ice for 1 h and centrifuged for 30 min at 10000g and 4°C. The supernatant was used for SOD zymogram detection. To determine the SOD isoforms, non-equilibrated isoelectric focusing was performed horizontally in the LKB 2117 Multiphor II system, using 0.5 mm thick polyacrylamide gels (7.5%), that contained 5% 3.5–10.0 ampholites. Gels were run at 5°C with the constant power of 0.25 W/cm width of gel, with limiting voltage of 1,000 V for 2 h. SOD isoenzymes were detected on the gels by staining for 20 minutes in the dark in 20 ml of 100 mM sodium phosphate buffer pH 7.8 with 4 mg of nitrobluetetrazolium, 0.6

mg of riboflavine, 2 µl of TEMED and 40 µl of 0.25 M NaEDTA by the photochemical method of Beauchamp and Fridovich (1971). After that, the gels were briefly rinsed with distilled water and illuminated for 15 min. To separate different types of SOD – manganese, gels were preincubated with 5 mM KCN (inhibits CuZnSOD) or 5 mM H_2O_2 (inhibits FeSOD).

2.3.8 Measuring Lipid Oxidation

Lipid oxidation was measured indirectly by measuring the presence of malondialdehyde (MDA), a by-product of lipid oxidation, using thiobarbituric acid reactive substances (TBARS). Cells were harvested by centrifuging 30 ml of dense cell culture at 14,000g for 5 min to collect a cell pellet and the supernatant removed. Cell pellets were lyophilised overnight. Lyophilised samples were weighed then dipped in liquid nitrogen. A 3 mm tungsten carbide bead was added to each Eppendorf tube and samples were ground using a Qiagen tissue lyser II. Ground samples were re-suspended in 1.1 ml of ddH_2O and 0.5 ml aliquot was added to fresh Eppendorf tubes containing 0.5 ml of either –TBA solution consisting of 20% trichloroacetic acid (TCA), 0.01% butylated hydroxytoluene and 0.2 M HCl or +TBA solution consisting of the –TBA solution with the addition of 0.65% thiobarbituric acid (TBA). Samples were heated at 95°C on a dry heating block for 1 h, then centrifuged at 3000g for 5 min to pellet cell debris. Samples were allowed to cool then 200 µl was aliquoted into a 96-well gannt plate and absorbance was read at 440 nm, 532 nm, and 600 nm using a BMG CLARIOStar Multi-mode microplate reader.

MDA equivalents were calculated using the equations described by (Hodges et al., 1999)

$$eq\ 1)\ (A532_{+TBA} - A600_{+TBA}) - (A532_{-TBA} - A600_{-TBA})$$

$$eq\ 2)(A440_{+TBA} - A600_{+TBA}) \times 0.0571$$

$$eq\ 3)\ \text{MDA equivalents}\ (\text{nmol ml}^{-1}) = \frac{(eq\ 1 - eq\ 2)}{137000} \times 10^6$$

2.4 *Results*

2.4.1 Growth Characteristics of Microalgae Strains Under Copper Stress

To understand how the different strains of microalgae tolerate and grow in the presence of copper three strains of *C. acidophila* and one strain of *C. reinhardtii* were measured with their ability to grow in the presence of high concentrations of copper. The copper concentrations presented were chosen due to their ability to reduce cell growth for their respective organisms, whilst still being able to produce enough biomass for analysis. Figure 2.1 (A) shows the copper tolerant strain of *C. acidophila* PM01 grown in the presence of 2 mM Cu. The cell count and OD measurements show a very similar trend in growth over 27 days. Copper significantly reduced the growth of PM01, cell counts show a 51.6% reduction in culture growth after 27 days compared to the control, whilst the OD_{750nm} measurements show only a 27.5% reduction in culture growth (Table 2.1). This was also the case half-way through the measurement as at day 15, the cell counts showed a 62.8% reduction for cell counts whilst only a 29.6% reduction for OD_{750nm}. The 75 µM copper stress seemed to have a slightly lesser impact to 11/32c, than the 2 mM copper stress did to PM01. 11/32c is similar to PM01 in which both the cell count and OD_{750nm} show similar trend patterns (Figure 2.1 (B)). However, the cell counts show a 35.6% reduction in culture growth after 27 days and a 13.8% for OD_{750nm},

suggesting this copper stress had a slightly lower impact on cell growth but not by much. The other *C. acidophila* strains, 11/136 and 11/137, showed a much lower tolerance for copper than PM01. For the controls both OD_{750nm} and cell counts show very similar patterns in terms of cell growth. However, both cultures did not grow in the presence of copper, however, 11/136 did appear to start growing between day 24 and day 27 (Figure 2.1 (C+D)). The correlation plots in Figure 2.3 show a high correlation between OD_{750nm} and cell number. This confers with the literature which recommend using OD_{750nm} as a measure of culture growth (Griffiths et al., 2011).

To test the effects of copper cell viability, Evans blue staining was used to count the percentage of dead cells. The long-term copper induced an increase in cell death for PM01, whilst the short-term copper stress induced an increase in cell death for both PM01 and 11/32c. 11.9% of cells were dead in the long-term copper treatment for PM01, which is 10.2 % higher than the control, whilst the short-term copper stress only caused 10% cell death. Both of these cell death ratios were substantially smaller than the 35.3% of dead cells found in the short-term copper stress for 11/32c. Interestingly, both copper treatments led to no significant differences in chlorophyll content in either species when compared to their respective controls (Figure 2.2).

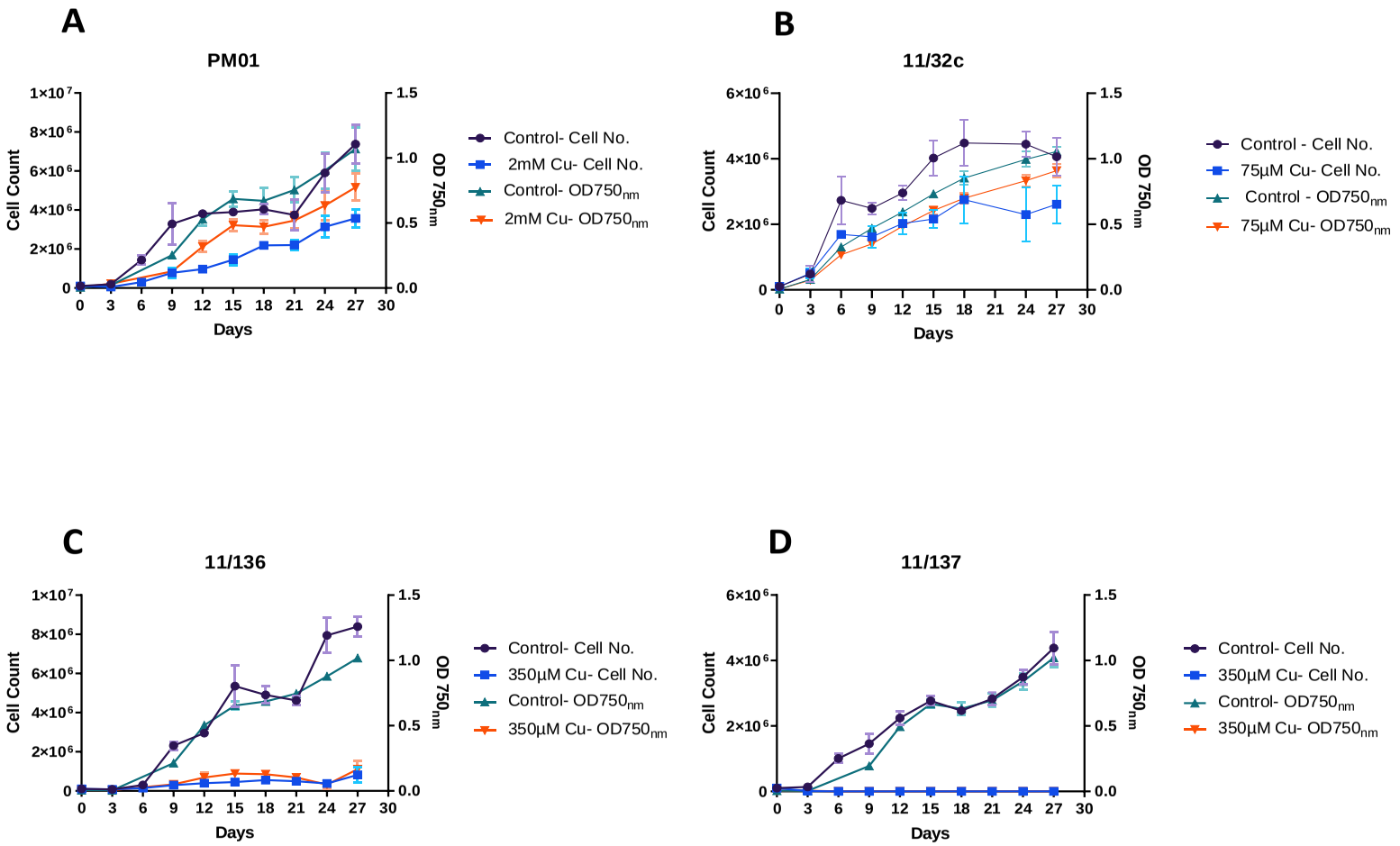

Figure 2.1 Measurement of cell growth parameters of 4 different strains of microalgae; (A) C. acidophila (PM01), (B) C. reinhardtii (11/32c), (C) C. acidophila (11/136), (D) C. acidophila (11/137), in the presence of copper. Cells were grown in triplicate and cell growth parameters taken every 3 days over 27 days. Cell counts were taken to show the growth of cultures and the optical density at 750nm was also measured as an indicator of cell growth.

	Day 14				Day 27			
	% Cell Count Reduction		% OD Reduction		% Cell Count Reduction		% OD Reduction	
	Mean (SD)	N	Mean	N	Mean	N	Mean	N
PM01	62.76 (7.25)	3	29.59 (6.63)	3	51.60 (6.35)	3	27.53 (9.75)	3
11/136	91.43 (1.3)	3	79.68 (2.45)	3	90.18 (4.92)	3	83.62 (6.48)	3
11/137	100 (0)	3	100 (0)	3	100 (0)	3	100 (0)	3
11/32c	46.31 (7.09)	3	17.27 (4.06)	3	35.63 (14.16)	3	13.83 (4.86)	3

Table 2.1 % reduction of cell growth parameters to an average of the control group. Cell growth parameters include cell counts and OD readings at 750nm.

	PM01			11/32c		
	Control	**Long-Term**	**Short-Term**	**Control**	**Long-Term**	**Short-Term**
% Dead Cells	1.7 ± 0.93	11.9 ± 2.8 **	10 ± 2.3 *	0.9 ± 0.25	2.7 ± 1.3	35.3 ± 6.2 ***
Chl *a* (pg cell $^{-1}$)	0.433 ± 0.131	0.419 ± 0.136	0.378 ± 0.064	0.414 ± 0.084	0.213 ± 0.01	0.313 ± 0.147
Chl *b* (pg cell $^{-1}$)	0.134 ± 0.044	0.133 ± 0.038	0.169 ± 0.058	0.169 ± 0.034	0.086 ± 0.038	0.142 ± 0.066
Total Chl (pg cell $^{-1}$)	0.567 ± 0.175	0.552 ± 0.174	0.547 ± 0.121	0.583 ± 0.118	0.299 ± .137	0.455 ± 0.212

*Figure 2.2 Physiological responses of PM01 and 11/32c in response to a shot-term and long-term copper stress. % dead were measured with Evans Blue staining and represent the number of blue cells as a percentage of the total cells counted. Chlorophyll a (Chl a) and Chlorophyll b (Chl b) were measured using spectroscopic methods. A two-way ANOVA was used to measure for significance. No significant differences were found for any chlorophyll measurements. Sidaks multiple comparison tests were conducted for the % dead cells (Adj. P values * =p<0.05, **= p<0.01, ***= p<0.001)*

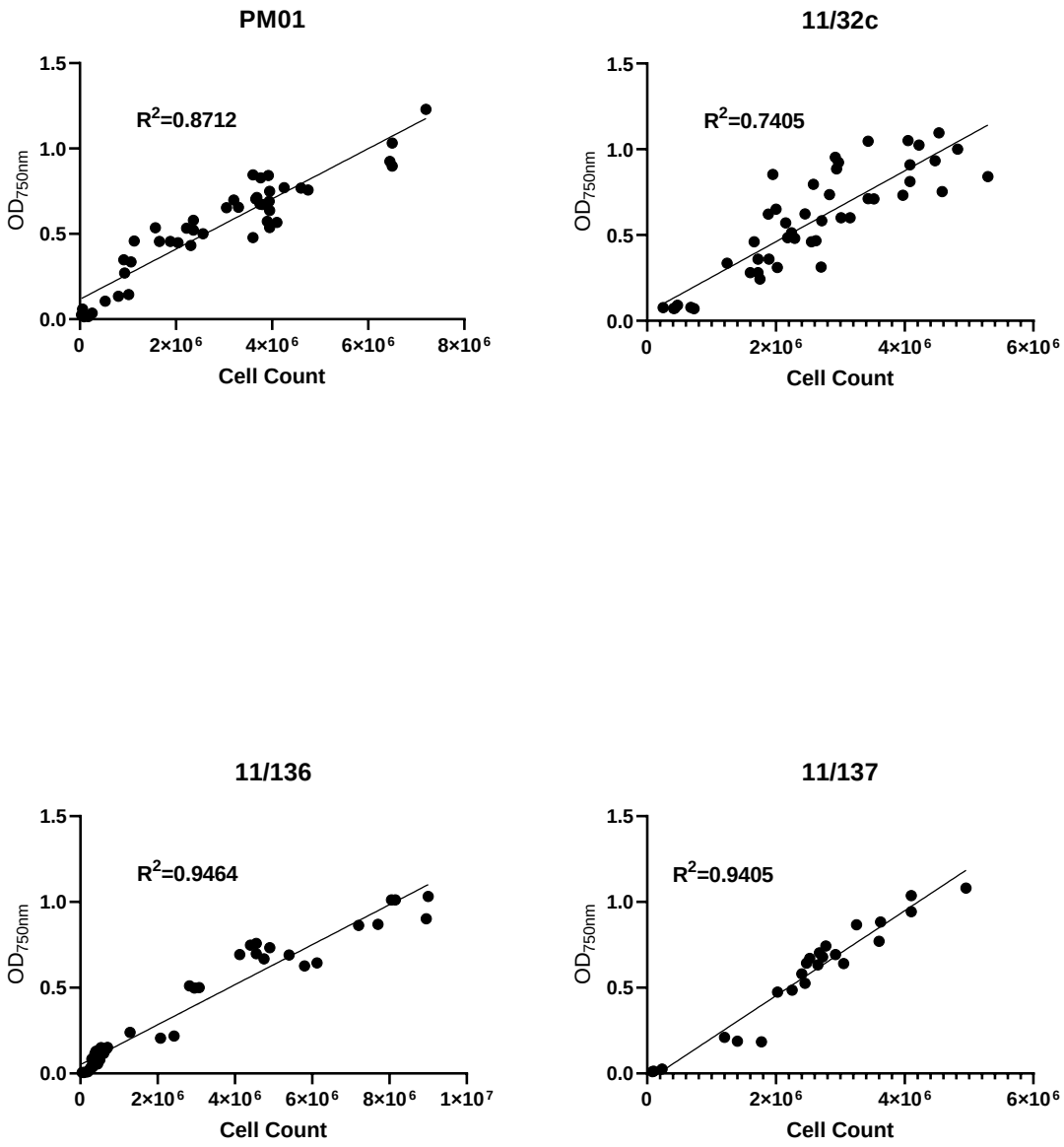

Figure 2.3 Cell counts plotted against the optical density at 750nm of cell cultures grown under control and copper stressed conditions. Four strains of microalgae were tested, three C. acidophila strains (PM01, 11/136 and 11/137) and one C. reinhardtii strain (11/32c). A simple linear regression was performed to test for correlation with the R^2 values stated on the graph.

2.4.2 *The Photosynthetic Response of Chlamydomonas acidophila and Chlamydomonas reinhardtii to Copper*

Photosynthesis is a finely tuned metabolic process that has the potential to generate a high number of radicals. Under normal physiological conditions these are maintained at non-damaging levels, some of which have been found to be used in cell signalling (Foyer, 2018). Excess copper is known to damage the photosystems and induce excess ROS (Pätsikkä et al., 2002; Sharma et al., 2012). I hypothesised that the extremophile *C. acidophila* may have an altered photosynthetic machinery to help it adapt to a highly metallic, and specifically copper, environment. F_v/F_m is a commonly used parameter to assess plant stress and measures the maximum quantum efficiency of PSII (Maxwell and Johnson, 2000). To test this, we utilised pulse amplitude modulated (PAM) fluorometry, which utilises chlorophyll fluorescence to measure the photosynthetic ability of samples. Briefly, light energy hitting a photosynthetic organisms can be converted 3-ways. It can be used for photochemistry, driving energy production, dissipated as non-photochemical quenching, using a variety of different processes or finally, chlorophyll fluorescence. In general, a decrease in photochemistry and NPQ will lead to an increase in chlorophyll fluorescence and vice versa. We can utilise these small changes in chlorophyll fluorescence to determine photochemistry and NPQ of a sample (Maxwell and Johnson, 2000).Figure 2.4 shows the F_v/F_m values of both *C. acidophila* and *C. reinhardtii* under control, long-term and short-term copper stresses. *C. reinhardtii* under control conditions had the highest F_v/F_m value, with a mean of 0.681 (±0.024 SD). Interestingly, PM01 had a significantly lower maximum quantum efficiency of PSII with a mean of 0.619 (±0.028 SD) a 10% lower maximum PS II efficiency when compared to the *C. reinhardtii* control. The PM01 strain value was found to not be statistically different from the *C. reinhardtii* long-term copper stress with a mean of 0.624 (±0.278 SD) which is a 9.2% reduction in the maximum photosynthetic efficiency of PSII of the *C. reinhardtii* control. The PM01 long-term treatment also showed a significant decrease in PSII with a F_v/F_m value of 0.541 (±0.048 SD), which is a 14.5% reduction in comparison to the PM01 control. Interestingly, PM01 did not a show a significant decrease in maximum photosynthetic efficiency of PSII for the more harsh, short-term copper treatment when compared to its control. The mean value was actually higher than for the control 0.644 (±0.065 SD) although this was not found to be significant. This is in stark contrast to the *C. reinhardtii* short-term treatment which had the lowest F_v/F_m value of all treatments with a mean of 0.495 (±0.09 SD).

The short-term treatments for both species show a lot of variability in the F_v/F_m values. To get a better understanding all F_v/F_m values these were plotted to the time of day they were collected (Figure 2.5). The F_v/F_m values for the control remained relatively stable throughout the day, whereas, both the short-term and long-term treatments showed a diurnal pattern (Figure 2.5 (A)). The long-term treatment showed the highest variability with a highest value of 0.624 at 11:00 and a low value of 0.355 at 15:20. The short-term treatment showed a similar variation from a high of 0.723 at 11:20 to a low of 0.552 at 15:00. Both copper treatments for PM01 appeared to show two peaks at the morning and evening with a trough at midday. Interestingly, the only copper treatment for *C. reinhardtii* which elicited a similar diurnal pattern for *C. reinhardtii* was the short-term copper treatment (Figure 2.5 (B)). Again, the *C. reinhardtii* short-term treatments showed peaks at both the morning and evening with a trough at midday.

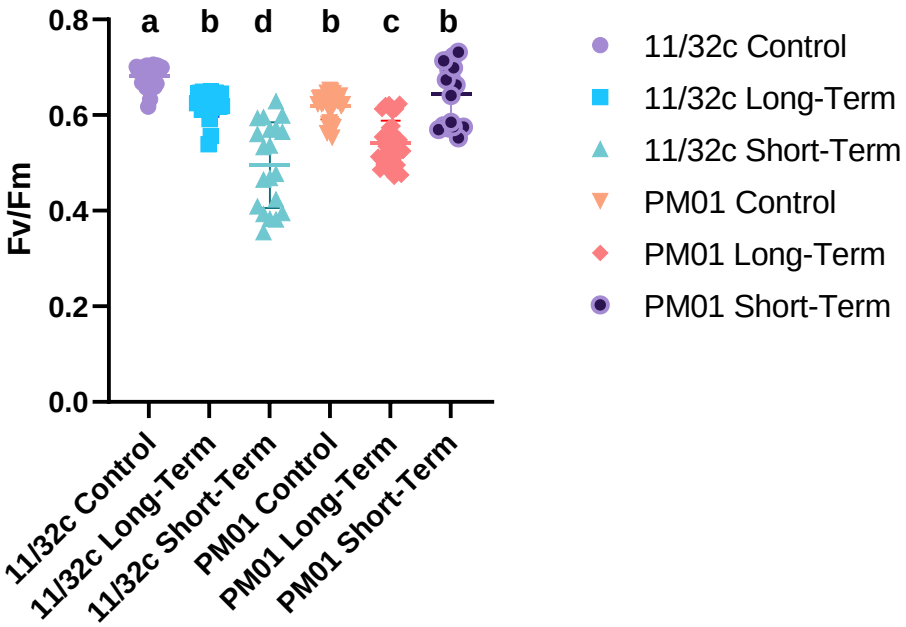

Figure 2.4 F_v/F_m of C. reinhardtii and C. acidophila under control (n=23/ n=30), long-term (n=24/ n=29) and short-term (n=19/ n=17) copper conditions. The mean and standard deviation for all treatments are shown and each data point is plotted. A one-way ANOVA was used to test for significance (P <0.05) with a least significant difference post-hoc test applied.

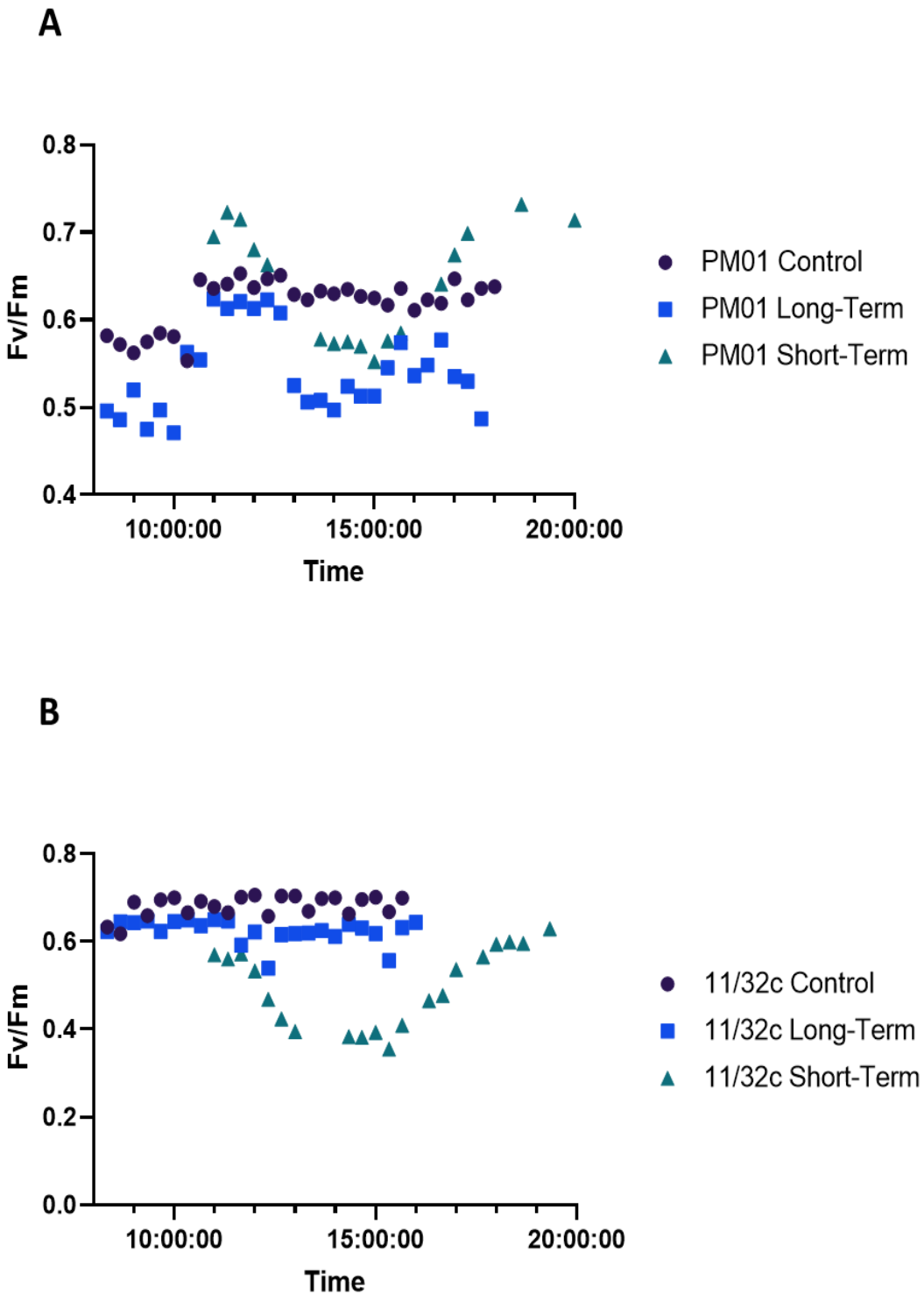

Figure 2.5 F_v/F_m values plotted at the time of day they were measured to show the diurnal cycles of the F_v/F_m values for certain copper treatments. (A) F_v/F_m values for PM01, (B) F_v/F_m values for C. reinhardtii. Samples were left to acclimate to the dark for 30 min before given saturating light pulses at 4200 µmol m^{-2} s^{-1}. Measurements were taken from 8 am through to 6 pm, The short-term treatment measurements were taken from 11 am as they had to be exposed to copper 3 hours prior to measurements. The photoperiod runs from 06:00 to 22:00

To gain a further understanding of the photosynthetic parameters, cultures were left for 15 min after taking the F_v/F_m measurements under different actinic lights to create a light response curve. Figure 2.6 (A) shows the efficiency of photosystem II (ΦPSII) of PM01 under both the long-term and short-term copper conditions. As would be expected, ΦPSII decreased as light intensity increased. ΦPSII for the long-term treatment was not significantly different to the control at any of the light intensities whilst the short-term treatment showed significantly lower ΦPSII than both the other treatments. ΦPSII for the short-term treatment was near 0 for all light intensities apart from 90 µmol m^{-2} s^{-1}, which for two replicates was near 0 and there was just one replicate with a higher ΦPSII of 0.222, leaving the mean as 0.094 for 90 µmol m^{-2} s^{-1}. Figure 2.6(B) shows ΦPSII for *C. reinhardtii* under both copper treatments. Like PM01, the *C. reinhardtii* ΦPSII decreased as light intensity increases across all treatments. The long-term treatment had a significantly lower ΦPSII at the 150 µmol m^{-2} s^{-1} actinic light, while for the 90, 150 and 250 µmol m^{-2} s^{-1} actinic light intensities there appeared to be a high amount of variation between the replicates before the variation appeared to be reduced at higher actinic light levels. Similar to PM01, the short-term treatment was significantly lower than all other treatments at all actinic light levels apart from 90 and 1500 µmol m^{-2} s^{-1}. At 90 µmol m^{-2} s^{-1} the short-term treatment was significantly lower than the control. One of the clearest differences between PM01 and *C. reinhardtii* was that at all actinic light intensities apart from 350 µmol m^{-2} s^{-1}, the short-term copper stress was still exhibiting some degree of ΦPSII. 90 and 150 µmol m^{-2} s^{-1} had a mean ΦPSII of 0.309 and 0116, respectively for the short-term treatments.

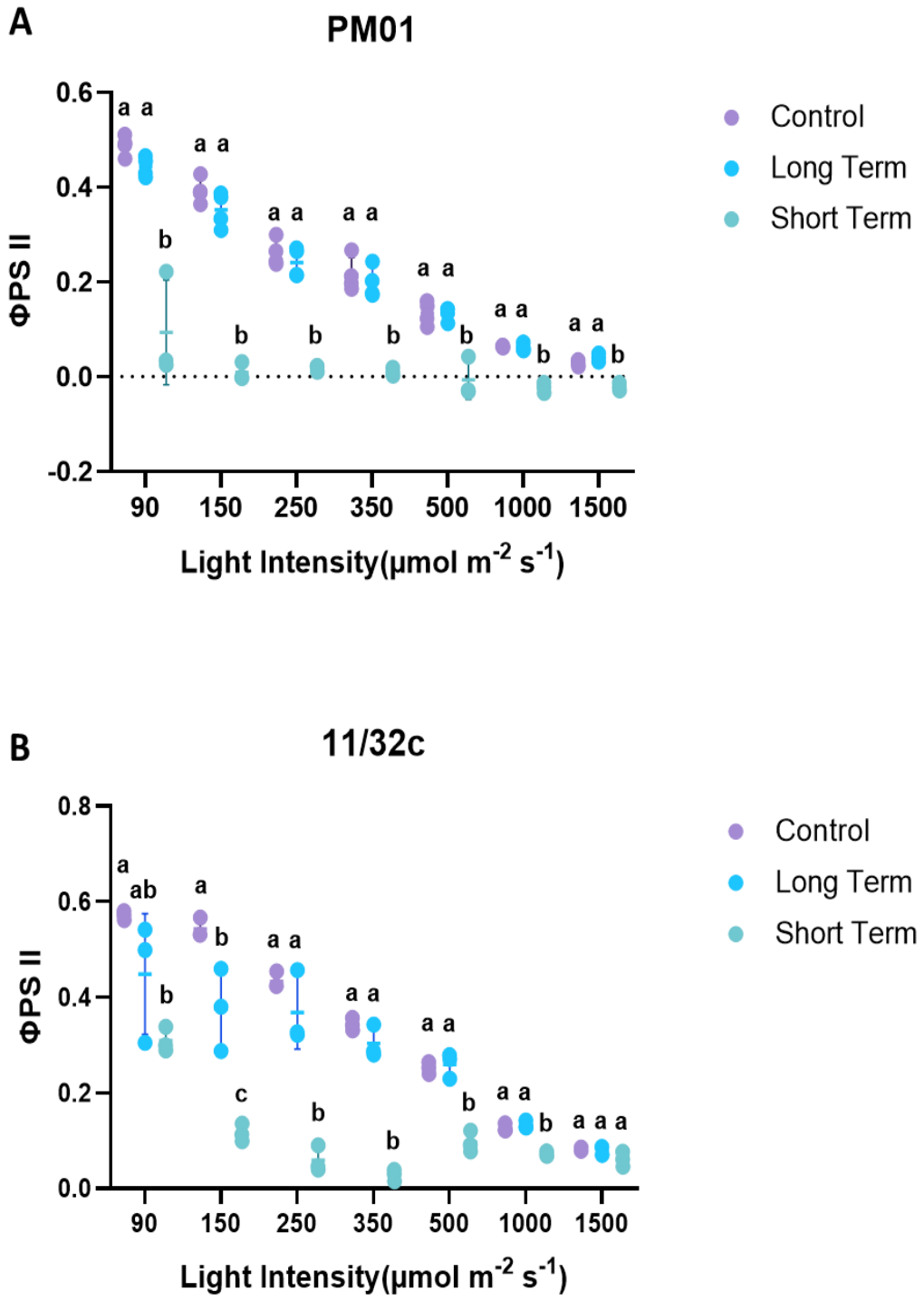

Figure 2.6 *Efficiency of photosystem II (ΦPSII) of two species of microalgae, (A) C. acidophila (PM01) and (B) C. reinhardtii (11/32c) under a long-term and short-term copper stress. Each data point is plotted with the and the line representing the mean and the bars showing the standard deviation. A one-way ANOVA was run at each light intensity with least significant difference multiple comparisons made to determine significant differences (P < 0.05), which are represented by different lowercase letters.*

Another photosynthetic parameter that was important to measure was the non-photochemical quenching (NPQ) capabilities of the two species. For both species, at lower light intensities there appeared to be negative NPQ values. For PM01 the control had negative NPQ values at 90 µmol m^{-2} s^{-1} (-0.031 ±0.033SD) whilst the long-term copper stress had negative values for both 90 and 150 µmol m^{-2} s^{-1}(-0.212 ±0.016 SD, -0.156 ±0.086 SD respectively) (Figure 2.7 (A)). On the other hand *C. reinhardtii* had negative values for the control at 90 and 150 µmol m^{-2} s^{-1} (-0.349 ±0.043 SD, -0.2 ±0.167 SD respectively) whilst the short-term copper stress had a negative value for 90 µmol m^{-2} s^{-1}(-0.147 ±0.045 SD) (Figure 2.7 (B)). This tells us that there is some mechanism that is repressing maximal fluorescence in the dark, and at low actinic light intensities, there is no pressure to reverse this.

The highest NPQ values seen between both species was found with the short-term copper treatment for PM01 at 90 µmol m^{-2} s^{-1} actinic light with a mean of 2.22 ±0.223 SD (Figure 2.7 (A)). The NPQ rapidly dropped to a low of 1.099 ±0.229 SD and 0.990 ±0.072 SD for the 250 and 350 µmol m^{-2} s^{-1} actinic light intensities, respectively, a 50% decrease to the highest value. The NPQ values then increased and levelled off to 1.735 ±0.27 SD. The short-term copper treatment had higher NPQ values than all other conditions for PM01 up until the 500 µmol m^{-2} s^{-1} actinic light intensity, where there is not statistical difference between the short-term and long-term copper treatment for the rest of the actinic lights (Figure 2.7 (A)). Whilst differing in values, both the long-term and the control NPQs for PM01 showed a similar pattern in that NPQ increases, linearly, as the actinic light intensity increases.

The long-term copper treatments showed consistently the lowest levels of NPQ for PM01, at 90 and 150 µmol m^{-2} s^{-1} light, the long-term treatment showed the lowest levels alongside the control, whilst for every other actinic light value the long-term treatment had the lowest NPQ values reaching a high of only 0.7 ±0.179 SD. The NPQ values for *C. reinhardtii* all showed a positive correlation with actinic light intensity for all treatments (Figure 2.7 (B)). Interestingly, the long-term copper treatment for *C. reinhardtii* has large variations between the biological replicates, the largest variation is soon in the long-term treatment at an actinic light intensity of 1500 µmol m^{-2} s^{-1} (0.842 ±0.41 SD). Although there is some degree of positive correlation between NPQ and actinic light intensity for *C. reinhardtii* under the short-term stress, most of the values are on either side of 0. The lowest NPQ value for the short-term stress was -0.147 ±0.045 SD whilst the highest value was 0.194 ±0.054 SD at 1500 µmol m^{-2} s^{-1} actinic light. For the most part there is no significant difference between the control and long-term treatments for *C. reinhardtii*. The two treatments only differed at 90, 150 and 1000 µmol m^{-2} s^{-1}, where the long-term treatment had the highest NPQ values for the former two, whilst the control had the highest NPQ value for the latter.

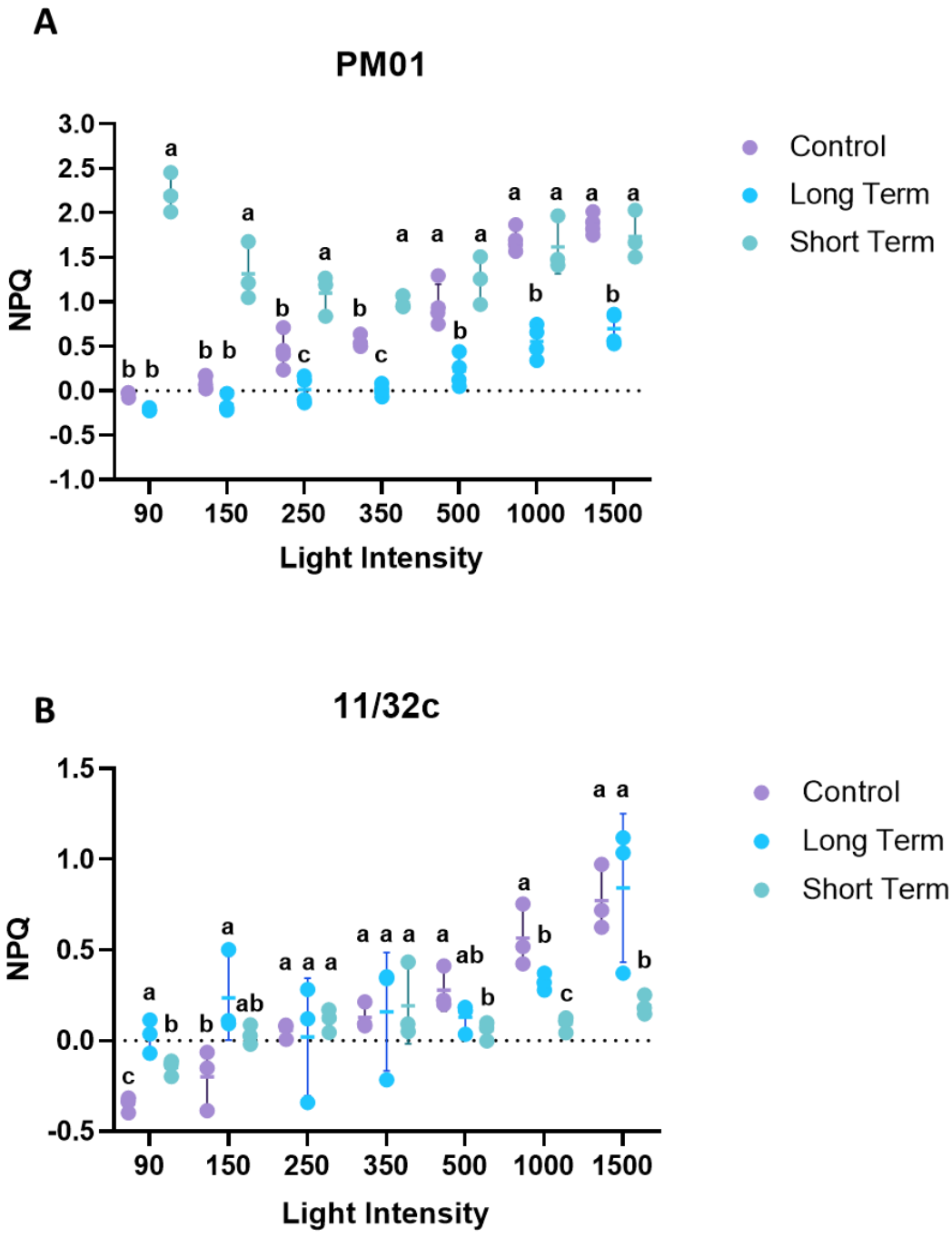

Figure 2.7 Non-photochemical quenching (NPQ) of two species of microalgae, (A) C. acidophila (PM01) and (B) C. reinhardtii (11/32c) under a long-term and short-term copper stress. A one-way ANOVA was run at each light intensity with least significant difference multiple comparisons made to determine significant differences (P < ?), which are represented by different lowercase letters.

Figure 2.4 showed that there was a clear species differentiation in photosynthetic capability. To be able to draw a more direct comparison between the species, the electron transport rate (ETR) was caluated by multiplying the ΦPSII by the light intensity. The NPQ values were normalised by subtracted from an average of their comparative controls (Figure 2.8). Figure 2.8 (A) clearly shows that the short-term treatment caused the largest reduction in ETR across both species at lower actinic light intensities. The short-term conditions significantly reduced ETR across all actinic light intensities measured from their respective controls. The long-term treatment for PM01 never significantly differed from its control with the ETR values remaining at around a constant 50 μmol $e^{-}m^{-2}$ s^{-1} . The long-term treatment for *C. reinhardtii* also showed very little perturbation from the control in terms of ETR. However, where different to PM01, the ETR seemingly increases with increasing actinic light intensity rather than levelling out like PM01.

Figure 2.8 (B) shows the relative NPQ changes compared to the control. The highest relative NPQ change compared to the control was for the PM01 short-term treatment at 90 μmol m^{-2} s^{-1}. Interestingly, both the relative long-term and short-term treatments for PM01 showed a similar downward trend as light intensity increases. Whilst the relative short-term treatment levelled off at around 0, the long-term treatment started at 0 and decreased further. These are the largest negative changes and Figure 2.8 (B) shows, statistically, that the PM01 long-term treatment had the lowest NPQ values across all treatments and species. This is particularly intriguing as the corresponding normalised long-term treatment shows very little deviation from 0, indicating no change from the control and was statistically similar to the normalised short-term treatment apart from at the highest 1500 μmol m^{-2} s^{-1} actinic light intensity.

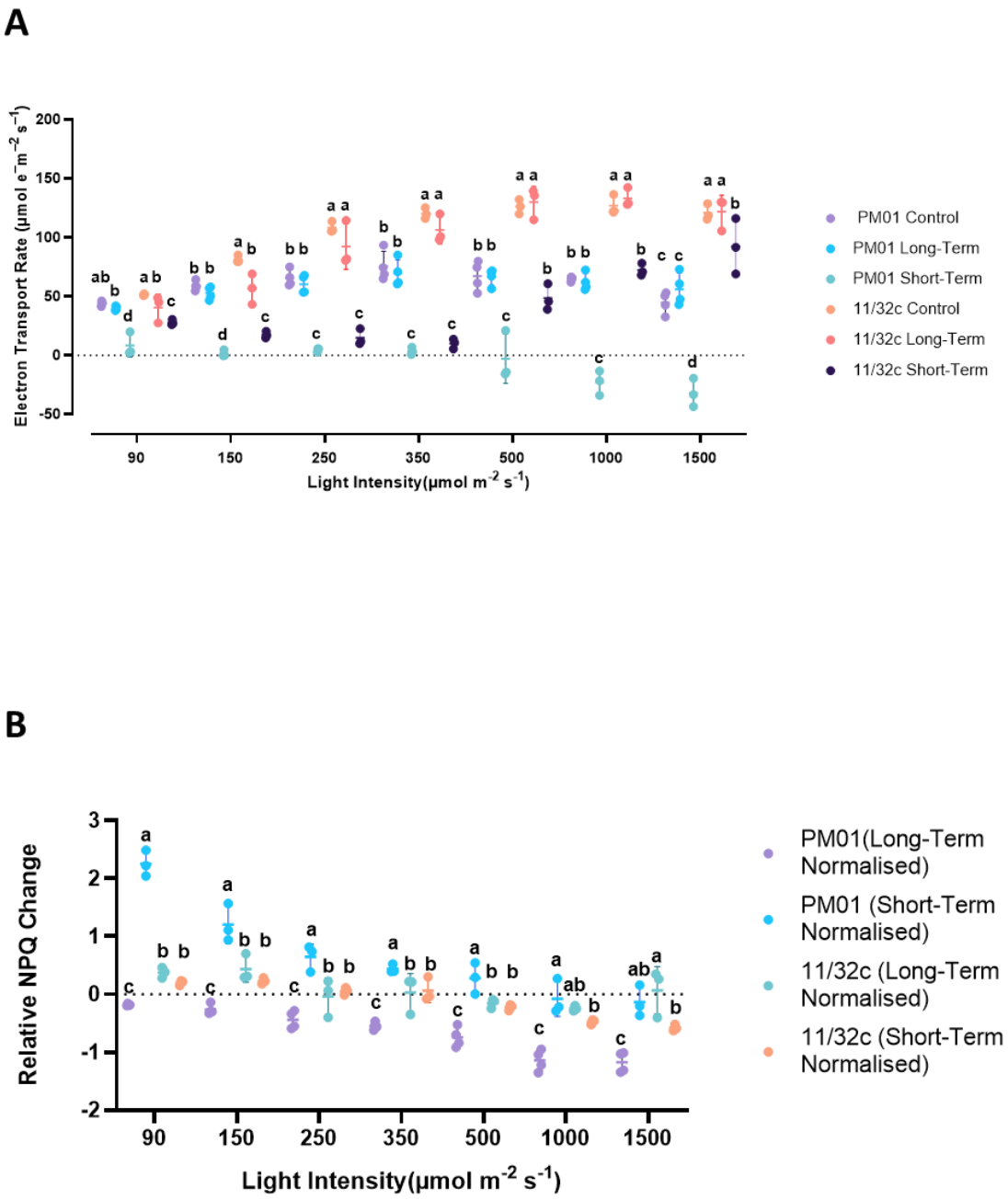

Figure 2.8 Comparative analysis of the photosynthetic parameters (A) Electron Transport Rate (ETR) and (B) NPQ for the extremophile C. acidophila (PM01) and the model organism C. reinhardtii (11/32c) under and long-term and short-term copper stress. ETR is calculated by multiplying ΦPSII by the light intensity. NPQ values were normalised by averaging the controls and subtracting them from the NPQ values from their respective copper treatments, at the specific light intensity. A one-way ANOVA was run at each light intensity with least significant difference multiple comparisons made to determine significant differences, which are represented by letters

Finally, when taking the short-term copper spike measurements, there were clear differences observed in the way the organisms fluoresce. To help picture this, Figure 2.9 and Figure 2.10 show the traces over the 15 min measurement period and chose a typical trace of the 3 biological replicates tested. What is evident is that the short-term copper stress seems to induce an increase in fluorescence in PM01 that is seemingly absent in *C. reinhardtii*. What is more interesting is that this increase in fluorescence seemed to occur in a time dependent manner depending on the actinic light intensity. At 90 µmol m^{-2} s^{-1} the increase in fluorescence was not apparent, however, it started to increase at around 670 s (Figure 2.9 (A)). The increase in fluorescence was more obvious for the 150, 250, 350, 500 and 1000 µmol m^{-2} s^{-1} intensity treatments (Figure 2.9 (B), (C), (D) and Figure 2.10 (A) and (B)), with the increase in fluorescence happening at 600, 420, 250, 410 and 580 s, respectively. Finally, it was examined whether this increase plateaued, therefore samples were left to run for 1 h to observe the behaviour of this fluorescence increase (Figure 2.10 (D)). For both the 150 and 350 µmol m^{-2} s^{-1} actinic light intensities, the fluorescence increased until 20 min, but interestingly the fluorescence did not plateau but steadily decreased. This response was in stark contrast to *C. reinhardtii* which did not seem to show any difference in basal fluorescence throughout the time course for any of the light intensities or even during 50 min durations (Figure 2.9 and Figure 2.10).

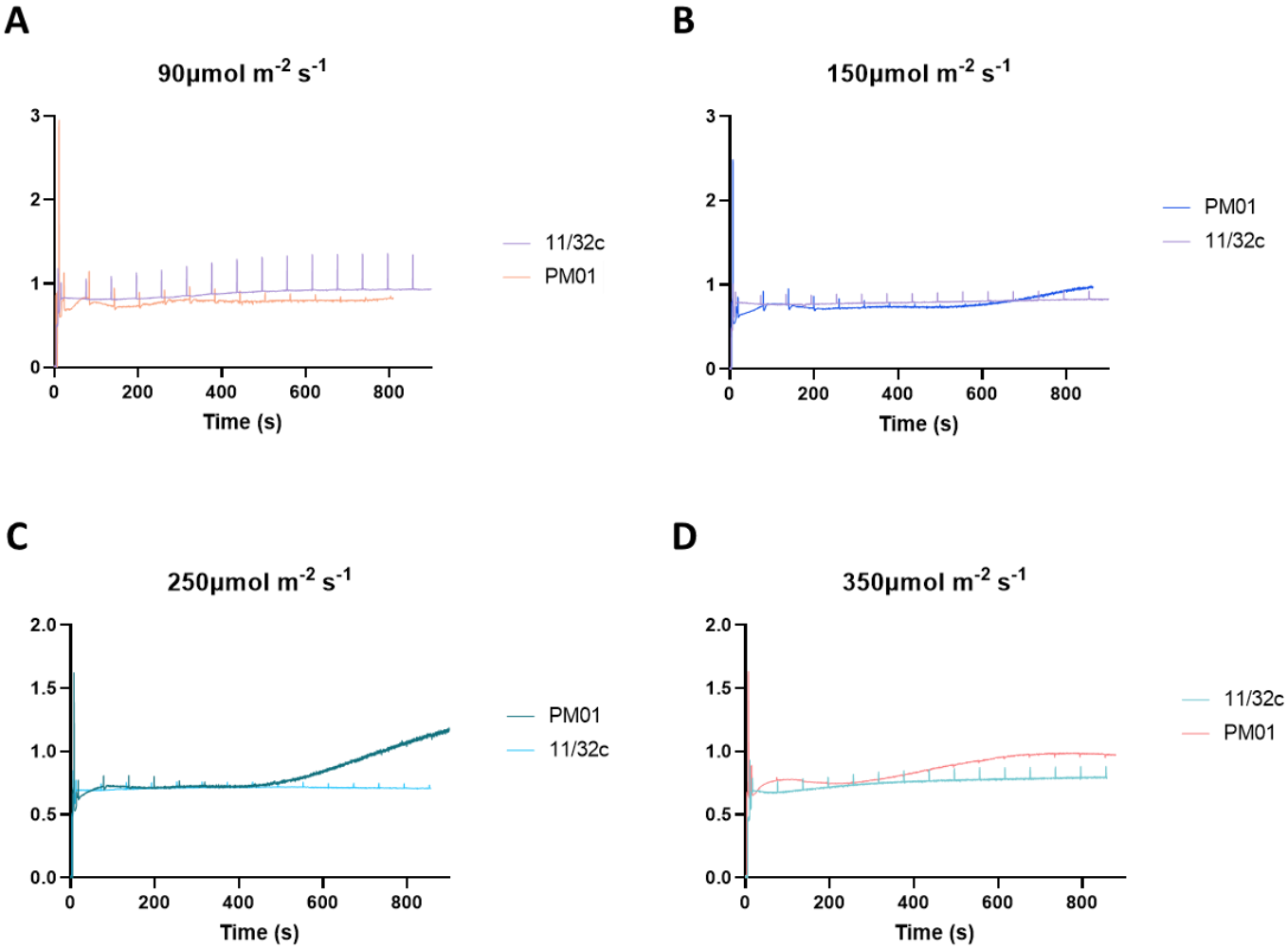

Figure 2.9 Traces of changing chlorophyll fluorescence taken during PAM measurements which were used to determine ΦPSII and NPQ in the short-term copper treatments for PM01 and 11/32c at (A) 90µmol m^{-2} s^{-1}, (B) 150µmol m^{-2} s^{-1}, (C) 250µmol m^{-2} s^{-1} and (D) 350µmol m^{-2} s^{-1}. Samples were measured over a 900 s period with saturating light pulses every 60 s.

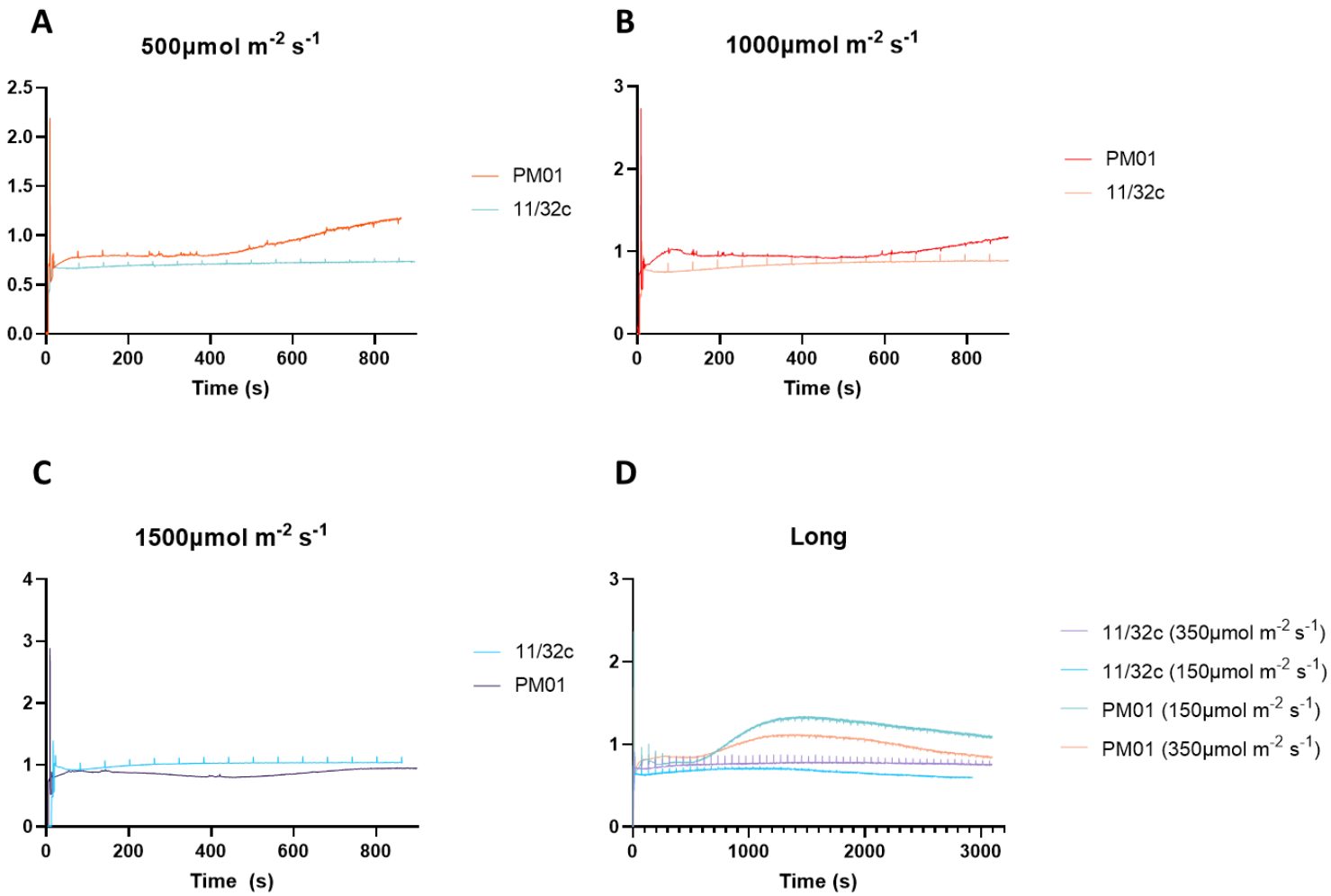

Figure 2.10 Traces of changing chlorophyll fluorescence taken during PAM measurements which were used to determine ΦPSII and NPQ in the short-term copper treatments for PM01 and 11/32c at (A) 500µmol m-2 s-1, (B) 1000µmol m-2 s-1, (C) 1500µmol m-2 s-1 and (D) long traces at 2 actinic lights (150µmol m-2 s-1 and 350µmol m-2 s-1). Samples were measured over a 900 s period with saturating light pulses every 60 s with the exception of (D) which was ran for

2.4.3 Quantifying ROS

To get a better idea of the stress microalgal cells experience under copper stress, the total quantity of ROS was measured over time after exposure to copper using a commercial fluorometric intracellular ROS stain kit from Sigma Adlrich, incubated with the cells and measured using fluorescence spectrometry. Figure 2.11 shows the total fluorescence emitted from algal samples after excitation at 490 nm and detection at 520 nm after allowing the total ROS stain to enter the cells. All the *C. acidophila* samples clearly show that under copper stress the fluorescence is immediately reduced (at most after 30 min) when compared to a control sample (Figure 2.11 A, C and D). Interestingly, the control samples also saw a decrease in fluorescence through the day, with a large decrease between the 1 h and 3 h time points, a response seen across all species. The copper treated sample for *C. reinhardtii* (11/32c) also followed this sharp decrease in fluorescence throughout the day evenly matching the control samples of all species up until the 8 h time point Figure 2.11 (B). However, after 24 h the fluorescence for this treatment decreased to almost zero along with all the other copper spiked samples. Within each plate a H_2O_2 standard was included to ensure that the fluorescence gain remained stable across multiple plate reads. Figure 2.11(E) shows the values of three independent replicates with H_2O_2 samples that were serially diluted from 1.5% to 0.0000015% in 10% reduction increments. After 0.015% the fluorescence values did not decrease further and in fact remained stable at around 450 arbitrary fluorescence units. When comparing the maximum fluorescence between the standards and the algal samples there is a clear discrepancy. The highest H_2O_2 standard (1.5%) fluoresced at around 10000 arbitrary units, whereas the algal samples were fluorescing at a maximum of 22000 arbitrary units.

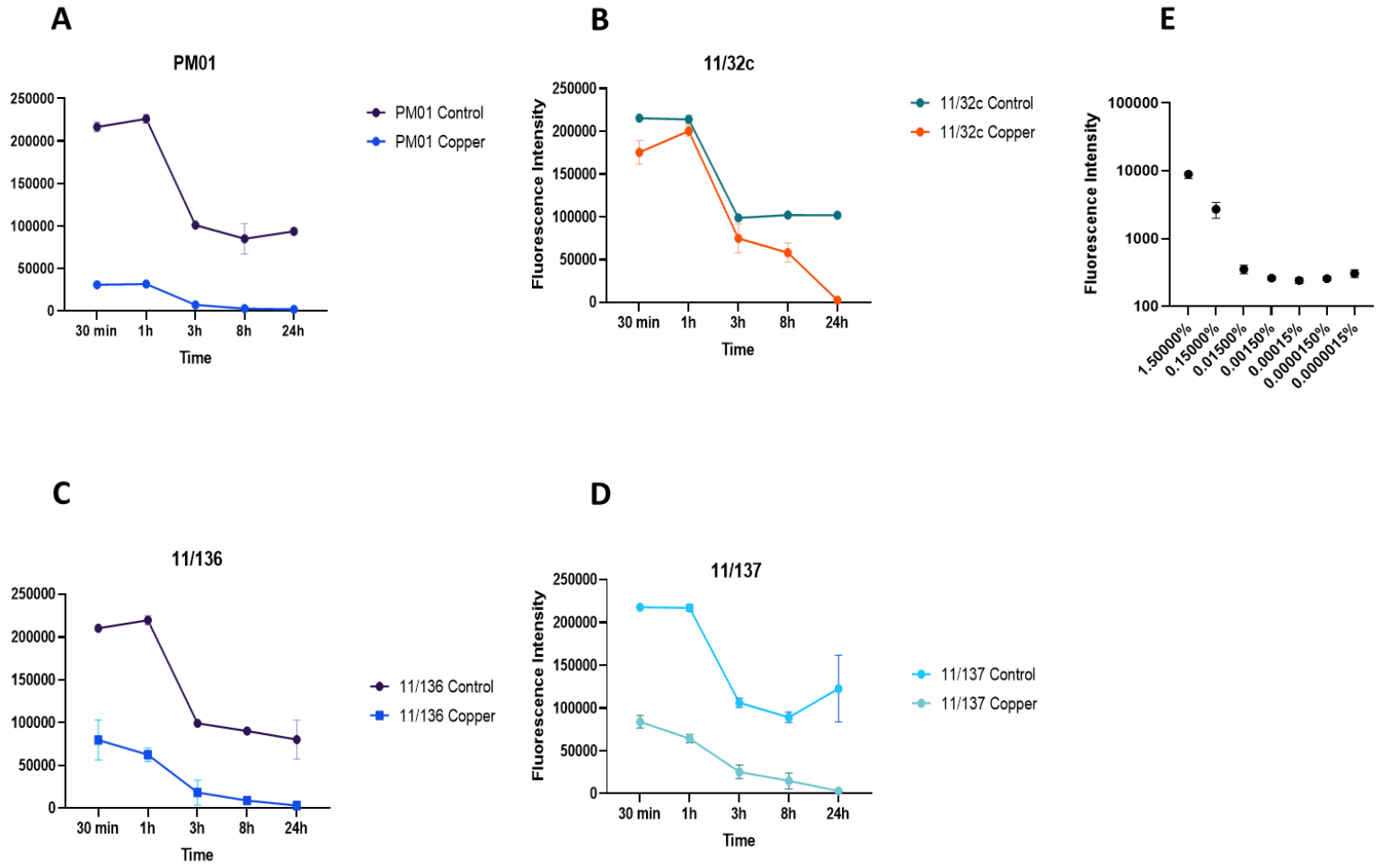

Figure 2.11 Estimation of total ROS using a fluorometric based assay. total ROS of intact algal samples under control and copper spiked conditions. 3 C. acidophila strains were tested; PM01 (A), 11/136 (C) and 11/137 (D) and a C. reinhardtii strain 11/32c (B) strain was also tested, samples were spiked with 8mM, 1.2mM, 1.2mM and 300µMof copper respectively. Data shows the mean of 4 biological replicates and standard deviation. (E) Hydrogen peroxide (H_2O_2) tested with the total ROS assay kit to create a standard curve. Data shows the mean of 3 independent replicates and the standard deviation.

2.4.4 C. acidophila Strain PM01 Shows Differences to C. reinhardtii in ROS Scavenging Enzyme Activity

To assess the responses of ROS to stress the activity of the ROS scavenging enzymes SOD and CAT was measured. SOD scavenges the radical superoxide and converts it into oxygen and hydrogen peroxide, whilst CAT scavenges hydrogen peroxide, converting it to water and oxygen. Figure 2.12 (A) shows the activity of CAT between *C. acidophila* PM01 and *C. reinhardtii* 11/32c. PM01 showed the highest level of CAT activity, compared to 11/32C. Interestingly the long-term copper stress for PM01 gave a lower level of CAT activity compared to the control, with a reduction of 37.9%. Although this was still significantly higher than the *C. reinhardtii* control activity (2.4-fold higher) (Figure 2.12 (A)). However, there was no difference in the *CAT* transcript abundance (collected from RNA-seq data; see chapter 4) between these treatments for PM01, as shown in Figure 2.13. CAT activity was significantly higher in the control treatment in PM01 when compared to both control and long-term *C. reinhardtii* treatments, which showed a 3.8-fold and 2.8-fold reduction in activity, respectively (Figure 2.12 (A)). This was roughly in line with the transcriptomic data which showed a 3.1-fold and 3.6-fold reduction in transcript abundance, respectively for the *CAT1* isoforms compared between PM01 and 11/32c (Figure 2.13). No CAT2 isoform could be found for PM01, however, the *CAT2* transcript abundance was very low across all treatments for *C. reinhardtii*. The CAT activity for *C. reinhardtii* was not significantly different between the control and long-term copper treatment (Figure 2.12 (A)), and the RNA-seq data also showed no difference in transcript abundance for the *CAT1* isoform between the control and long-term copper treatment (Figure 2.13). Finally, the short-term copper spike treatment increased *CAT1* transcript abundance for both strains, although the relative abundance of *CAT1* in this condition was significantly higher for PM01 than for 11/32c.

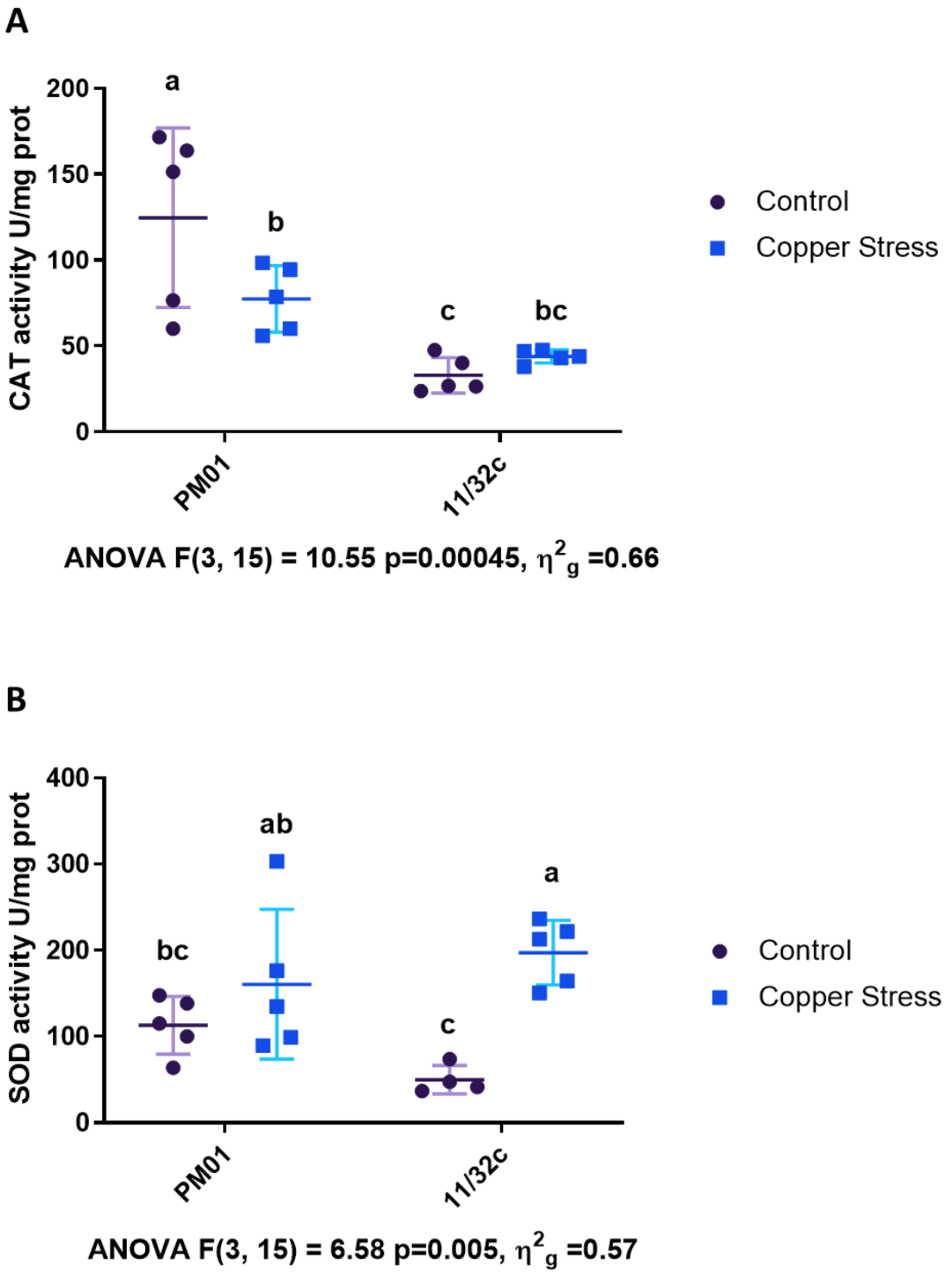

Figure 2.12 Activity of the ROS scavenging enzymes (A) Catalase (CAT) and (B) Superoxide dismutase (SOD) of C. acidophila (PM01) and C. reinhardtii (11/32c). Cells were grown with a long term copper stress of 2 mM (PM01) and 75 µM (11/32c) copper. ROS enzymes activity was normalised to units of activity per mg of protein. Five biological replicates were measured for each treatment with each data point plotted, the bars represent the mean and SD for each treatment. A one-way ANOVA was run to test for significance (P < 0.05) , with a Fisher's least significant difference post hoc test applied for comparisons between species and treatments.

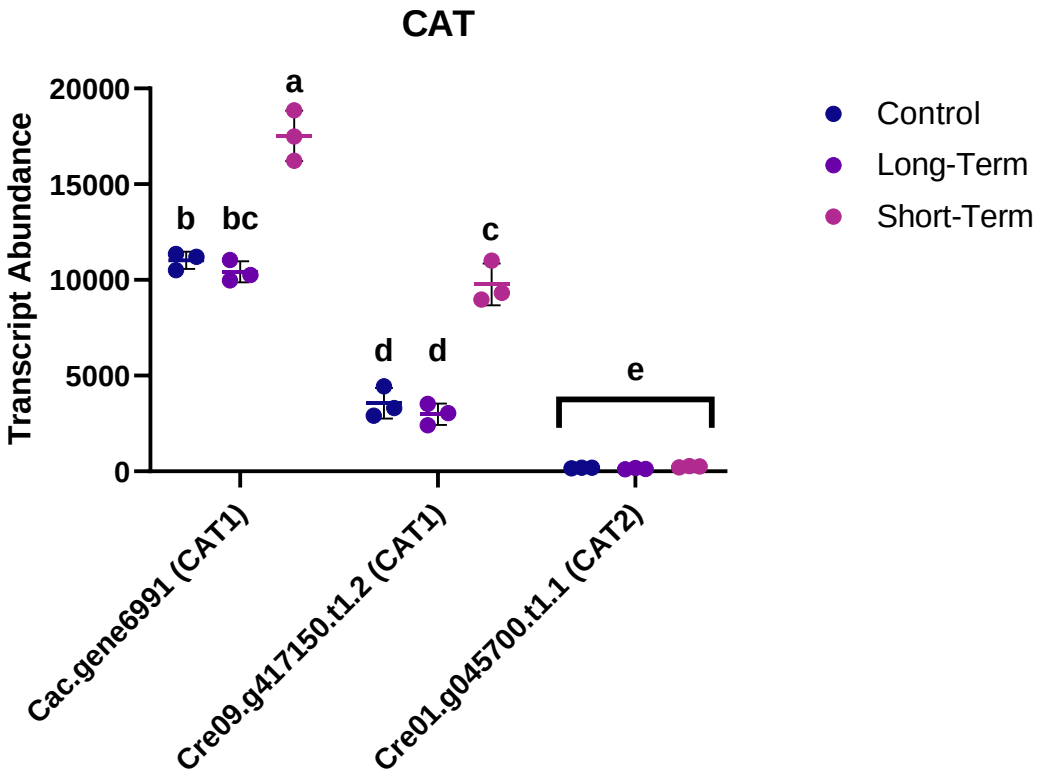

Figure 2.13 Transcript abundance of ROS scavenging enzyme Catalase (CAT). The figures present transcript abundance of two different species of microalgae, C. acidophila (transcripts prefixed with Cac) and C. reinhardtii (transcripts prefixed with Cre). Data shows 3 biological replicates (all data points plotted) with the mean and SD represented by the bars. A one-way ANOVA was performed for statistical analysis and Fisher's least significant difference was applied as a post-hoc test.

SOD activity shows a different picture than CAT activity, where there was no difference in activity between control and the long-term copper treatment for PM01 but SOD activity was significantly higher (by 4-fold) under copper treatment for 11/32c (Figure 2.12 (B)). However, the long-term copper treatment for PM01 did give a significant increase in SOD activity when compared to the *C. reinhardtii* control. However, Figure 2.14 shows that SOD gene expression is more complicated and does not directly correspond with this observed enzyme activity. Three isoforms of the MnSOD were identified in PM01 and four isoforms in 11/32c (Figure 2.14 (A)). All of the isoforms showed no difference in expression level between the control and long-term copper stress. One *C. acidophila* isoform, Cac.gene7511, showed significantly higher expression levels under both control and long-term copper conditions than most other isoforms. This expression was further increased under the short-term copper conditions where it increases 5-fold to its already highly expressed control (Figure 2.14 (A)). A similar pattern was also seen in the *C. reinhardtii* isoform Cre02.g096150.t1.2. One FeSOD isoform was identified in PM01 and two FeSOD isoforms in 11/32c (Figure 2.14 (B)). The Cre17.g703176.t1.1 isoform showed almost no expression for all treatments, so is unlikely to have much effect in the SOD activity. As seen for some of the MnSOD isoforms, short-term copper conditions increased expression for Cac.gene8132 and Cre10.g436050.t1.2 compared to the other treatments. Figure 2.15 shows the different isoforms that could be identified from protein extracts of the two strains. Two isoforms of MnSOD with a pI of 8 - 9 were identified in both species. Two FeSOD isoforms were found in *C. reinhardtii* with a pI of 6 - 7, whilst two FeSODs were found with a pI of 3 - 4 in PM01. PM01 also had one MnSOD isoform at pI of 3 - 4 whilst 11/32c had two isoforms of MnSOD with a pI of 3 - 4.

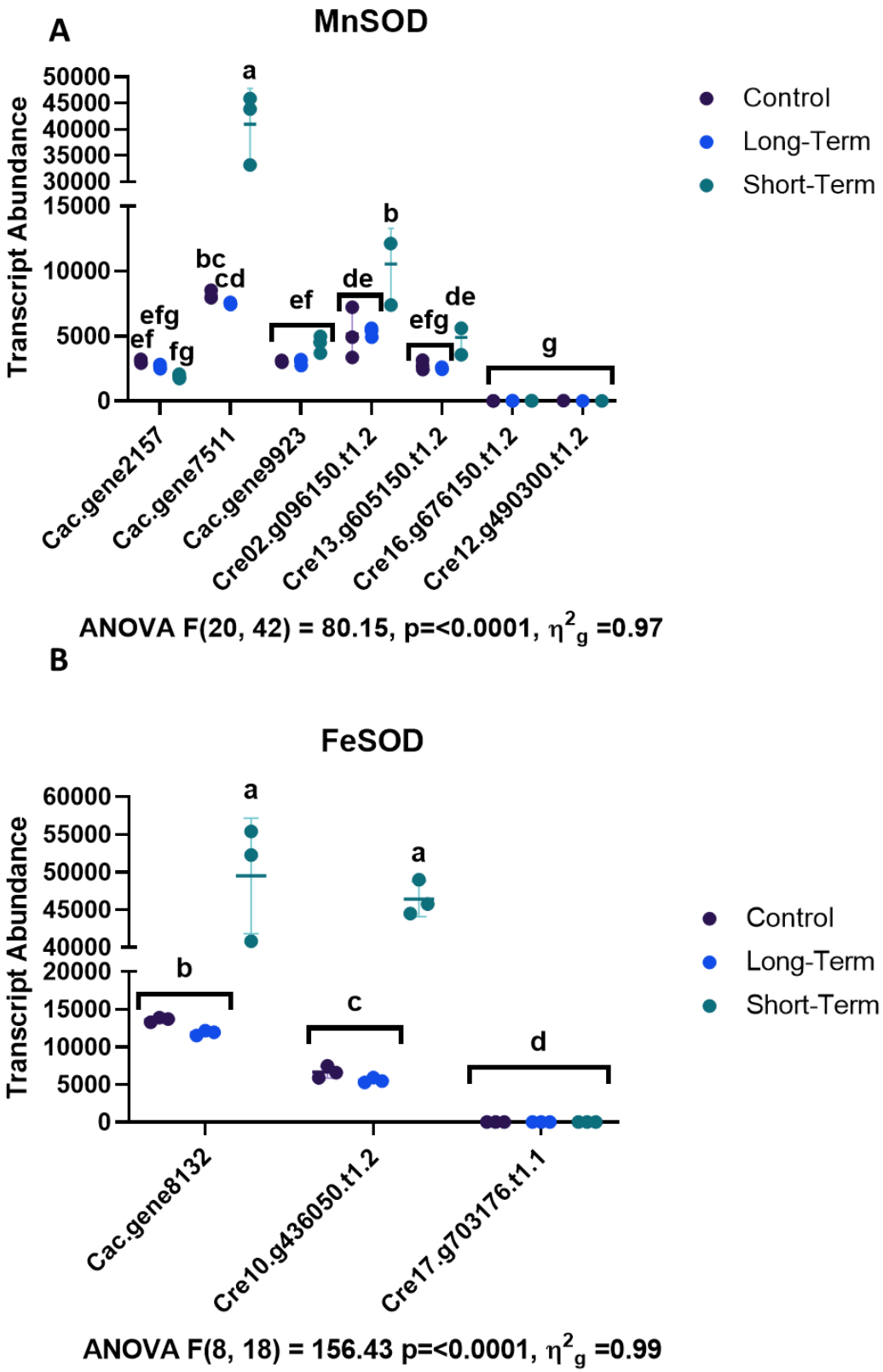

Figure 2.14 Transcript abundance of different isoforms of Superoxide dismutase (SOD). Data shows to different forms of SOD with different metallic cores (A) MnSOD and (B) FeSOD. The figures present transcript abundance of two different species of microalgae, C. acidophila (transcripts prefixed with Cac) and C. reinhardtii (transcripts prefixed with Cre). Data shows 3 biological replicates (all data points plotted) with the mean and SD represented by the bars. A one-way ANOVA was performed for statistical analysis and Fisher's least significant difference was applied as a post-hoc test.

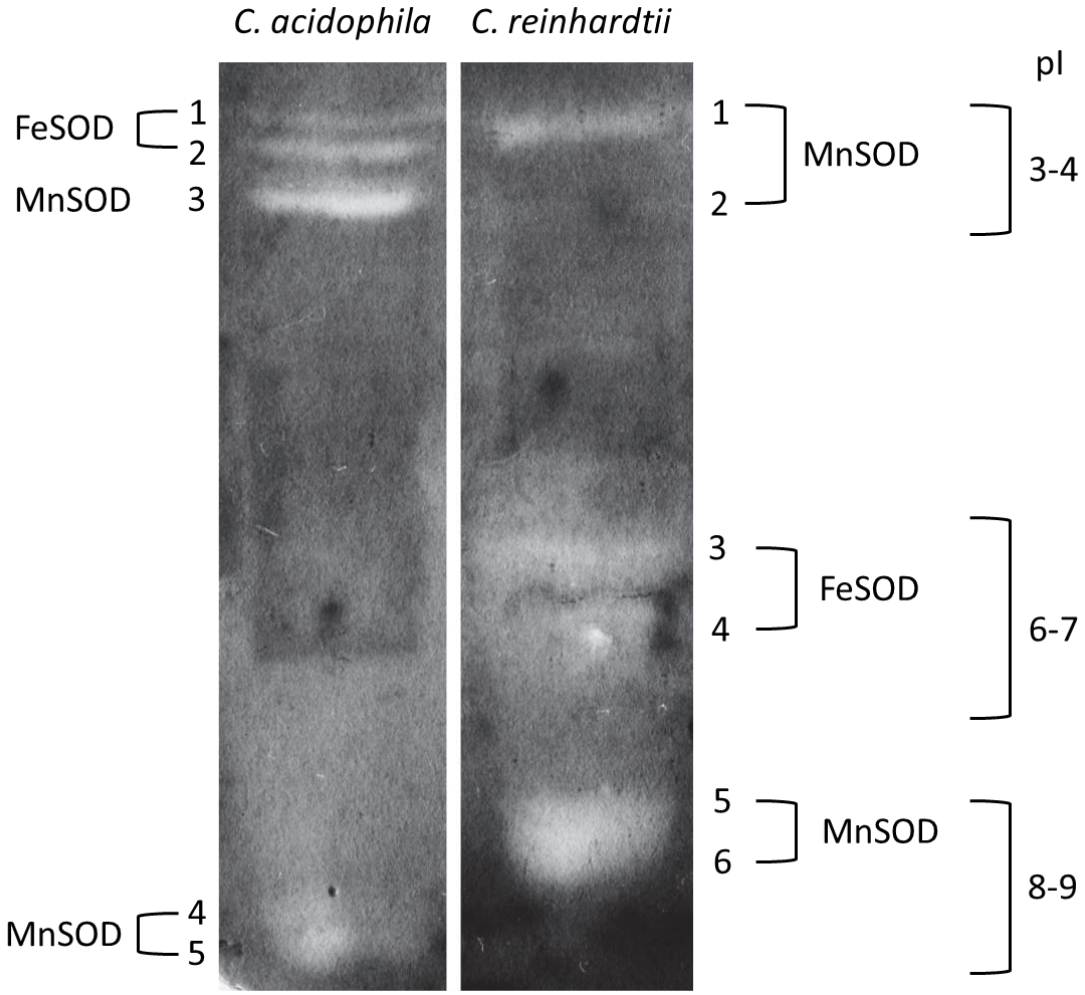

Figure 2.15 Isoelectric focussing of superoxide dismutase (SOD) to identify different isoforms. To test for SOD activity gels were stained with nitrobluetetrazolium in conjuncture with riboflavin. Different metal core SODs were identified using the inhibitors KCN (inhibiting CuZnSOD) or H_2O_2 (inhibits FeSOD).

To get a better understanding of the differences in the pI of the FeSOD between *C. acidophila and C. reinhardtii* the predicted protein sequences of the genes that were mapped from the RNA-seq data (chapter 4) were aligned. As *C. acidophila* has not been well described previously, protein sequence was taken from *Chlamydomonas eustigma*, which is closely related to *C. acidophila* (see Figure 4.1) and the *C. eustigma* genome was used to map *C. acidophila* sequence reads for the RNA-seq experiment. Figure 2.16 shows the aligned sequences for two FeSOD protein sequences for *C. reinhardtii* (Cre17.g703176 and Cre10.g436050) whilst only one FeSOD isoform protein sequence could be found for *C. eustigma* (CEUSTIGMA_g8133). All three genes show a high protein sequence similarity and show core conserved amino acid sequences such as DVWEHAYY starting at amino acid 275 for Cre17.g703176, amino acid 204 for CEUSTIGMA_g8133 and amino acid 203 for Cre10.g436050. Interestingly, Cre10.g436050 shows a higher protein similarity to CEUSTGIMA_g8133 than it does to Cre17.g703176, showing 8 regions of 5 or more shared amino acid sequences that are not present in Cre17.g703176.

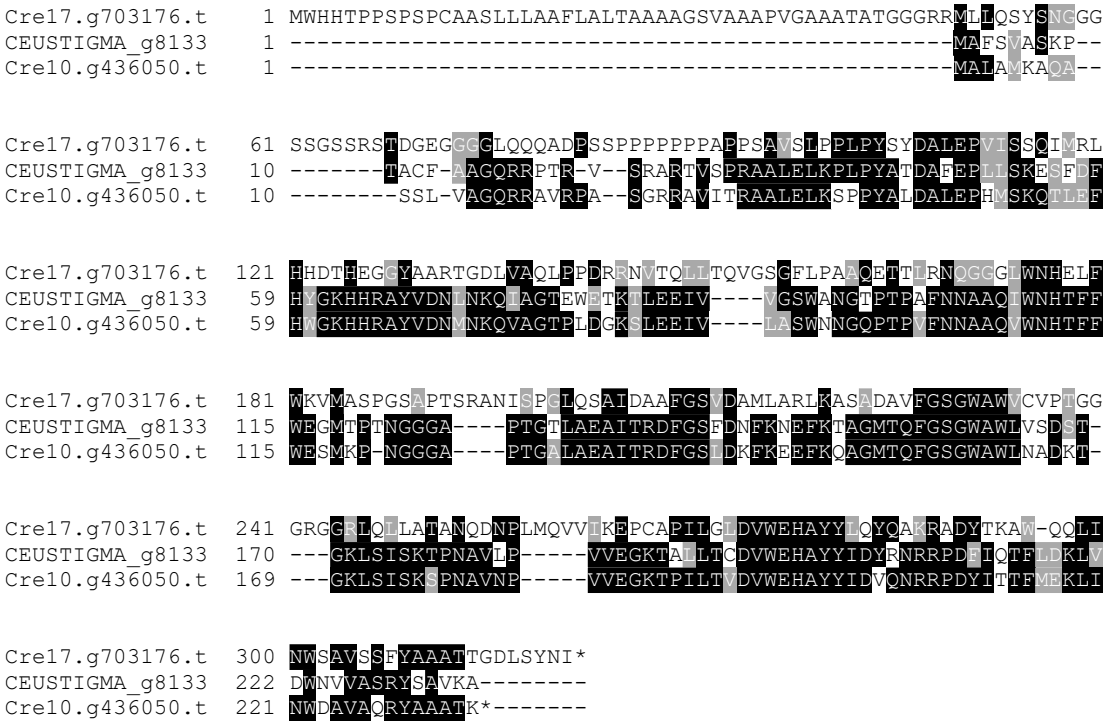

Figure 2.16 Aligned protein sequences of identified FeSOD for C. eustigma and C. reinhardtii. Protein sequences were obtained from Genbank (C. esutigma) and phytozome (C. reinhardtii), aligned in Clustal Omega and coloured using Boxshade.

2.4.5 PM01 Shows High Lipid Oxidation Under Copper Stress

Lipids are an easy target for oxidation by ROS, and thiobarbituric acid can bind to lipid oxidation by-products such as malondialdehyde causing a colour change to be detected. Figure 2.17 shows the estimated lipid oxidation between the three strain of *C. acidophila* (PM01, 11/136 and 11/137) and *C. reinhardtii* (11/32c). Only three samples showed significantly elevated levels of lipid oxidation. The short-term copper treatment induced lipid oxidation in both 11/32c and PM01, causing an increase of MDA or MDA like by-products to their corresponding controls by 3.8-fold and 3.6-fold respectively. Interestingly, the PM01 long-term copper treatment also caused a significant 4-fold increase in lipid oxidation. There was no significant changes in the levels of lipid oxidation for the other strains of *C. acidophila* 11/136 and 11/137.

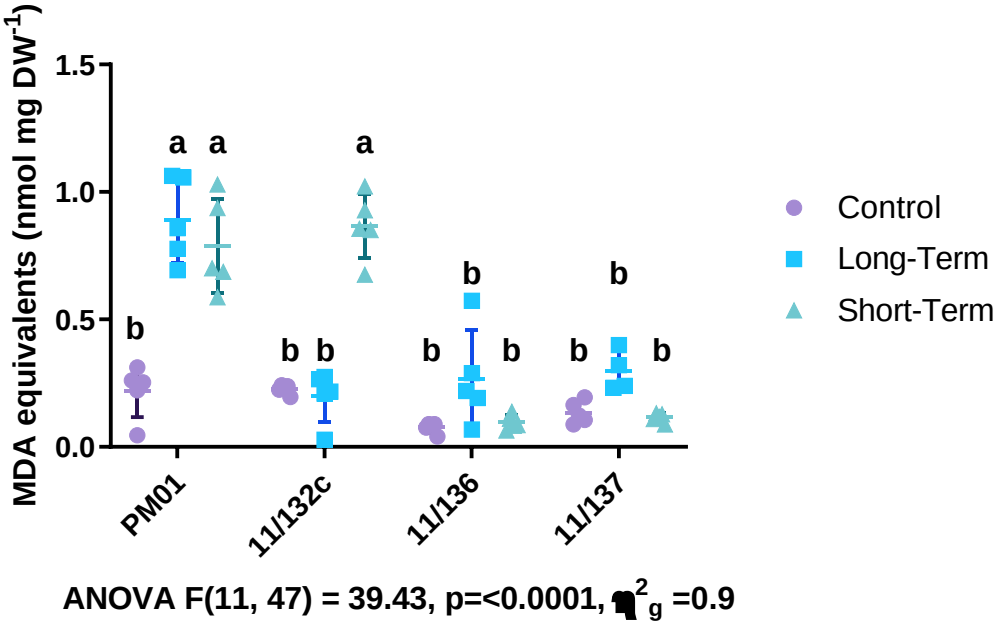

Figure 2.17 Estimations of lipid oxidation by measuring malondialdehyde (MDA) or MDA equivalents detected using the TBARS assay. Three strains of C. acidophila were tested (PM01, 11/136 and 11/137) and C. reinhardtii (11/32c). Five biological replicates were tested for each treatment apart from the long-term treatment for 11/137 which has four, with each biological replicate plotted. The mean and standard deviations are represented by the bars. A one-way ANOVA was performed to test for significance with a Tukeys post-hoc test to find significant differences between treatments.

2.5 Discussion

2.5.1 PM01 can Survive Much Higher Copper Concentrations than Other Microalgae

C. acidophila is an extremophile microalga that has been found to inhabit many acidic and metal-rich water bodies (Dean et al., 2019; Nishikawa and Tominaga, 2001; Olsson et al., 2015; Spijkerman et al., 2007). Due to the diverse range of extreme environments *C. acidophila* has adapted to, it is perhaps unsurprising that the different strains have different traits. *C. acidophila* PM01 was isolated from an acid mine drainage pond within an abandoned open cast copper mine, which had a pH < 2.0 and high concentration of dissolved trace metals including copper within the pond, typically at 60 mg/L (~1 mM Cu) (Dean et al., 2019). Therefore, in order to grow in these conditions, the PM01 strain must be able to tolerate extreme concentrations of copper. However, the *C. acidophila* strains 11/136 and 11/137 were isolated from different environments that were not known to be copper-rich and as such may not have been exposed to the quantities of copper PM01 has adapted to tolerate (Bissinger et al., 2000; Fott and Mccarthy, 1964; Gerloff-Elias et al., 2005). The findings described here, show that PM01 has a greater copper tolerance than 11/136 and 11/137, which struggle to grow in 350 µM Cu and certainly cannot grow in 2 mM Cu, in agreement with my previous analysis (Dean et al., 2019). Another strain of *C. acidophila* (RT46) has been isolated from the Rio Tinto, which shows high heavy metal tolerance, and has been shown to grow up to 500 µm copper. However, the Rio Tinto is known to reach up to 6 mM Cu in places (Olsson et al., 2015), indicating that RT46 may also have adapted tolerance to very high copper exposure. Additionally, *Desmodesmus* sp. AARLG074 has been shown to grow in 50 mg L^{-1} (the equivalent to 790 µM) (Buayam et al., 2019), *Nannochloropsis oculata* has been grown in 250 µM Cu (Martínez-Macias et al., 2019) and *Enteromorpha compressa* was found to grow in 100 µM of copper (Correa et al., 1996). To the best of my knowledge PM01 shows some of the highest tolerance ranges to copper among the green algae, if not the highest, providing a fantastic model to glean insights into the mechanisms of adaptation to a high copper environment. I aimed to find a relative copper stress dose between organisms that was not fully lethal, but impacted cultures growth rate. For *C. acidophila*, a 2 mM copper treatment inhibited culture growth by 52% (if using cell counts) or 28% (if using OD750nm). This is a higher level of inhibition than seen in *C. reinhardtii* however, 11/32c was only exposed to 75 µM of copper. Although a higher inhibition is seen in PM01 at 2 mM of copper the 75 µM copper stress for 11/32c gives a close enough relative comparison for a inhibition. A 100 µM copper stress was tested for 11/32c however, the cultures did not grow (data not shown). It is interesting that the 350 µM copper dose was lethal for the other 2 *C. acidophila* strains, as previous experimental work in our lab has shown they are capable of growth (data not shown). Therefore, for the rest of the experiments using these two strains, and they were exposed to only 300 µM.

2.5.2 Shutting Down Photosynthetic Activity as a Short-Term Tolerance Mechanism to Excess Copper

The PAM data has provided evidence that short term copper stresses inhibits linear electron transport in both species as shown by the reduction in ΦPSII. This response is much more evident in PM01 and occurs at lower actinic light intensities than 11/32c. However, both species are capable of restoring ΦPSII over a long-term copper stress, to the point where there is no difference in ΦPSII between the control and long-term copper treatments. Further, there was no significant reduction in chlorophyll content in any of the copper treatments for both species.

The photosynthetic machinery has been shown to be particularly sensitivity to excess heavy metals, in particular, copper (Küpper et al., 2003). One of the most commonly used stress parameters of photosynthetic organisms is the F_v/F_m ratio. Typically, a decrease in F_v/F_m is indicative of higher stress levels (Maxwell and Johnson, 2000). Interestingly, the short-term copper treatment shows no significant decrease in the F_v/F_m for PM01, although it did show a pattern of diurnal cycling. This is in stark contrast to *C. reinhardtii* which shows the lowest of all F_v/F_m values tested whilst still showing a diurnal pattern. The diurnal pattern was an unexpected result was observed during the experimental procedure. For both species the copper spikes show a diurnal pattern whilst the long-term copper treatment also induces this pattern in PM01. Due to the process of performing photosynthetic parameter measurements in a different laboratory, the cultures (including the control) were exposed to natural light from a window after copper spiking rather than artificial light, so it is possible that any changes in sunlight intensity could be altering the F_v/F_m ratio throughout the day. The lowest dips in F_v/F_m do seem to regularly occur just after midday, where the sunlight levels may be highest and providing the highest stress levels. As there is no apparent pattern seen in either control, it is obvious that the copper is eliciting this response. A similar diurnal pattern has been seen in lichens, where the F_v/F_m reaches its lowest point at 13:00, with the authors attributing it to the high heat and light temperatures of the midday sun (Wu et al., 2013). An opposite response is seen in *Heterosigma akashiwo*, where F_v/F_m started increasing during daylight hours. The authors contributed NPQ and photochemistry changes to this diurnal pattern where they also noticed a similar diurnal pattern of NPQ (Hennige et al., 2013).

It is not clear whether it is changes in photochemistry or external factors that could be influencing these changes in F_v/F_m. It is well known that many, if not all organisms, including microalgae, have some form of internal biological clock, with genes fluctuating throughout the day to help them anticipate for daily cycles of light and darkness (Annunziata et al., 2019; Fustin et al., 2020). It has even been shown that chloroplasts in *C. reinhardtii* show differential gene expression throughout the day (Idoine et al., 2014). Copper replete conditions were shown to alter an internal biological clock of soybeans (Jiang et al., 2006). Okamoto et al. (1999) did suggest that heavy metals affect the biological clock mechanisms, that controls luminescence, of the diatom *Gonyaulax polyedra.* However, they did notice that all the metals tested, including copper, did cause some offset in the regular luminescence of *G. polyedra,* It is very possible that excess copper present in the cell could influence this biological clock and cause changes in the F_v/F_m throughout the day. Olsson et al. (2015) found that the F_v/F_m of another strain of *C. acidophila*, RT46, was 0.57 under control conditions. However, under a 500 µM copper stress for 24 h, there was a minimal change in the maximal quantum efficiency of PSII detected (Olsson et al., 2015), suggesting that it may take longer than 24 hours to elicit the decrease in F_v/F_m seen with the data in this study. A reduction of F_v/F_m was also seen in a *C. reinhardtii* strain (CC-124) at 1, 3 and 5 days after a 250 µM copper stress (Jiang et al., 2016). CC-124 is capable at growing at much higher concentrations of copper than 11/32c. However, both the short and long-term copper stress reduced the F_v/F_m in this study suggesting that *C. reinhardtii* 11/32c is still much more susceptible to copper inhibition of photosynthesis in both the short and long-term compared to PM01. At the point of measurement the cells were dark adapted. As such it is unlikely that high -energy state quenching processes, such as dissipation through carotenoids, would be taking place (Demmig-Adams and Adams, 1990). This leaves two other

alternatives of either photoinhibition (damage to PS II reaction centres), or state transitions. Photoinhibition is a slower and progressive process (Maxwell and Johnson, 2000), so could be a candidate for some of the fluctuations we see in the diurnal pattern that is seen. However, it is unclear if it would happen that quickly over the time course of a day and could warrant further investigation. The other, and most likely candidate are state transitions, in *C. reinhardtii* state transitions are common and can vary on a range of factors such as the redox state of the cell. As they rely on phosphorylation, this process can happen, and reverse quickly (Finazzi, 2005).

Juneau et al. (2002) have previously shown that both *C. reinhardtii* and *Selenastrum capricornutum* are both highly susceptible to copper with the efficiency of PSII reducing significantly upon copper addition. Photo-autotrophic, and, to some extent, photo-heterotrophic organisms, depend on photosynthesis to produce a reliable energy source. Therefore, minimising the impact of copper on the photosynthetic machinery would be paramount to adapting to a high copper environment. This data shows that both PM01 and 11/32c can both maintain high levels Φ PSII under their respective long-term copper treatments (Figure 2.6 and Figure 2.8). Interestingly, the PM01 long-term copper stress loses less efficiency than 11/32c at lower light levels. Kupper et al. (1996) have shown that at lower light intensities there is more heavy metal, particularly copper and zinc, displacement of magnesium in the chlorophylls of Light harvesting complex 2 (LHCII), which they coined the shade-reaction. However, the authors did note that a dark phase period was required after this low light irradiation for the metal displacement to occur. In this experimental procedure cell cultures were spiked with copper and left on a windowsill for 2.5 hours before being dark acclimated for 30 min prior to measurements. It is unclear as to what further low-light irradiance does to chlorophylls that have undergone the shade-reaction, however, it is possible that these lower actinic lights could further exacerbate metal displacement over 3 hours. As PM01 has adapted to a high copper environment it is likely that it may have strategies to either prevent, fix or replace substituted chlorophylls, which could explain why we see high ΦPSII even at lower actinic light intensities. Additionally, this could explain some of the high variation seen between the biological replicates of 11/32c as the metal displacement rates could be variable.

This model could be of great interest for further study as not only could it provide insights for an organism's ability to adapt to copper but also an interesting model to further study the mechanisms of heavy metal displacement in chlorophylls. At the highest actinic light intensities, the reduction in ΦPSII becomes minimal and hard to distinguish. This is likely due to the oversaturation of the electron transport chain and the high light intensity providing a greater stress than copper. However, both the short-term copper stress condition still showed significantly reduced ΦPSII, with PM01 having the lowest level. Even with the additional high light stress, PM01 still reduces its ΦPSII with the addition of copper, suggesting that shutting down PSII is an essential requirement to a short-term adaptation to copper. An obvious question to ask at this point is, if there was no detected PSII activity how are the cells producing energy to survive? Under copper stress, barley has been shown to induce a state transition from state 1 to 2 shifting photosynthetic activity from PSII to PSI (Lysenko et al., 2020). Additionally, PSII was significantly inhibited upon copper stress to *Microcystis aerugeinosa*, but PSI activity was seen to increase concurrently (Deng et al., 2014). This study did not measure any PSI parameters, therefore, it is difficult to say if this is the case with microalgae and there appears to be

very little literature on the subject. However, it is possible that a switch to PSI could provide a less redox intense energy production method.

The NPQ measurements for PM01 could hint to a shift towards PSI being utilised. High NPQ values have been shown throughout all the actinic light intensities but more specifically at lower and higher actinic lights (Figure 2.7 and Figure 2.8). Cyclic electron flow (CEF) is a method of NPQ in which electrons are taken from NADPH or ferrodoxin and cycled through PSI to the plastoquinone pool, whilst driving protons across the thylakoid membrane generating a proton gradient for ATP synthesis (Huang et al., 2018). An increase in PSI activity in response to copper was found to be due to an increase in CEF. The CEF increased in a dose dependent manner with copper (Deng et al., 2014). Whilst this is likely not the only contributing factors to increasing NPQ in copper stressed PM01 it is likely to play a role and could explain the high NPQ values seen. Additionally, CEF around PSI has been found to promote ATP synthesis, and has been suggested to help repair photodamaged PSII (Huang et al., 2018). According to Maxwell and Johnson (2000) as NPQ is calculated as a relative change from the dark-adapted state, if the F_v/F_m values are markedly different between treatments, direct comparisons to NPQ should be avoided. In this case the PM01 F_v/F_m ratios did not markedly change, however, there was a significant reduction between the control and short-term copper treatment in *C. reinhardtii*. With these results where ΦPSII is close to 0, especially for PM01, the NPQ values show very little variation and whilst the values may not be completely true, should give a good estimate to the amount of NPQ happening. Whilst *C. reinhardtii* showed an increasing NPQ with the actinic light levels these did not reach the same levels as PM01, especially at the lower actinic lights. Interestingly, Jiang et al. (2016) have found that NPQ in *C. reinhardtii* decreases in the short-term respective to the control in a time and copper concentration dependent manner until 5 days where the NPQ increases significantly. The results seem to somewhat contradict this as at lower actinic light intensities both the short-term and long-term copper treatments appear to have higher NPQ values than the controls. There are a few caveats to this comparison however, firstly, and most likely is that the time points from this study do not match, NPQ could vary greatly between the time points matched. Additionally, the actinic light intensity was not described, this is important as at higher actinic light intensities smaller NPQ values were seen in the copper treatments when compared to the control. Finally, it appears that the strain of *C. reinhardtii* used by Jiang et al. (2016) could grow at 250 µM copper, so is almost certainly more copper tolerant than the 11/32c strain tested here. It seems that one adaptive mechanism for PM01 to survive high copper conditions, at least in the short-term, is to shut down PSII, possibly through the increase NPQ. This appears to be in stark contrast to the data presented in this study for *C. reinhardtii* and the data shown by Jiang et al. (2016).

The final bit of intrigue from these PAM results are the differences in fluorescence traces in the short-term copper treatments (Figure 2.9 and Figure 2.10). The increase in the steady state fluorescence in a supposedly time-dependent manner. Typically, I waited for the fluorescence to stabilise before taking the ΦPSII and NPQ readings. However as can be seen in the long traces this was impossible, and so readings were taken when the control samples stabilised after 15 mins. A steady decrease in basal fluorescence was seen in algal species exposed to metolachlor over time (Juneau et al., 2001). The basal fluorescence of a desiccation tolerant lichen, *Cladonia borealis*, was much higher than a less desiccation tolerant species of lichen, *Usnea* sp, during periods of drought (Cho et al., 2020).

Whist it is hard to draw parallels between this study and the Cho et. al (2020) study, as *C. borealis* still showed levels of ΦPSII, as opposed to PM01 which effectively shut down PSII under copper stress, it provides an interesting insight into possible mechanisms of stress tolerance. An obvious explanation for this increase in fluorescence could be the upregulation of NPQ. However, this seems unlikely in this study as the increase in basal fluorescence seems to correspond to increasing light intensity between 150 µmol m^{-2} s^{-1} and 350 µmol m^{-2} s^{-1} which shows a negative correlation with the NPQ data. Additionally, the actinic light which exhibited the highest NPQ values, 90 µmol m^{-2} s^{-1} showed no apparent increase in basal fluorescence. This is a fascinating area for further study which could provide greater insights into an extremophile photosynthetic response to copper.

2.5.3 ROS Detection Kits May Not be Accurate for Photosynthetic Organisms

Using the ROS detection kit gave us interesting results, what was most striking is that the copper stress seemingly caused a decrease in ROS according to the data. This would be in contrast to most, if not all published data, as many studies have described an increase in ROS generation when exposed to copper stress (Che et al., 2018; Janani et al., 2020; Sabatini et al., 2009). Arsenic, cadmium and silver nanoparticles have also been found to increase ROS generation in *C. acidophila* (Díaz et al., 2020; Oukarroum et al., 2014). As a result, it seems hard to justify that the ROS decreased in all tested strains, even *C. reinhardtii*. When the H_2O_2 standards were ran the highest fluorescence intensity was 10000, a much lower than many ROS measurements for the microalgal samples. This hints that there could be some background interference in the detectable fluorescence coming of the microalgae. Considering that there is a complete reduction in fluorescence, for PM01, with the stain after copper exposure, the most obvious candidate would be that chlorophyll could be being detected. However, the fluorescence detection range was 520 nm, whilst chlorophyll fluoresces around the 450 nm and 700 nm range (Pfündel, 2021; Ritchie and Sma-Air, 2020). It is unclear what we could be detecting at the 520 nm range, but there is obviously some cellular interference making this particular ROS stain unreliable for detecting ROS in microalgal strains. The fact that we see a steep drop off as with the photosynthetic parameters in PM01, leads me to believe that it could be something related to photosynthesis we are detecting. However, with the present data it is impossible to come to any conclusions. Electron Paramagnetic resonance spin trapping (EPR) spectroscopy has previously been used to detect ROS as well as reactive nitrogen species ,this could be a more accurate method of detection in the future (Villamena and Zweier, 2004).

2.5.4 ROS Enzyme Activity Hints at PM01 Having a Greater Antioxidant Capabilities

Catalase activity has previously been shown to increase in multiple microalgae species when exposed to copper (Chen et al., 2016; Sabatini et al., 2011, 2009). Whilst the copper appears to cause an increase in CAT activity in *C. reinhardtii*, although not significant, it significantly decreases CAT activity in PM01. The PM01 control showed the highest level of CAT activity, interestingly, CAT activity significant decreased in the long-term copper treatment suggesting there is less of a need for antioxidative capability. It could also be possible that low copper levels could be inducing stress on PM01 under 'control' conditions. Despite there being only a minor transcript decrease in the long-term copper treatment for PM01 compared to the control this equated to a large decrease in CAT activity. This could suggest that either the transcripts are not being converted to protein or that some post-translational modifications may prevent the PM01 CAT1 enzyme becoming fully active. Chen et al. (2016) did find that there is not a linear relationship between copper concentration and CAT

activity. Concentrations above 2 µM actually started to decrease CAT activity to the extent that 5 µM copper conditions actually decreased CAT activity when compared to the control. Unfortunately, due to time constraints I was not able to get the short-term copper stress CAT assays working as they showed the highest transcript abundance and it would have been interesting to see if this was converted into CAT activity. A loss of CAT activity could result from damage to the enzyme in a high H_2O_2 environment. Further studies could determine if there was a loss or degradation of protein, using Western Blots or mass spectrometry to look for fragments of the protein.

SOD activity has also been shown to increase with increasing copper concentrations (Chen et al., 2016; Piotrowska-Niczyporuk et al., 2012; Wang et al., 2018). The data appears to have shown that with both copper treatments seemingly increasing SOD activity, however, only the *C. reinhardtii* SOD activity was significantly increased. Comparing SOD transcript abundance to activity is more complicated due to the many different isoforms identified. Between the control and long-term copper treatments there does not appear to be much difference in the transcript abundance. Again, it is unfortunate the short-term treatments assays could not be performed as they may have solicited a stronger response based on the transcriptomic data set. The isoelectric focussing identified interesting differences between PM01 and 11/32c. Firstly 11/32c has an extra MnSOD isoform than PM01. The SOD isozymes identified in *C. reinhardtii* confer with most of the literature, I identified an additional Mn and FeSOD than Sakurai' et al. (1993) and one additional FeSOD than Kitayama et al. (1999). To the best of my knowledge this is the first attempt at identifying SOD isozymes in *C. acidophila*. Interestingly, an additional isozyme was potentially found in the protein fraction than in the RNA-seq experiment. However, the migration of this protein could be altered due to post-translational modifications, therefore, sequencing the protein would be needed to investigate this further.

The most interesting difference between *C. acidophila* and *C. reinhardtii* is the pI differences between the FeSOD isozymes. When the protein sequences of the FeSOD isozymes were compared the sequences are not highly divergent. There actually appears to be a greater difference in the protein sequence between Cre17.g703176 and Cre10.g436050. The pI is mainly determined by the charged amino acids glutamate, aspartate, cysteine, tyrosine, histidine, lysine and arginine (Kozlowski, 2017). This could suggest that some form of post-translational modification could be happening to cause a change in pI between the two FeSODs. Alternatively the extraction process could have also differentially affected one species isoform of the FeSOD (Pace et al., 2009). The *C. acidophila* FeSOD isoforms are found at a pI of 1-2, indicating that they are acidic. It is important to note that whilst *C. acidophila* is found in a highly acidic environment, all acidophiles have a near neutral internal pH (Spijkerman, 2011). Most FeSODs are found either in the cytoplasm or within the stroma of the chloroplast associated to PSI (Wolfe-Simon et al., 2005). It could be possible that either one or both the *C. acidophila* FeSOD have moved to the thylakoid lumen side of the chloroplast, where the pH is lower, and having an acidic charge provides better function. Given that we have already seen PM01 and 11/32c behave very differently in the presence of copper it is well within reason that the FeSOD isoforms associated in the chloroplast may have evolved different properties to alter its function, causing the different pIs observed.

2.5.5 Lipid Oxidation- A By-Product or Tolerance Mechanism?

Copper inhibits photosynthetic electron transport creating superoxide radical and catalyses the destruction of unsaturated membrane fatty acids (Sandmann and Böger, 1980). A by-product of lipid oxidation is malondialdehyde, which was detected using the TBARs assay. Interestingly, PM01 showed the highest levels of lipid peroxidation for both copper treatments. An increase in lipid oxidation is seen across many species in response to copper (Chen et al., 2016; Jiang et al., 2016). Extremely high levels of copper have actually been found to reduce lipid oxidation, whilst 4 µM copper was sufficient to significantly increase MDA content in *C. vulgaris*, 5 µM actually significantly reduced MDA when compared to the control (Chen et al., 2016). To the best of my knowledge this is the first study to assess the MDA content in *C. acidophila.* It is fascinating that even in the long-term copper stress we still see higher levels of lipid oxidation when compared to other strains of *C. acidophila* and *C. reinhardtii*. This leads to two possible conclusions, either PM01 cannot control ROS generation, leading to the oxidation of lipids but has other methods of preventing ROS damaging core processes or there are some form of "sacrificial" lipids that could form the basis of the antioxidant defence in PM01, preventing greater damage to more central molecules. This would require further study to identify the key lipids being oxidised to gain any further insight.

2.6 Conclusion

PM01 exhibits a much higher copper tolerance to 11/32c and PM01 differs in many ways to 11/32c both physiologically and biochemically. The abrupt loss of ΦPSII under a short-term copper stress in PM01 is stark response, and a surprising finding. As are the high lipid oxidation levels seen in PM01 for both a short-term and long-term copper stress. Whereas 11/32c only exhibits high lipid oxidation levels under a short-term copper stress.

2.7 References

Annunziata, R., Ritter, A., Fortunato, A.E., Manzotti, A., Cheminant-Navarro, S., Agier, N., Huysman, M.J.J., Winge, P., Bones, A.M., Bouget, F.Y., Lagomarsino, M.C., Bouly, J.P., Falciatore, A., 2019. BHLH-PAS protein RITMO1 regulates diel biological rhythms in the marine diatom Phaeodactylum tricornutum. Proc. Natl. Acad. Sci. U. S. A. 116, 13137–13142. https://doi.org/10.1073/pnas.1819660116

Bazihizina, N., Colzi, I., Giorni, E., Mancuso, S., Gonnelli, C., 2015. Photosynthesizing on metal excess: Copper differently induced changes in various photosynthetic parameters in copper tolerant and sensitive Silene paradoxa L. populations. Plant Sci. 232, 67–76. https://doi.org/10.1016/j.plantsci.2014.12.015

Bissinger, V., Jander, J., Tittel, J., 2000. A New Medium Free of Organic Carbon to Cultivate Organisms from Extremely Acidic Mining Lakes (pH 2.7). Acta Hydrochim. Hydrobiol. 28, 310–312. https://doi.org/10.1002/1521-401X(200012)28:6<310::AID-AHEH310>3.0.CO;2-H

Buayam, N., Davey, M.P., Smith, A.G., Pumas, C., 2019. Effects of copper and pH on the growth and physiology of Desmodesmus sp. AARLG074. Metabolites 9, 84. https://doi.org/10.3390/metabo9050084

Che, X., Ding, R., Li, Y., Zhang, Z., Gao, H., Wang, W., 2018. Mechanism of long-term toxicity of CuO NPs to microalgae. Nanotoxicology 12, 923–939. https://doi.org/10.1080/17435390.2018.1498928

Chen, Z., Song, S., Wen, Y., Zou, Y., Liu, H., 2016. Toxicity of Cu (II) to the green alga Chlorella vulgaris: a perspective of photosynthesis and oxidant stress. Environ. Sci. Pollut. Res. 23, 17910–17918. https://doi.org/10.1007/s11356-016-6997-2

Cho, S.M., Lee, H., Hong, S.G., Lee, J., 2020. Study of ecophysiological responses of the antarctic fruticose lichen cladonia borealis using the PAM fluorescence system under natural and laboratory conditions. Plants 9, 85. https://doi.org/10.3390/plants9010085

Choo, K.S., Snoeijs, P., Pedersén, M., 2004. Oxidative stress tolerance in the filamentous green algae Cladophora glomerata and Enteromorpha ahlneriana. J. Exp. Mar. Bio. Ecol. 298, 111–123. https://doi.org/10.1016/j.jembe.2003.08.007

Correa, J.A., González, P., Sánchez, P., Muñoz, J., Orellana, M.C., 1996. Copper-algae interactions: Inheritance or adaptation? Environ. Monit. Assess. 40, 41–54. https://doi.org/10.1007/BF00395166

Dean, A.P., Hartley, A., McIntosh, O.A., Smith, A., Feord, H.K., Holmberg, N.H., King, T., Yardley, E., White, K.N., Pittman, J.K., 2019. Metabolic adaptation of a Chlamydomonas acidophila strain isolated from acid mine drainage ponds with low eukaryotic diversity. Sci. Total Environ. 647, 75–87. https://doi.org/10.1016/j.scitotenv.2018.07.445

Demmig-Adams, B., Adams, W.W., 1990. The carotenoid zeaxanthin and “high-energy-state quenching” of chlorophyll fluorescence. Photosynth. Res. 25, 187–197. https://doi.org/10.1007/BF00033160

Deng, C., Pan, X., Wang, S., Zhang, D., 2014. Cu2+ inhibits photosystem II activities but enhances photosystem I quantum yield of Microcystis aeruginosa. Biol. Trace Elem. Res. 160, 268–275. https://doi.org/10.1007/s12011-014-0039-z

Díaz, S., de Francisco, P., Olsson, S., Aguilera, Á., González-Toril, E., Martín-González, A., 2020. Toxicity, physiological, and ultrastructural effects of arsenic and cadmium on the extremophilic microalga Chlamydomonas acidophila. Int. J. Environ. Res. Public Health 17, 1650. https://doi.org/10.3390/ijerph17051650

Fernandes, J.C., Henriques, F.S., 1991. Biochemical, physiological, and structural effects of excess copper in plants. Bot. Rev. 57, 246–273. https://doi.org/10.1007/BF02858564

Finazzi, G., 2005. The central role of the green alga Chlamydomonas reinhardtii in revealing the mechanism of state transitions, in: Journal of Experimental Botany. Oxford Academic, pp. 383–388. https://doi.org/10.1093/jxb/erh230

Fott, B., Mccarthy, A.J., 1964. Three Acidophilic Volvocine Flagellates in Pure Culture. J. Protozool. 11, 116–120. https://doi.org/10.1111/j.1550-7408.1964.tb01731.x

Foyer, C.H., 2018. Reactive oxygen species, oxidative signaling and the regulation of photosynthesis. Environ. Exp. Bot. 154, 134- 142. https://doi.org/10.1016/j.envexpbot.2018.05.003

Fustin, J.M., Ye, S., Rakers, C., Kaneko, K., Fukumoto, K., Yamano, M., Versteven, M., Grünewald, E., Cargill, S.J., Tamai, T.K., Xu, Y., Jabbur, M.L., Kojima, R., Lamberti, M.L., Yoshioka-Kobayashi, K., Whitmore, D., Tammam, S., Howell, P.L., Kageyama, R., Matsuo, T., Stanewsky, R., Golombek, D.A., Johnson, C.H., Kakeya, H., van Ooijen, G., Okamura, H., 2020. Methylation deficiency disrupts biological rhythms from bacteria to humans. Commun. Biol. 3, 211. https://doi.org/10.1038/s42003-020-0942-0

Galván, L., Olías, M., Cerón, J.C., de Villarán, R.F., 2021. Inputs and fate of contaminants in a reservoir with circumneutral water affected by acid mine drainage. Sci. Total Environ. 762, 143614. https://doi.org/10.1016/j.scitotenv.2020.143614

Gerloff-Elias, A., Spijkerman, E., Pröschold, T., 2005. Effect of external pH on the growth, photosynthesis and photosynthetic electron transport of Chlamydomonas acidophila Negoro, isolated from an extremely acidic lake (pH 2.6). Plant, Cell Environ. 28, 1218–1229. https://doi.org/10.1111/j.1365-3040.2005.01357.x

Gross, W., 2000. Ecophysiology of algae living in highly acidic environments. Hydrobiologia 433, 31–37. https://doi.org/10.1023/A:1004054317446

Griffiths, M.J., Garcin, C., van Hille, R.P., Harrison, S.T.L., 2011. Interference by pigment in the estimation of microalgal biomass concentration by optical density. J. Microbiol. Methods 85, 119–123. https://doi.org/10.1016/j.mimet.2011.02.005

Halliwell, B., 2006. Reactive species and antioxidants. Redox biology is a fundamental theme of aerobic life. Plant Physiol. 141, 312–322. https://doi.org/10.1104/pp.106.077073

Harris, E.H., 2009. The Chlamydomonas Sourcebook. Academic Press, San Diego.

Hennige, S.J., Coyne, K.J., Macintyre, H., Liefer, J., Warner, M.E., 2013. The Photobiology of Heterosigma akashiwo. Photoacclimation, Diurnal Periodicity, and its Ability to Rapidly Exploit Exposure to High Light. J. Phycol. 49, 349–360. https://doi.org/10.1111/jpy.12043

Hodges, D.M., DeLong, J.M., Forney, C.F., Prange, R.K., 1999. Improving the thiobarbituric acid-reactive-substances assay for estimating lipid peroxidation in plant tissues containing anthocyanin and other interfering compounds. Planta 207, 604–611. https://doi.org/10.1007/s004250050524

Huang, W., Yang, Y.J., Zhang, S.B., Liu, T., 2018. Cyclic electron flow around photosystem i promotes ATP synthesis possibly helping the rapid repair of photodamaged photosystem ii at low light. Front. Plant Sci. 9, 239. https://doi.org/10.3389/fpls.2018.00239

Idoine, A.D., Boulouis, A., Rupprecht, J., Bock, R., 2014. The Diurnal Logic of the Expression of the Chloroplast Genome in Chlamydomonas reinhardtii. PLoS One 9, e108760. https://doi.org/10.1371/journal.pone.0108760

Janani, B., Al Farraj, D.A., Raju, L.L., Elshikh, M.S., Alkubaisi, N.A., Thomas, A.M., Das, A., Sudheer Khan, S., 2020. Cytotoxicological evaluation of copper oxide nanoparticles on green algae, bacteria and crustacean systems. J. Environ. Heal. Sci. Eng. 18, 1465–1472. https://doi.org/10.1007/s40201-020-00561-1

Jiang, Y., Zhu, Y., Hu, Z., Lei, A., Wang, J., 2016. Towards elucidation of the toxic mechanism of copper on the model green alga Chlamydomonas reinhardtii. Ecotoxicology 25, 1417–1425. https://doi.org/10.1007/s10646-016-1692-0

Jiang, Z., Morré, D.M., Morré, D.J., 2006. A role for copper in biological time-keeping. J. Inorg. Biochem. 100, 2140–2149. https://doi.org/10.1016/j.jinorgbio.2006.08.007

Juneau, P., Dewez, D., Matsui, S., Kim, S.G., Popovic, R., 2001. Evaluation of different algal species sensitivity to mercury and metolachlor by PAM-fluorometry. Chemosphere 45, 589–598.

https://doi.org/10.1016/S0045-6535(01)00034-0

Juneau, P., El Berdey, A., Popovic, R., 2002. PAM fluorometry in the determination of the sensitivity of Chlorella vulgaris, Selenastrum capricornutum, and Chlamydomonas reinhardtii to copper. Arch. Environ. Contam. Toxicol. 42, 155–164. https://doi.org/10.1007/s00244-001-0027-0

Kitayama, K., Kitayama, M., Osafune, T., Togasaki, R.K., 1999. Subcellular localization of iron and manganese superoxide dismutase in Chlamydomonas reinhardtii (Chlorophyceae). J. Phycol. 35, 136–142. https://doi.org/10.1046/j.1529-8817.1999.3510136.x

Kozlowski, L.P., 2017. Proteome-pI: Proteome isoelectric point database. Nucleic Acids Res. 45, D1112–D1116. https://doi.org/10.1093/nar/gkw978

Küpper, H., Küpper, F., Spiller, M., 1996. Environmental relevance of heavy metal-substituted chlorophylls using the example of water plants. J. Exp. Bot. 47, 259–266. https://doi.org/10.1093/jxb/47.2.259

Küpper, H., Šetlík, I., Šetliková, E., Ferimazova, N., Spiller, M., Küpper, F.C., 2003. Copper-induced inhibition of photosynthesis: Limiting steps of in vivo copper chlorophyll formation in Scenedesmus quadricauda. Funct. Plant Biol. 30, 1187–1196. https://doi.org/10.1071/FP03129

Küpper, H., Šetlík, I., Spiller, M., Küpper, F.C., Prášil, O., 2002. Heavy metal-induced inhibition of photosynthesis: Targets of in vivo heavy metal chlorophyll formation. J. Phycol. 38, 429–441. https://doi.org/10.1046/j.1529-8817.2002.t01-1-01148.x

Li, M., Hu, C., Zhu, Q., Chen, L., Kong, Z., Liu, Z., 2006. Copper and zinc induction of lipid peroxidation and effects on antioxidant enzyme activities in the microalga Pavlova viridis (Prymnesiophyceae). Chemosphere 62, 565–572. https://doi.org/10.1016/j.chemosphere.2005.06.029

Lichtenthaler, H.K., Wellburn, A.R., 1983. Determinations of total carotenoids and chlorophylls a and b of leaf extracts in different solvents. Biochem. Soc. Trans. 11, 591–592. https://doi.org/10.1042/bst0110591

Lysenko, E.A., Klaus, A.A., Kartashov, A. V., Kusnetsov, V. V., 2020. Specificity of Cd, Cu, and Fe effects on barley growth, metal contents in leaves and chloroplasts, and activities of photosystem I and photosystem II. Plant Physiol. Biochem. 147, 191–204. https://doi.org/10.1016/j.plaphy.2019.12.006

Martínez-Macias, M. del R., Correa-Murrieta, M.A., Villegas-Peralta, Y., Dévora-Isiordia, G.E., Álvarez-Sánchez, J., Saldivar-Cabrales, J., Sánchez-Duarte, R.G., 2019. Uptake of copper from acid mine drainage by the microalgae Nannochloropsis oculata. Environ. Sci. Pollut. Res. 26, 6311–6318. https://doi.org/10.1007/s11356-018-3963-1

Maxwell, K., Johnson, G.N., 2000. Chlorophyll fluorescence--a practical guide. J. Exp. Bot. 51, 659–668. https://doi.org/10.1093/jexbot/51.345.659

Mehta, R., Templeton, D.M., O'Brien, P.J., 2006. Mitochondrial involvement in genetically determined transition metal toxicity. II. Copper toxicity. Chem. Biol. Interact. 163, 77–85. https://doi.org/10.1016/j.cbi.2006.05.011

Nalewajko, C., Colman, B., Olaveson, M., 1997. Effects of pH on growth, photosynthesis, respiration, and copper tolerance of three Scenedesmus strains. Environ. Exp. Bot. 37, 153–160. https://doi.org/10.1016/S0098-8472(96)01029-5

Nalewajko, C., Olaveson, M.M., 1995. Differential responses of growth, photosynthesis, respiration, and phosphate uptake to copper in copper-tolerant and copper-intolerant strains of Scenedesmus acutus (Chlorophyceae). Can. J. Bot. 73, 1295–1303. https://doi.org/10.1139/b95-141

Nishikawa, K., Tominaga, N., 2001. Isolation, growth, ultrastructure, and metal tolerance of the green alga, Chlamydomonas acidophila (Chlorophyta). Biosci. Biotechnol. Biochem. 65, 2650- 2656. https://doi.org/10.1271/bbb.65.2650

Okamoto, O.K., Shao, L., Woodland Hastings, J., Colepicolo, P., 1999. Acute and chronic effects of

toxic metals on viability, encystment and bioluminescence in the dinoflagellate Gonyaulax polyedra. Comp. Biochem. Physiol. - C Pharmacol. Toxicol. Endocrinol. 123, 75–83. https://doi.org/10.1016/S0742-8413(99)00013-4

Olaveson, M.M., Stokes, P.M., 1989. Responses of the acidophilic alga *Euglena mutabilis* (euglenophyceae) to carbon enrichment at pH 3. J. Phycol. 25, 529–539. https://doi.org/10.1111/j.1529-8817.1989.tb00259.x

Olsson, S., Puente-Sánchez, F., Gómez, M.J., Aguilera, A., 2015. Transcriptional response to copper excess and identification of genes involved in heavy metal tolerance in the extremophilic microalga Chlamydomonas acidophila. Extremophiles 19, 657–672. https://doi.org/10.1007/s00792-015-0746-1

Oukarroum, A., Samadani, M., Dewez, D., 2014. Influence of pH on the toxicity of silver nanoparticles in the green alga Chlamydomonas acidophila. Water. Air. Soil Pollut. 225, 2038. https://doi.org/10.1007/s11270-014-2038-2

Ouzounidou, G., Symeonidis, L., Babalonas, D., Karataglis, S., 1994. Comparative Responses of a Copper-tolerant and a Copper-sensitive Population of Minuartia hirsuta to Copper Toxicity. J. Plant Physiol. 144, 109–115. https://doi.org/10.1016/S0176-1617(11)81001-1

Pace, C.N., Grimsley, G.R., Scholtz, J.M., 2009. Protein ionizable groups: pK values and their contribution to protein stability and solubility. J. Biol. Chem. 284, 13285- 13289. https://doi.org/10.1074/jbc.R800080200

Pätsikkä, E., Kairavuo, M., Šeršen, F., Aro, E.M., Tyystjärvi, E., 2002. Excess copper predisposes photosystem II to photoinhibition in vivo by outcompeting iron and causing decrease in leaf chlorophyll. Plant Physiol. 129, 1359–1367. https://doi.org/10.1104/pp.004788

Pfündel, E.E., 2021. Simultaneously measuring pulse-amplitude-modulated (PAM) chlorophyll fluorescence of leaves at wavelengths shorter and longer than 700 nm. Photosynth. Res. 147, 345–358. https://doi.org/10.1007/s11120-021-00821-7

Piotrowska-Niczyporuk, A., Bajguz, A., Zambrzycka, E., Godlewska-żyłkiewicz, B., 2012. Phytohormones as regulators of heavy metal biosorption and toxicity in green alga Chlorella vulgaris (Chlorophyceae). Plant Physiol. Biochem. 52, 52–65. https://doi.org/10.1016/j.plaphy.2011.11.009

Puente-Sánchez, F., Olsson, S., Aguilera, A., 2016. Comparative Transcriptomic Analysis of the Response of Dunaliella acidophila (Chlorophyta) to Short-Term Cadmium and Chronic Natural Metal-Rich Water Exposures. Microb. Ecol. 72, 595–607. https://doi.org/10.1007/s00248-016-0824-7

Ritchie, R.J., Sma-Air, S., 2020. Solvent-free chlorophyll spectrometry in unicellular algal research. J. Appl. Phycol. 32, 2711–2723. https://doi.org/10.1007/s10811-020-02233-x

Sabatini, S.E., Juárez, Á.B., Eppis, M.R., Bianchi, L., Luquet, C.M., Ríos de Molina, M. del C., 2009. Oxidative stress and antioxidant defenses in two green microalgae exposed to copper. Ecotoxicol. Environ. Saf. 72, 1200–1206. https://doi.org/10.1016/j.ecoenv.2009.01.003

Sabatini, S.E., Leonardi, P.I., Rodríguez, M.C., 2011. Responses to sublethal copper exposure in two strains of Chlamydomonas reinhardtii (Volvocales, Chlorophyceae) in autotrophic and mixotrophic conditions. Phycologia 50, 78–88. https://doi.org/10.2216/09-101.1

Sakurai, H., Kusumoto, N., Kitayama, K., Togasaki, R.K., 1993. Isozymes of superoxide dismutase in chlamydomonas and purification of one of the major isozymes containing fe. Plant Cell Physiol. 34, 1133–1137. https://doi.org/10.1093/oxfordjournals.pcp.a078528

Sandmann, G., Böger, P., 1980. Copper-mediated Lipid Peroxidation Processes in Photosynthetic Membranes. Plant Physiol. 66, 797–800. https://doi.org/10.1104/pp.66.5.797

Sharma, P., Jha, A.B., Dubey, R.S., Pessarakli, M., 2012. Reactive Oxygen Species, Oxidative Damage, and Antioxidative Defense Mechanism in Plants under Stressful Conditions. J. Bot. 2012, 1–26. https://doi.org/10.1155/2012/217037

Spijkerman, E., 2011. The expression of a carbon concentrating mechanism in Chlamydomonas

acidophila under variable phosphorus, iron, and CO2 concentrations, in: Photosynthesis Research. Springer Netherlands, pp. 179–189. https://doi.org/10.1007/s11120-010-9607-z

Spijkerman, E., Barua, D., Gerloff-Elias, A., Kern, J., Gaedke, U., Heckathorn, S.A., 2007. Stress responses and metal tolerance of Chlamydomonas acidophila in metal-enriched lake water and artificial medium. Extremophiles 11, 551–562. https://doi.org/10.1007/s00792-007-0067-0

Stoiber, T.L., Shafer, M.M., Armstrong, D.E., 2013. Induction of reactive oxygen species in chlamydomonas reinhardtii in response to contrasting trace metal exposures. Environ. Toxicol. 28, 516–523. https://doi.org/10.1002/tox.20743

Szivák, I., Behra, R., Sigg, L., 2009. Metal-induced reactive oxygen species production in chlamydomonas reinhardtii (chlorophyceae). J. Phycol. 45, 427–435. https://doi.org/10.1111/j.1529-8817.2009.00663.x

Villamena, F.A., Zweier, J.L., 2004. Detection of Reactive Oxygen and Nitrogen Species EPR Spin Trapping. Antioxidants Redox Signal. 6, 619-629. https://doi.org/10.1089/152308604773934387

Wang, H., Ebenezer, V., Ki, J.S., 2018. Photosynthetic and biochemical responses of the freshwater green algae Closterium ehrenbergii Meneghini (Conjugatophyceae) exposed to the metal coppers and its implication for toxicity testing. J. Microbiol. 56, 426–434. https://doi.org/10.1007/s12275-018-8081-8

Wolfe-Simon, F., Grzebyk, D., Schofield, O., Falkowski, P.G., 2005. The role and evolution of superoxide dismutases in algae. J. Phycol. 41, 4553-465. https://doi.org/10.1111/j.1529-8817.2005.00086.x

Wu, L., Zhang, G., Lan, S., Zhang, D., Hu, C., 2013. Microstructures and photosynthetic diurnal changes in the different types of lichen soil crusts. Eur. J. Soil Biol. 59, 48–53. https://doi.org/10.1016/j.ejsobi.2013.10.001

Ye, N., Li, H., Zhu, G., Liu, Y., Liu, R., Xu, W., Jing, Y., Peng, X., Zhang, J., 2014. Copper suppresses abscisic acid catabolism and catalase activity, and inhibits seed germination of rice. Plant Cell Physiol. 55, 2008–2016. https://doi.org/10.1093/pcp/pcu136

3 Metabolic Responses of *Chlamydomonas acidophila* and *Chlamydomonas reinhardtii* to Copper

3.1 Abstract

A whole host of metabolites have been found to play important roles in organisms in response to a variety of abiotic stresses. Several biochemical and physiological differences were identified between the extremophile microalga *C. acidophila* (PM01) and the model organism *C. reinhardtii*. To get a better understanding of some of these differences and to further elucidate adaptations of PM01 to copper we utilise broad scale metabolomic approaches to understand metabolic changes under a copper stress. Firstly, a high throughput FT-IR spectroscopy approach allowed us to do a rapid screening and assess changes in an array of biomolecules such as lipids, carbohydrates and proteins. FT-IR spectroscopy data identified an increase in protein and decrease in lipid and carbohydrate content in both organisms under a long-term copper stress. To assess this protein content change further MALDI-TOF spectroscopy was used as a rapid proteomic screen, with minimal processing required. I identified several protein peaks appearing in the long-term copper stress in both organisms. One peak with a high m/z also shows an equivalent peak if it were doubly charged suggesting it may play a role in oxidation-reduction reactions. Finally, a broad scale, untargeted metabolomic approach was employed to identify possible metabolites involved in PM01's adaption to copper. From it was identified that glutathione plays an important role in the response to copper in both organisms, although PM01 appears to show more pathways involved in glutathione metabolism were upregulated in response to copper. The two organisms appear to differ in amino acid preferences, with *C. reinhardtii* appearing to favour amino acids such as methionine in response to copper whilst PM01 upregulates amino acids such as proline.

3.2 Introduction

Chapter 2 focussed on some of the physiological capabilities of *Chlamydomonas acidophila* and *Chlamydomonas reinhardtii* under both a short-term and long-term copper stress. These gave novel insights into some of the biological processes that were occurring inside the cell. However, there are too many biological processes to measure in a reasonable time frame and a more rapid method of analysis is needed to identify other key processes that could be worth investigating further.

Fourier Transform Infrared (FT-IR) spectroscopy is one such method used for the rapid detection of biomolecules such as lipids, carbohydrates nucleic acids and proteins. Different functional groups that characterise these biomolecules will stretch and vibrate at specific infrared light intensities (D'Souza et al., 2008), meaning that we can detect absorbance of the infrared light at specific wavelengths to determine the molecular make up of a particular sample. Additionally, the only sample processing required is to dry the biomass prior to measurement as water can interfere with vibrational absorbance, so needs to be completely removed from the sample. FT-IR spectroscopy has been used for characterisation of microalgae in many studies. Both Dean et al. (2010) and Driver et al. (2015) found shifts and changes in lipid peak intensities in response to nutrient stress by *C. reinhardtii*. FT-IR spectroscopy has also been used to identify different growth stages of the diatom *Ditylum brightwellii*, although the authors did note that Raman spectroscopy could confer a greater accuracy than FT-IR spectroscopy (Rüger et al., 2016). FT-IR spectroscopy has even been used to assess metal impacts such as cadmium or CuO nanoparticles on microalgae (D'Souza et al., 2008; Fazelian et al., 2019). This rapid characterisation of functional groups that might be important in the response to abiotic stresses means FT-IR spectroscopy provides an exciting tool to give insights into the metal adaptation of *C. acidophila*.

Another fingerprinting technique that can provide rapid insights into cells is Matrix Assisted Laser Desorption/Ionisation- Time of Flight Mass Spectroscopy (MALDI-TOF-MS). Following mixing of a cell sample on an artificial, energy absorbent, organic matrix, the samples are then ionised. The desorption and ionisation of samples generates typically singly protonated ions from analytes which can then be separated by their mass to charge ration (m/z) using a mass spectrometer (Singhal et al., 2015). MALDI-TOF has previously been used to characterise and identify microalgae (Barbano et al., 2015; Emami et al., 2015) and extracellular polymeric substances (EPS) (Mishra et al., 2011). MALDI-TOF analysis of *Escherichia coli* exposed to copper found an increase in copper-binding proteins with a concurrent decrease in lipids (Calvano et al., 2016). In these studies, a fingerprint of the samples was easily obtained with little sample preparation required. However, more extensive sample preparation, including protein extraction and digestion, combined with MALDI-TOF techniques, can provide full proteomic information, including the identification of proteins. This has been undertaken in many studies including ones looking into the proteomic response of an acidophilic *Chlamydomonas* sp. (Cid et al., 2010; Lee et al., 2006). Cid et al. (2010), identified a reduction in photosynthetic proteins, complementing the physiological data seen in chapter 2, alongside an increase in stress response proteins such as heat-shock proteins (HSP).

Finally, protein-mediated processes are not the only method of detoxification occurring inside the cells when exposed to metals. The amino acid proline, an osmolyte has been suggested to confer tolerance in *Vigna radiata* to nickel (Yusuf et al., 2012). Copper stresses were also seen to induce

an increase in a host of amino acids, including cysteine, valine, lysine, isoleucine, leucine and methionine alongside other metabolites such as fatty acids and oxylipins in the brown alga *Ectocarpus siliculosus* (Ritter et al., 2014a). An NMR- based metabolomics experiment identified a rapid decrease in the GSH/ GSSG ratio in copper spiked conditions, an indication of oxidative stress, but also determined an absence of phytochelatins and increase in EPS, suggesting that copper is immobilised outside of the cell during the copper response by *Chlorella* sp, (Zhang et al., 2015). Interestingly, the metabolite responses might not always be as expected. Major lichen secondary metabolites atranorin and stictic acid are reported to be associated with heavy metal adsorption. However, the copper hyperaccumulator lichen species *Stereocaulon japonicum,* was found to decrease these metabolites under copper exposure (Nakajima et al., 2019). A study into another copper accumulator *Celosia argentea* found that elevated sugar, polyamines, and organic acid content could help mitigate oxidative stress, whilst organic acids and amino acids such as proline, aspartic acid and glutamic acid may be playing a role in chelating copper (Wang et al., 2021).

While LC- and GC-MS approaches have been used extensively to examine metabolites in microalgae under various conditions, no (or few) studies have used these techniques to understand metal stress response processes. Mass spectrometry methods such as liquid chromatography (LC) -MS or gas chromatography (GC)-MS have long been used as a method of metabolite analysis (Fiehn, 2016). Nuclear magnetic resonance (NMR) has been used to study metabolic changes in *C. reinhardtii* exposed to copper, however, the authors stated that this methodology did not give as high a sensitivity as they were hoping for analysis (Jamers et al., 2013). Another NMR based metabolomic approach, coupled with GC-MS analysis in cucumber exposed to revealed several interesting metabolite changes in response to copper. In the roots a metabolites involved in alanine glutamate and aspartate were upregulated in response to copper, as well as ROS quenching metabolites such as ascorbate and phenolic compounds. Interestingly, citric acid was down-regulated to reduce copper mobilisation (Zhao et al., 2016). A broad scale metabolomic experiment of biofilms in AMD found that taurine, ectoine, and hydroxyectoine play important roles in both acid and metal tolerance of the microbial community. However, many of the metabolites could not be identified and could represent a fantastic source of novel biomolecules with the potential for an array of applications (Mosier et al., 2013). Currently, there are very few untargeted metabolite studies looking into the effects of copper on microalgae, and to the best of my knowledge, none looking into the metabolic responses of extremophile microalgae to a highly acidic and copper polluted environment.

To understand the full adaptation mechanisms of PM01 to a high copper environment, we must examine other pathways and processes in addition to the physiological and biochemical responses assessed in chapter 2. Here high throughput screening techniques FT-IR and MALDI-TOF spectroscopy were used to identify possible areas of change in response to copper that may help direct future research into the adaption of PM01 to copper. I also provide a more in-depth analysis of metabolites using LC-MS and use heat map analysis to find clusters of metabolites that are differentially expressed to help us identify key pathways of the metabolic response to copper in an extremophile.

3.3 Materials and methods

3.3.1 Growth Conditions

C. acidophila (PM01) and *C. reinhardtii* (CCAP 11/32c) (referred to subsequently as PM01 and 11/32c) were grown in triplicate at 24 °C and 16 h:8 h light:dark cycle at 150 µmol m^{-2} s^{-1} light intensity on an orbital shaker (120 rpm). PM01 was grown in a modified acid medium (MAM), described by Olaveson & Stokes (1989) which was adjusted to pH 3. Conversely 11/32c was grown in a Tris-minimal phosphate media (TP) described in Harris (2009), at pH7. Both strains were grown in control conditions or in continuous (long-term) copper stressed conditions that were appropriate for each strain for 2 weeks: 2 mM $CuCl_2$ for PM01 and 75 µM $CuCl_2$ for 11/32c. Both strains were also grown in control conditions for two weeks and were then spiked with 4 times the concentration of the long-term copper stress: 8 mM for PM01 and 300 µM for 11/32c, then incubated in these conditions for 3 h (short-term copper stress).

3.3.2 Fourier Transform Infrared Spectroscopy (FT-IR) Analysis of Intact Algal Cell Pellets

Cells were harvested by centrifuging 30ml of dense algal cell culture at 10,000 g for 5 min. The supernatant was removed, cells were washed with 1 ml of ddH_2O, centrifuged again at 10,000 g for 5 min and the supernatant removed leaving a dense cell pellet. Each replicate culture was then normalised to 30 mg (fresh weight) and plated onto a 96-well silicon microplate, with the first well left blank to take a background measurement. The cultures were left to dry in an oven set to 40°C for 30 mins until all water had evaporated. The plate was placed into the FT-IR spectrometer (Bruker Equinox 55 FTIR spectrometer) equipped with a HTS-XT high-throughput microplate extension and a deuterated triglycerine sulfate (DTGS) detector. Spectra were collected from wavenumbers 4000-600 cm^{-1}. Data was analysed using MATLAB, and the spectra were baseline corrected using extended multiplicative scatter correction (EMSC). Further statistical analyses such as principle component analysis was performed on MATLAB using the cluster v2.0 toolbox from biospec.net.

3.3.3 Matrix-Assisted Laser Desorption/Ionization- Time of Flight (MALDI-TOF) Analyses of Intact Algal-Cell Pellets

Cells were harvested by centrifuging 30 ml of dense algal cell culture at 10,000 g for 5 min. The supernatant was removed, cells were washed with 1 ml of ddH_2O, centrifuged again at 10,000 g for 5 min and the supernatant removed leaving a dense cell pellet. The fresh weight (FW) was measured and an aliquot containing 20 mg FW of algal biomass was taken for MALDI analysis. Algal biomass was resuspended in a matrix of alpha-cyano-4-hydroxy-cinnamic acid (CHCA) (10mg ml^{-1}), 2.5% acetonitrile (ACN) and dried onto an aluminium plate. Measurements were taken in reflection/ linear mode and masses ranging from 500-25000 m/z were taken and 81 profiles were collected, for each sample, using a Axima Confidence MALDI-TOF-MS (Shimadzu Biotech). Samples were then processed in mMAss v5.5 (Niedermeyer and Strohalm, 2012) by aligning the spectra and normalising the spectra to relative intensity.

3.3.4 Metabolite Extraction

After cell harvest cultures were snap frozen in liquid nitrogen and stored at -80°C. Cell pellets were ground using a 2 mm tungsten ball in a Qiagen tissue lyser II then 1 ml of a methanol: chloroform: water (2.5:1:1) mix was added to each sample and vortexed. Samples were shaken at room temperature for 15 min. Samples were centrifuged at 14,000 g for 5 min at 24 °C, then 1 ml of supernatant was recovered to a fresh Eppendorf tube and 500 µl of ddH20 was added to each. The sample was vortexed and centrifuged at 14,000 g for 10 min at 24 °C to aid phase separation. Up to 1.2 ml of the upper, polar phase was recovered (normalised to 30 mg (FW) of biomass) for LC-MS analysis. 100 µl of an internal standard containing 30 mg Lysine d_4 and 30 mg Succinic-d_4 acid was added to each sample. Samples were then left to dry in a speed vacuum concentrator overnight.

3.3.5 LC-MS Analysis of Polar Phase Metabolites

Metabolite analysis using LC-MS techniques were run at the University of Liverpool with the help of personnel from the Goodacre lab group. Metabolites were reconstituted in 200 µl of LC-MS grade H_20. 100 µl of sample was aliquoted into auto sample vials and mass spectrum data was collected using a ThermoFisher Scientific Vanquish UHP-LC system coupled to a ThermoFisher Scientific Q-Exactive mass spectrometer (ThermoFisher Scientific, UK), with an untargeted LC-MS/MS data acquisition performed. Sample vials were stored at 4 °C, 5 µl aliquots were injected for positive ionisation.

3.3.6 Data Analysis

Raw spectra were processed in Compound Discoverer 3.1, for deconvolution, alignment and annotation. Annotated peak areas were exported into Morpheus to generate a heat map. Metabolites were sorted based on their peak area across the 6 different treatments into 8 separate clusters using k means analysis. Metabolite names from each cluster were then put into the MBROLE conversion utility, to generate IDs for the metabolites across 11 different databases. These ID's were then used to get functional annotation across BioCyc, The Small Molecule Pathway database (SMPDB) (including the human metabolome database; HMDB, The Yeast Metabolome Database; YMDB and E. Coli Metabolome Database; ECMDB), UniPathway, KEGG, KEGG module and Chemical Entities of Biological Interest (ChEBI) pathways, interactions and roles, using MRBOLE. Enrichment analysis was then performed to see if any functional annotations appeared significantly enriched against a randomly generated list to identify any key pathways that are involved within that cluster. A cut of >0.05 for the false discovery rate (FDR) to test for significant enrichment within the cluster.

3.4 Results

3.4.1 FT-IR Spectroscopy Determines Quantities of Metabolites Change in Response to Copper

FT-IR spectroscopy can determine and quantify different molecules of a biological sample using the vibrations of chemical bonds of certain metabolites. Principal component analysis (PCA) of the FT-IR spectra shows a clear differentiation between the *C. acidophila* PM01 and *C. reinhardtii* 11/32c species across principle component (PC) 1 (Figure 3.1). PC1 accounts for 64.9% of the variation of the data, showing that this is the main differential factor of the data and highlights how different the two species are. The more extreme copper stress (short-term) *C. reinhardtii* samples are distinguished from the control samples at the more negative values of PC1. PC2 accounts for the next highest percentage of the variation in the data (15.8%), and whilst it slightly differentiates some

of the copper treatments of *C. reinhardtii*, it clearly differentiates the treatments of *C. acidophila*. The long-term copper stress also has a highly variable effect on the metabolites of *C. reinhardtii*, as two of the biological replicates cluster near the control samples whilst the other two replicates cluster with the short-term copper stress samples (Figure 2.1). The mean FT-IR spectra for each treatment indicates that there are only very subtle differences between the species and between treatments in terms of the spectra patterns (Figure 3.2(A and B)). The PC1 loading plot shows a peak at 1270 cm^{-1} as a major determinant of PC1 variance, which is clearly distinguished in the *C. reinhardtii* spectra but not as large in the *C. acidophila* spectra. This likely corresponds to phosphoryl groups (Table 3.1). The PC2 loading plot shows that the two amide peaks (Amide I and amide II) at 1655 cm^{-1} and 1543 cm^{-1} mainly explain the variance between spectra on the basis of PC2. Therefore these peaks are potentially associated with adaptation by PM01 to copper. The peak at 3014cm^{-1} appears more prominent in control and short- term copper stress conditions than the long-term copper stress for both organisms (Figure 3.2 (A and B)).

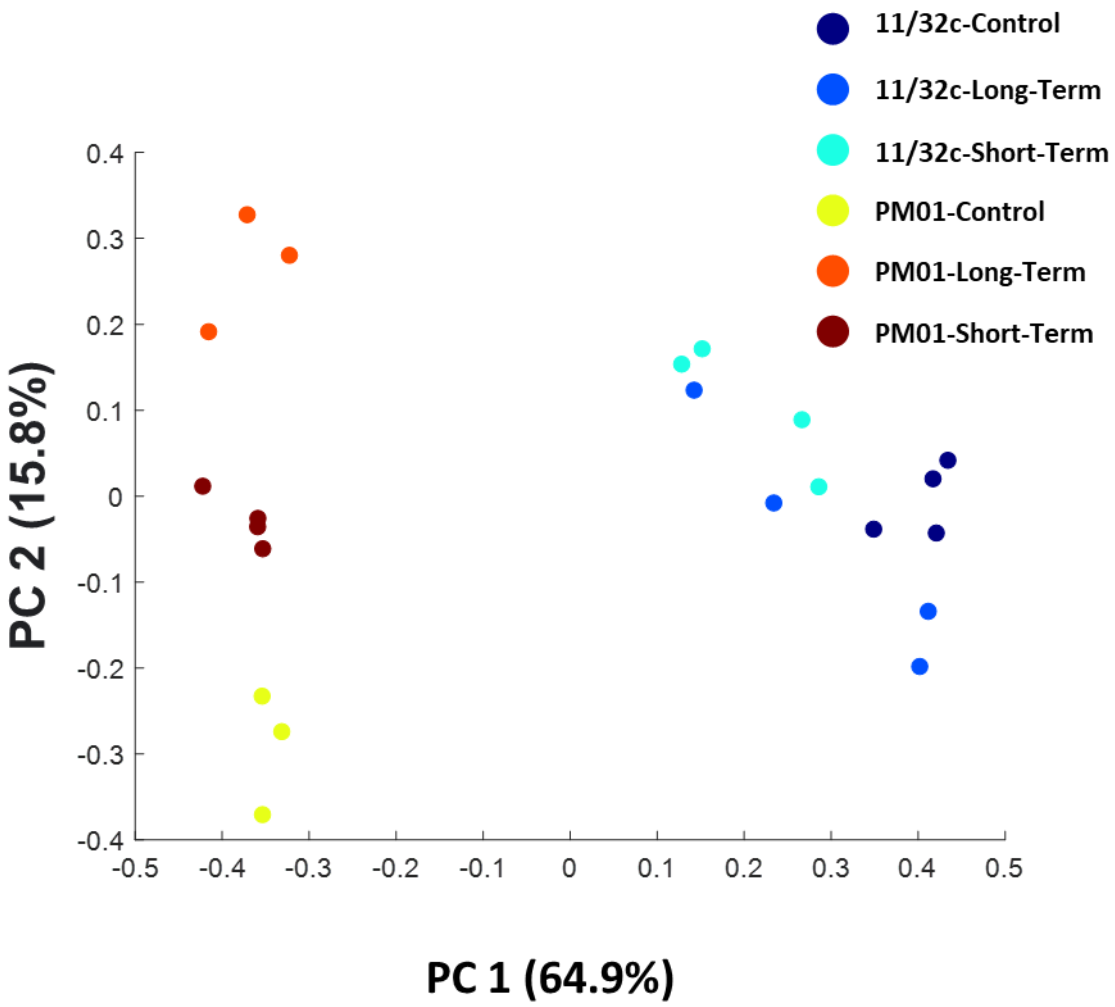

Figure 3.1 Principal component analysis (PCA) of FT-IR spectra of two microalgae species C. reinhardtii (11/32c) and C. acidophila (PM01), under both a long-term and a short-term copper stress. Each point represents an individual biological replicate that has been averaged over nine technical replicates.

Peaks 3014 cm^{-1} , 1456 cm^{-1} and 1740 cm^{-1} from the FT-IR spectra can all detect functional groups in lipids. The peak at 3014 cm^{-1} is associated with vC-H of C=CH- chains of lipids (Table 3.1). All of the PM01 treatments were significantly lower than their respective *C. reinhardtii* treatments at the 3014 cm^{-1}. Other than the PM01 control compared to the *C. reinhardtii* short-term copper treatment, all the PM01 peaks were significantly smaller than any of the *C. reinhardtii* peaks (Table 2.1). No differences were seen between the long-term and the control in both organisms, whilst the short-term copper stress was significantly lower in PM01. Lipids can also be detected at 1456 cm^{-1} which detects the vibration of δ_{as} CH_3 and δ_{as} CH_2 in lipids and proteins (Table 3.1). Conversely to the peak at 3014 cm^{-1}, the control and short-term copper treatment in PM01 show the highest values for these peaks. The control and long-term copper treatments in *C. reinhardtii* are significantly reduced compared to their respective treatments in PM01, however, they are not significantly smaller than the long-term treatment in PM01. The last peak with functional groups associated to lipids is the one at 1740 cm^{-1}, which detects the vC=O ester of lipids and fatty acids (Table 3.1). The peak at 1740 cm^{-1}, show the PM01 peaks are significantly higher than the corresponding *C. reinhardtii* treatment, and, with the exception of the *C. acidophila* long-term treatment and the *C. reinhardtii* control, all PM01 treatments are significantly higher than the *C. reinhardtii* treatments. For peak 1740 cm^{-1} there is a different response to copper between the two species. PM01 has a reduction in peak height with a positive correlation with time in copper. The PM01 control treatment has the highest peak heights, whilst the long-term copper treatment has the smallest peak height which is significantly reduced compared to the control. Like for PM01 the highest peak height in the *C. reinhardtii* samples is seen in the control. However, the two organism differ in that it is the short-term copper treatment with the smallest peak height which is significantly lower than the control.

The 1740 cm^{-1} peak also contains functional groups that can be associated to fatty acids, whilst these can be a component of lipids, they can also be exist as distinct functional molecules. Other than the 1740 cm^{-1} peak, there are four other peaks that can be associated to fatty acids, which are, 2957 cm^{-1}, 2928 cm^{-1}, 2872 cm^{-1} and 2852 cm^{-1}. These peaks are all associated to v_sCH_2 and $v_{as}CH_2$, v_sCH_3 and $v_{as}CH_3$ of fatty acids (Table 3.1) The 2872 cm^{-1} peak shows no significant difference across any of the species and treatments. For the peak at 2852 cm^{-1} only the short-term copper stress for *C. reinhardtii* was significantly lower than the control and long-term copper treatments, whilst all the other comparisons showed no significant changes in peak height. For the 2957 cm^{-1} peak the short-term copper stresses for both species were significantly lower than every other treatment except for the PM01 long-term copper treatment. The 2928 cm^{-1} peak shows the most differences of the fatty acid peaks between the treatments. The PM01 control has the highest peak height and is significantly higher than all other treatments. The long-term and short-term copper stress induce a significant reduction of peak height for PM01, these peak heights are also statistically similar to the control and long-term copper treatment in *C. reinhardtii*. The short-term copper stress for *C. reinhardtii* caused a significant reduction in peak height compared to all other treatments across both species.

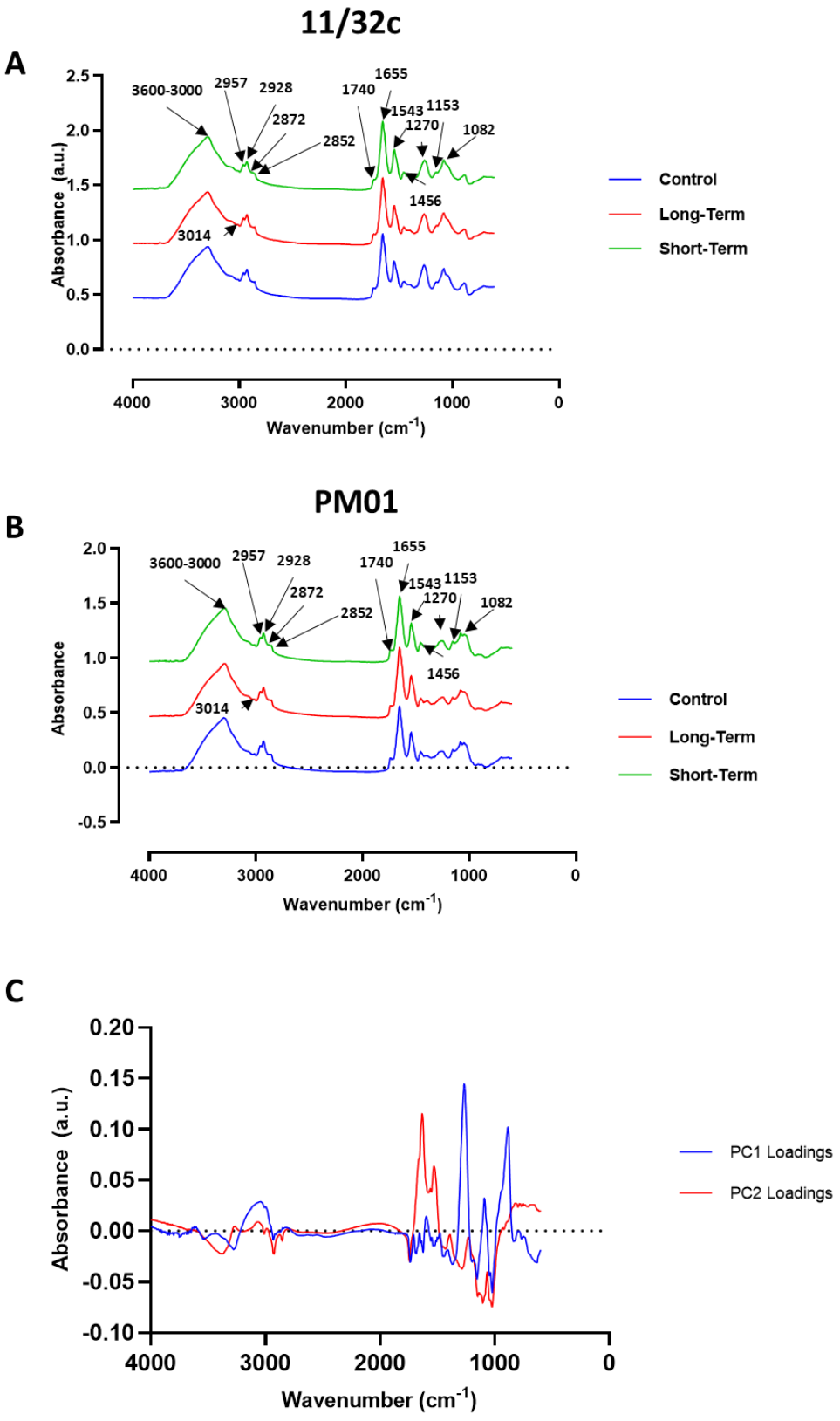

Figure 3.2 FT-IR spectra of two microalgae species (A) C. reinhardtii (11/32c) and (B) C. acidophila (PM01), spectra are offset from each other and are the average of either 3 or 4 biological replicates. The principal component loading plots for both principal component 1 and 2 are also shown to highlight the main regions of difference. Wavenumbers were collected from 4000-600cm^{-1}.

The aforementioned 1456 cm^{-1} peak also detects the δ_{as} CH_3 and δ_{as} CH_2 of proteins as well as lipids. There are three other peaks that can be associated to proteins. First, 1655 cm^{-1} can detect vC=O of amides associated with protein (Amide I) (Table 3.1). The long-term copper stress in PM01 resulted in the highest peak at 1655 cm^{-1}, this was significantly higher than any of the other treatments for PM01. Both the short-term and long-term copper stress in *C. reinhardtii* were statistically similar to the long-term copper stress in PM01 although they were not quite as high. The *C. reinhardtii* long-term copper stress peak heights did not significantly differ from any other treatment across both species. The second peak associated to proteins is 1543 cm^{-1} which detects δN-H of amides associated with protein (Amide II). Again the long-term copper stress in PM01 resulted in the highest peak across all species and treatments, and the short-term copper stress in *C. reinhardtii* was the only treatment that was not statistically different to the long-term copper stress in PM01. The final wavenumber associated to proteins is 1270 cm^{-1} which detects the V_{as} P=O of nucleic acids, phosphoryl groups and phosphorylated proteins. For this wavenumber the control in *C. reinhardtii* had the highest peak and was statistically higher than every other treatment.

Finally, the carbohydrate peaks at 1153 cm^{-1} and 1082 cm^{-1} show similar patterns to each other. For the first peak PM01 has the highest peak height, which is significantly bigger than any other treatment across both species and copper treatments (Table 3.1). However, both the short-term and long-term copper stress were enough to induce an 11.6% and 19.1% decrease in peak height from the control, respectively. Conversely, there was no significant reduction in carbohydrates under either of the copper stresses in 11/32c, and actually the long-term copper stress significantly increases the carbohydrate peak height at 1153 cm^{-1}. The same pattern is seen at the carbohydrate peak at 1082 cm^{-1}, except that the long-term copper stress did not induce an increase in the carbohydrate peak height in 11/32c (Table 3.1).

		C. reinhardtii			*C. acidophila*		
Peak	**Functional Group**	**Control**	**Long-Term**	**Short-Term**	**Control**	**Long-Term**	**Short-Term**
3600-3000	vO-H of water, vN-H of amide, vC-O of carbohydrates	n/a	n/a	n/a	n/a	n/a	n/a
3014	vC-H of C=CH- chains of lipids	0.143 ±0.003 ^{a}	0.143 ±0.004 ^{a}	0.136 ±0.003 ^{ab}	0.129 ±0.003 ^{bc}	0.124 ±0.003 ^{cd}	0.12 ±0.003 ^{d}
2957	v_sCH_2 and $v_{as}CH_2$, v_sCH_3 and $v_{as}CH_3$ of fatty acids	0.198 ±0.002 ^{a}	0.198 ±0.005 ^{a}	0.189 ±0.003 ^{b}	0.198 ±0.0004 ^{a}	0.192 ±0.004 ^{ab}	0.186 ±0.004 ^{b}
2928	v_sCH_2 and $v_{as}CH_2$, v_sCH_3 and $v_{as}CH_3$ of fatty acids	0.231 ±0.003 ^{b}	0.229 ±0.003 ^{b}	0.215 ±0.003 ^{c}	0.243 ±0.002 ^{a}	0.229 ±0.004 ^{b}	0226 ±0.006 ^{b}
2872	v_sCH_2 and $v_{as}CH_2$, v_sCH_3 and $v_{as}CH_3$ of fatty acids	0.122 ±0.002 ^{ns}	0.121 ±0.004 ^{ns}	0.116 ±0.003 ^{ns}	0.123 ±0.001 ^{ns}	0.119 ±0.001 ^{ns}	0.119 ±0.002 ^{ns}
2852	v_sCH_2 and $v_{as}CH_2$, v_sCH_3 and $v_{as}CH_3$ of fatty acids	0.119 ±0.002 ^{a}	0.118 ±0.003 ^{a}	0.11 ±0.003 ^{b}	0.118 ±0.002 ^{ab}	0.112 ±0.001 ^{ab}	0.112 ±0.006 ^{ab}
1740	vC=O ester functional groups from lipids and fatty acids	0.062 ±0.001 ^{cd}	0.053 ±0.004 ^{de}	0.049 ±0.006 ^{e}	0.085 ±0.005 ^{a}	0.067 ±0.004 ^{bc}	0.076 ±0.004 ^{ab}
1655	vC=O of amides associated with protein (Amide I)	0.558 ±0.011 ^{c}	0.57 ±0.015 ^{abc}	0.584 ±0.006 ^{ab}	0.558 ±0.003 ^{c}	0.593 ±0.018 ^{a}	0.561 ±0.005 ^{bc}

		C. reinhardtii			*C. acidophila*		
Peak	**Functional Group**	**Control**	**Long-Term**	**Short-Term**	**Control**	**Long-Term**	**Short-Term**
1543	δN-H of amides associated with protein (Amide II)	0.309 ±0.005 ^{c}	0.314 ±0.011 ^{bc}	0.324 ±0.007 ^{ab}	0.313 ±0.001 ^{bc}	0.338 ±0.008 ^{a}	0.316 ±0.003 ^{bc}
1456	δ_{as} CH_3 and δ_{as} CH_2 of lipids and proteins	0.127 ±0.004 ^{bc}	0.118 ±0.005 ^{c}	0.122 ±0.006 ^{bc}	0.145 ±0.004 ^{a}	0.132 ±0.0005 ^{ab}	0.141 ±0.008 ^{a}
1270	V_{as} P=O of nucleic acids, phosphoryl groups, phosphorylated proteins	0.265 ±0.004 ^{a}	0.233 ±0.027 ^{b}	0.219 ±0.013 ^{b}	0.154 ±0.004 ^{c}	0.133 ±0.010 ^{c}	0.153 ±0.002 ^{c}
1153	vC-O of carbohydrates	0.117 ±0.006 ^{e}	0.129 ±0.004 ^{d}	0.118 ±0.003 ^{e}	0.173 ±0.004 ^{a}	0.14 ±0.003 ^{c}	0.153 ±0.001 ^{b}
1082	vC-O of carbohydrates	0.24 ±0.005 ^{abc}	0.249 ±0.005 ^{a}	0.231 ±0.006 ^{bc}	0.244 ±0.002 ^{ab}	0.208 ±0.012 ^{d}	0.228 ±0.001 ^{c}

Table 3.1 Functional groups of peak heights identified in the FT-IR spectra of two microalgae species (A) C. reinhardtii (11/32c) and (B) C. acidophila (PM01). Peak heights were compared using a one- way ANOVA and Tukey's multiple comparison test was used as a post-hoc test to test for significant differences between the treatments represented by letters in superscript.

Due to the broad nature of the peaks some information can be lost in the data. To get around this we can take the second derivative to help identify any hidden peaks. PCA of the 2nd derivative data shows a clear separation between species and treatments. PC 1, which accounts for 62.1% of the variation of the data, separates both species and copper treatments. PM01 is associated with higher PC 1 values, which increase for the long-term and short-term copper treatment samples, with the short-term copper treatment having the highest PC 1 values in both organisms. PC 2 also separates both organisms and treatments, with negative PC 2 values being more associated to PM01 under control conditions whilst higher PC 2 values are more associated to *C. reinhardtii* under the short-term copper stress. It would seem logical that areas of interest in this data would be points on the spectra that corresponded with higher PC 1 values and lower regions of PC 2 values are they are more tightly associated to PM01 under copper stress and control conditions.

When looking at the 2nd derivative data, it is difficult to distinguish any noticeable peaks (Figure 3.4 (A and B)). To be more easily able to distinguish interesting peaks, the PC loadings plots are presented (Figure 3.4 (C)). A subtraction plot of PC 1 – PC 2 was also made to help exaggerate further areas of interest. There are 14 possible peaks of interest which have high PC 1 and low PC 2 plot points, as identified by the subtraction plot. High peaks are seen at 1749 cm^{-1}, 1712 cm^{-1}, 1698 cm^{-1}, 1679 cm^{-1}, 1635 cm^{-1}, 1664 cm^{-1}, 1611 cm^{-1}, 1472 cm^{-1}, 1456 cm^{-1}, 1259 cm^{-1}, 1082 cm^{-1}, 1065 cm^{-1}, 1032 cm^{-1} and 1005 cm^{-1}. However, currently, not functional groups can be assigned to these peak heights.

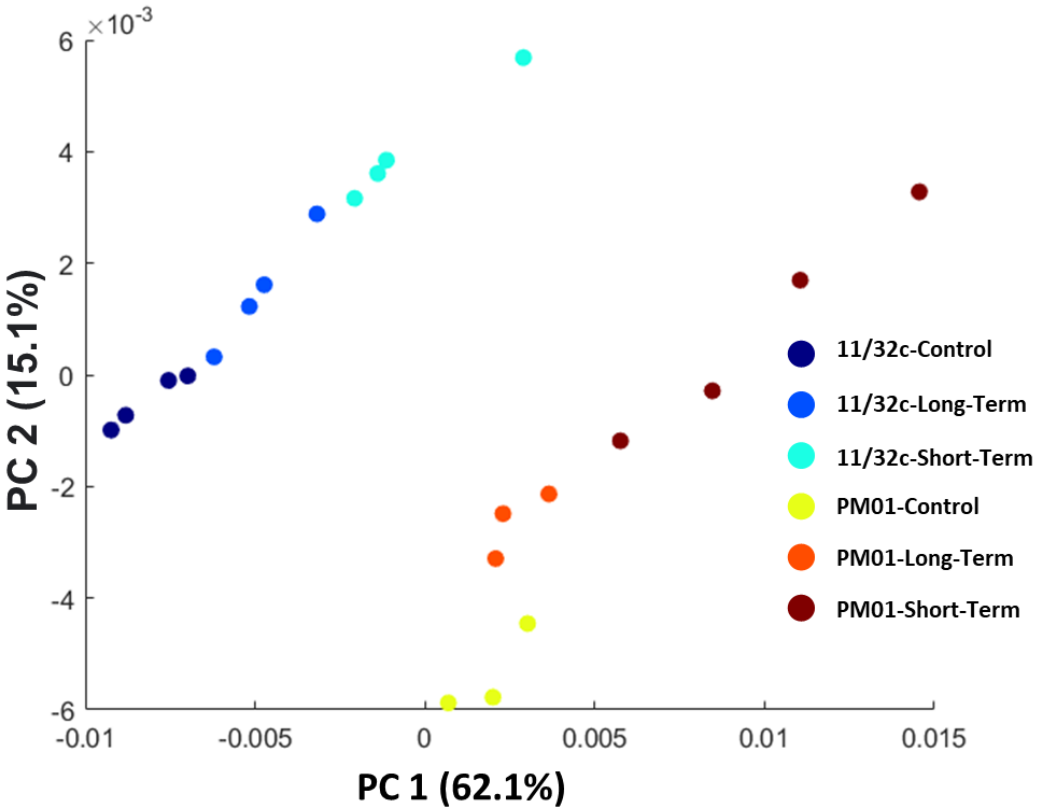

Figure 3.3 Principal component analysis (PCA) of the 2nd derivative of FT-IR spectra of two microalgae species C. reinhardtii (11/32c) and C. acidophila (PM01), under both long-term and a short-term copper stress. Each point represents an individual biological replicate that has been averaged over 9 technical replicates.

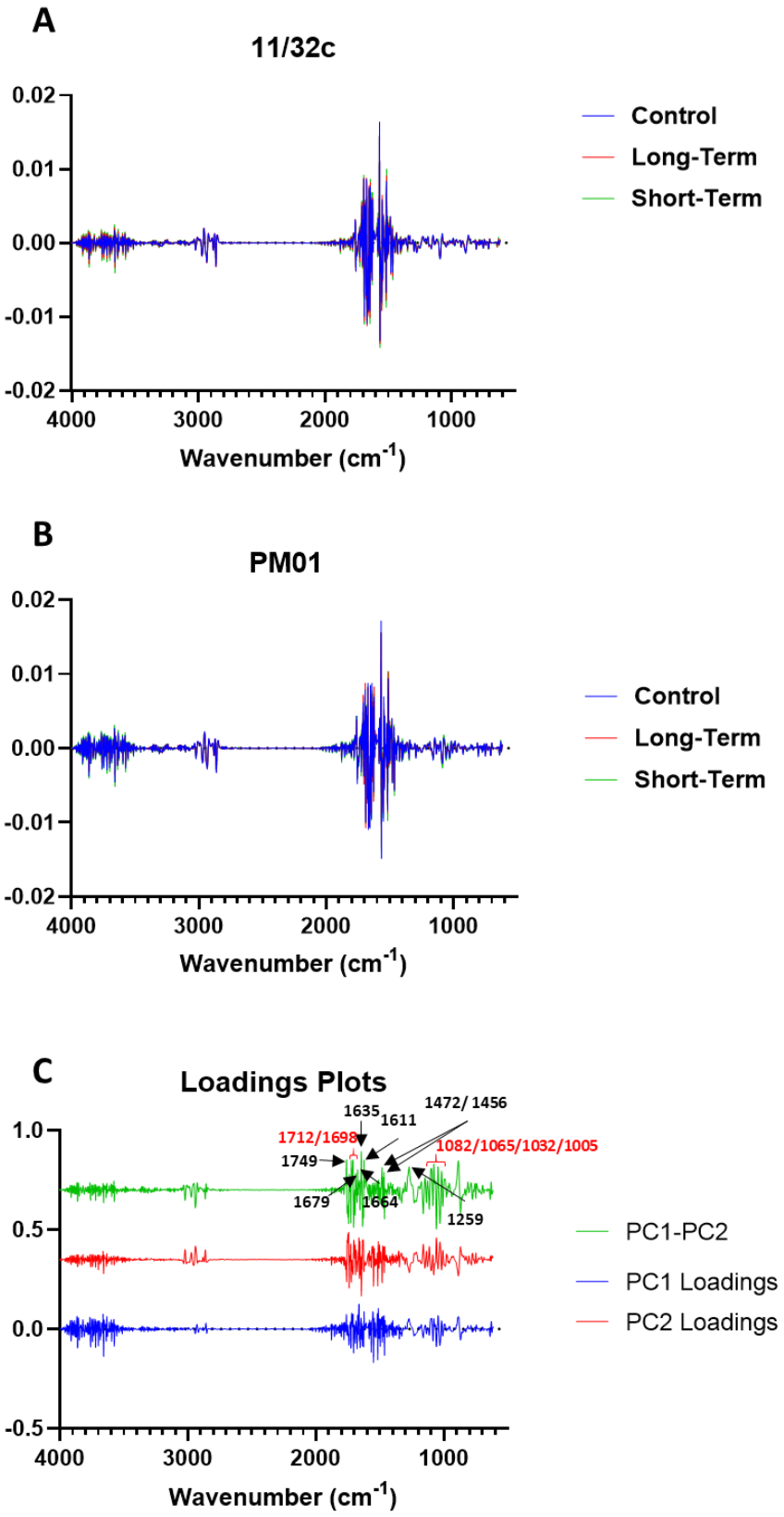

Figure 3.4 2nd derivative of FT-IR spectra of two microalgae species (A) C. reinhardtii (11/32c) and (B) C. acidophila (PM01), spectra are offset from each other and are the average of either 3 or 4 biological replicates. The principal component loading plots for both principal component 1 and 2 are also shown to highlight the main regions of difference, with a subtraction plot of PC 2 from PC 1 to identify key zones associated with copper stress also plotted.

3.4.2 MALDI Analysis Gives a Rapid Compound Profile of Intact Organisms

MALDI analysis can be used as a proteomics tool to quantify proteins. As the proteins were not extracted and digested, identification of the proteins is not possible. MALDI analysis of the intact algal samples has provided a rapid mode of detecting compound differences between the two species under copper stresses (Figure 3.5 (A and B)). Figure 3.5 (C) shows a heat map of the two sets of spectra based on peak intensity which provides an easy comparison between all the spectra and copper treatments. The first noticeable difference between the two organisms is a shift in peaks. The highest peaks for both organisms are seen at 8269 m/z for *C. reinhardtii* and 8513 m/z for PM01, and likely represent equivalent proteins between the two organisms despite PM01 showing a shift to a higher m/z. However, another set of likely equivalent proteins, show a peak at 17806 m/z in *C. reinhardtii*, whilst in PM01, the protein appears to have a lower m/z at 17590 m/z in the acidophile. One of the first noticeable effects of a long-term copper treatment is the presence of a peak at 17590 m/z and 17806 m/z for PM01 and *C. reinhardtii* respectively which is not seemingly present in the other copper treatments for both organisms. In addition to this major peak, other peaks appear in the long-term copper treatment that are not seemingly present in the other treatments for both organisms. Peaks are present at 8903 m/z, 9178 m/z, 11039 m/z, 11587 m/z and 13462 m/z in the *C. reinhardtii* long-term copper treatment (Figure 3.5 (A)). Fewer peaks are seen in the PM01 long-term copper treatment with unique peaks appearing at 8796 m/z and 11047 m/z (Figure 3.5 (B)).

Another region of interest is at 4864 m/z where there is a greater peak intensity for all of the PM01 treatments, in comparison to their relative treatment in *C. reinhardtii*, but is most prevalent under the long-term copper treatment. The highest peak intensity is reduced under a long-term copper stress in PM01 however, copper stresses in *C. reinhardtii* do not seemingly change the peak intensity. The peak at 10318 m/z shows a high peak intensity for a certain compound in *C. reinhardtii*, which is much reduced in PM01 with a likely equivalent peak at 10217 m/z.

PCA shows that the long-term treatments for both species are very similar, with very little variation across PC 1 and PC 2 between most of the long-term data sets, which accounts for 86.6% of the variation within the data Figure 3.6 (A). The two species are then separated across PC 1 with higher values being associated with *C. reinhardtii* and lower values being more associated with PM01. PC 2 separates the copper treatments, with all of the short-term copper treatments in *C. reinhardtii* show positive values across PC 2. Conversely most of the short-term copper treatments in PM01 show positive PC 2 values, but not all. Additionally, these are interspersed between two control replicates of PM01, which has both low PC 1 and high PC 2 values (Figure 3.6 (A)). The PC loading plots were plotted against the reference m/z to see key areas of differences in the data set Figure 3.6 (B). Based on this, there could be further interesting peaks, in relation to PM01 adaptation to copper, at 4819 m/z which shows high PC 2 and low PC 1 values.

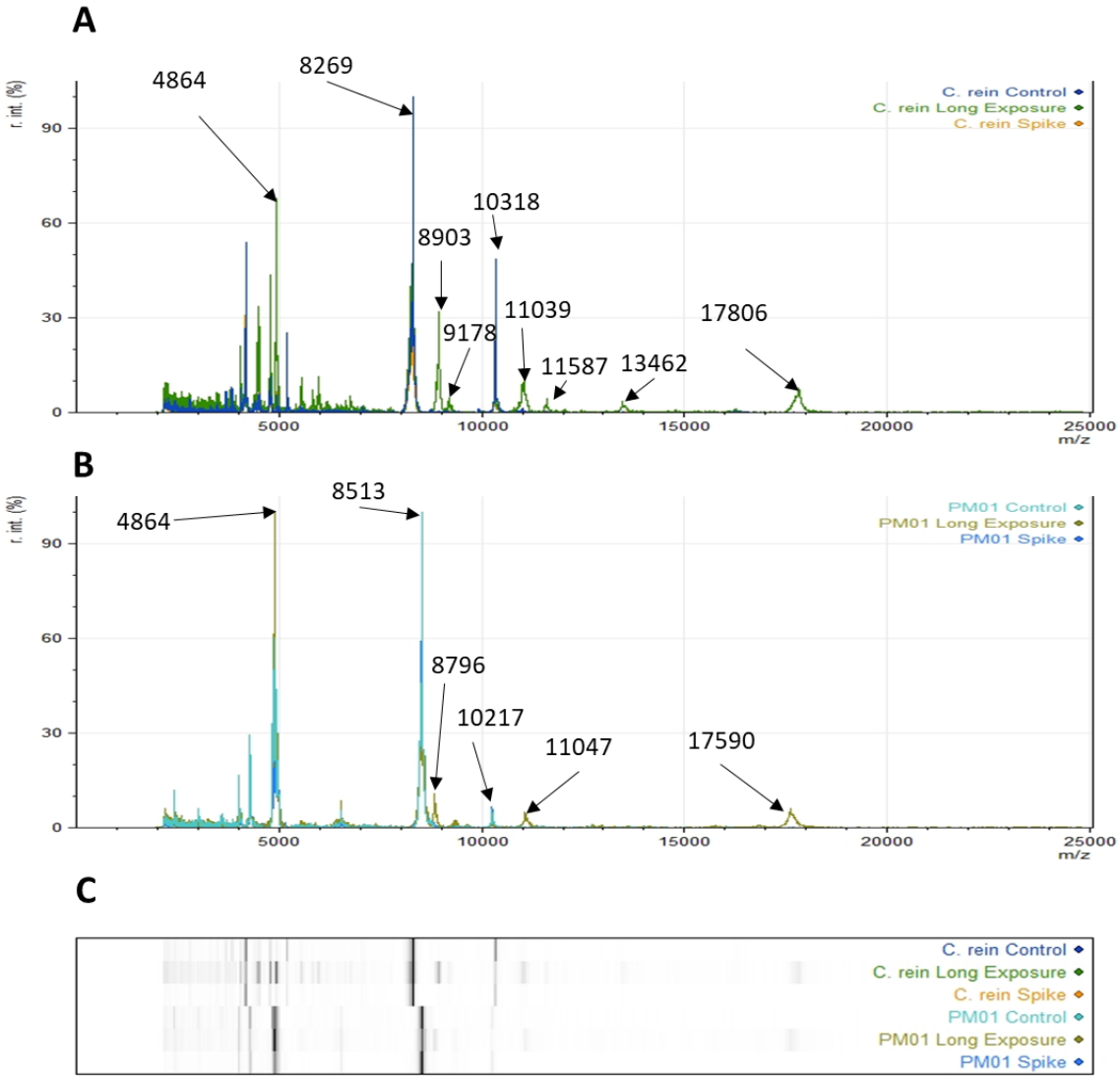

Figure 3.5 MALDI spectra of two species of microalgae (A) C. reinhardtii (11/32c) and (B) C. acidophila (PM01). A heat map of peak heights is also presented (C) to observe differences more easily between the two sets of spectra. Data was normalised to relative intensity and normalised in mMass v5.5

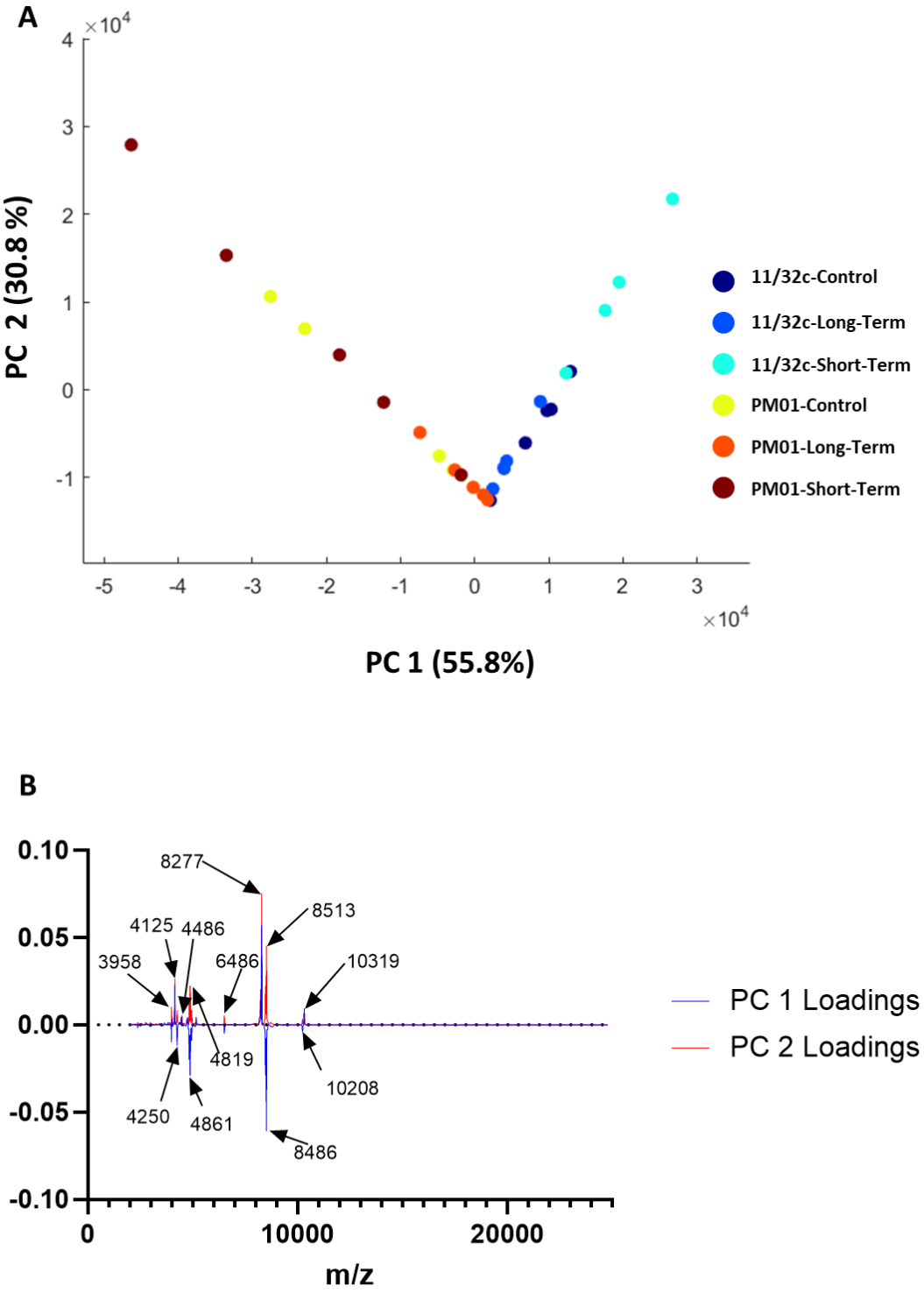

Figure 3.6 Principal component analysis of MALDI spectra of two intact microalgal species PM01 (C. acidophila) and 11/32c (C. reinhardtii) under long-term and short-term copper conditions. (A) Principal component plots, plotting PC 1 vs PC 2. (B) PC 1 and 2 loading plots across the m/z.

3.4.3 Broad-Scale, Untargeted Metabolomic Analyses

Polar fraction metabolites were extracted using a methanol/chloroform extraction process and analysed using LC-MS. PCA shows the best separation and clustering of data points when comparing PC 1 and PC 3 which account for 20.8% and 9.9 % of the variation in the data set, respectively (Figure 3.7). Clear separation of the two species is seen across PC 1, although one replicate of both the PM01 short-term and control appear to cluster more towards the *C. reinhardtii* replicates (Figure 3.7). There is a high amount of variation within the PM01 short-term treatments, whilst most data sets appear within negative PC 3 values. Most of the long-term copper treatments and controls for PM01 appear to cluster closely together, however, one replicate for both the control and long-term copper treatment show very high PC 3 values and separate further from the main cluster containing their other respective data points. Whilst the *C. reinhardtii* treatments appear to cluster together there is very little separation between the copper treatments. PC 1 vs PC2 can still discriminate against species (mainly across PC 1). However, it is less able to discriminate between treatments across either PC1 or PC 2 and many of the treatment points within the species are intertwined (Figure 3.7 (C)).

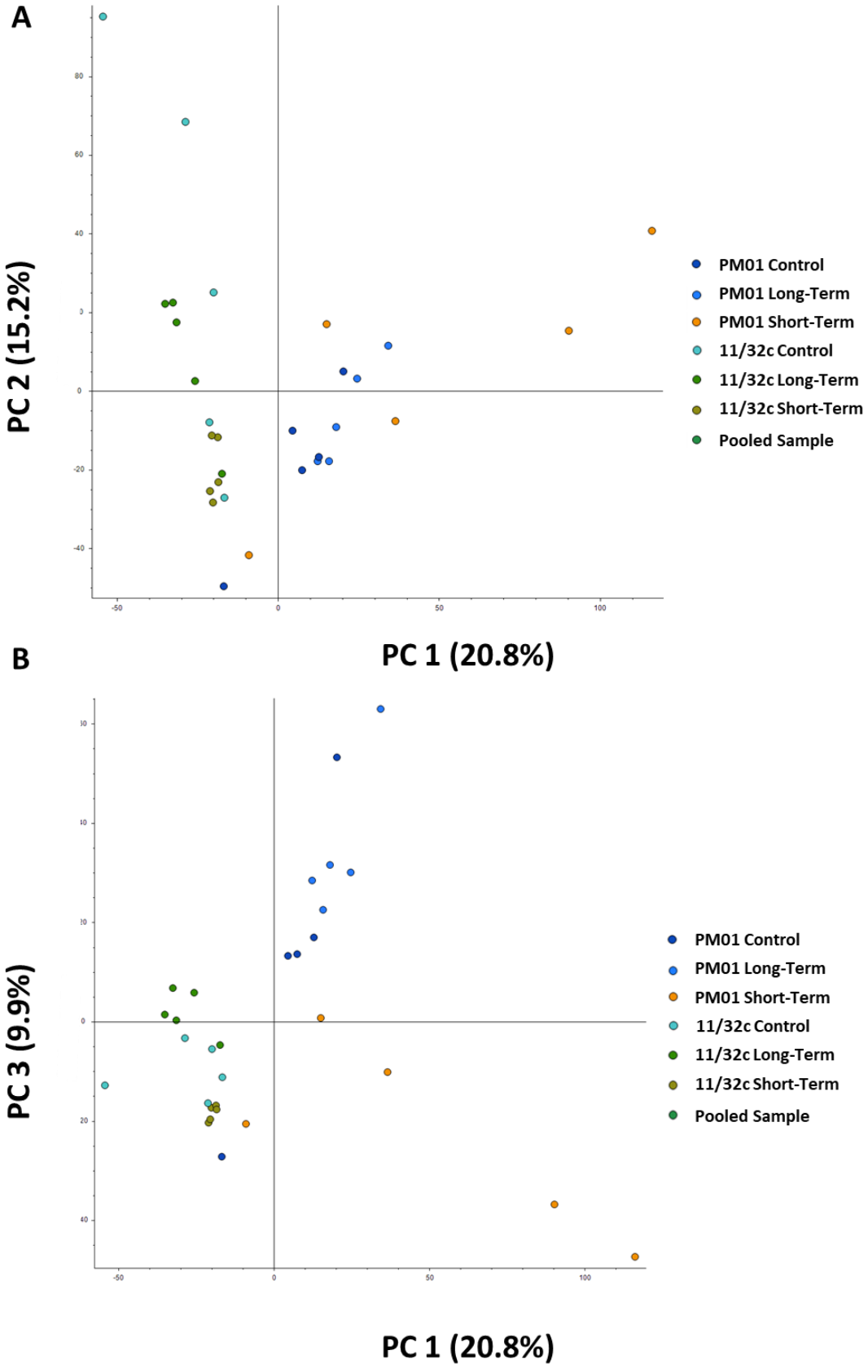

Figure 3.7 Principal component analysis of polar metabolites using LC-MS of 2 microalgal species 11/32c (C. reinhardtii) and PM01 (C. acidophila) under a short-term and long-term copper stress. Data also shows a pooled sample containing aliquots of all replicates. (A) Principle component 1 (20.8%) vs principle component 2 (15.2 %). (B) Principle component 1 (20.8%) vs principle component 3 (9.9%)

A total of 3010 putative metabolites were identified from the positive ion LC-MS dataset. To get a greater understanding of the biological processes that may be happening, the metabolites were sorted on a heat map, based on the peak area of the metabolites, and sorted using k-means clustering using the online Morpheus software tool. The heatmap separates into 8 clusters, separating metabolites based on their expression profiles (Figure 3.8). These clusters were then utilised to test for any enrichment of metabolites assigned to a variety of biological processes. The first cluster contains 655 metabolites, and of those metabolites 141 had at least one form of ID number from the various databases tested, giving rise to a total of 502 metabolite IDs for that cluster. Of those 502 ID's 127 had some form of annotation of biological function associated to it, leading to a 19.4% hit rate from the total metabolites of the cluster (Table 3.2). Cluster 1 shows the highest relative abundance of the metabolites in the 11/32c control, the long-term treatment for 11/32c also shows some relatively high quantities, whilst the rest of the treatments show the lowest metabolite quantities. The PM01 control and the 11/32c short-term copper treatment showed the lowest quantities of the metabolites found in Cluster 1. Cluster 7 had the highest hit rate of annotated ID's to total metabolites with 43.7% containing ID's with a form of annotation. Within Cluster 7 the PM01 control shows the highest quantities of metabolites, with metabolites in the PM01 long-term treatment also showing higher quantities of metabolites. The most annotated clusters thereafter are as follows; Cluster 8 (31.1%), Cluster 6 (24.9%), Cluster 4 (19.9%), Cluster 3 (17.3%), Cluster 5 (17.2%) and Cluster 2 (14.5%) (Table 3.2). Cluster 8 shows the highest relative quantities within the 11/32c long-term treatment, whilst the short-term treatment shows the lowest quantities of the metabolites. The long-term copper treatment for *C. reinhardtii* also has the highest quantities of metabolites within Cluster 2 with relatively low quantities of the metabolites for all other treatments (Figure 3.8). The short-term copper treatment on 11/32c yielded the highest quantities of metabolites in Cluster 3, with the rest of the treatments of 11/32c also showing relatively high quantities of the metabolites (Figure 3.8). The short-term copper treatment in PM01 yielded the highest quantities of metabolites in both Cluster 4 and 5. The main difference between the two clusters being that the long-term copper treatment also shows high quantities of the metabolites in Cluster 4 (Figure 3.8). The final cluster, Cluster 6, has the highest quantities of metabolites in the PM01 long-term copper treatment.

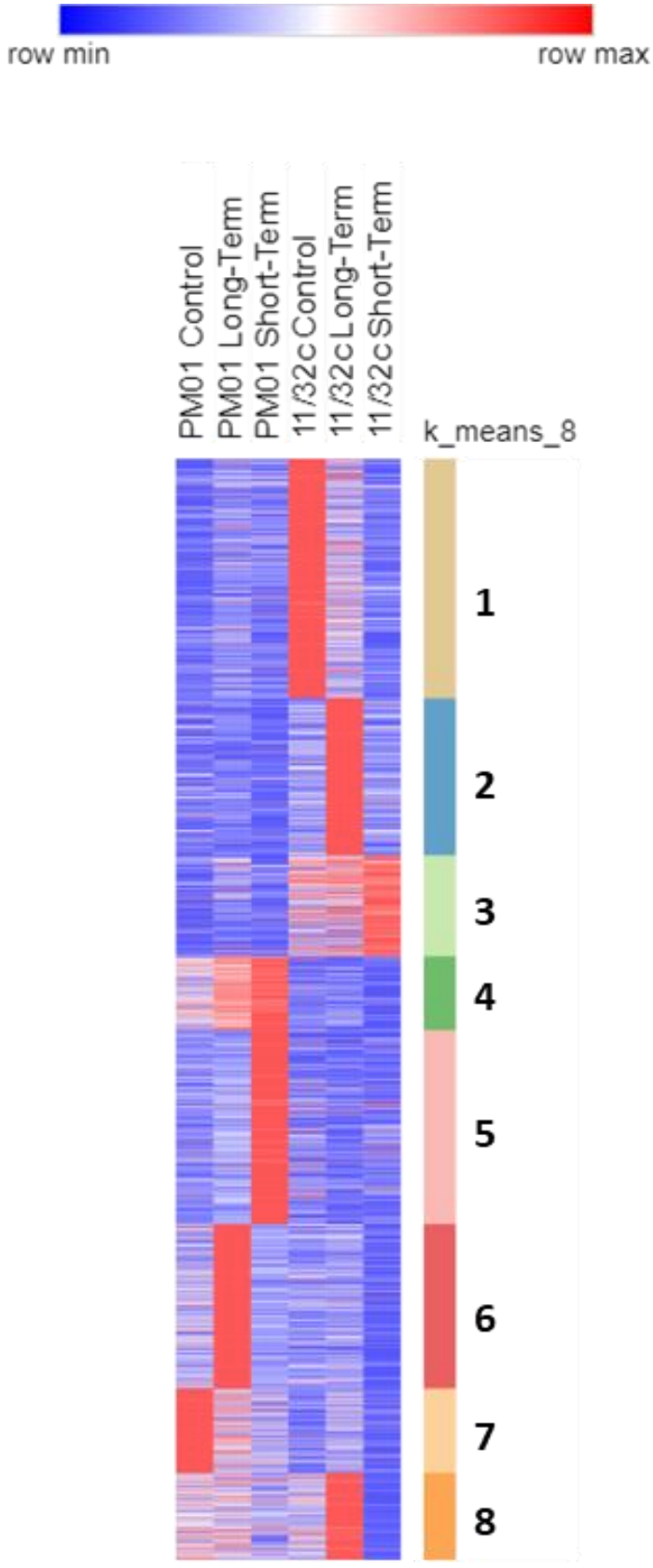

Figure 3.8 Heatmap of metabolites extracted from two microalgae species 11/32c (C. reinhardtii) and PM01 (C. acidophila) under a short-term and long-term copper stress. Metabolites were sorted using k-means clustering to organise into 8 different expression profiles using the Morpheus online heatmap tool.

	Total Metabolites	Metabolites ID'd	Total ID's Identified from Metabolite ID	Annotated ID's
Cluster 1	655	141	502	127
Cluster 2	429	79	234	62
Cluster 3	277	59	174	48
Cluster 4	201	54	168	40
Cluster 5	530	119	371	91
Cluster 6	449	110	381	112
Cluster 7	231	80	311	101
Cluster 8	238	76	284	74

Table 3.2 Overview of the annotations of metabolites from the clustered heatmap. Metabolite ID's across 11 databases were obtained from metabolites names for each individual cluster using the automatic ID conversion from MBROLE 2.0. The ID's were then analysed for any annotations of biological function and enriched using MBROLE 2.0.

The annotations of the metabolites yielded a large number of annotations across a variety of databases for every cluster. A total of 2105, 2024, 1974, 936, 2830, 2354, 3327 and 2913 annotations were found for Clusters 1 – 8, respectively (Figure 3.9). Metabolites related to protein interactions dominate the number of annotations, containing well over half the annotations for each cluster. The classification of enzyme interactions is very prevalent within Cluster 1, 5, 6 and 8 across all species, and specifically in *C. reinhardtii* (Figure 3.9). Both the SMPDB and *C. reinhardtii* pathways were prevalent in Cluster 6. Biofunctions and Chebi roles also make up a relatively large fraction of the annotations in Cluster 1, 4, 5, 6 and 8. Whilst not many metabolites were annotated with the KEGG modules, other interactions and UniPathway Pathways databases (Figure 3.9). As protein interactions consisted of the bulk of the annotations, they were removed for the metabolite enrichment analysis. This is, in part due to the nature of the data, and with just protein names assigned we could not easily identify processes the metabolites would be involved in. Also due to the sheer bulk of the data, it warrants further investigation and analysis of the proteins involved. Metabolite enrichment classifies metabolites to certain pathways or interactions and calculates whether the number of metabolites found within these pathways are found in higher quantities than would be expected if you were to generate a list of the pathways at random. This gives an excellent overview and insight into the metabolite changes within the algae.

Supplementary Table 3.1 shows significantly enriched metabolite annotations within Cluster 1. 63 of the 89 significantly enriched annotations are associated to biofunctions. Of specific interest within this biofunction category 2, metabolite ID's related to free radical scavenging were identified and four metabolites involved in purine metabolism. In addition to purine metabolism, two metabolites were also identified as purines within the KEGG compounds with biological roles database. Tryptophan metabolism was also found to be enriched within this cluster, being independently found enriched in both SMPDB pathway and the KEGG modules database. One metabolite involved in glutathione metabolism was also found in this cluster.

Supplementary Table 3.2 shows significantly enriched metabolites annotations within Cluster 2. A total of 88 annotation terms were found to be enriched within this cluster. Enzyme interactions consist of the highest amount of metabolite assignations found within this cluster, with 12 enzyme interactions being involved in *C. reinhardtii* databases and a further 27 enzyme interactions being found within other species. 25 metabolites have also been found in the biofunctions database. Three metabolites involved in protein and amino acid synthesis were found in the biofunctions pathway. Lipid synthesis also appears to play an important role within this cluster, with metabolites involved in glycerol-3-phoosphate dehydrogenase being found to play an important role and enriched independently in the enzyme interactions classification of the KEGG database, ECMDB and the Biocyc database. Glycerolipid metabolism was also found to be enriched within the SMPDB pathway.

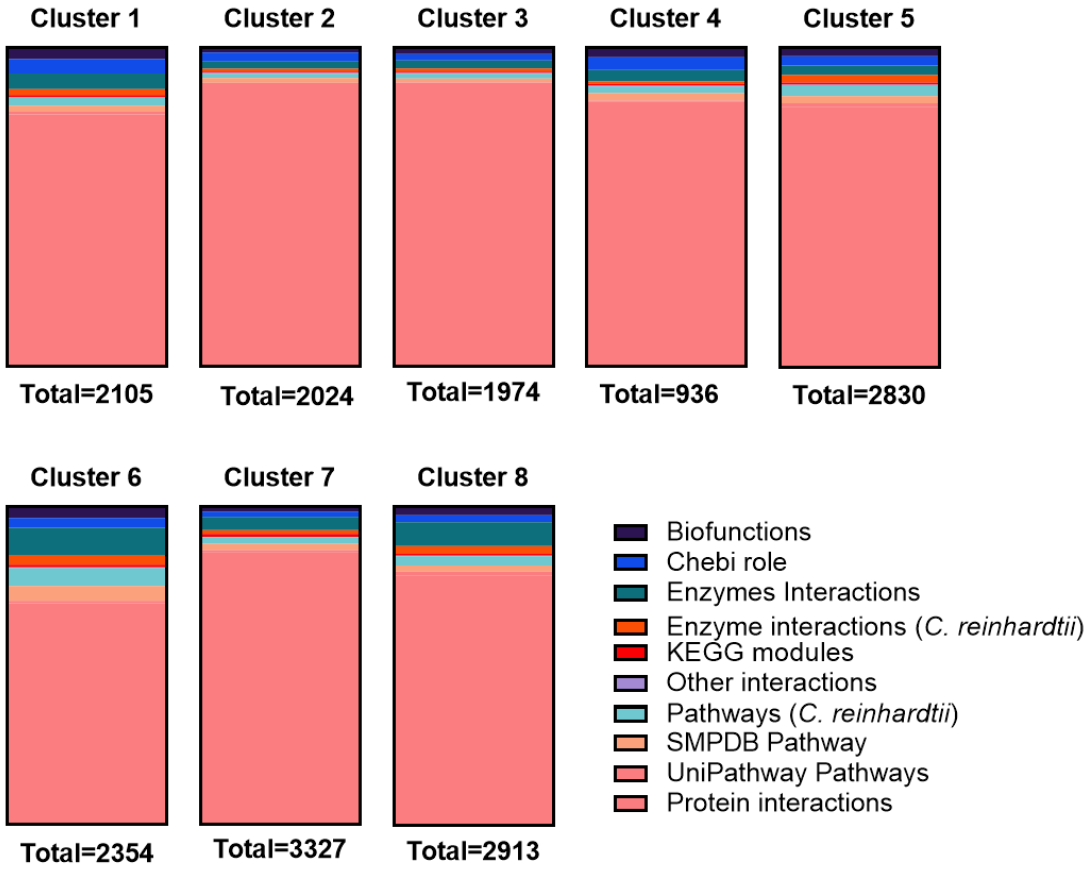

Figure 3.9 Annotations of metabolites for each cluster identified over several data bases. Total number of annotations are presented under each cluster and the colours represent relative quantities within each cluster.

Supplementary Table 3.3 shows significantly enriched metabolite annotations within Cluster 3. A total of 85 metabolite annotations were found to be enriched within the cluster. 35 of the annotations came from the biofunctions classification in the HMDB. Amino acid biosynthesis plays a large role within this cluster with glycine serine, threonine and tyrosine metabolism all being significantly enriched pathways within the cluster as identified from the HMDB. Methionine metabolism may also be important within this cluster as it was found to be significantly enriched within the HMDB of biofunctions and methionine synthase, methionine adenosyltransferase and methionine. tRNA ligase was also found to be enriched within the KEGG enzyme interactions pathway.

Supplementary Table 3.4 shows significantly enriched metabolites annotations within Cluster 4. A total of 77 pathways and interactions were found to be significantly enriched within this cluster. Again, biofunction and enzyme interaction were the most abundant terms containing 22 and 26 terms, respectively. Thiamine biosynthesis pathways are significantly enriched within this cluster. Two metabolites are predicted to be involved in thiamine metabolism in the *C. reinhardtii* pathways from the KEGG database. Thiamin salvage II, thiamine diphosphate biosynthesis II and the superpathway of thiamin diphosphate biosynthesis III (eukaryotes) were also found enriched within the *C. reinhardtii* pathways from the BioCyc database. Biotin metabolism is also enriched within the cluster, with metabolites being found enriched within the SMPDB pathway. Additionally, metabolites involved in the biotin---[propionyl-CoA-carboxylase (ATP-hydrolysing)] ligase and biotin---[methylmalonyl-CoA-carboxytransferase] ligase enzyme interactions were found within the YMDB. Metabolites involved in the Biotin--[acetyl-CoA-carboxylase] ligase enzyme interactions were found within the ECMDB. Metal chelators and radical scavengers are also found in the biofunctions of the HMDB containing 1 and 2 metabolites respectively.

Supplementary Table 3.5 shows significantly enriched metabolites annotations within Cluster 5. Biofunctions consist of the large majority of metabolite pathways and functions enriched within this cluster, containing 50 out of 57 categories. Metabolites involved in radical scavenging were found to be enriched within the cluster containing two metabolites. A metabolite involved in metal chelation was also found to be significantly enriched. Two metabolites involved in the oxidoreductant, 3-phenylpropanoate dioxygenase, were also found to be enriched within Cluster 5. Finally, 59 metabolites involved in Cytochrome P450 substrates as part of the CYP1 family. Metabolites involved in cysteine, glutamine, glutamate, lysine, phenylalanine, tyrosine, tryptophan, valine, leucine and isoleucine biosynthesis were also found within Cluster 5. A metabolite involved in glutathione metabolism was also found within this cluster.

Supplementary Table 3.6 shows significantly enriched metabolites annotations within Cluster 6. Like Cluster 5, the biofunction category consists of the most enriched pathways within this cluster, containing 73 out of 88 terms. Five metabolites involved in protein synthesis and amino acid biosynthesis were enriched within this cluster. Alongside, metabolites involved in glycine, serine, threonine, glutamate, purine, alanine, aspartate, phenylalanine, taurine, tyrosine, tryptophan and cysteine metabolism, which were also found to be enriched within this cluster. In addition to that, broader terms involved in amino acid biosynthesis have been found enriched within this cluster including essential amino acid and seleno amino acid metabolism terms. Lipid catabolism, fatty acid transport and energy production terms were found within this cluster, as well as components of

glycerophospholipid metabolism. Three metabolites involved in glutathione metabolism were also found enriched within the cluster and two metabolites involved in glutathione biosynthesis were identified from the KEGG module. Finally, 41 metabolites involved in ABC transporters were also found to be enriched within this cluster.

Supplementary Table 3.7 shows significantly enriched metabolites annotations within Cluster 7. As with the previous two clusters the biofunction category consists of the most enriched pathways within this cluster, containing 50 out of 72 terms. As with the last cluster, there appears to be a large quantity of metabolites involved in protein synthesis. These include Biofunctions involved in histidine, phenylalanine, tyrosine, tryptophan, histidine, arginine, proline, valine, leucine, isoleucine, cysteine, alanine and aspartate biosynthesis. Five metabolites are involved in transcription and translation as identified in the SMPDB pathway. Five are metabolites involved in the panthothenate and CoA biosynthesis. In addition, metal chelators and free radical scavengers were found enriched within Cluster 7, with three metabolites being assigned to those biofunctions. A metabolite categorised as an electron donor has also been found enriched within Cluster 7. Again CYP1, part of the cytochrome p450 family was found enriched within this cluster as 48 metabolites involved in this process were found enriched within Cluster 7. We also see a high number of metabolites (45) associated with the cyc-loop superfamily of the ion channel ligands enriched within Cluster 7. A metabolite involved in glutathione metabolism was also found within this cluster.

Supplementary Table 3.8 shows significantly enriched metabolites annotations within Cluster 8. Like previous clusters, biofunctions dominate the categories enriched within the cluster, consisting of 70 out of a total of 80 functional annotations. Amino acid metabolism plays a large role within the cluster, with metabolites involved in alanine, aspartate, arginine, proline, glutamate, glycine, serine, threonine, histidine, phenylalanine, tyrosine, tryptophan, valine, methionine, leucine and isoleucine metabolism all found enriched within the cluster. In addition, two metabolites were found enriched within the essential amino acids and protein, synthesis and amino acid biosynthesis biofunction annotation within the HMDB. Four metabolites involved in transcription and translation, were also found enriched within the cluster. Energy metabolism also plays a role within this cluster, with metabolites involved in fatty acid and pyruvate metabolism also being found enriched within the cluster. Finally, more metabolites involved in the CYP1 family within the cytochrome p450 superfamily. A metabolite involved in glutathione metabolism was also found within this cluster.

3.5 Discussion

3.5.1 MALDI-TOF as a Better Finger-Printing Tool, but Currently Less Informative

The FT-IR spectra of both the PM01 and 11/32c controls were surprisingly similar. This is even more so when the samples have been exposed to copper. FT-IR spectra have been shown to distinguish both species and state of microalgae can differ in both peaks and peaks size when exposed to nutrient stress (Driver et al., 2015), nutrient stress and species dependent (Domenighini and Giordano, 2009) and plastic pollutants (Déniel et al., 2020). However, this study did not observe this, with the only major difference between the two species, and copper treatments being seen in a few peak heights. The peak at ν_{as} P=O of nucleic acids, phosphoryl groups and phosphorylated proteins does appear to slightly distinguish the species, with it being much more prevalent in the 11/32c samples as all treatments were significantly higher than any of the PM01 treatments. In comparison,

MALDI-TOF provided a much more distinct molecular fingerprint of intact algal samples. MALDI-TOF has been used on intact algal cells to provide an overview of the proteome (Emami et al., 2015), and on protein extracted samples (Barbano et al., 2015), to successfully distinguish microalgae down to the species level. However, without some form of protein digestion, any more in-depth information, such as protein composition, is unable to be collected. The MALDI-TOF spectra were much more distinguishable between the species, especially so under a long-term copper stress. Interestingly, the PCA of the FT-IR spectra gave better separation than that of the MALD-TOF.

Despite a lesser ability to easily distinguish organisms and treatments, the FT-IR spectra do undoubtedly give greater insights into the cellular conditions than MALDI-TOF. The data indicated that PM01 may accumulate greater content of lipids and fatty acids, than 11/32c. This is significantly decreased upon a long-term copper stress, whilst a decrease was also seen in the short-term copper stress, but was not significant. My results seem to contradict that of Yang et al. (2015) who showed that copper stress can significantly induce lipid accumulation in *Chlorella minutissima* alongside other metals. However, there are two main differences between these two experiments, firstly, *C. minutissima* was grown in an artificial wastewater, containing very high concentrations of nitrogen and phosphates. Secondly, cultures were stressed with only up to 1 mM Cu for 7 days, which was less than the exposure conditions of PM01. Although FT-IR spectra can give hints of the metabolic composition and changes of the cell, the results presented here would need to be confirmed by further molecular characterisation methods for a lipid decrease, such as use of the neutral lipid dye Nile Red or by mass spectrometry analysis. Lipid mobilisation was found to be crucial to the survival of extremophile species of the *Rhodococcus* genus, such that upon inhibition of triacylglycerol (TAG) degradation, cultures were unable to survive osmotic stress, UV irradiation and perhaps unsurprisingly, carbon starvation (Urbano et al., 2013; Urbano et al., 2014). A reduction in carbohydrate content in the PM01 strain as indicated by both the 1153 cm^{-1} and 1082 cm^{-1} peaks under both a short-term and long-term copper stress when compared to the control, also indicates some sort of energy demand to dealing with the copper stress.

The second derivative spectra have the potential to give further insights, due to the broad nature of peaks from the FT-IR spectra, spectral information can be lost. By taking the 2^{nd} derivative we are able to identify many hidden peaks (Gough et al., 2010). Although I was not able to assign any functional annotation to them, most of the hidden peaks were found between 1749 cm^{-1} and 1005 cm^{-1}. Due to the noise of the data, a likely artefact of taking the 2^{nd} derivative, a method of focussing the data was needed to identify peaks that are having the greatest impact on the variation in my data. Further investigation into the functional annotation of these peaks will provide a greater insight into the copper adaptation of PM01 and provide more detailed information in the rapid metabolic characterisation of microalgae.

Although no specific proteins were identified within the MALDI-TOF data, we can certainly gain insights. The appearance to new peaks under the long-term copper stress for both species are very interesting and likely explain why to long-term treatments for both species cluster together in the PCA analysis. What is more interesting is that most of these new peaks have high a high m/z value suggesting that very large proteins could be involved in the long-term copper adaptation of microalgae to copper. It is possible that the large protein peaks observed could just be due to

changes in the charge of the protein. Both the 17806 and 17590 m/z peaks for 11/32c and PM01, respectively have peaks at the 2-charge mass of 8903 and 8796 m/z. However, once again these peaks are only predominant in the long-term copper stress. These peaks are likely to be the same proteins seen at 7806 and 17590 m/z but in a 2^+ charge state as opposed a single 1^+ charge. This change in charge could be through either damage or quenching of ROS, or through the direct reduction of Cu^{2+} to Cu^+. Copper is renowned for its ability to accept and donate electrons, one of the reasons it can be so damaging to cells in excess quantities (Printz et al., 2016). Therefore, it is entirely feasible that we could see proteins donating electrons and increasing their charge state under copper stressed conditions. Whatever the mechanisms, this could be an interesting protein to either assess the damaging impact of copper, or alternatively, one of the adaptive mechanisms of microalgae to copper.

3.5.2 Protein Synthesis Increases in Response to Copper

FT-IR spectra data shown in Figure 3.2 and Table 3.1 clearly shows an increase in peaks associated to proteins in both *C. acidophila* and *C. reinhardtii*. The long-term copper stress elicited the strongest increase in protein peak height in *C. acidophila*, whilst the short-term copper stress elicited the strongest increase in *C. reinhardtii*. The metabolomic data analyses further elucidate to an increase in protein content in the long-term copper stress for PM01, as Cluster 6 contains metabolites elevated at high quantities in the long-term copper stress of PM01 involved in amino acid metabolism and protein synthesis. Clusters 2, 3, 5 and 8 all also show metabolites involved in amino acid and protein biosynthesis, with the clusters showing elevated metabolites in copper stressed conditions for both species of microalgae. This is slightly confounded as the FT-IR spectra data shows that only protein peaks in the short-term copper stress for 11/32c and the long-term copper stress for PM01 were significantly increased in response to copper (Table 3.1). The matter is further complicated as an abundance of metabolites involved in amino acid and protein synthesis were also found in cluster 7, in which, the control for PM01 had the highest quantity of metabolites. A species of marine alga that dominates copper polluted waters in Chile, *Ulva compressa*, was found to increase expression of proteins involved in a variety of processes including carbon, nitrogen and sulphur assimilation, suggesting a need for increased protein synthesis (Laporte et al., 2020). Conversely, copper was found to negatively affect soluble protein content in the lichen *Trebxia erici* and the microalga *Scenedesmus quadricauda* (Piovár et al., 2011). Copper has also been shown to dramatically alter nitrogen metabolism leading to a reduction in amino acid and protein content within plants (Llorens et al., 2000). It is evident there is no clear universal strategy to whether an increase in protein content is beneficial to copper adaptation. It is likely that specific protective proteins will confer the most resilience to copper, rather than just sheer quantity of total protein. The increase in protein peak size seen in the long-term copper adaptation of PM01 could be due to an accumulation of proteins helping to keep an optimum copper homeostasis. Although the short-term copper stress does show an increase in protein peaks, 3 hours is likely not enough time for the full protective measures to take place.

However, there is another potential explanation for the increase in protein peak height seen. Excess copper has been shown to induce proteins involved in the ubiquitin pathway. This pathway is involved in the break down and removal of damaged and/ or misfolded proteins in response to abiotic stresses (Contreras-Porcia et al., 2011; Wang et al., 2017). It is possible that the increase in protein content

seen in the short-term copper stress of 11/32c is due to an increase in misfolded proteins, that have not yet been degraded. The ubiquitin-proteosome protein degradation pathway is capable of the breakdown of proteins from a couple of minutes up to days (Glickman and Ciechanover, 2002). Further, the ubiquitin proteasome pathway in *C. reinhardtii* can be hindered as excessive reactive oxygen species (ROS) accumulate (Vallentine et al., 2014). Therefore, damaged and unfunctional proteins could accumulate inside the cell of 11/32c, whilst the cell is producing more proteins to make up for the loss of function, leading to the increase in peak heights, functionally associated to proteins seen in the FT-IR data.

3.5.3 Thiols Playing an Important Role in Copper Detoxification

An abundance of metabolites either containing or directly involved with proteins containing thiols were indicated from the LC-MS dataset. Thiol groups play a key role in plant abiotic stress, they are integral to cysteine and methionine amino acids which can undergo ROS mediated transformation and as such are important amino acids in stress response proteins (Zagorchev et al., 2013). Additionally, thiols also play an important role in glutathione, a metabolite than can not only detoxify metals and ROS itself, but are also precursors to larger biomolecules such as phytochelatins and enzyme cofactors in ROS quenching enzymes such as glutathione peroxidase and ascorbate peroxidase (Mallick and Mohn, 2000; Zagorchev et al., 2013).

The PM01 long-term copper treatment had the highest-level metabolites compared to the other treatments in Cluster 6. Within this cluster, three metabolites were identified to be involved in glutathione metabolism. This cluster had the most biological functions associated to glutathione, with Clusters 1, 5, 7 and 8 also having metabolites involved in glutathione metabolism significantly enriched within their cluster. *Scenedesmus bijugatus* cells exposed to copper for 3 days increased their total cellular thiol content. However, cellular glutathione was found to decrease in a copper concentration dependent manner (Nagalakshmi and Prasad, 2001). The authors stated that glutathione is being depleted rapidly, through various mechanisms of metal toxicity. At lower copper levels a copper sensitive strain of *Silene cucubalus* was found to contain higher quantities of reduced and oxidised glutathione than a copper tolerant strain of the same species. However, at higher concentrations of copper (>100 μM), the total glutathione concentrations and total phytochelatin content was much higher in the tolerant species than in the sensitive species (Ric De Vos et al., 1992). This can help explain why we may see the highest concentration of metabolites involved in glutathione metabolism within the long-term copper treatment for PM01. Under a short-term copper stress, these metabolites are likely being used and depleted rapidly either through interactions directly with copper, as co-factors for enzymes, or synthesis into phytochelatins. However, over a long period of stress it is easy to see why the copper tolerant extremophile may want to accumulate these important biomolecules to deal with a lower, more persistent copper stress.

As mentioned in Section 3.5.2, amino acid biosynthesis has been found enriched within many of the clusters, including for cysteine. Cysteine is an important amino acid, crucial for glutathione synthesis (the main limiting substrate for glutathione synthesis (Torricelli et al., 2004)), in addition it is the only sulphur containing amino acid which is part of a thiol group, which have been shown to have metal chelating and radical scavenging capabilities (Deneke, 2001). Among all the clusters containing amino acid enrichment, Clusters 5, 6 and 7 all contain elements of cysteine metabolism enriched

within them. A different PM01 treatment represents the highest quantities of metabolites within each cluster, suggesting that cysteine metabolism is an important process in PM01, even in non- copper stressed cells. This could potentially help explain how the PM01 long-term treatment shows a higher quantity of metabolites related to glutathione metabolism in Cluster 6. My findings are consistent with those of Ritter et al. (2014b), who, alongside a whole host of other amino acids saw a significant increase in cysteine residues under a copper stress in the brown alga *E. siliculosus.*

Other amino acids that contain sulphur groups are methionine and taurine. Methionine rich clusters have been identified in the N-terminal motif of the high affinity copper transport proteins (CTR) and suggested to play a role in copper binding (Puig and Thiele, 2002). Cluster 3, which shows the highest quantity of metabolites in the 11/32c short-term treatment, but also higher quantities in the long-term and control of 11/32c, shows a significant amount of metabolites annotated to roles involved in methionine biosynthesis or biological processes involving methionine. Metabolites involved in methionine synthesis and its incorporation into proteins, including methionine synthase and methionine tRNA ligase were found to be enriched within this cluster. In addition, methionine adenosyl transferase catalyses the synthesis of S-adenosylmethionine (Kotb and Geller, 1993). S-adenosylmethionine has been shown to be upregulated in response to heavy metal stress across a variety of organisms (Lee et al., 2006; Requejo and Tena, 2005), including copper stress in *Ectocarpus siliculosus* (Ritter et al., 2010). This could be a distinguishing factor between the two species of *Chlamydomonas*, as it suggests that PM01 may have an amino acid preference for cysteine biosynthesis which contain important metal binding and redox active thiol groups, whereas 1132c may have a preference for methionine based detoxification methods and proteins.

We have previously discussed how one of the main causes of damage to cells under copper stress is by disturbing the balance of ROS (Knauert and Knauer, 2008). Therefore, it was no surprise that metabolites involved in radical scavenging have been found in some of the clusters showing metabolite enrichment under a copper stress. These include Clusters 3, 4 and 5. Clusters 4 and 5 show metabolites enriched within the PM01 in the long-term and short-term copper stress treatments. The ROS scavenging enzyme data from Chapter 2 shows that PM01 may have a higher antioxidant capability than 11/32c. Other studies have also shown that ROS scavenging enzyme activity increases in response to copper (Laporte et al., 2016; Li et al., 2006; Sabatini et al., 2009; Wang et al., 2018). Interestingly, both Clusters 1 and 7, which had the highest metabolite expression in the 11/32c and PM01 controls, respectively, also showed enrichment of metabolites involved in radical scavenging. ROS are ever present in algal cells and are known to be useful at low concentrations for processes such as cell signalling (Devasagayam et al., 2004). It could be that the metabolites enriched in the control samples that are involved in radical scavenging, could be more focussed around ROS homeostasis in non-stressed states and a host of other metabolites are used for radical scavenging under copper stressed states. This would require further investigation into the specific metabolites involved in both the control and copper stressed states in regards to ROS homeostasis.

3.5.4 Amino Acids Playing a direct Role in Copper Chelation

Section 3.5.3 focussed on one important amino acid, cysteine in the role of copper detoxification. However, other amino acids such as proline have long been known to chelate copper (Farago and Mullen, 1979). Copper has been shown to induce proline synthesis in *C. reinhardtii* (Zhang et al.,

2008), whilst proline content was also seen to increase when the copper tolerant *C. argentea* was exposed to copper (Wang et al., 2021). Three metabolites assigned as a component of arginine and proline metabolism were found in Cluster 7 and one metabolite enriched in Cluster 8. Cluster 7 has the highest number of metabolites in the PM01 control but also relatively high quantities in the long-term treatment of PM01, whilst these metabolites were much reduced in the short-term copper treatment. This could suggest that high quantities of proline are present under non-stressed conditions in preparation for an unexpected stress (such as the short-term copper stress), where they can chelate metals such as copper. Once the proline is depleted under a short-term copper stress the cell can then build back up the cellular proline over time, once the copper has been sequestered. Two metabolites involved in alanine and aspartate metabolism were found in both Clusters 6 and 7, whilst one was found in both Cluster 1 and 8. Buayam et al. (2019), found that alanine and aspartate metabolism were more sensitive to pH change than copper whilst proline was more sensitive to copper changes. However, Wang et al. (2021) also found alanine and aspartate pathways upregulated in response to copper in *C. argentea.* It seems that amino acids could play an important role in either both or one adapting to copper and pH stress.

3.5.5 Cytochrome P450 Metabolites are Abundant Across Both Species and Most Treatments

Metabolites identified as substrates for the cytochrome P450 (CYTP450) monooxygenase system were found enriched within 6 out of 8 of the clusters. Not only that, but they also were present in very high numbers. CYTP450 is a thiol-based protein and as such copper has been found to bind and inhibit activity of this monooxygenase (Letelier et al., 2009). The CYTP450 is involved in metabolising xenobiotics in the microsome and has been found in a variety of marine microalgae phyla and shown to metabolise various marine pollutants (Pflugmacher and Sandermann, 1998). My dataset shows no clear pattern of CYTP450 metabolites by either copper treatment or species. It is possible that copper is inhibiting the enzymatic reactions, causing a build up of metabolites that are being detected in the copper treated samples. Cu^{2+} ions have previously been found to inhibit cytochrome P450 reactions in rat liver microsomes, where other metal ions such as Mg^{2+}, Mn^{2+} and Zn^{2+} did not (Kim et al., 2002). However, this does not explain the enrichment within the control samples. Another cause could be different biomolecules are being broken down processes that are occurring between the treatments, requiring a host of different enzymes and metabolites depending on the substrates that are being degraded. It would also be worth examining whether there are any differences between the copper treatments, or if the CYTP450 complex remains highly active regardless of copper treatment.

3.6 Conclusion

It appears that there is a high energy burden upon PM01 in adapting to a copper stress as shown by the reduction in both lipid and carbohydrates as seen in the FT-IR spectra. Concurrent increases in protein suggest that this utilisation of carbohydrates and lipids could be to provide energy for protein synthesis and to meet the energy demands of said proteins for them to function. In chapter 3 we saw how copper stress completely inhibited photosynthesis in the short-term copper stress in PM01 whilst, significantly but not completely inhibited photosynthesis in 11/32c. This could, in part explain some of the reduction in lipids and carbohydrate. However, under the long-term copper stress photosynthetic efficiency of PS II was completely restored compared to the control. MALDI-TOF

data provided an insight into some of the proteomic changes of the cells, where, in both species, various protein peaks appeared in the long-term copper stress for both species. A large protein with a high m/z charge was found which also showed peaks where would expect to see it should it be doubly charged. This could indicate it may play a role in either redox, or metal binding activities. This clarifies my FT-IR spectra data suggesting that proteins could play an important role in copper adaptation, especially in PM01. Metabolomic data analyses by LC-MS further support the idea of proteins playing an important role in copper detoxification, with many metabolite functional annotations being linked to protein interactions. On top of this a possible distinguishing feature between PM01 and 11/32c is with regard to amino acid preference. 11/32c samples show enrichment a lot of metabolites involved in methionine-based processes, whilst PM01 saw a lot of processes involved cysteine amino acid metabolism. Cysteines contain thiol groups, a functional group that is known to have potent ROS and metal detoxification properties, therefore their abundant presence in PM01 is not too surprising. This could be one of the methods in which PM01 can confer greater tolerance to copper. However, as this study undertook an untargeted metabolomic approach, no substantiated claims can be made. Further investigations would have to look at specific metabolites of interest with the appropriate standards run. Finally, in this analysis a large chunk of metabolite annotations were discounted, those associated to protein interactions. This could be a great source of information in PM01s adaptation to copper and could compliment the data in the following chapter. Further work will look into combining these two data sets. There are also samples ready for both GC-MS for the polar fraction, and LC-MS samples for non-polar metabolites to be analysed. Once able these will be run and may give further insights into some of these adaptation mechanisms.

3.7 References

Barbano, D., Diaz, R., Zhang, L., Sandrin, T., Gerken, H., Dempster, T., 2015. Rapid characterization of microalgae and microalgae mixtures using matrix-assisted laser desorption ionization time-of-flight mass spectrometry (MALDI-TOF MS). PLoS One 10, e0135337. https://doi.org/10.1371/journal.pone.0135337

Bequer Urbano, S., Albarracín, V.H., Ordoñez, O.F., Farías, M.E., Alvarez, H.M., 2013. Lipid storage in high-altitude Andean Lakes extremophiles and its mobilization under stress conditions in Rhodococcus sp. A5, a UV-resistant actinobacterium. Extremophiles 17, 217–227. https://doi.org/10.1007/s00792-012-0508-2

Buayam, N., Davey, M.P., Smith, A.G., Pumas, C., 2019. Effects of copper and pH on the growth and physiology of Desmodesmus sp. AARLG074. Metabolites 9. https://doi.org/10.3390/metabo9050084

Calvano, C.D., Picca, R.A., Bonerba, E., Tantillo, G., Cioffi, N., Palmisano, F., 2016. MALDI-TOF mass spectrometry analysis of proteins and lipids in Escherichia coli exposed to copper ions and nanoparticles. J. Mass Spectrom. 828–840. https://doi.org/10.1002/jms.3823

Cid, C., Garcia-Descalzo, L., Casado-Lafuente, V., Amils, R., Aguilera, A., 2010. Proteomic analysis of the response of an acidophilic strain of Chlamydomonas sp. (Chlorophyta) to natural metal-rich water. Proteomics 10, 2026–2036. https://doi.org/10.1002/pmic.200900592

Contreras-Porcia, L., Dennett, G., Gonzalez, A., Vergara, E., Medina, C., Correa, J.A., Moenne, A., 2011. Identification of Copper-Induced Genes in the Marine Alga Ulva compressa (Chlorophyta). Mar. Biotechnol. 13, 544–556. https://doi.org/10.1007/s10126-010-9325-8

D'Souza, L., Devi, P., Divya Shridhar, M.P., Naik, C.G., 2008. Use of Fourier Transform Infrared (FTIR) spectroscopy to study cadmium-induced changes in Padina tetrastromatica (Hauck). Anal. Chem. Insights 2008, 135–143. https://doi.org/10.4137/aci.s0

Dean, A.P., Sigee, D.C., Estrada, B., Pittman, J.K., 2010. Using FTIR spectroscopy for rapid determination of lipid accumulation in response to nitrogen limitation in freshwater microalgae. Bioresour. Technol. 101, 4499–4507. https://doi.org/10.1016/j.biortech.2010.01.065

Deneke, S.M., 2001. Thiol-based antioxidants. Curr. Top. Cell. Regul. 36, 151–180. https://doi.org/10.1016/S0070-2137(01)80007-8

Déniel, M., Lagarde, F., Caruso, A., Errien, N., 2020. Infrared spectroscopy as a tool to monitor interactions between nanoplastics and microalgae. Anal. Bioanal. Chem. 412, 4413–4422. https://doi.org/10.1007/s00216-020-02683-9

Devasagayam, T.P.A., Tilak, J., Boloor, K.K., Sane, K.S., Ghaskadbi, S.S., Lele, R.D., 2004. Free radicals and antioxidants in human health: current status and future prospects. J Assoc Physicians India 52, 794–804. https://doi.org/10.1016/S0300-483X(03)00149-5

Domenighini, A., Giordano, M., 2009. Fourier transform infrared spectroscopy of microalgae as a novel tool for biodiversity studies, species identification, and the assessment of water quality. J. Phycol. 45, 522–531. https://doi.org/10.1111/j.1529-8817.2009.00662.x

Driver, T., Bajhaiya, A.K., Allwood, J.W., Goodacre, R., Pittman, J.K., Dean, A.P., 2015. Metabolic responses of eukaryotic microalgae to environmental stress limit the ability of FT-IR spectroscopy for species identification. Algal Res. 11, 148–155. https://doi.org/10.1016/j.algal.2015.06.009

Emami, K., Hack, E., Nelson, A., Brain, C.M., Lyne, F.M., Mesbahi, E., Day, J.G., Caldwell, G.S., 2015. Proteomic-based biotyping reveals hidden diversity within a microalgae culture collection: An example using Dunaliella. Sci. Rep. 5, 1–15. https://doi.org/10.1038/srep10036

Farago, M.E., Mullen, W.A., 1979. Plants which accumulate metals. Part IV. A possible copper-proline complex from the roots of armeria maritima. Inorganica Chim. Acta 32, L93–L94. https://doi.org/10.1016/S0020-1693(00)91627-X

Fazelian, N., Movafeghi, A., Yousefzadi, M., Rahimzadeh, M., 2019. Cytotoxic impacts of CuO nanoparticles on the marine microalga Nannochloropsis oculata. Environ. Sci. Pollut. Res. 26,

17499–17511. https://doi.org/10.1007/s11356-019-05130-0

Fiehn, O., 2016. Metabolomics by gas chromatography-mass spectrometry: Combined targeted and untargeted profiling. Curr. Protoc. Mol. Biol. 2016, 30.4.1. https://doi.org/10.1002/0471142727.mb3004s114

Glickman, M.H., Ciechanover, A., 2002. The ubiquitin-proteasome proteolytic pathway: Destruction for the sake of construction. Physiol. Rev. 82, 373-428. https://doi.org/10.1152/physrev.00027.2001

Gough, K.M., Tzadu, L., Kastyak, M.Z., Kuzyk, A.C., Julian, R.L., 2010. Theoretical and experimental considerations for interpretation of amide I bands in tissue. Vib. Spectrosc. 53, 71–76. https://doi.org/10.1016/j.vibspec.2010.01.015

Harris, E.H., 2009. The Chlamydomonas Sourcebook. Academic Press, San Diego.

Jamers, A., Blust, R., De Coen, W., Griffin, J.L., Jones, O.A.H., 2013. Copper toxicity in the microalga Chlamydomonas reinhardtii: An integrated approach. BioMetals 26, 731–740. https://doi.org/10.1007/s10534-013-9648-9

Kim, J.S., Ahn, T., Yim, S.K., Yun, C.H., 2002. Differential effect of copper (II) on the cytochrome P450 enzymes and NADPH-cytochrome P450 reductase: Inhibition of cytochrome P450-catalyzed reactions by copper (II) ion. Biochemistry 41, 9438–9447. https://doi.org/10.1021/bi025908b

Knauert, S., Knauer, K., 2008. The role of reactive oxygen species in copper toxicity to two freshwater green algae. J. Phycol. 44, 311–319. https://doi.org/10.1111/j.1529-8817.2008.00471.x

Kotb, M., Geller, A.M., 1993. Methionine adenosyltransferase: Structure and function. Pharmacol. Ther. 59, 125- 143. https://doi.org/10.1016/0163-7258(93)90042-C

Laporte, D., Rodríguez, F., González, A., Zúñiga, A., Castro-Nallar, E., Saéz, C.A., Moenne, A., 2020. Copper-induced concomitant increases in photosynthesis, respiration, and C, N and S assimilation revealed by transcriptomic analyses in Ulva compressa (Chlorophyta). BMC Plant Biol. 20. https://doi.org/10.1186/s12870-019-2229-5

Laporte, D., Valdés, N., González, A., Sáez, C.A., Zúñiga, A., Navarrete, A., Meneses, C., Moenne, A., 2016. Copper-induced overexpression of genes encoding antioxidant system enzymes and metallothioneins involve the activation of CaMs, CDPKs and MEK1/2 in the marine alga Ulva compressa. Aquat. Toxicol. 177, 433–440. https://doi.org/10.1016/j.aquatox.2016.06.017

Lee, S.E., Yoo, D.H., Son, J., Cho, K., 2006. Proteomic evaluation of cadmium toxicity on the midge Chironomus riparius Meigen larvae. Proteomics 6, 945–957. https://doi.org/10.1002/pmic.200401349

Letelier, M.E., Faúndez, M., Jara-Sandoval, J., Molina-Berríos, A., Cortés-Troncoso, J., Aracena-Parks, P., Marín-Catalán, R., 2009. Mechanisms underlying the inhibition of the cytochrome P450 system by copper ions. J. Appl. Toxicol. 29, 695–702. https://doi.org/10.1002/jat.1460

Li, M., Hu, C., Zhu, Q., Chen, L., Kong, Z., Liu, Z., 2006. Copper and zinc induction of lipid peroxidation and effects on antioxidant enzyme activities in the microalga Pavlova viridis (Prymnesiophyceae). Chemosphere 62, 565–572. https://doi.org/10.1016/j.chemosphere.2005.06.029

Llorens, N., Arola, L., Bladé, C., Mas, A., 2000. Effects of copper exposure upon nitrogen metabolism in tissue cultured Vitis vinifera. Plant Sci. 160, 159–163. https://doi.org/10.1016/S0168-9452(00)00379-4

Mallick, N., Mohn, F.H., 2000. Reactive oxygen species: response of algal cells. J. Plant Physiol. 157, 183–193. https://doi.org/10.1016/S0176-1617(00)80189-3

Mishra, A., Kavita, K., Jha, B., 2011. Characterization of extracellular polymeric substances produced by micro-algae Dunaliella salina. Carbohydr. Polym. 83, 852–857. https://doi.org/10.1016/j.carbpol.2010.08.067

Mosier, A.C., Justice, N.B., Bowen, B.P., Baran, R., Thomas, B.C., Northen, T.R., Banfield, J.F.,

2013. Metabolites associated with adaptation of microorganisms to an acidophilic, metal-rich environment identified by stable-isotope-enabled metabolomics. MBio 4. https://doi.org/10.1128/mBio.00484-12

Nagalakshmi, N., Prasad, M.N.V., 2001. Responses of glutathione cycle enzymes and glutathione metabolism to copper stress in Scenedesmus bijugatus. Plant Sci. 160, 291–299. https://doi.org/10.1016/S0168-9452(00)00392-7

Nakajima, H., Fujimoto, N., Yamamoto, Y., Amemiya, T., Itoh, K., 2019. Response of secondary metabolites to Cu in the Cu-hyperaccumulator lichen Stereocaulon japonicum. Environ. Sci. Pollut. Res. 26, 905–912. https://doi.org/10.1007/s11356-018-3624-4

Niedermeyer, T.H.J., Strohalm, M., 2012. mMass as a Software Tool for the Annotation of Cyclic Peptide Tandem Mass Spectra. PLoS One 7, e44913. https://doi.org/10.1371/journal.pone.0044913

Olaveson, M.M., Stokes, P.M., 1989. Responses of the acidophilic alga *Euglena mutabilis* (euglenophyceae) to carbon enrichment at ph 3. J. Phycol. 25, 529–539. https://doi.org/10.1111/j.1529-8817.1989.tb00259.x

Pflugmacher, S., Sandermann, H., 1998. Cytochrome P450 monooxygenases for fatty acids and xenobiotics in marine macroalgae. Plant Physiol. 117, 123–128. https://doi.org/10.1104/pp.117.1.123

Piovár, J., Stavrou, E., Kaduková, J., Kimáková, T., Bačkor, M., 2011. Influence of long-term exposure to copper on the lichen photobiont Trebouxia erici and the free-living algae Scenedesmus quadricauda. Plant Growth Regul. 63, 81–88. https://doi.org/10.1007/s10725-010-9515-4

Printz, B., Lutts, S., Hausman, J.F., Sergeant, K., 2016. Copper trafficking in plants and its implication on cell wall dynamics. Front. Plant Sci. 7, 601. https://doi.org/10.3389/fpls.2016.00601

Puig, S., Thiele, D.J., 2002. Molecular mechanisms of copper uptake and distribution. Curr. Opin. Chem. Biol. 6, 171-180. https://doi.org/10.1016/S1367-5931(02)00298-3

Requejo, R., Tena, M., 2005. Proteome analysis of maize roots reveals that oxidative stress is a main contributing factor to plant arsenic toxicity. Phytochemistry 66, 1519–1528. https://doi.org/10.1016/j.phytochem.2005.05.003

Ric De Vos, C.H., Vonk, M.J., Vooijs, R., Schat, H., 1992. Glutathione depletion due to copper-induced phytochelatin synthesis causes oxidative stress in Silene cucubalus. Plant Physiol. 98, 853–858. https://doi.org/10.1104/pp.98.3.853

Ritter, A., Dittami, S.M., Goulitquer, S., Correa, J.A., Boyen, C., Potin, P., Tonon, T., 2014a. Transcriptomic and metabolomic analysis of copper stress acclimation in Ectocarpus siliculosus highlights signaling and tolerance mechanisms in brown algae. BMC Plant Biol. 14, 116. https://doi.org/10.1186/1471-2229-14-116

Ritter, A., Ubertini, M., Romac, S., Gaillard, F., Delage, L., Mann, A., Cock, J.M., Tonon, T., Correa, J.A., Potin, P., 2010. Copper stress proteomics highlights local adaptation of two strains of the model brown alga Ectocarpus siliculosus. Proteomics 10, 2074–2088. https://doi.org/10.1002/pmic.200900004

Rüger, J., Unger, N., Schie, I.W., Brunner, E., Popp, J., Krafft, C., 2016. Assessment of growth phases of the diatom Ditylum brightwellii by FT-IR and Raman spectroscopy. Algal Res. 19, 246–252. https://doi.org/10.1016/j.algal.2016.09.007

Sabatini, S.E., Juárez, Á.B., Eppis, M.R., Bianchi, L., Luquet, C.M., Ríos de Molina, M. del C., 2009. Oxidative stress and antioxidant defenses in two green microalgae exposed to copper. Ecotoxicol. Environ. Saf. 72, 1200–1206. https://doi.org/10.1016/j.ecoenv.2009.01.003

Singhal, N., Kumar, M., Kanaujia, P.K., Virdi, J.S., 2015. MALDI-TOF mass spectrometry: An emerging technology for microbial identification and diagnosis. Front. Microbiol. 6, 791. https://doi.org/10.3389/fmicb.2015.00791

Torricelli, E., Gorbi, G., Pawlik-Skowronska, B., Di Toppi, L.S., Corradi, M.G., 2004. Cadmium

tolerance, cysteine and thiol peptide levels in wild type and chromium-tolerant strains of Scenedesmus acutus (Chlorophyceae). Aquat. Toxicol. 68, 315–323. https://doi.org/10.1016/j.aquatox.2004.03.020

Urbano, S.B., Di Capua, C., Cortez, N., Farías, M.E., Alvarez, H.M., 2014. Triacylglycerol accumulation and oxidative stress in Rhodococcus species: Differential effects of pro-oxidants on lipid metabolism. Extremophiles 18, 375–384. https://doi.org/10.1007/s00792-013-0623-8

Vallentine, P., Hung, C.Y., Xie, J., Van Hoewyk, D., 2014. The ubiquitin-proteasome pathway protects Chlamydomonas reinhardtii against selenite toxicity, but is impaired as reactive oxygen species accumulate. AoB Plants 6, 1–11. https://doi.org/10.1093/aobpla/plu062

Wang, C., Wang, J., Wang, X., Xia, Y., Chen, C., Shen, Z., Chen, Y., 2017. Proteomic analysis on roots of Oenothera glazioviana under copper-stress conditions. Sci. Rep. 7, 1–12. https://doi.org/10.1038/s41598-017-10370-6

Wang, H., Ebenezer, V., Ki, J.S., 2018. Photosynthetic and biochemical responses of the freshwater green algae Closterium ehrenbergii Meneghini (Conjugatophyceae) exposed to the metal coppers and its implication for toxicity testing. J. Microbiol. 56, 426–434. https://doi.org/10.1007/s12275-018-8081-8

Wang, S., He, T., Xu, F., Li, X., Yuan, L., Wang, Q., Liu, H., 2021. Analysis of physiological and metabolite response of Celosia argentea to copper stress. Plant Biol. 23, 391–399. https://doi.org/10.1111/plb.13160

Yang, J.S., Cao, J., Xing, G.L., Yuan, H.L., 2015. Lipid production combined with biosorption and bioaccumulation of cadmium, copper, manganese and zinc by oleaginous microalgae Chlorella minutissima UTEX2341. Bioresour. Technol. 175, 537–544. https://doi.org/10.1016/j.biortech.2014.10.124

Yusuf, M., Fariduddin, Q., Ahmad, A., 2012. 24-Epibrassinolide modulates growth, nodulation, antioxidant system, and osmolyte in tolerant and sensitive varieties of Vigna radiata under different levels of nickel: A shotgun approach. Plant Physiol. Biochem. 57, 143–153. https://doi.org/10.1016/j.plaphy.2012.05.004

Zagorchev, L., Seal, C.E., Kranner, I., Odjakova, M., 2013. A central role for thiols in plant tolerance to abiotic stress. Int. J. Mol. Sci. 14, 7405- 7432. https://doi.org/10.3390/ijms14047405

Zhang, L.P., Mehta, S.K., Liu, Z.P., Yang, Z.M., 2008. Copper-induced proline synthesis is associated with nitric oxide generation in Chlamydomonas reinhardtii. Plant Cell Physiol. 49, 411–419. https://doi.org/10.1093/pcp/pcn017

Zhang, W., Tan, N.G.J., Fu, B., Li, S.F.Y., 2015. Metallomics and NMR-based metabolomics of Chlorella sp. reveal the synergistic role of copper and cadmium in multi-metal toxicity and oxidative stress. Metallomics 7, 426–438. https://doi.org/10.1039/c4mt00253a

Zhao, L., Huang, Y., Hu, J., Zhou, H., Adeleye, A.S., Keller, A.A., 2016. 1H NMR and GC-MS Based Metabolomics Reveal Defense and Detoxification Mechanism of Cucumber Plant under Nano-Cu Stress. Environ. Sci. Technol. 50, 2000–2010. https://doi.org/10.1021/acs.est.5b05011

3.8 Supplementary Tables

Supplementary Table 3.1- Functional Annotations and Enrichment of Metabolites From Cluster 1

ID Annotation	Annotation	Category	Database	In Set	FDR correction
PWY-6605	adenine and adenosine salvage II	Pathways (Chlamydomonas reinhardtii)	BioCyc	2	0.033413
2.4.2.7	Adenine phosphoribosyltransferase	Enzyme interactions	ECMDB	2	0.039139
SALVADEHYPOX-PWY	adenosine nucleotides degradation	Pathways (Chlamydomonas reinhardtii)	BioCyc	2	0.033413
N/A	Adjuvants	Biofunctions	HMDB	1	0.02391
N/A	Adrenergic Agents	Biofunctions	HMDB	1	0.038302
N/A	Analgesics, Opioid	Biofunctions	HMDB	1	0.041945
N/A	Anorexigenic Agents	Biofunctions	HMDB	1	0.021885
N/A	Anti-anxiety Agents	Biofunctions	HMDB	2	0.006397
N/A	anti-arthritic	Biofunctions	HMDB	1	0.017928
N/A	anti-cancer	Biofunctions	HMDB	1	0.038302
N/A	Anticonvulsants	Biofunctions	HMDB	4	2.29E-05
N/A	Antiepileptic Agents	Biofunctions	HMDB	1	0.015579
N/A	anti-fungal	Biofunctions	HMDB	1	0.043865
N/A	anti-inflammatory	Biofunctions	HMDB	2	0.012341
N/A	anti-mutagen	Biofunctions	HMDB	1	0.008233
N/A	anti-mycotic	Biofunctions	HMDB	1	0.017928
N/A	anti-nociceptive	Biofunctions	HMDB	1	0.029188
N/A	anti-tumor	Biofunctions	HMDB	2	0.004749
N/A	Antitussive Agents	Biofunctions	HMDB	1	0.02391
N/A	Antitussives	Biofunctions	HMDB	1	0.022224
N/A	Antiviral Agents	Biofunctions	HMDB	1	0.043865
N/A	apoptotic	Biofunctions	HMDB	1	0.042857
N/A	Appetite Depressants	Biofunctions	HMDB	1	0.021885
N/A	Barbiturates	Biofunctions	HMDB	1	0.02391
N/A	Bases	Compounds with biological roles	KEGG	3	0.005695
N/A	catabolic	Biofunctions	HMDB	1	0.022224
N/A	Central Nervous System Agents	Biofunctions	HMDB	1	0.029188
N/A	Central Nervous System Stimulants	Biofunctions	HMDB	1	0.029188
SMP00405	Codeine Pathway	SMPDB Pathway	HMDB	1	0.034649
N/A	Component of Alanine and aspartate metabolism	Biofunctions	HMDB	1	0.036837
N/A	Component of beta-Alanine metabolism	Biofunctions	HMDB	1	0.036837
N/A	Component of Biotin metabolism	Biofunctions	HMDB	1	0.017928
N/A	Component of Butanoate metabolism	Biofunctions	HMDB	1	0.035187
N/A	Component of Glutamate metabolism	Biofunctions	HMDB	1	0.049213
N/A	Component of Glutathione metabolism	Biofunctions	HMDB	1	0.029188
N/A	Component of Methionine metabolism	Biofunctions	HMDB	1	0.031956
N/A	Component of Purine metabolism	Biofunctions	HMDB	3	0.000635
N/A	Component of Riboflavin metabolism	Biofunctions	HMDB	1	0.02391

N/A	Component of Selenoamino acid metabolism	Biofunctions	HMDB	1	0.029188
N/A	Component of Taurine and hypotaurine metabolism	Biofunctions	HMDB	1	0.021885
N/A	Cross-Linking Reagents	Biofunctions	HMDB	1	0.021422
Cytochrome P450 substrates	CYP1 family	Other interactions	KEGG	40	8.91E-07
Ion channel ligands	Cys-loop superfamily	Other interactions	KEGG	50	0.004402
N/A	Dermatologicals	Biofunctions	HMDB	1	0.015579
N/A	DNA component	Biofunctions	HMDB	1	0.036837
3.2.2.7	EC number	Enzyme interactions (Chlamydomonas reinhardtii)	BioCyc	2	0.007364
3.2.2.1	EC number	Enzyme interactions (Chlamydomonas reinhardtii)	BioCyc	2	0.022485
N/A	Essential amino acid	Biofunctions	HMDB	1	0.029188
N/A	Essential amino acids	Biofunctions	HMDB	1	0.02391
N/A	Essential vitamins	Biofunctions	HMDB	1	0.029188
N/A	GABA Modulators	Biofunctions	HMDB	2	0.004749
3.5.4.3	Guanine deaminase	Enzyme interactions	BioCyc	2	0.007364
3.5.4.3	Guanine deaminase	Enzyme interactions	ECMDB	2	0.013049
PWY-6606	guanosine nucleotides degradation II	Pathways (Chlamydomonas reinhardtii)	BioCyc	2	0.033413
N/A	hepatoprotective	Biofunctions	HMDB	2	0.001131
N/A	Hypnotics and Sedatives	Biofunctions	HMDB	2	0.008233
N/A	Hypoglycemic Agents	Biofunctions	HMDB	1	0.038302
2.4.2.8	Hypoxanthine phosphoribosyltransferase	Enzyme interactions	ECMDB	3	0.006152
N/A	metal chelator	Biofunctions	HMDB	1	0.015579
N/A	Muscle Relaxants, Central	Biofunctions	HMDB	1	0.029188
N/A	Narcotics	Biofunctions	HMDB	1	0.039316
N/A	neuroprotectant	Biofunctions	HMDB	2	0.001373
N/A	neuroprotective	Biofunctions	HMDB	2	0.001112
N/A	Neuroprotective Agents	Biofunctions	HMDB	1	0.029188
N/A	Nootropic Agents	Biofunctions	HMDB	1	0.022224
N/A	Opiate Agonists	Biofunctions	HMDB	1	0.025851
PWY4LZ-81	Organic Nitrogen Assimilation	Pathways (Chlamydomonas reinhardtii)	BioCyc	3	0.033413
N/A	Osmolyte, enzyme cofactor, signalling	Biofunctions	HMDB	2	0.010816
N/A	Photosensitizing Agents	Biofunctions	HMDB	1	0.021885
N/A	Pigmenting Agents	Biofunctions	HMDB	1	0.012341
N/A	Prodrugs	Biofunctions	HMDB	1	0.02391
N/A	Protein component	Biofunctions	HMDB	2	0.001112
SMP00050	Purine Metabolism	SMPDB Pathway	HMDB	4	0.007059
2.4.2.1	Purine-nucleoside phosphorylase	Enzyme interactions	ECMDB	4	0.004078
N/A	Purines	Compounds with biological roles	KEGG	2	0.010798
N/A	radical scavenger	Biofunctions	HMDB	2	0.001112
N/A	Ribonucleosides	Compounds with biological roles	KEGG	2	0.041627

3.2.2.8	Ribosylpyrimidine nucleosidase	Enzyme interactions	ECMDB	5	9.35E-06
N/A	Stimulants	Biofunctions	HMDB	1	0.022224
ULS00086	sulfite from sulfate	UniPathway Pathways	ChEBI	2	0.038699
N/A	Sympathomimetics	Biofunctions	HMDB	1	0.043865
N/A	Thazolidinediones	Biofunctions	HMDB	1	0.012341
SMP00063	Tryptophan Metabolism	SMPDB Pathway	HMDB	3	0.01926
SMP00063	Tryptophan Metabolism	SMPDB Pathway	ECMDB	5	0.035311
M00066	Tryptophan metabolism, tryptophan => serotonin =>	KEGG modules	KEGG	2	0.035028
3.2.2.3	uridine nucleosidase	Enzyme interactions	YMDB	3	0.017728
N/A	Waste products	Biofunctions	HMDB	5	0.029604
ULS00321	xanthine from guanine	UniPathway Pathways	ChEBI	2	0.014541
2.4.2.22	Xanthine phosphoribosyltransferase	Enzyme interactions	ECMDB	2	0.035548

Supplementary Table 3.2- Functional Annotations and Enrichment of Metabolites From Cluster 2

ID Annotation	Annotation	Category	Database	In Set	FDR correction
3.5.4.2	Adenine deaminase	Enzyme interactions	BioCyc	1	0.026281
3.5.4.2	Adenine deaminase	Enzyme interactions	ECMDB	1	0.039989
2.4.2.7	Adenine phosphoribosyltransferase	Enzyme interactions	BioCyc	1	0.026281
2.4.2.7	Adenine phosphoribosyltransferase	Enzyme interactions	ECMDB	1	0.039989
2.4.2.7	Adenine phosphoribosyltransferase	Enzyme interactions	KEGG	1	0.047909
3.2.2.9	Adenosylhomocysteine nucleosidase	Enzyme interactions	BioCyc	1	0.026281
3.2.2.9	Adenosylhomocysteine nucleosidase	Enzyme interactions	ECMDB	1	0.039989
N/A	adenylate cyclase agonist	Chebi role	ChEBI	1	0.037629
N/A	Adrenergic Agents	Biofunctions	HMDB	1	0.02555
N/A	Adrenergic beta-Antagonists	Biofunctions	HMDB	2	0.001853
ULS00309	AMP from adenine	UniPathway Pathways	ChEBI	1	0.006443
3.2.2.4	AMP nucleosidase	Enzyme interactions	ECMDB	1	0.039989
N/A	Anti-anxiety Agents	Biofunctions	HMDB	1	0.030231
N/A	anticonvulsant	Chebi role	ChEBI	3	0.037629
N/A	Anticonvulsants	Biofunctions	HMDB	2	0.002623
N/A	Antidotes	Biofunctions	HMDB	1	0.014247
N/A	Antihypertensive Agents	Biofunctions	HMDB	2	0.007487
N/A	Antiviral Agents	Biofunctions	HMDB	1	0.028028
3.6.3.16	arsenite-transporting ATPase	Enzyme interactions (Chlamydomonas reinhardtii)	BioCyc	1	0.027781
3.6.3.16	arsenite-transporting ATPase	Enzyme interactions (Chlamydomonas reinhardtii)	KEGG	1	0.047909
N/A	Barbiturates	Biofunctions	HMDB	1	0.014247
N/A	Bases	Compounds with biological roles	KEGG	2	0.004094

M00084	beta-Alanine biosynthesis, cytosine / uracil => beta-alanine	KEGG modules	KEGG	1	0.033606
M00173	beta-Oxidation, acyl-CoA synthesis	KEGG modules	KEGG	1	0.033606
SMP00299	Betaxolol Pathway	SMPDB Pathway	HMDB	1	0.020382
SMP00300	Bisoprolol Pathway	SMPDB Pathway	YMDB	3	0.001651
SMP00300	Bisoprolol Pathway	SMPDB Pathway	HMDB	1	0.020382
SMP00300	Bisoprolol Pathway	SMPDB Pathway	YMDB	2	0.033445
N/A	catabolic	Biofunctions	HMDB	1	0.014112
2.7.8.5	CDP-diacylglycerol--glycerol-3-phosphate 3-phosphatidyltransferase	Enzyme interactions	BioCyc	1	0.026281
2.7.8.5	CDP-diacylglycerol--glycerol-3-phosphate 3-phosphatidyltransferase	Enzyme interactions	KEGG	1	0.047909
N/A	Component of Glycerolipid metabolism	Biofunctions	HMDB	1	0.026462
N/A	Component of Glycerophospholipid metabolism	Biofunctions	HMDB	1	0.030231
N/A	Component of Purine metabolism	Biofunctions	HMDB	1	0.033363
N/A	curing agent	Chebi role	ChEBI	1	0.037629
3.5.4.1	Cytosine deaminase	Enzyme interactions	BioCyc	1	0.026281
3.5.4.1	Cytosine deaminase	Enzyme interactions	ECMDB	1	0.039989
N/A	DNA component	Biofunctions	HMDB	1	0.024534
N/A	EC 1.1.1.189 (prostaglandin-E2 9-reductase) inhibitor	Chebi role	ChEBI	1	0.037629
N/A	EC 2.6.1.19 (4-aminobutyrate--2-oxoglutarate transaminase) inhibitor	Chebi role	ChEBI	1	0.037629
2.1.1.137	EC number	Enzyme interactions (Chlamydomonas reinhardtii)	BioCyc	2	0.005455
4.1.1.48	EC number	Enzyme interactions (Chlamydomonas reinhardtii)	BioCyc	1	0.026281
1.20.4.1	EC number	Enzyme interactions (Chlamydomonas reinhardtii)	BioCyc	1	0.026281
5.3.1.24	EC number	Enzyme interactions (Chlamydomonas reinhardtii)	BioCyc	1	0.026281
3.2.2.7	EC number	Enzyme interactions (Chlamydomonas reinhardtii)	BioCyc	1	0.026281
N/A	EENT Drugs	Biofunctions	HMDB	1	0.011096
N/A	Enzyme Inhibitors	Biofunctions	HMDB	2	0.004252
N/A	GABA Agents	Biofunctions	HMDB	1	0.006347
2.7.1.30	Glycerol kinase	Enzyme interactions	BioCyc	1	0.026281
2.7.1.30	Glycerol kinase	Enzyme interactions	ECMDB	1	0.039989
2.7.1.30	Glycerol kinase	Enzyme interactions	KEGG	1	0.047909
2.3.1.15	Glycerol-3-phosphate 1-O-acyltransferase	Enzyme interactions	BioCyc	1	0.027781
2.3.1.15	Glycerol-3-phosphate 1-O-acyltransferase	Enzyme interactions	KEGG	1	0.047909
1.1.5.3	Glycerol-3-phosphate dehydrogenase	Enzyme interactions	BioCyc	1	0.034869

1.1.5.3	Glycerol-3-phosphate dehydrogenase	Enzyme interactions	ECMDB	1	0.039989
1.1.5.3	Glycerol-3-phosphate dehydrogenase	Enzyme interactions	KEGG	1	0.047909
1.1.1.94	Glycerol-3-phosphate dehydrogenase (NAD(P)(+))	Enzyme interactions	BioCyc	1	0.026281
1.1.1.94	Glycerol-3-phosphate dehydrogenase (NAD(P)(+))	Enzyme interactions	ECMDB	1	0.039989
1.1.1.8	glycerol-3-phosphate dehydrogenase (NAD+)	Enzyme interactions (Chlamydomonas reinhardtii)	BioCyc	1	0.026281
1.1.1.8	glycerol-3-phosphate dehydrogenase (NAD+)	Enzyme interactions (Chlamydomonas reinhardtii)	KEGG	1	0.047909
SMP00039	Glycerolipid Metabolism	SMPDB Pathway	HMDB	2	0.020382
3.1.4.46	Glycerophosphodiester phosphodiesterase	Enzyme interactions	BioCyc	1	0.026281
3.1.4.46	Glycerophosphodiester phosphodiesterase	Enzyme interactions	ECMDB	1	0.039989
3.1.4.46	Glycerophosphodiester phosphodiesterase	Enzyme interactions	KEGG	1	0.047909
N/A	hepatitis C protease inhibitor	Chebi role	ChEBI	2	0.015256
N/A	Hypnotics and Sedatives	Biofunctions	HMDB	2	0.002623
6.2.1.3	Long-chain-fatty-acid--CoA ligase	Enzyme interactions	ECMDB	1	0.039989
3.2.2.16	methylthioadenosine nucleosidase	Enzyme interactions (Chlamydomonas reinhardtii)	KEGG	1	0.047909
N/A	neuroprotectant	Biofunctions	HMDB	1	0.017982
N/A	neuroprotective	Biofunctions	HMDB	1	0.01477
3.1.2.22	palmitoyl[protein] hydrolase	Enzyme interactions (Chlamydomonas reinhardtii)	BioCyc	1	0.026281
3.1.2.22	palmitoyl[protein] hydrolase	Enzyme interactions (Chlamydomonas reinhardtii)	KEGG	1	0.047909
M00182	Phosphatidic acid (PA) biosynthesis	KEGG modules	KEGG	1	0.033606
M00184	Phosphatidylcholine (PC) biosynthesis, PE => PC	KEGG modules	KEGG	1	0.033606
N/A	Prodrugs	Biofunctions	HMDB	1	0.014247
N/A	protein kinase A agonist	Chebi role	ChEBI	1	0.037629
N/A	Protein synthesis, amino acid biosynthesis	Biofunctions	HMDB	3	0.002124
N/A	Purines	Compounds with biological roles	KEGG	1	0.044655
3.2.2.8	Ribosylpyrimidine nucleosidase	Enzyme interactions	ECMDB	2	0.010446
N/A	Signaling	Biofunctions	HMDB	1	0.027284
N/A	signalling	Biofunctions	HMDB	1	0.018221
ULS00433	S-methyl-5-thio-alpha-D-ribose 1-phosphate from S-methyl-5'-thioadenosine (phosphorylase route)	UniPathway Pathways	ChEBI	1	0.006443
N/A	Styrenes	Compounds with biological roles	KEGG	1	0.033595
N/A	Succinimides	Biofunctions	HMDB	1	0.007487
N/A	sympatholytic agent	Chebi role	ChEBI	2	0.037629
N/A	Sympatholytics	Biofunctions	HMDB	2	0.001853

M00181	Triacylglycerol biosynthesis	KEGG modules	KEGG	1	0.033606
ULS00346	uracil from cytosine	UniPathway Pathways	ChEBI	1	0.006443

Supplementary Table 3.3- Functional Annotations and Enrichment of Metabolites From Cluster 3

ID Annotation	Annotation	Category	Database	In Set	FDR correction
1.97.1.4	[Formate-C-acetyltransferase]-activating enzyme	Enzyme interactions	BioCyc	1	0.049235
2.1.1.14	5-methyltetrahydropteroyl triglutamate--homocysteine S-methyltransferase	Enzyme interactions	BioCyc	1	0.049235
N/A	Adjuvants, Anesthesia	Biofunctions	HMDB	1	0.016317
N/A	Adrenergic alpha-Agonists	Biofunctions	HMDB	1	0.016317
N/A	Adrenergic beta-Agonists	Biofunctions	HMDB	1	0.016067
N/A	Anesthetics, Intravenous	Biofunctions	HMDB	1	0.015332
N/A	Anti-anxiety Agents	Biofunctions	HMDB	1	0.020712
N/A	Anticonvulsants	Biofunctions	HMDB	1	0.025384
N/A	Antiemetics	Biofunctions	HMDB	1	0.020712
N/A	Antifibrinolytic Agents	Biofunctions	HMDB	1	0.006955
N/A	Antimetabolites	Biofunctions	HMDB	1	0.018601
4.1.1.28	aromatic-L-amino-acid decarboxylase	Enzyme interactions (Chlamydomonas reinhardtii)	KEGG	1	0.032763
ULS00183	betaine from betaine aldehyde	UniPathway Pathways	ChEBI	2	0.003988
SMP00123	Betaine Metabolism	SMPDB Pathway	HMDB	3	0.000889
1.2.1.8	Betaine-aldehyde dehydrogenase	Enzyme interactions	KEGG	2	0.003035
1.2.1.8	Betaine-aldehyde dehydrogenase	Enzyme interactions	BioCyc	2	0.010999
1.2.1.8	Betaine-aldehyde dehydrogenase	Enzyme interactions	ECMDB	2	0.01598
2.8.1.6	Biotin synthase	Enzyme interactions	KEGG	1	0.032763
2.8.1.6	Biotin synthase	Enzyme interactions	BioCyc	1	0.049235
N/A	Bronchodilator Agents	Biofunctions	HMDB	1	0.019394
N/A	Cardiotonic Agents	Biofunctions	HMDB	1	0.016067
N/A	Component of Aminoacyl-tRNA biosynthesis	Biofunctions	HMDB	1	0.016067
N/A	Component of Glycine, serine and threonine metabolism	Biofunctions	HMDB	3	3.43E-05
N/A	Component of Histidine metabolism	Biofunctions	HMDB	1	0.016269
N/A	Component of Methionine metabolism	Biofunctions	HMDB	2	0.000305
N/A	Component of Riboflavin metabolism	Biofunctions	HMDB	1	0.0125
N/A	Component of Selenoamino acid metabolism	Biofunctions	HMDB	1	0.015332
N/A	Component of Stilbene, coumarine and lignin biosynthesis	Biofunctions	HMDB	1	0.009479
N/A	Component of Tyrosine metabolism	Biofunctions	HMDB	3	3.43E-05
1.3.99.22	Coproporphyrinogen dehydrogenase	Enzyme interactions	KEGG	1	0.032763
1.3.99.22	Coproporphyrinogen dehydrogenase	Enzyme interactions	BioCyc	1	0.049235
Cytochrome P450 substrates	CYP1 family	Other interactions	KEGG	16	1.25E-05

2.5.1.47	cysteine synthase	Enzyme interactions	YMDB	1	0.030358
N/A	Dermatologicals	Biofunctions	HMDB	1	0.006955
1.1.1.303	Diacetyl reductase ((R)-acetoin forming)	Enzyme interactions	YMDB	1	0.018363
M00076	Dopamine / noradrenaline / adrenaline metabolism	KEGG modules	KEGG	2	0.04417
4.4.1.11	EC number	Enzyme interactions (Chlamydomonas reinhardtii)	BioCyc	1	0.049235
1.8.4.14	EC number	Enzyme interactions (Chlamydomonas reinhardtii)	BioCyc	1	0.049235
3.2.2.1	EC number	Enzyme interactions (Chlamydomonas reinhardtii)	BioCyc	1	0.049235
3.4.13.18	EC number	Enzyme interactions (Chlamydomonas reinhardtii)	BioCyc	2	0.049235
2.6.1.88	EC number	Enzyme interactions (Chlamydomonas reinhardtii)	BioCyc	1	0.049235
2.7.1.1	EC number	Enzyme interactions (Chlamydomonas reinhardtii)	BioCyc	1	0.049235
2.4.1.141	EC number	Enzyme interactions (Chlamydomonas reinhardtii)	BioCyc	1	0.049235
3.4.11.18	EC number	Enzyme interactions (Chlamydomonas reinhardtii)	BioCyc	1	0.049235
1.2.1.28	EC number	Enzyme interactions (Chlamydomonas reinhardtii)	BioCyc	1	0.049235
2.1.1.192	EC number	Enzyme interactions (Chlamydomonas reinhardtii)	BioCyc	1	0.049235
2.4.1.142	EC number	Enzyme interactions (Chlamydomonas reinhardtii)	BioCyc	1	0.049235
4.1.99.17	EC number	Enzyme interactions (Chlamydomonas reinhardtii)	BioCyc	1	0.049235
N/A	Enzyme cofactor	Biofunctions	HMDB	1	0.015332
N/A	Enzyme Inhibitors	Biofunctions	HMDB	2	0.002956
N/A	Enzyme Inhibitors Antimetabolites	Biofunctions	HMDB	1	0.005963
N/A	Essential amino acids	Biofunctions	HMDB	1	0.0125
N/A	Essential minerals	Biofunctions	HMDB	1	0.016317
N/A	Free Radical Scavengers	Biofunctions	HMDB	1	0.010424
N/A	GABA Modulators	Biofunctions	HMDB	1	0.018668
PWY1F-353	glycine betaine biosynthesis III (plants)	Pathways (Chlamydomonas reinhardtii)	BioCyc	2	0.021823
N/A	Good's buffer substance	Chebi role	ChEBI	2	0.010946

N/A	Gout Suppressants	Biofunctions	HMDB	1	0.008344
3.5.4.3	Guanine deaminase	Enzyme interactions	BioCyc	1	0.049235
2.1.1.10	Homocysteine S-methyltransferase	Enzyme interactions	BioCyc	1	0.049235
N/A	Hypnotics and Sedatives	Biofunctions	HMDB	1	0.024325
N/A	Hypoglycemic Agents	Biofunctions	HMDB	1	0.016317
2.4.2.8	Hypoxanthine phosphoribosyltransferase	Enzyme interactions	BioCyc	1	0.049235
2.8.1.8	Lipoyl synthase	Enzyme interactions	KEGG	1	0.032763
2.8.1.8	Lipoyl synthase	Enzyme interactions	BioCyc	1	0.049235
2.5.1.6	Methionine adenosyltransferase	Enzyme interactions	YMDB	1	0.01227
2.5.1.6	Methionine adenosyltransferase	Enzyme interactions	KEGG	1	0.032763
2.5.1.6	Methionine adenosyltransferase	Enzyme interactions	BioCyc	1	0.049235
2.1.1.13	Methionine synthase	Enzyme interactions	KEGG	1	0.032763
2.1.1.13	Methionine synthase	Enzyme interactions	BioCyc	1	0.049235
6.1.1.10	Methionine--tRNA ligase	Enzyme interactions	KEGG	1	0.032763
6.1.1.10	Methionine--tRNA ligase	Enzyme interactions	BioCyc	1	0.049235
N/A	Muscle Relaxants, Central	Biofunctions	HMDB	1	0.015332
N/A	Osmolyte	Biofunctions	HMDB	2	7.13E-05
1.8.4.11	Peptide-methionine (S)-S-oxide reductase	Enzyme interactions	KEGG	1	0.032763
N/A	plant growth retardant	Chebi role	ChEBI	2	0.010946
N/A	Sympathomimetic	Biofunctions	HMDB	1	0.0125
N/A	Sympathomimetics	Biofunctions	HMDB	2	0.000765
SMP00287	Tranexamic Acid Pathway	SMPDB Pathway	HMDB	1	0.034649
2.4.2.29	tRNA-guanine(34) transglycosylase	Enzyme interactions	KEGG	1	0.032763
2.4.2.29	tRNA-guanine(34) transglycosylase	Enzyme interactions	BioCyc	1	0.049235
SMP00006	Tyrosine Metabolism	SMPDB Pathway	HMDB	3	0.026522
3.2.2.3	uridine nucleosidase	Enzyme interactions	YMDB	1	0.030358
N/A	Vasoconstrictor Agents	Biofunctions	HMDB	1	0.016317
N/A	xenobiotic metabolite	Chebi role	ChEBI	2	0.027168

Supplementary Table 3.4- Functional Annotations and Enrichment of Metabolites From Cluster 4

ID Annotation	Annotation	Category	Database	In Set	FDR correction
PWY-6890	4-amino-2-methyl-5-diphosphomethylpyrimidine biosynthesis	Pathways (Chlamydomonas reinhardtii)	BioCyc	1	0.039181
ULS00057	4-amino-2-methyl-5-diphosphomethylpyrimidine from 5-amino-1-(5-phospho-D-ribosyl)imidazole	UniPathway Pathways	ChEBI	1	0.007729
ULS00058	4-methyl-5-(2-phosphoethyl)-thiazole from 5-(2-hydroxyethyl)-4-methylthiazole	UniPathway Pathways	ChEBI	1	0.007729
6.3.4.-	5-(carboxyamino)imidazole ribonucleotide synthase	Enzyme interactions	YMDB	1	0.039694
3.2.1.86	6-phospho-beta-glucosidase	Enzyme interactions	ECMDB	1	0.037886

2.4.2.7	Adenine phosphoribosyltransferase	Enzyme interactions	ECMDB	1	0.037886
3.1.3.73	Adenosylcobalamin/alpha-ribazole phosphatase	Enzyme interactions	ECMDB	1	0.032272
N/A	Adjuvants, Anesthesia	Biofunctions	HMDB	1	0.019742
N/A	Analgesics	Biofunctions	HMDB	1	0.026786
N/A	Anesthetics, Intravenous	Biofunctions	HMDB	1	0.014829
N/A	Anti-anxiety Agents	Biofunctions	HMDB	1	0.025633
N/A	anti-arthritic	Biofunctions	HMDB	1	0.005947
N/A	Anticonvulsants	Biofunctions	HMDB	2	0.001673
N/A	Antiemetics	Biofunctions	HMDB	1	0.025633
N/A	anti-fungal	Biofunctions	HMDB	1	0.024339
N/A	anti-inflammatory	Biofunctions	HMDB	2	0.002273
N/A	anti-mutagen	Biofunctions	HMDB	1	0.00248
N/A	anti-mycotic	Biofunctions	HMDB	1	0.005947
N/A	anti-nociceptive	Biofunctions	HMDB	1	0.014829
N/A	Anti-oxidant	Biofunctions	HMDB	1	0.012148
N/A	anti-spectic	Biofunctions	HMDB	1	0.005576
N/A	anti-tumor	Biofunctions	HMDB	2	0.000872
SMP00066	Biotin Metabolism	SMPDB Pathway	YMDB	2	0.00281
SMP00066	Biotin Metabolism	SMPDB Pathway	YMDB	1	0.03387
SMP00066	Biotin Metabolism	SMPDB Pathway	HMDB	1	0.035486
SMP00066	Biotin Metabolism	SMPDB Pathway	ECMDB	2	0.044936
6.3.4.15	Biotin--[acetyl-CoA-carboxylase] ligase	Enzyme interactions	ECMDB	1	0.032272
6.3.4.9	biotin---[methylmalonyl-CoA-carboxytransferase] ligase	Enzyme interactions	YMDB	1	0.039694
6.3.4.10	biotin---[propionyl-CoA-carboxylase (ATP-hydrolysing)] ligase	Enzyme interactions	YMDB	1	0.039694
N/A	Component of Tyrosine metabolism	Biofunctions	HMDB	1	0.026786
M00229	Conjugated bile acid biosynthesis, choloyl-CoA =>	KEGG modules	KEGG	1	0.022925
Cytochrome P450 substrates	CYP1 family	Other interactions	KEGG	19	0.000181
1.3.5.2	dihydroorotate dehydrogenase	Enzyme interactions (Chlamydomonas reinhardtii)	KEGG	1	0.005166
3.2.2.1	EC number	Enzyme interactions (Chlamydomonas reinhardtii)	BioCyc	1	0.020558
6.3.4.3	EC number	Enzyme interactions (Chlamydomonas reinhardtii)	BioCyc	1	0.020558
2.3.2.2	EC number	Enzyme interactions (Chlamydomonas reinhardtii)	BioCyc	1	0.020558
6.3.2.17	EC number	Enzyme interactions (Chlamydomonas reinhardtii)	BioCyc	1	0.020558
2.3.1.84	EC number	Enzyme interactions (Chlamydomonas reinhardtii)	BioCyc	1	0.033428

PWY-2161	folate polyglutamylation	Pathways (Chlamydomonas reinhardtii)	BioCyc	1	0.039905
N/A	GABA Modulators	Biofunctions	HMDB	1	0.024339
1.1.5.3	glycerol-3-phosphate dehydrogenase	Enzyme interactions (Chlamydomonas reinhardtii)	KEGG	1	0.005166
PWY-6599	guanine and guanosine salvage II	Pathways (Chlamydomonas reinhardtii)	BioCyc	1	0.039181
3.5.4.3	Guanine deaminase	Enzyme interactions	BioCyc	1	0.020558
3.5.4.3	Guanine deaminase	Enzyme interactions	ECMDB	1	0.032272
PWY-6606	guanosine nucleotides degradation II	Pathways (Chlamydomonas reinhardtii)	BioCyc	1	0.039181
N/A	hepatoprotective	Biofunctions	HMDB	2	0.000206
N/A	human xenobiotic metabolite	Chebi role	ChEBI	3	0.03871
2.7.1.50	Hydroxyethylthiazole kinase	Enzyme interactions	BioCyc	1	0.020558
2.7.1.50	Hydroxyethylthiazole kinase	Enzyme interactions	ECMDB	1	0.032272
2.7.1.49	Hydroxymethylpyrimidine kinase	Enzyme interactions	ECMDB	1	0.032272
2.7.1.49	Hydroxymethylpyrimidine kinase	Enzyme interactions	YMDB	1	0.039694
PWY-6910	hydroxymethylpyrimidine salvage	Pathways (Chlamydomonas reinhardtii)	BioCyc	1	0.039181
N/A	Hypnotics and Sedatives	Biofunctions	HMDB	1	0.026786
2.4.2.8	Hypoxanthine phosphoribosyltransferase	Enzyme interactions	BioCyc	1	0.020558
2.4.2.8	Hypoxanthine phosphoribosyltransferase	Enzyme interactions	ECMDB	1	0.037886
M00070	Lignin biosynthesis, coniferyl alcohol => lignin	KEGG modules	KEGG	1	0.022925
N/A	metal chelator	Biofunctions	HMDB	1	0.005576
N/A	Muscle Relaxants, Central	Biofunctions	HMDB	1	0.014829
2.7.4.7	Phosphomethylpyrimidine kinase	Enzyme interactions	BioCyc	1	0.020558
2.7.4.7	Phosphomethylpyrimidine kinase	Enzyme interactions	ECMDB	1	0.032272
2.7.4.7	Phosphomethylpyrimidine kinase	Enzyme interactions	YMDB	1	0.039694
M00096	Purine alkaloid biosynthesis, xanthosine => theobromine, caffeine,	KEGG modules	KEGG	1	0.030777
N/A	Purines	Compounds with biological roles	KEGG	1	0.040257
N/A	radical scavenger	Biofunctions	HMDB	2	0.000206
3.2.2.8	Ribosylpyrimidine nucleosidase	Enzyme interactions	ECMDB	1	0.037886
THISYNARA-PWY	superpathway of thiamin diphosphate biosynthesis III (eukaryotes)	Pathways (Chlamydomonas reinhardtii)	BioCyc	1	0.039181
PWY-6908	thiamin diphosphate biosynthesis IV (eukaryotes)	Pathways (Chlamydomonas reinhardtii)	BioCyc	1	0.039181
PWY-6897	thiamin salvage II	Pathways (Chlamydomonas reinhardtii)	BioCyc	2	0.002386
3.5.99.2	thiaminase	Enzyme interactions	YMDB	2	0.010832
M00252	Thiamine biosynthesis, AIR => thiamine-P/thiamine-2P	KEGG modules	KEGG	2	0.001063

cre00730	Thiamine metabolism	Pathways (Chlamydomonas reinhardtii)	KEGG	2	0.048368
2.5.1.3	thiamine-phosphate diphosphorylase	Enzyme interactions	BioCyc	1	0.020558
2.4.2.4	Thymidine phosphorylase	Enzyme interactions	ECMDB	1	0.037886
2.4.2.29	tRNA-guanine(34) transglycosylase	Enzyme interactions	KEGG	1	0.005166
2.4.2.29	tRNA-guanine(34) transglycosylase	Enzyme interactions	BioCyc	1	0.020558
2.4.2.29	tRNA-guanine(34) transglycosylase	Enzyme interactions	ECMDB	1	0.032272
ULS00321	xanthine from guanine	UniPathway Pathways	ChEBI	1	0.007729
2.4.2.22	Xanthine phosphoribosyltransferase	Enzyme interactions	ECMDB	1	0.037886

Supplementary Table 3.5- Functional Annotations and Enrichment of Metabolites From Cluster 5

ID Annotation	Annotation	Category	Database	In Set	FDR correction
2.5.1.10	(2E,6E)-farnesyl diphosphate synthase	Enzyme interactions	YMDB	2	0.029038
1.14.12.19	3-phenylpropanoate dioxygenase	Enzyme interactions	ECMDB	2	0.025153
N/A	Abortifacient Agents	Biofunctions	HMDB	1	0.026798
N/A	Abortifacient Agents, Nonsteroidal	Biofunctions	HMDB	1	0.035666
N/A	Amphetamines	Biofunctions	HMDB	1	0.022008
N/A	Anesthetics, Intravenous	Biofunctions	HMDB	1	0.042148
N/A	Anticholesteremic Agents	Biofunctions	HMDB	1	0.041768
N/A	Antidyskinetics	Biofunctions	HMDB	2	0.006713
N/A	anti-hypertensive	Biofunctions	HMDB	1	0.031732
N/A	anti-inflammatory	Biofunctions	HMDB	2	0.026798
N/A	Antilipemic Agents	Biofunctions	HMDB	2	0.001092
N/A	anti-mutagen	Biofunctions	HMDB	1	0.014318
N/A	Antiparkinson Agents	Biofunctions	HMDB	2	0.007814
N/A	anti-tumor	Biofunctions	HMDB	4	1.46E-05
N/A	Anti-Ulcer Agents	Biofunctions	HMDB	1	0.042148
2.6.1.42	branched-chain-amino-acid transaminase	Enzyme interactions (Chlamydomonas reinhardtii)	KEGG	2	0.045772
M00232	C21-Steroid hormone biosynthesis, progesterone => cortisol/cortisone	KEGG modules	KEGG	2	0.045159
N/A	catabolic	Biofunctions	HMDB	2	0.001092
N/A	Cell signalling	Biofunctions	HMDB	1	0.039978
N/A	Central Nervous System Stimulants	Biofunctions	HMDB	1	0.042148
N/A	Component of Biotin metabolism	Biofunctions	HMDB	1	0.031732
N/A	Component of Cysteine metabolism	Biofunctions	HMDB	1	0.043276
N/A	Component of D-Glutamine and D-glutamate metabolism	Biofunctions	HMDB	1	0.035666
N/A	Component of Glutathione metabolism	Biofunctions	HMDB	1	0.042148
N/A	Component of Lysine biosynthesis	Biofunctions	HMDB	1	0.037182
N/A	Component of Nitrogen metabolism	Biofunctions	HMDB	1	0.047977

N/A	Component of Novobiocin biosynthesis	Biofunctions	HMDB	1	0.039873
N/A	Component of Pantothenate and CoA biosynthesis	Biofunctions	HMDB	1	0.042148
N/A	Component of Phenylalanine metabolism	Biofunctions	HMDB	1	0.042148
N/A	Component of Phenylalanine, tyrosine and tryptophan biosynthesis	Biofunctions	HMDB	1	0.043276
N/A	Component of Terpenoid biosynthesis	Biofunctions	HMDB	1	0.039978
N/A	Component of Tyrosine metabolism	Biofunctions	HMDB	3	0.001092
N/A	Component of Valine, leucine and isoleucine biosynthesis	Biofunctions	HMDB	1	0.039978
N/A	Component of Vitamin B6 metabolism	Biofunctions	HMDB	1	0.042148
Cytochrome P450 substrates	CYP1 family	Other interactions	KEGG	59	9.4E-23
2.5.1.1	dimethylallyltranstransferase	Enzyme interactions	YMDB	2	0.002882
N/A	Dopamine Agents	Biofunctions	HMDB	1	0.039978
N/A	Dopamine Agonists	Biofunctions	HMDB	1	0.042148
N/A	Dopamine Uptake Inhibitors	Biofunctions	HMDB	1	0.039978
N/A	Enzyme cofactor	Biofunctions	HMDB	1	0.042148
N/A	Essential amino acids	Biofunctions	HMDB	1	0.039978
N/A	Essential vitamins	Biofunctions	HMDB	1	0.042148
N/A	Fribic Acid Derivatives	Biofunctions	HMDB	1	0.022008
N/A	hepatoprotective	Biofunctions	HMDB	1	0.042148
N/A	Hormones, Membrane component	Biofunctions	HMDB	7	1.49E-05
N/A	Hydroxymethylglutaryl-CoA Reductase Inhibitors	Biofunctions	HMDB	1	0.037182
N/A	metal chelator	Biofunctions	HMDB	1	0.026798
N/A	Muscle Relaxants, Central	Biofunctions	HMDB	2	0.003353
N/A	Nucleoside and Nucleotide Reverse Transcriptase Inhibitors	Biofunctions	HMDB	1	0.039873
N/A	Oxytocics	Biofunctions	HMDB	1	0.037182
SMP00463	Phosphatidylinositol Phosphate Metabolism	SMPDB Pathway	ECMDB	3	0.038083
N/A	Progestagens	Compounds with biological roles	KEGG	2	0.016835
N/A	Prostaglandins	Biofunctions	HMDB	1	0.022008
N/A	Protein component	Biofunctions	HMDB	1	0.039978
N/A	radical scavenger	Biofunctions	HMDB	2	0.001212
N/A	Reverse Transcriptase Inhibitors	Biofunctions	HMDB	1	0.042148
N/A	signalling	Biofunctions	HMDB	1	0.042148
N/A	Skeletal Muscle Relaxants	Biofunctions	HMDB	1	0.041768
N/A	Steroid hormones	Compounds with biological roles	KEGG	4	0.016835

Supplementary Table 3.6- Functional Annotations and Enrichment of Metabolites From Cluster 6

ID Annotation	Annotation	Category	Database	In Set	FDR correction
3.5.4.2	Adenine deaminase	Enzyme interactions	ECMDB	2	0.032978
3.5.4.2	Adenine deaminase	Enzyme interactions	BioCyc	2	0.039548
N/A	adenosine receptor antagonist	Chebi role	ChEBI	2	0.002722

N/A	Adjuvants, Anesthesia	Biofunctions	HMDB	1	0.024592
N/A	Amino acids	Compounds with biological roles	KEGG	6	0.001068
N/A	Anesthetics, Intravenous	Biofunctions	HMDB	2	0.000266
N/A	Anti-anxiety Agents	Biofunctions	HMDB	1	0.035297
N/A	Anticonvulsants	Biofunctions	HMDB	2	0.00189
N/A	Antiemetics	Biofunctions	HMDB	2	0.001223
N/A	anti-fungal	Biofunctions	HMDB	1	0.032018
N/A	anti-microbial	Biofunctions	HMDB	1	0.034971
N/A	anti-tumor	Biofunctions	HMDB	1	0.03159
6.3.4.5	Argininosuccinate synthase	Enzyme interactions	ECMDB	2	0.032978
6.3.4.5	Argininosuccinate synthase	Enzyme interactions	BioCyc	2	0.045913
N/A	Aromatase Inhibitors	Biofunctions	HMDB	1	0.009629
N/A	B vitamin	Chebi role	ChEBI	2	0.015971
N/A	Common amino acids	Compounds with biological roles	KEGG	5	0.000124
N/A	Component of Alanine and aspartate metabolism	Biofunctions	HMDB	2	0.000493
N/A	Component of Aminoacyl-tRNA biosynthesis	Biofunctions	HMDB	3	4.08E-06
N/A	Component of Arginine and proline metabolism	Biofunctions	HMDB	3	3.49E-05
N/A	Component of Biotin metabolism	Biofunctions	HMDB	1	0.008003
N/A	Component of Cysteine metabolism	Biofunctions	HMDB	2	0.000289
N/A	Component of Folate biosynthesis	Biofunctions	HMDB	1	0.020695
N/A	Component of Glutamate metabolism	Biofunctions	HMDB	1	0.034971
N/A	Component of Glutathione metabolism	Biofunctions	HMDB	1	0.020138
N/A	Component of Glycine, serine and threonine metabolism	Biofunctions	HMDB	1	0.046896
N/A	Component of Histidine metabolism	Biofunctions	HMDB	3	4.28E-06
N/A	Component of Indole and ipecac alkaloid biosynthesis	Biofunctions	HMDB	1	0.004527
N/A	Component of Methionine metabolism	Biofunctions	HMDB	1	0.020695
N/A	Component of Nicotinate and nicotinamide metabolism	Biofunctions	HMDB	1	0.020695
N/A	Component of Nitrogen metabolism	Biofunctions	HMDB	3	4.08E-06
N/A	Component of Novobiocin biosynthesis	Biofunctions	HMDB	1	0.012121
N/A	Component of Pantothenate and CoA biosynthesis	Biofunctions	HMDB	1	0.020138
N/A	Component of Phenylalanine metabolism	Biofunctions	HMDB	2	0.000266
N/A	Component of Phenylalanine, tyrosine and tryptophan biosynthesis	Biofunctions	HMDB	3	4.08E-06
N/A	Component of Purine metabolism	Biofunctions	HMDB	4	1.68E-06
N/A	Component of Pyrimidine metabolism	Biofunctions	HMDB	1	0.046958
N/A	Component of Selenoamino acid metabolism	Biofunctions	HMDB	1	0.020138
N/A	Component of Tryptophan metabolism	Biofunctions	HMDB	2	0.000924
N/A	Component of Tyrosine metabolism	Biofunctions	HMDB	4	1.68E-06
N/A	Component of Valine, leucine and isoleucine biosynthesis	Biofunctions	HMDB	2	0.00012

N/A	cyclooxygenase 3 inhibitor	Chebi role	ChEBI	2	0.006003
Cytochrome P450 substrates	CYP1 family	Other interactions	KEGG	48	9.2E-12
Ion channel ligands	Cys-loop superfamily	Other interactions	KEGG	45	0.026458
N/A	DNA component	Biofunctions	HMDB	1	0.024592
N/A	EC 3.1.4.* (phosphoric diester hydrolase) inhibitor	Chebi role	ChEBI	2	0.030375
2.6.1.42	EC number	Enzyme interactions (Chlamydomonas reinhardtii)	BioCyc	2	0.045913
3.4.13.18	EC number	Enzyme interactions (Chlamydomonas reinhardtii)	BioCyc	3	0.045913
N/A	Electron donor	Biofunctions	HMDB	1	0.010753
N/A	Enzyme cofactor	Biofunctions	HMDB	2	0.000266
N/A	Enzyme co-factor	Biofunctions	HMDB	1	0.020695
N/A	Essential amino acid	Biofunctions	HMDB	3	4.08E-06
N/A	Essential amino acids	Biofunctions	HMDB	2	0.000141
N/A	Essential vitamins	Biofunctions	HMDB	2	0.000266
N/A	Free Radical Scavengers	Biofunctions	HMDB	1	0.010753
N/A	GABA Modulators	Biofunctions	HMDB	1	0.03159
N/A	hepatoprotective	Biofunctions	HMDB	1	0.017825
N/A	Hypnotics and Sedatives	Biofunctions	HMDB	2	0.001713
N/A	metabolite	Chebi role	ChEBI	12	0.030375
N/A	metal chelator	Biofunctions	HMDB	1	0.006245
N/A	Muscle Relaxants, Central	Biofunctions	HMDB	1	0.020138
N/A	Non-essential amino acid	Biofunctions	HMDB	1	0.006245
N/A	nutraceutical	Chebi role	ChEBI	6	9.48E-06
cre00770	Pantothenate and CoA biosynthesis	Pathways (Chlamydomonas reinhardtii)	KEGG	4	0.01435
SMP00027	Pantothenate and CoA Biosynthesis	SMPDB Pathway	ECMDB	5	0.001387
M00244	Pantothenate biosynthesis, valine/L-aspartate=> pantothenate	KEGG modules	KEGG	3	0.01746
N/A	Peptides	Compounds with biological roles	KEGG	6	0.001663
N/A	Protein synthesis, amino acid biosynthesis	Biofunctions	HMDB	5	4.08E-06
2.4.2.1	Purine-nucleoside phosphorylase	Enzyme interactions	ECMDB	3	0.032978
N/A	radical scavenger	Biofunctions	HMDB	1	0.0134
SMP00019	Transcription/Translation	SMPDB Pathway	HMDB	5	0.003569
ULS00322	urate from hypoxanthine	UniPathway Pathways	ChEBI	2	0.036669
N/A	Waste products	Biofunctions	HMDB	9	1.06E-05
N/A	Water-soluble vitamins	Compounds with biological roles	KEGG	2	0.045586
1.17.1.4	Xanthine dehydrogenase	Enzyme interactions	ECMDB	2	0.032978
1.17.1.4	Xanthine dehydrogenase	Enzyme interactions	BioCyc	2	0.045913

Supplementary Table 3.7- Functional Annotations and Enrichment of Metabolites From Cluster 7

ID Annotation	Annotation	Category	Database	In Set	FDR correction
3.5.4.2	Adenine deaminase	Enzyme interactions	ECMDB	2	0.032978
3.5.4.2	Adenine deaminase	Enzyme interactions	BioCyc	2	0.039548
N/A	adenosine receptor antagonist	Chebi role	ChEBI	2	0.002722
N/A	Adjuvants, Anesthesia	Biofunctions	HMDB	1	0.024592
N/A	Amino acids	Compounds with biological roles	KEGG	6	0.001068
N/A	Anesthetics, Intravenous	Biofunctions	HMDB	2	0.000266
N/A	Anti-anxiety Agents	Biofunctions	HMDB	1	0.035297
N/A	Anticonvulsants	Biofunctions	HMDB	2	0.00189
N/A	Antiemetics	Biofunctions	HMDB	2	0.001223
N/A	anti-fungal	Biofunctions	HMDB	1	0.032018
N/A	anti-microbial	Biofunctions	HMDB	1	0.034971
N/A	anti-tumor	Biofunctions	HMDB	1	0.03159
6.3.4.5	Argininosuccinate synthase	Enzyme interactions	ECMDB	2	0.032978
6.3.4.5	Argininosuccinate synthase	Enzyme interactions	BioCyc	2	0.045913
N/A	Aromatase Inhibitors	Biofunctions	HMDB	1	0.009629
N/A	B vitamin	Chebi role	ChEBI	2	0.015971
N/A	Common amino acids	Compounds with biological roles	KEGG	5	0.000124
N/A	Component of Alanine and aspartate metabolism	Biofunctions	HMDB	2	0.000493
N/A	Component of Aminoacyl-tRNA biosynthesis	Biofunctions	HMDB	3	4.08E-06
N/A	Component of Arginine and proline metabolism	Biofunctions	HMDB	3	3.49E-05
N/A	Component of Biotin metabolism	Biofunctions	HMDB	1	0.008003
N/A	Component of Cysteine metabolism	Biofunctions	HMDB	2	0.000289
N/A	Component of Folate biosynthesis	Biofunctions	HMDB	1	0.020695
N/A	Component of Glutamate metabolism	Biofunctions	HMDB	1	0.034971
N/A	Component of Glutathione metabolism	Biofunctions	HMDB	1	0.020138
N/A	Component of Glycine, serine and threonine metabolism	Biofunctions	HMDB	1	0.046896
N/A	Component of Histidine metabolism	Biofunctions	HMDB	3	4.28E-06
N/A	Component of Indole and ipecac alkaloid biosynthesis	Biofunctions	HMDB	1	0.004527
N/A	Component of Methionine metabolism	Biofunctions	HMDB	1	0.020695
N/A	Component of Nicotinate and nicotinamide metabolism	Biofunctions	HMDB	1	0.020695
N/A	Component of Nitrogen metabolism	Biofunctions	HMDB	3	4.08E-06
N/A	Component of Novobiocin biosynthesis	Biofunctions	HMDB	1	0.012121
N/A	Component of Pantothenate and CoA biosynthesis	Biofunctions	HMDB	1	0.020138
N/A	Component of Phenylalanine metabolism	Biofunctions	HMDB	2	0.000266
N/A	Component of Phenylalanine, tyrosine and tryptophan biosynthesis	Biofunctions	HMDB	3	4.08E-06
N/A	Component of Purine metabolism	Biofunctions	HMDB	4	1.68E-06

N/A	Component of Pyrimidine metabolism	Biofunctions	HMDB	1	0.046958
N/A	Component of Selenoamino acid metabolism	Biofunctions	HMDB	1	0.020138
N/A	Component of Tryptophan metabolism	Biofunctions	HMDB	2	0.000924
N/A	Component of Tyrosine metabolism	Biofunctions	HMDB	4	1.68E-06
N/A	Component of Valine, leucine and isoleucine biosynthesis	Biofunctions	HMDB	2	0.00012
N/A	cyclooxygenase 3 inhibitor	Chebi role	ChEBI	2	0.006003
Cytochrome P450 substrates	CYP1 family	Other interactions	KEGG	48	9.2E-12
Ion channel ligands	Cys-loop superfamily	Other interactions	KEGG	45	0.026458
N/A	DNA component	Biofunctions	HMDB	1	0.024592
N/A	EC 3.1.4.* (phosphoric diester hydrolase) inhibitor	Chebi role	ChEBI	2	0.030375
2.6.1.42	EC number	Enzyme interactions (Chlamydomonas reinhardtii)	BioCyc	2	0.045913
3.4.13.18	EC number	Enzyme interactions (Chlamydomonas reinhardtii)	BioCyc	3	0.045913
N/A	Electron donor	Biofunctions	HMDB	1	0.010753
N/A	Enzyme cofactor	Biofunctions	HMDB	2	0.000266
N/A	Enzyme co-factor	Biofunctions	HMDB	1	0.020695
N/A	Essential amino acid	Biofunctions	HMDB	3	4.08E-06
N/A	Essential amino acids	Biofunctions	HMDB	2	0.000141
N/A	Essential vitamins	Biofunctions	HMDB	2	0.000266
N/A	Free Radical Scavengers	Biofunctions	HMDB	1	0.010753
N/A	GABA Modulators	Biofunctions	HMDB	1	0.03159
N/A	hepatoprotective	Biofunctions	HMDB	1	0.017825
N/A	Hypnotics and Sedatives	Biofunctions	HMDB	2	0.001713
N/A	metabolite	Chebi role	ChEBI	12	0.030375
N/A	metal chelator	Biofunctions	HMDB	1	0.006245
N/A	Muscle Relaxants, Central	Biofunctions	HMDB	1	0.020138
N/A	Non-essential amino acid	Biofunctions	HMDB	1	0.006245
N/A	nutraceutical	Chebi role	ChEBI	6	9.48E-06
cre00770	Pantothenate and CoA biosynthesis	Pathways (Chlamydomonas reinhardtii)	KEGG	4	0.01435
SMP00027	Pantothenate and CoA Biosynthesis	SMPDB Pathway	ECMDB	5	0.001387
M00244	Pantothenate biosynthesis, valine/L-aspartate=> pantothenate	KEGG modules	KEGG	3	0.01746
N/A	Peptides	Compounds with biological roles	KEGG	6	0.001663
N/A	Protein synthesis, amino acid biosynthesis	Biofunctions	HMDB	5	4.08E-06
2.4.2.1	Purine-nucleoside phosphorylase	Enzyme interactions	ECMDB	3	0.032978
N/A	radical scavenger	Biofunctions	HMDB	1	0.0134
SMP00019	Transcription/Translation	SMPDB Pathway	HMDB	5	0.003569
ULS00322	urate from hypoxanthine	UniPathway Pathways	ChEBI	2	0.036669
N/A	Waste products	Biofunctions	HMDB	9	1.06E-05

N/A	Water-soluble vitamins	Compounds with biological roles	KEGG	2	0.045586
1.17.1.4	Xanthine dehydrogenase	Enzyme interactions	ECMDB	2	0.032978
1.17.1.4	Xanthine dehydrogenase	Enzyme interactions	BioCyc	2	0.045913

Supplementary Table 3.8 -Functional Annotations and Enrichment of Metabolites From Cluster 8

ID Annotation	Annotation	Category	Database	In Set	FDR correction
N/A	Adjuvants, Anesthesia	Biofunctions	HMDB	1	0.032124
N/A	Adrenergic Agents	Biofunctions	HMDB	1	0.032944
N/A	Adrenergic beta-Antagonists	Biofunctions	HMDB	2	0.001682
N/A	Alkylating Agents	Biofunctions	HMDB	1	0.01813
N/A	anesthetic	Biofunctions	HMDB	1	0.024796
N/A	Anesthetics, Intravenous	Biofunctions	HMDB	1	0.026882
N/A	Anti-anxiety Agents	Biofunctions	HMDB	2	0.002904
N/A	Anti-Arrhythmia Agents	Biofunctions	HMDB	3	0.000215
N/A	Antiarrhythmic Agents	Biofunctions	HMDB	1	0.035859
N/A	anti-cancer	Biofunctions	HMDB	1	0.032944
N/A	Antidyskinetics	Biofunctions	HMDB	1	0.032944
N/A	Antiemetics	Biofunctions	HMDB	2	0.002904
N/A	Antifibrinolytic Agents	Biofunctions	HMDB	1	0.012382
N/A	anti-fungal	Biofunctions	HMDB	1	0.036873
N/A	Antihypertensive Agents	Biofunctions	HMDB	2	0.016796
N/A	anti-microbial	Biofunctions	HMDB	1	0.041438
N/A	Antineoplastic Agents, Alkylating	Biofunctions	HMDB	1	0.029455
N/A	Antiparkinson Agents	Biofunctions	HMDB	1	0.034741
N/A	apoptotic	Biofunctions	HMDB	1	0.035859
N/A	beta-oxidant	Biofunctions	HMDB	1	0.01813
N/A	Cardiotonic Agents	Biofunctions	HMDB	1	0.029436
N/A	catabolic	Biofunctions	HMDB	2	0.000303
N/A	Central Nervous System Agents	Biofunctions	HMDB	1	0.026882
N/A	Component of Alanine and aspartate metabolism	Biofunctions	HMDB	1	0.032124
N/A	Component of Aminoacyl-tRNA biosynthesis	Biofunctions	HMDB	4	2.9E-07
N/A	Component of Arginine and proline metabolism	Biofunctions	HMDB	1	0.048344
N/A	Component of Biotin metabolism	Biofunctions	HMDB	1	0.015125
N/A	Component of Fatty acid metabolism	Biofunctions	HMDB	1	0.029455
N/A	Component of Glutamate metabolism	Biofunctions	HMDB	2	0.002904
N/A	Component of Glutathione metabolism	Biofunctions	HMDB	1	0.026882
N/A	Component of Glycine, serine and threonine metabolism	Biofunctions	HMDB	2	0.005113
N/A	Component of Histidine metabolism	Biofunctions	HMDB	2	0.001178
N/A	Component of Lysine biosynthesis	Biofunctions	HMDB	1	0.01813
N/A	Component of Methionine metabolism	Biofunctions	HMDB	2	0.001002
N/A	Component of Nitrogen metabolism	Biofunctions	HMDB	1	0.029455
N/A	Component of Novobiocin biosynthesis	Biofunctions	HMDB	2	0.000303

N/A	Component of Phenylalanine metabolism	Biofunctions	HMDB	2	0.000831
N/A	Component of Phenylalanine, tyrosine and tryptophan biosynthesis	Biofunctions	HMDB	3	2.52E-05
N/A	Component of Porphyrin and chlorophyll metabolism	Biofunctions	HMDB	1	0.035859
N/A	Component of Propanoate metabolism	Biofunctions	HMDB	1	0.030582
N/A	Component of Purine metabolism	Biofunctions	HMDB	3	0.000215
N/A	Component of Pyruvate metabolism	Biofunctions	HMDB	1	0.033858
N/A	Component of Riboflavin metabolism	Biofunctions	HMDB	1	0.023956
N/A	Component of Selenoamino acid metabolism	Biofunctions	HMDB	2	0.000831
N/A	Component of Stilbene, coumarine and lignin biosynthesis	Biofunctions	HMDB	1	0.016796
N/A	Component of Sulfur metabolism	Biofunctions	HMDB	1	0.026882
N/A	Component of Thiamine metabolism	Biofunctions	HMDB	1	0.016796
N/A	Component of Tryptophan metabolism	Biofunctions	HMDB	1	0.036873
N/A	Component of Tyrosine metabolism	Biofunctions	HMDB	3	0.000215
N/A	Component of Valine, leucine and isoleucine biosynthesis	Biofunctions	HMDB	1	0.021951
Cytochrome P450 substrates	CYP1 family	Other interactions	KEGG	29	3.15E-07
N/A	depressant	Biofunctions	HMDB	1	0.015125
N/A	DNA component	Biofunctions	HMDB	1	0.032124
N/A	Dopamine Agents	Biofunctions	HMDB	1	0.021951
N/A	EC 3.1.1.3 (triacylglycerol lipase) inhibitor	Chebi role	ChEBI	2	0.028682
N/A	Essential amino acids	Biofunctions	HMDB	2	0.000403
N/A	Essential vitamins	Biofunctions	HMDB	1	0.026882
N/A	Excitatory Amino Acid Antagonists	Biofunctions	HMDB	1	0.020458
N/A	flavouring agent	Chebi role	ChEBI	3	0.028682
N/A	GABA Modulators	Biofunctions	HMDB	1	0.036654
N/A	Glucocorticoids	Biofunctions	HMDB	1	0.032944
N/A	hepatoprotective	Biofunctions	HMDB	1	0.026168
N/A	Muscle Relaxants, Central	Biofunctions	HMDB	1	0.026882
N/A	neuroprotectant	Biofunctions	HMDB	1	0.026882
N/A	neuroprotective	Biofunctions	HMDB	1	0.024796
N/A	Neuroprotective Agents	Biofunctions	HMDB	1	0.026882
N/A	neurotransmitter	Biofunctions	HMDB	1	0.012382
N/A	nutraceutical	Chebi role	ChEBI	4	0.009977
SMP00304	Oxprenolol Pathway	SMPDB Pathway	YMDB	3	0.030779
SMP00304	Oxprenolol Pathway	SMPDB Pathway	ECMDB	3	0.039805
cre00360	Phenylalanine metabolism	Pathways (Chlamydomonas reinhardtii)	KEGG	5	0.000636
N/A	phosphoantigen	Chebi role	ChEBI	2	0.045864
N/A	Phosphodiesterase Inhibitors	Biofunctions	HMDB	1	0.028187
N/A	Protein synthesis, amino acid biosynthesis	Biofunctions	HMDB	4	0.00038
N/A	signalling	Biofunctions	HMDB	1	0.026882
N/A	Sympatholytics	Biofunctions	HMDB	2	0.001498

SMP00019	Transcription/Translation	SMPDB Pathway	HMDB	4	0.031315
M00072	Tyrosine biosynthesis, phenylalanine => tyrosine	KEGG modules	KEGG	2	0.00249
N/A	Vasodilator Agents	Biofunctions	HMDB	2	0.005296
N/A	Waste products	Biofunctions	HMDB	5	0.024796

4 Transcriptomic Changes of *Chlamydomonas acidophila* and *Chlamydomonas reinhardtii* to a Short-and Long-Term Copper Stress

4.1 Abstract

Genetic adaptation likely underpins a high percentage of the adaptation mechanisms of extremophile organisms to their harsh environments. Using a highly copper tolerant strain of the extremophile microalga *C. acidophila* (PM01), this study aimed to understand the genes important to surviving a copper contaminated environment. Using Illumina HiSeq RNA analysis changes in the transcriptome in response to a short-term and long-term copper stress between the extremophile *C. acidophila* and a close relative *C. reinhardtii* were identified and quantified. Through heatmap generation and Gene Ontology (GO) term analysis 3 main processes were found to be important, an increase in intracellular transport and decrease in photosynthesis were found to be important in PM01 adaptation to copper. An increase in the oxidative response was seen in *C. reinhardtii*. Individual genes of interest were also identified and analysed with the metal transporters CTP3 and HMA1 seemingly playing an important role in the copper adaptation of PM01 alongside other genes involved in glutathione biosynthesis and metabolism. One cluster in the heatmap which shows an array of genes upregulated in the short-term response to copper in PM01 was of particular interest, however, these represent a wide array of cellular processes. This study presents exciting insights for mechanisms of copper adaptation and suggests some genes that could play a crucial role.

4.2 Introduction

There are many different environments across the planet that species may colonise and form ecological niches. These environments can be variable, providing new challenges for organisms to adapt to. In the introduction (chapter 1) we have seen how some of the more extreme environments produce harsh conditions that many organisms cannot survive, but for those organisms that can tolerate a particular stress, understanding the mechanisms of tolerance and adaptation may provide greater insight into the impact and the way the organisms have on their environmental and be a potential source for novel biotechnological applications.

There are three main strategies by which an organism can adapt to a new environment. The first is a behavioural change in which an organism can alter their strategy, one of the most obvious in green algae is negative phototaxis, in which cells swim in the opposite direction of a light source under high light intensities (Erickson et al., 2015). Another behavioural change is forming symbioses, in which two organisms form an association to help them overcome stresses that may have killed them individually. One such example are lichens in which an algal primary producer can partner with a fungal consumer. Through this partnership lichens are able to survive extreme desiccation and have been found colonising the polar regions and deserts (Kranner et al., 2008). The second strategy is through physiological metabolic changes, allowing metabolic pathways in the cells to respond to stresses through various different methods. One of the more well-known microalgal responses is the accumulation of storage lipids under nutrient stress (Driver et al., 2017; Tan et al., 2016), which has been a popular area of study recently due to their potential as a renewable biofuel source. It is important to note that these processes may also be underpinned by tranascriptional changes, although this is not exclusive to it. The final strategy, that likely underpins both the previous strategies, is genetic adaptation. Genes form the template of all organisms, encoding for proteins which drive cellular functions and synthesis of other key molecules. Genetic adaptations could arise from either novel genes providing new functions or an increase in expression level, leading to an increase in protein quantity in the cell. Understanding the genetic basis of an extremophile microorganisms by identifying genes which are increased in response to a stress or are novel in extremophile organisms, can help identify key pathways in stress tolerance.

Several studies have looked at the transcriptomic response of algae to copper. The marine macroalga *Ulva compressa* was studied for transcriptional changes to 50 µM copper over 5 days (Laporte et al., 2016). The authors identified that copper induced increased expression of photosynthesis, photosynthetic repair mechanisms and respiration. An increase in transcripts related to photosynthesis was also seen in a strain of the extremophile microalga *C. acidophila* isolated from the Rio Tinto (Olsson et al., 2015). A transcriptomic analysis on the marine alga *Chromera velia* exposed to Hg found that a whole host of oxidative response genes were involved in the response to Hg stress. These included genes encoding ROS scavenging enzymes such as peroxidase and pathways involving glutathionylation (Sharaf et al., 2019). In contrast to the other two previous papers this study did not identify any transcripts related to photosynthesis.

Olsson et al. (2015) have previously looked at the transcriptional response of *C. acidophila* to a low concentration of copper. However, this was only a short-term response and did not compare to a non-extremophile organism. Among the differentially expressed genes Olsson et al. (2015) saw

transcripts involved in processes such as photosynthesis, carbohydrate metabolism and general stress response increased in expression. Among the down regulated transcripts, processes such as signallying and gene transcription regulation, growth and mobility and transporters were found. Within the stress response genes they particularly focussed on heat-shock proteins. As such there is a chance that any constitutively expressed genes and conserved responses that are not unique to *C. acidophila* involved in this stress response may have been overlooked. In this study I compared the transcriptomic response of *C. acidophila* to *C. reinhardtii* under both short- and long-term copper responses in order to elucidate many more genetic mechanisms involved in the response of *C. acidophila.*

4.3 Materials and Methods

4.3.1 Growth Conditions

Chlamydomonas acidophila (PM01) and *Chlamydomonas reinhardtii* (CCAP 11/32c) (referred to subsequently as PM01 and 11/32c, respectively) were grown in triplicate at 24 °C and 16 h:8 h light:dark cycle at 150 µmol m^{-2} s^{-1} light intensity on an orbital shaker (120 rpm). PM01 was grown in a modified acid media (MAM), described by Olaveson & Stokes, (1989) which was adjusted to pH 3. Conversely 11/32c was grown in a Tris-minimal phosphate media (TP) described in Harris (2009), at pH 7. Both strains were grown in control conditions or in continuous (long-term) copper stressed conditions that were appropriate for each strain for 2 weeks: 2 mM $CuCl_2$ for PM01 and 75 µM $CuCl_2$ for 11/32c. Both strains were also grown in control conditions for two weeks and were then spiked with four times the concentration of the long-term copper stress: 8 mM for PM01 and 300 µM for 11/32c, then incubated in these conditions for 3 h (short-term copper stress). Cells were harvested by centrifuging 30 ml of dense algal cell culture at 10,000 g for 5 min. The supernatant was removed, cells were washed with 1 ml of ddH_2O, centrifuged again at 10,000 g for 5 min and the supernatant removed leaving a dense cell pellet for RNA extraction.

4.3.2 Phylogenetic Tree Generation

To compare the evolutionary relatedness of PM01 to *C. reinhardtii* a phylogenetic tree was generated. 18S rRNA gene sequences were obtained from GenBank, NCBI (https://www.ncbi.nlm.nih.gov/genbank/) from an array of species from the Chlorophyta. Additional 18S sequences of PM01 and other strains of *C. acidophila* (11/136 and 11/137) were obtained from Dean et al. (2019). phylogenetic tree was generated using the maximum likelihood method using RAxMLGUI and the GTR-GAMMA model (Stamatakis, 2006).

4.3.3 RNA Extraction

RNA extraction was performed by the addition of 1 ml TRIzol Reagent (Sigma), which was added to each cell pellet and left to incubate at room temperature for 5 min then 200 µl of chloroform was added to each sample for further extraction. Samples were briefly vortexed until they were completely mixed and left to stand for a further 5 min. To isolate the RNA from DNA, proteins and other cell debris the samples were centrifuged for 15 min at 12,000 g and 4 °C, the upper layer was then aliquoted into a new Eppendorf tube taking care not to disturb the lower layers. To precipitate the RNA, 500 µl of isopropanol was added to each sample and left for 15 min at room temperature. To collect the precipitated RNA, samples were centrifuged for 10 min at 12,000 g and 4°C and the supernatant was removed. The RNA pellet was washed with 1 ml of 75% (v/v) ethanol, centrifuged

at 12,000 g for 5 min at 4 °C, and the wash step was repeated once more. Samples were left on ice for 30 min to allow any remnant ethanol to evaporate. The RNA pellet was then resuspended in 50 µl ddH_2O.

4.3.4 Library Preparation and Sequencing

Total RNA was submitted to the University of Manchester Faculty of Biology, Medicine and Health Genomic Technologies Core Facility. Quality and integrity of the RNA samples were assessed using a 2200 TapeStation (Agilent Technologies) and then libraries were generated using the TruSeq® Stranded mRNA assay (Illumina, Inc.) according to the manufacturer's protocol. Briefly, total RNA (0.1 – 4 µg) was used as input material from which polyadenylated mRNA was purified using poly-T, oligo-attached, magnetic beads. The mRNA was then fragmented using divalent cations under elevated temperature and then reverse transcribed into first strand cDNA using random primers. Second strand cDNA was then synthesised using DNA Polymerase I and RNase H. Following a single 'A' base addition, adapters were ligated to the cDNA fragments, and the products then purified and enriched by PCR to create the final cDNA library. Adapter indices (IDT for Illumina TruSeq UD Indexes (Illumina, cat# 20022371)) were used to multiplex libraries, which were pooled prior to cluster generation using a cBot instrument. The loaded flow-cell was then paired-end sequenced (76 + 76 cycles, plus indices) on an Illumina HiSeq4000 instrument. Finally, the output data was demultiplexed (allowing one mismatch) and BCL-to-Fastq conversion performed using Illumina's bcl2fastq software, version 2.20.0.422.

4.3.5 Data Analysis

A total of 322,702,415 and 339,124,886 uniquely mapped reads across all treatments for PM01 and 11/32c, respectively were obtained. This data needed to be pre-processed, mapped and normalised before any further analysis could take place. Firstly, all reads were pre-processed using the Trimmomatic filter to remove adapters and contaminants from the data. After the data was cleaned *C. reinhardtii* reads were mapped and counted to *C. reinhardtii* CC-503 genome assembly version 5.0 (https://phytozome.jgi.doe.gov/pz/portal.html#!info?alias=Org_Creinhardtii). Initially *C. acidophila* reads were attempted to be mapped to the *C. reinhardtii* genome for ease of comparison. However, this resulted in poor mapping (<1%). As a result *C. acidophila* reads were mapped and counted to the more closely related *Chlamydomonas eustigma* genome (Figure 4.1) assembly version 1.0 (https://www.ncbi.nlm.nih.gov/genome/57939) generated by Hirooka et al., (2017). Mapping was performed using STAR mapping software whilst the counting was performed using htseq- count software. Finally, principal component analysis (PCA), normalisation and differential expression calculations were performed using DEseq2. Where mentioned in the thesis, transcript abundance is shown as normalised counts (NC) obtained from the DEseq2 software.

4.3.6 Heatmap Generation

In order to compare both *C. acidophila* and *C. reinhardtii* to each other, all sequences were ran through Inparanoid software to identify potential orthologues between the two species. Out of the identified orthologues, other likely paralogues for the genes were identified for both species. The likely orthologues identified for

PM01 were kept in the heatmap but 11/32c likely paralogues were removed for simplicity. From this a total of 7740 transcripts were identified out of the 14,232 and 19,256 total transcripts identified for PM01 and 11/32c, respectively. These were then filtered to pass two tests. The first, if the $\log_2$ fold change was >±1 and, secondly, if this change was significant (p value <0.05). Four data points were plotted for each gene, these were the log fold changes between long term stress and control, and the short-term stress and control for both species, described subsequently as relative transcription. The data was then z-transformed to allow for direct comparison between the species. Eight clusters were then generated using k-means clustering using maxdView software.

4.3.7 Gene Ontology (GO) Enrichment

Once the clusters were generated, the gene list for each cluster was run through the agriGO v.20 software for gene ontology enrichment (Tian et al., 2017). Genes were enriched using the Singular Enrichment Analysis (SEA) against transcript ID v5.5 (Phytozome v11.0) for *C. reinhardtii.* To identify significantly enriched Gene Ontology (GO) terms the fisher statistical test was applied and then further tested using the Yekutieli (false discovery rate under dependency test). Any terms that were under a significance level of 0.05 were removed.

4.4 Results and Discussion

4.4.1 PM01 Exhibits a Stronger More Directional Transcriptomic Response to Copper

The aim of this study was to identify potential classes of genes which may explain how *C. acidophila* strain PM01 can tolerate a much higher copper stress than the closely related non-extremophile *C. reinhardtii* (strain 11/32c). A *C. acidophila* genome was unavailable therefore PM01 transcript sequence reads had to be either assembled *de novo* or mapped to a related reference genome. There was difficulty mapping PM01 sequence reads to the *C. reinhardtii* genome. This is evidenced in Table 4.1 where we can see a much lower mapping rate with 0% of the reads being uniquely mapped and at most 2% of the reads being mapped to multiple loci. Conversely when PM01 reads were mapped to the *C. eustigma* genome where18% of reads were uniquely mapped and up to 57% of reads mapped to multiple loci. While strains of *C. acidophila* (including PM01, as well as CCAP 11/136 and CCAP11/137) are closely related to *C. reinhardtii*, there is still enough evolutionary distance to explain why there was difficulty mapping PM01 to the *C. reinhardtii* genome (Figure 4.1). In contrast, the acidophile *C. eustigma* is much more closely related to *C. acidophila* and justifies the approach in mapping PM01 to the *C. eustigma* genome.

It is likely that there are novel genes that have allowed PM01 to adapt to such a hostile environment and identifying these genes could help us understand metal homeostasis in extremophile organisms in much greater detail. Unfortunately, the PM01 read mapping rates are still not optimum in contrast to the mapping of 11/32c reads to the *C. reinhardtii* genome, which elicited 95% uniquely mapped reads. This could suggest that there is still room for improvement of the mapping for PM01 and some genes could have been missed in this analysis. That being said 75% of reads were mapped which was able to provide enough coverage for analysis. Table 4.1 also shows that PM01 had more unique orthologous genes identified when compared to 11/32c. There was also a higher number of orthologous genes expressed over 0.15 $\log_2$-fold in PM01 compared to the corresponding treatments in 11/32c.

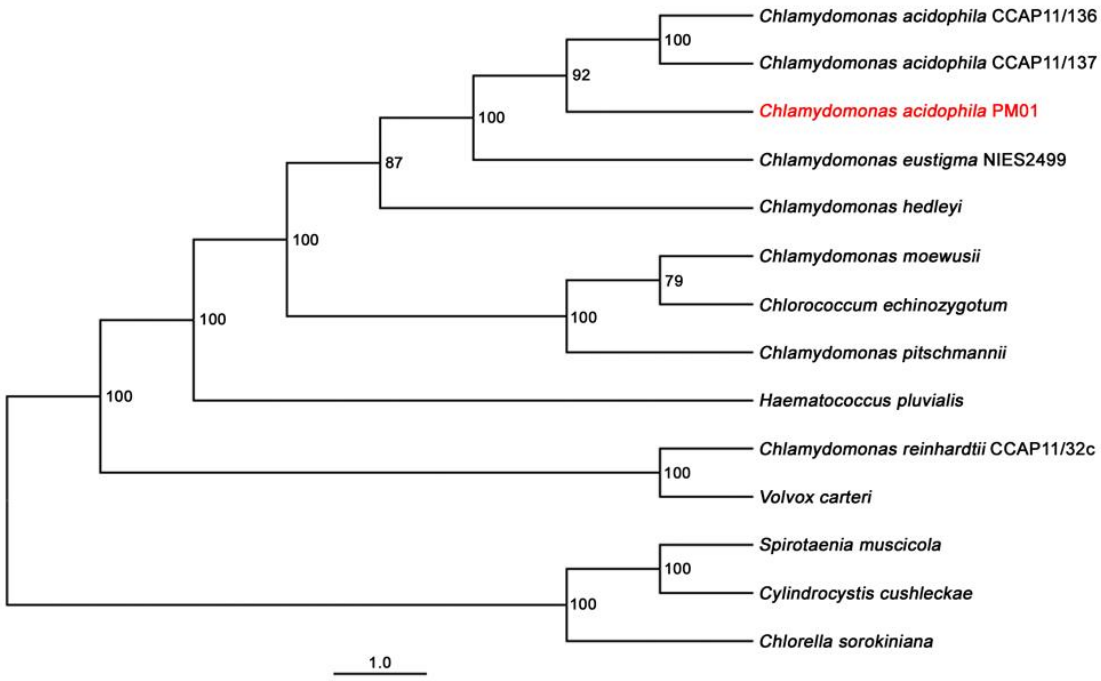

Figure 4.1 Phylogenetic tree of 18s sequences of the Chlorophyta microalgae indicating relatedness of PM01 to other extremophiles and a clear evolutionary divergence from non-extremophile organisms such as C. reinhardtii. bootstrap percentage values are indicated at the tree nodes of branches for 1000 replications and indicate confidence in tree node positions. The branch length scale bar indicates evolutionary distance.

	PM01 (mapped to *C. eustigma*)			PM01 (mapped to *C. reinhardtii*)			11/32c (mapped to *C. reinhardtii)*		
	Control	Long Stress	Short Stress	Control	Long Stress	Short Stress	Control	Long Stress	Short Stress
Mapping rate	147.5	143.4	145.1	10.8	10.8	11.1	498.1	481.5	398.7
Number of input reads	37,502,690	36,735,182	33,329,599	37,502,690	36,735,182	33,329,599	37,083,930	39,708,081	36,249,618
Average input read length	150.0	149.7	150.0	150.0	149.7	150.0	150.0	150.0	150.0
Uniquely mapped reads %	17%	18%	17%	0%	0%	0%	95%	95%	94%
Average mapped length	148.2	148.0	147.8	127.4	129.4	131.3	149.8	149.8	149.7
% reads mapped to multiple loci	57%	55%	42%	0%	1%	2%	3%	3%	3%
% reads mapped to too many loci	18%	19%	27%	0%	0%	0%	0%	0%	0%
Transcripts identified	13742	13771	13708	-	-	-	15622	15882	15122
Orthologous Genes Identified	7009	7009	7009	-	-	-	7009	7009	7009
Unique Orthologous Genes Identified To Corresponding Treatment	466	458	516	-	-	-	3	2	4
Orthologous Genes Expressed 0.15 log_2-Fold Higher than Corresponding Treatment in Other Organisms	5135	5069	4612	-	-	-	1523	1551	2105

Table 4.1 Mapping statistics of an RNA sequencing experiment performed on C. acidophila PM01 and C. reinhardtii 11/32c under a long and short-term copper stress conditions. PM01 reads were mapped to the C. eustigma and C. reinhardtii genomes and 11/32c reads were mapped to only the C. reinhardtii genome.

Once the data was mapped, patterns within the expression data were able to be investigated. PCA provides useful summary data to differentiate samples. Unfortunately, as *C. acidophila* and *C. reinhardtii* reads were not be mapped to the same genome, PCA could only be run within the species. PCA of the RNA-seq data shows a similar pattern between *C. reinhardtii* and *C. acidophila* (Figure 4.2(A and C)). Short term copper stress accounts for the most variation in the data as seen by Principal Component (PC) 1 (98% and 92% of the variance for PM01 and 11/32c, respectively) and separates the control and long-term copper stress from the short-term copper stress in both organisms. Long term copper stress is then distanced from both the control and short-term copper stress across PC2 in both organisms (7% and 1% of the variance for 11/32c and PM01, respectively). The short-term copper stress elicited a much stronger genetic response as shown in Figure 4.2(E), where more genes were differentially expressed in the short-term treatment vs control as opposed to the long-term treatment vs control.

Copper stress also seems to elicit a larger transcriptional response in *C. reinhardtii* when compared to PM01, and this is most evident when looking at increased and decreased gene sets in the long-term treatment vs control, where *C. reinhardtii* shows much higher Log_2 fold change values (Figure 4.2(E)). The short-term treatment elicits the largest transcriptional response in both organisms, when compared with the control and with the long-term treatment, with every comparison apart from one having over 5000 transcripts significantly changing (Figure 4.2(E)). Increased expression and decreased expression are equally distributed for both number of transcripts and size of response for *C. reinhardtii* (Figure 4.2(B and E)). The highest number of differential gene expression were seen in *C. reinhardtii* across all treatments (Figure 4.2(E)). In a previous study the highest change in gene expression was 3 hours after copper stress in *C. acidophila* (Puente-Sánchez et al., 2018), so the fact that we see a higher expression is perhaps unsurprising. *C. acidophila* appears to have a more skewed response to copper. The control and short-term copper treatment cause more genes to increase in expression, whilst the long-term copper treatment causes more genes decrease in expression. *C. reinhardtii* on the other hand, shows a much more balanced levels of increased and decreased expression in terms of numbers and size (Figure 4.2 (B, D and E)). This is most evident for the *C. acidophila* long-term copper stress vs control where there were more genes (153) up regulated than down regulated. In contrast for the same treatment in *C. reinhardtii* there was a difference of less than 40 genes between the up and down regulated sets whilst the increased genes were only 1.4 log_2 fold times higher on average. This could suggest that *C. acidophila* has a much more directed and concise response to copper.

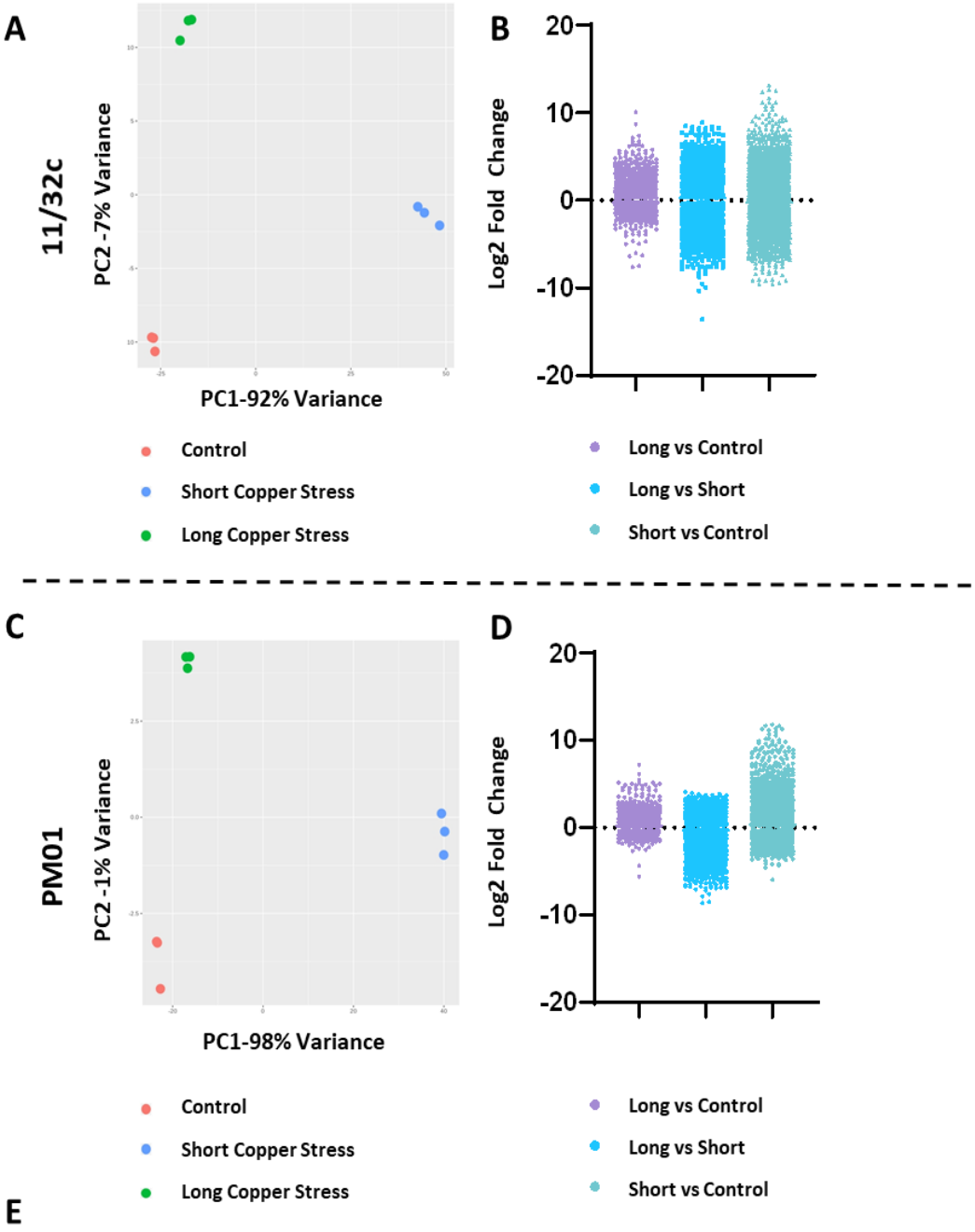

E

		Long vs Control		Long vs Short		Short vs Control	
		Up	Down	Up	Down	Up	Down
11/32c	N	3005	3042	5417	5292	5406	5425
	Average Log_2Fold Change	1.0459	-0.7427	1.6744	-1.7027	1.8534	-1.7031
PM01	N	1557	1398	4891	5068	5192	5028
	Average Log_2Fold Change	1.9236	-0.2989	0.9391	-1.4428	1.6187	-0.9633

Figure 4.2 An overview of the transcriptomic data sets collected for PM01 (C. acidophila) and 11/32c (C. reinhardtii) exposed to short term copper stress and a long term copper stress. A and C show PCA of the data for each species, each point represents a biological replicate for each treatment. B and D show the average Log2 fold change, across 3 biological replicates, for each gene transcript detected in all three treatments. (E)Table showing a more detailed overview of the differential gene expression changes between both species and under the three treatments.

4.4.2 *Gene Clustering and Enrichment of the Transcriptome Indicates Cell Transport, Photosynthetic and Oxido-Reductase Genes May Play an Important Role in Copper Adaptation*

I wanted a better understanding of some of the mechanisms in which the green microalgae *C. acidophila* and *C. reinhardtii* respond to copper. In order to do so the transcriptomic data sets were clustered based on expression data, these clusters were then further enriched to GO terms to identify which cellular processes dominated each cluster. To do that probable orthologues between *C. reinhardtii* and *C. acidophila* were identified. Orthologues were identified using the Inparanoid software, short- and long-term treatments were normalised to their respective controls, leaving 4 total data sets of the short and long-term copper stresses for both organisms. The datasets were then z-transformed so the means across the four datasets were set to 0, and ± 1 represents 1 standard deviation. The heatmap was separated by k-means clustering into 8 distinct clusters containing 5029 genes in total, in which at least one of the four data sets passed the test of having a Log_2 fold change value of >±1 whilst also showing a significant change (p value <0.05). The most likely paralogues for *C. reinhardtii* were removed during the analysis for simplicity. However, all paralogues identified in *C. acidophila* were retained in the data sets as these could be a potential source of adaptation due to gene duplication and functional changes. A total of 265 *C. acidophila* paralogues were identified across five clusters, however, of these clusters, Cluster 2 and 6 contained the most paralogues, with 153 and 101, respectively. GO enrichment was performed for each cluster to predict what cellular processes were being affected by copper treatment. Generally, the clusters showed very little overlap, with most having predominantly unique GO terms. Not only that, but for many clusters GO terms were specific to certain cellular functions, showing a clear difference in cellular response between the treatments.

To get an idea of the relationship of the transcriptomics response between the two species, the mean number of copies for each transcript across all the treatments were plotted for all identified orthologues (Figure 4.3). The first thing that is obvious when looking at the plots is that there is no significant correlation between the two species with R^2 values of 0.4992, 0.5235 and 0.4686 for the control, long stress and short stress, respectively when a linear regression was performed on the data sets. It is also evident looking across all the plots that *C. reinhardtii* shows the highest levels of expression across all treatments including the control. It also highlights, as has been previously described, that the short-term treatment elicits the highest transcriptomic response. The most abundant transcript had 958,206 copies and 381,199 copies for *C. reinhardtii* and PM01 respectively in the short-term treatment (Figure 4.3C).

Clusters 1,5,6 and 8 all contain genes related to either energy or protein metabolism these account for 2342 of the total orthologues identified. Another study has found that a 55 µM copper stress was enough to significantly reduce growth rates of *C. reinhardtii* and that energy metabolism and protein metabolism accounted for 49% of all the differentially expressed genes for all of their copper treatments (Jamers et al., 2013). Although slightly lower than the numbers seen in Jamers et al. (2006), the data shows numbers similar, considering we could only look at a much smaller sample set. Taking into account the inhibition of culture growth and high cell death seen in the long-term

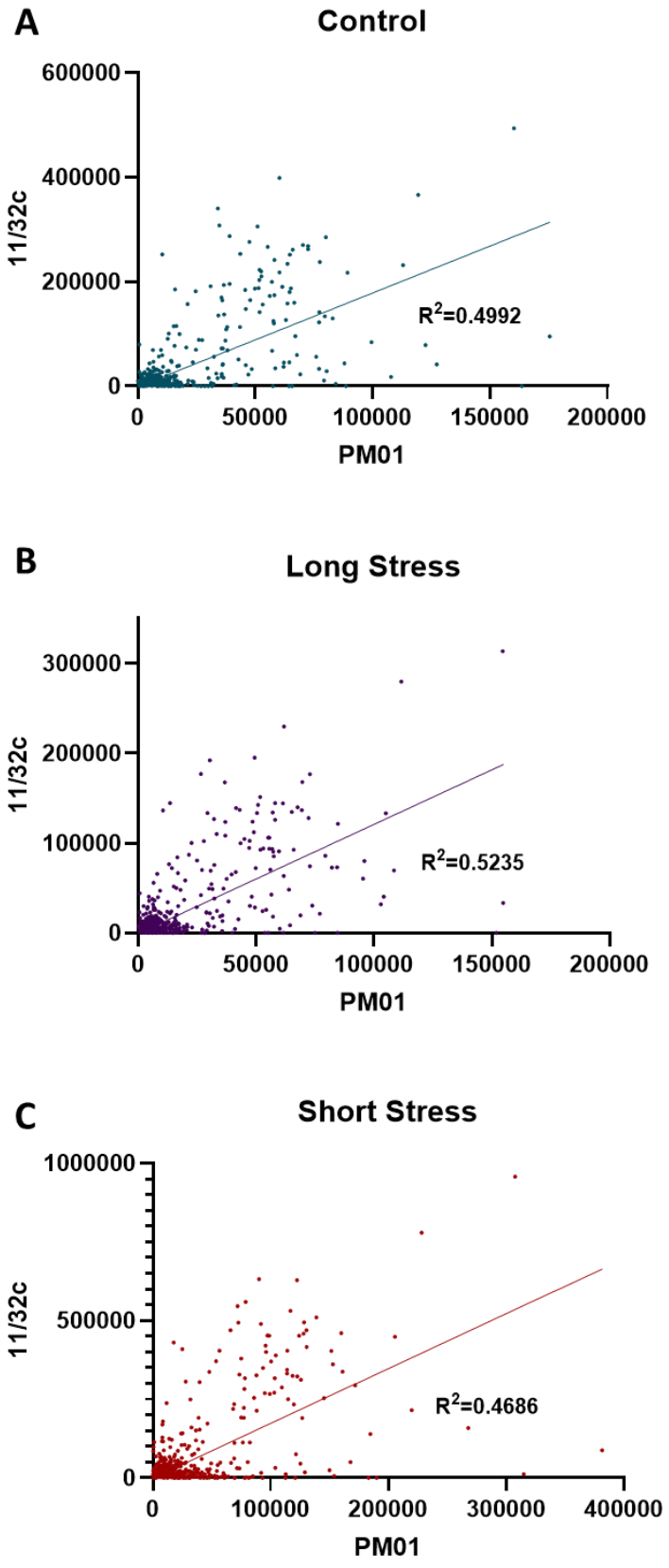

Figure 4.3 Orthologues identified between C. acidophila (PM01) and C. reinhardtii (11/32c) with the mean values of normalised expression of three replicates for each treatment plotted as a dot using linear regression (A) control conditions, (B) long-term copper stress and (C) short-term copper stress. The R^2 values indicate the correlation between the two species expression values.

and short-term copper stresses for both species, it is likely that at least a portion of the differentially expressed genes seen here are due to a reduction in cell growth.

Cluster 1 is the only cluster in which the gene sets respond to the different copper stress treatments in a similar manner between *C. acidophila* and *C. reinhardtii*. Both species showed a higher expression of genes under short-term copper stress whilst the expression was lower under long term copper stress (Figure 4.4). *C. acidophila* showed a slightly higher increase in expression of 0.968 standard deviations whilst *C. reinhardtii* increased by 0.621 standard deviations. Cluster 1 also had the most diverse GO enriched terms consisting of 61 terms, of which 54 terms were unique to this cluster (Table 4.2). Also located in this cluster were three *C. acidophila* genes identified as likely paralogues to *C. reinhardtii* genes.

There is a wide array of functions associated to these terms, mostly associated with primary metabolic processes, protein turnover including prot ubiquitination, degradation and synthesis. Excess cellular copper is well known to induce oxidative stress in a variety of organisms. This can cause the oxidation of proteins, leading to protein carbonylation and/ or ubiquitination in a variety of organisms such as *S. cerevisiae, Zea mays* and *C. reinhardtii* (McConnell et al., 2018; Pena et al., 2007; Shanmuganathan et al., 2004). Pena et al. (2007) also found an accumulation of oxidised and ubiquitinated proteins in the leaves of maize under a moderate cadmium stress. The ubiquitin-proteasome pathway (UPP) identifies ubiquitinated proteins and targets them for degradation. This is a crucial process in protein cycling and can increase survivability of organisms under stressed conditions. However, a study has found that the UPP process can be severely impaired under excessive ROS conditions in *C. reinhardtii* in a time dependent manner (Vallentine et al., 2014). An increase is seen in transcription for such proteins for both species in Cluster 1 under the short-term stress when compared to the control, whilst in contrast a decrease under the long-term copper stress. This suggests that immediately after a copper stress, proteins may become dysfunctional and need recycling. However, Vallentine et al. (2014) noted a decrease in proteasome activity after 3 hours, the same amount of time as the short-term copper stress, so this response could be short-lived. There is very little to differentiate the species under this cluster. However, it is likely that both species will be experiencing different cellular conditions for example PM01 was grown in a much more acidic environment. From chapter 2 we have seen how PM01 has the potential to deal with ROS stress more efficiently through processes such as ROS quenching enzymes, as well as an increase in transcripts in the oxidative stress response as we will see in section 4.4.3. it is also possible that the UPP complex could be adapted to work under more oxidising conditions. Extremophilic proteases are well classified and their properties have made them popular for use within industry (Białkowska et al., 2016).There is very little literature that suggests the UPP has been modified in extremophiles, in fact a study has suggested that this UPP complex plays a more conserved role under stress (Maniatsi et al., 2015). However, many transcripts related to ubiquitin processes were observed within this transcriptomic data set (data not shown), so this could warrant further investigation within PM01.

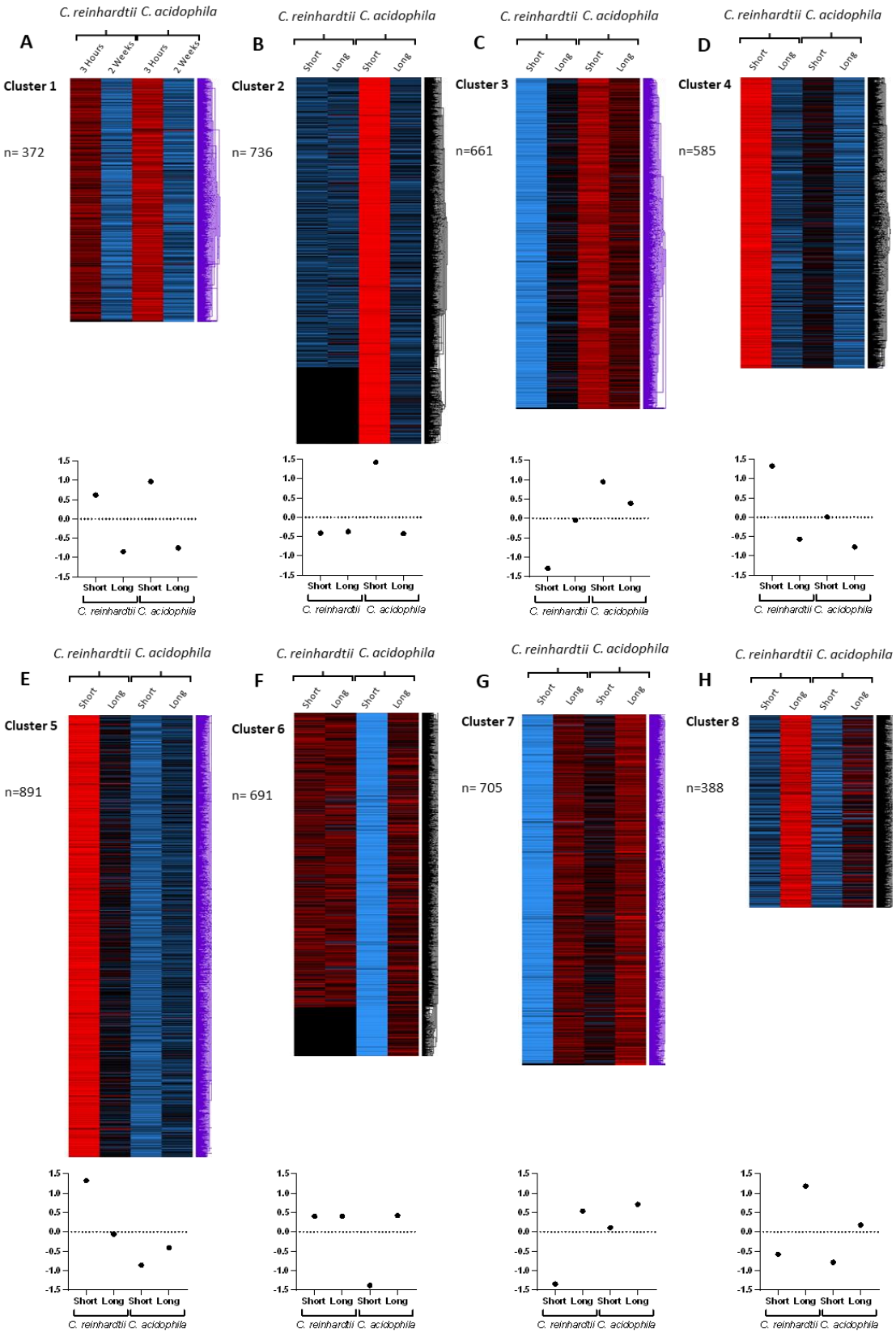

Figure 4.4 Heatmap representation of RNA-seq expression data from C. reinhardtii and C. acidophila under short and long term copper stress. Red represents more highly expressed genes, black is neutral and blue represents more lower expression. Orthologues between species were identified, using the Inparanoid software, so that expression profiles between the species could be matched. Most likely paralogues were identified but for simplicity only the most likely paralogues for C. acidophila were kept and these can be identified in the heatmap where there is no corresponding C. reinhardtii data. Short and long term treatments were normalised to their corresponding controls then the four data sets were z transformed, the mean across the data sets was defined as 0 and ±1 represents a standard deviation.

GO Term	Description	Cluster 1	Cluster 7	Cluster 8
GO:0043043	peptide biosynthetic process	7.70E-24 (59)		
GO:0043604	amide biosynthetic process	7.70E-24 (59)		
GO:0006412	translation	7.70E-24 (59)		
GO:0043603	cellular amide metabolic process	9.30E-24 (59)		
GO:1901566	organonitrogen compound biosynthetic process	9.30E-24 (75)		
GO:0006518	peptide metabolic process	9.30E-24 (59)		
GO:1901564	organonitrogen compound metabolic process	2.40E-20 (79)		
GO:0034645	cellular macromolecule biosynthetic process	1.90E-13 (68)		
GO:0009059	macromolecule biosynthetic process	1.90E-13 (68)		
GO:0044271	cellular nitrogen compound biosynthetic process	6.10E-12 (77)		
GO:0009058	biosynthetic process	1.30E-11 (93)		
GO:1901576	organic substance biosynthetic process	1.50E-11 (89)		
GO:0044249	cellular biosynthetic process	2.30E-11 (88)		
GO:0010467	gene expression	2.90E-11 (69)		1.40E-04 (40)
GO:0030163	protein catabolic process	6.60E-08 (16)		
GO:0051603	proteolysis involved in cellular protein catabolic process	9.50E-08 (15)		
GO:0044257	cellular protein catabolic process	9.50E-08 (15)		
GO:0019538	protein metabolic process	2.30E-07 (106)		
GO:0044265	cellular macromolecule catabolic process	1.10E-06 (15)		
GO:0009057	macromolecule catabolic process	1.70E-06 (16)		
GO:0006807	nitrogen compound metabolic process	1.90E-06 (96)		
GO:0044267	cellular protein metabolic process	2.60E-06 (92)		
GO:0044248	cellular catabolic process	2.50E-05 (17)		
GO:0034641	cellular nitrogen compound metabolic process	5.80E-05 (85)		
GO:0006508	proteolysis	3.30E-04 (28)		
GO:0043632	modification-dependent macromolecule catabolic process	3.30E-04 (9)		
GO:0006511	ubiquitin-dependent protein catabolic process	3.30E-04 (9)		
GO:0019941	modification-dependent protein catabolic process	3.30E-04 (9)		
GO:1901575	organic substance catabolic process	8.80E-04 (18)		
GO:0009056	catabolic process	9.4E-04 (18)		
GO:0043170	macromolecule metabolic process	2.60E-03 (119)		
GO:0071704	organic substance metabolic process	2.60E-03 (154)		
GO:0044238	primary metabolic process	7.60E-03 (145)		
GO:0044237	cellular metabolic process	8.60E-03 (138)		
GO:0008152	metabolic process	9.20E-03 (182)		
GO:0044260	cellular macromolecule metabolic process	1.70E-02 (105)		
GO:0003735	structural constituent of ribosome	2.50E-28 (55)		
GO:0005198	structural molecule activity	3.70E-27 (55)		
GO:0004298	threonine-type endopeptidase activity	2.20E-06 (11)		
GO:0070003	threonine-type peptidase activity	2.20E-06 (11)		
GO:0004175	endopeptidase activity	1.00E-04 (19)		
GO:0008233	peptidase activity	3.90E-03 (24)		
GO:0005840	ribosome	7.20E-29 (55)		
GO:1990904	ribonucleoprotein complex	3.30E-26 (56)		
GO:0030529	intracellular ribonucleoprotein complex	3.30E-26 (56)		
GO:0044444	cytoplasmic part	4.80E-17 (59)		
GO:0005737	cytoplasm	3.30E-16 (65)		
GO:0032991	macromolecular complex	3.30E-15 (78)		
GO:0043232	intracellular non-membrane-bounded organelle	5.60E-15 (57)		
GO:0043228	non-membrane-bounded organelle	5.60E-15 (57)		
GO:0005622	intracellular	1.30E-12 (96)	0.028 (67)	
GO:0044424	intracellular part	4.00E-12 (92)	0.028(68)	
GO:0044464	cell part	4.00E-12 (96)	0.028(68)	
GO:0005623	cell	4.00E-12 (96)	0.026(65)	
GO:0000502	proteasome complex	2.20E-09 (14)		
GO:0043229	intracellular organelle	9.10E-08 (67)	2.30E-03 (59)	
GO:0005839	proteasome core complex	1.20E-07 (11)		
GO:0043226	organelle	1.20E-07 (67)	2.30E-03 (60)	
GO:0019773	proteasome core complex, alpha-subunit complex	7.80E-04 (5)		
GO:0044391	ribosomal subunit	6.50E-03 (5)		
GO:0015934	large ribosomal subunit	2.50E-02 (4)		

Table 4.2. GO terms identified in Cluster 1. Some of these GO terms were also present within Cluster 7 and 8. The probability of being statistically overrepresented is shown for each GO term. Numbers in parentheses indicate the numbers of genes represented by each GO term.

Cluster 4 and 5 (Figure 4.4D and E) are interesting as they both show how *C. reinhardtii* under a short-term copper stress has a much higher expression change (over 1.3 standard deviations) for a subset of genes when compared to the long-term treatment and both *C. acidophila* treatments, all of which have lower levels of expression for this cluster. Significantly enriched GO terms found in Cluster 4 consisted of mainly metal ion binding and antioxidative properties (Table 4.4). A large proportion of this cluster presented genes with oxidoreductase activity (n=44). A significant proportion of these genes also included iron-sulphur cluster binding domains and metal binding domains indicating they have some role in metal binding. In *C. acidophila* there was very little change in the short-term copper stress as the relative expression value was close to the mean across the four data sets, whilst for long term copper exposure conditions across both species, the genes showed a lower expression in comparison to the mean for Cluster 4. This could suggest that they play a less important role in the copper adaptation over a long period of time. Cluster 5 on the other hand consists of photosynthesis and chloroplast structure genes (Table 4.5). These genes are expressed at a reduced relative expression in both *C. acidophila* copper treatments, however, much more so under the short-term copper stress. The cluster remains relatively unchanged under long term copper stress for *C. reinhardtii*. In contrast to these two clusters, Cluster 8 shows higher expression for *C. reinhardtii* under long term copper stress conditions whilst all other treatments stayed similar or were expressed at reduced expression. There were many GO terms associated to Cluster 8 (31) that are mostly focussed around gene expression and RNA processing (Table 2.7).

GO Term	Description	Cluster 3	Cluster 7
GO:0006928	movement of cell or subcellular component	2.00E-06 (18)	3.70E-02 (13)
GO:0007017	microtubule-based process	2.00E-06 (21)	3.70E-02 (16)
GO:0007018	microtubule-based movement	6.50E-06 (17)	3.70E-02 (13)
GO:0044763	single-organism cellular process	2.60E-02 (62)	
GO:0003777	microtubule motor activity	1.20E-04 (15)	2.20E-02 (13)
GO:0003774	motor activity	1.20E-04 (15)	2.20E-02 (13)
GO:0015630	microtubule cytoskeleton	3.90E-07 (21)	2.30E-03 (16)
GO:0044430	cytoskeletal part	1.10E-06 (21)	2.30E-03 (17)
GO:0005856	cytoskeleton	1.30E-06 (21)	2.30E-03 (17)
GO:0005875	microtubule associated complex	6.50E-06 (16)	3.00E-03 (13)
GO:0030286	dynein complex	1.90E-05 (9)	2.30E-03 (8)
GO:0042995	cell projection	3.20E-02 (5)	
GO:0005929	cilium	3.20E-02 (5)	

Table 4.3 GO terms identified in Cluster 3. Many of these GO terms were also present within Cluster 7. The probability of being statistically overrepresented is shown for each GO term. Numbers in parentheses indicate the numbers of genes represented by each GO term.

GO Term	Description	Cluster 4
GO:0016491	oxidoreductase activity	3.30E-02 (44)
GO:0051536	iron-sulfur cluster binding	3.70E-02 (12)
GO:0051540	metal cluster binding	3.70E-02 (12)

Table 4.4 GO terms identified in Cluster 4. The probability of being statistically overrepresented is shown for each GO term. Numbers in parentheses indicate the numbers of genes represented by each GO term.

GO Term	Description	Cluster 5	Cluster 6
GO:0034357	photosynthetic membrane	1.50E-03 (12)	
GO:0044436	thylakoid part	1.50E-03 (12)	
GO:0009521	photosystem	1.50E-03 (12)	
GO:0009579	thylakoid	1.50E-03 (12)	
GO:0009522	photosystem I	1.40E-02 (6)	
GO:0019684	photosynthesis, light reaction		4.20E-03 (10)
GO:0015979	photosynthesis		4.20E-03 (14)
GO:0009765	photosynthesis, light harvesting		4.90E-03 (9)

Table 4.5 GO terms identified in Cluster 5 or 6. The probability of being statistically overrepresented is shown for each GO term. Numbers in parentheses indicate the numbers of genes represented by each GO term.

GO Term	Description	Cluster 7
GO:0044422	organelle part	2.30E-03 (37)
GO:0044446	intracellular organelle part	2.30E-03 (36)
GO:0005634	nucleus	2.30E-03 (28)
GO:0043231	intracellular membrane-bounded organelle	3.50E-03 (37)
GO:0043227	membrane-bounded organelle	3.50E-03 (37)
GO:1902494	catalytic complex	7.20E-03 (15)

Table 4.6 GO terms identified in Cluster 7. The probability of being statistically overrepresented is shown for each GO term. Numbers in parentheses indicate the numbers of genes represented by each GO term.

GO Term	Description	Cluster 8
GO:0042254	ribosome biogenesis	3.50E-09 (16)
GO:0022613	ribonucleoprotein complex biogenesis	9.50E-09 (16)
GO:0016070	RNA metabolic process	1.10E-08 (43)
GO:0006396	RNA processing	3.30E-07 (23)
GO:0034660	ncRNA metabolic process	3.50E-07 (19)
GO:0034470	ncRNA processing	7.50E-07 (15)
GO:0006364	rRNA processing	3.40E-06 (10)
GO:0016072	rRNA metabolic process	3.40E-06 (10)
GO:0090304	nucleic acid metabolic process	5.70E-06 (45)
GO:0044085	cellular component biogenesis	4.60E-05 (16)
GO:0071840	cellular component organization or biogenesis	1.90E-04 (22)
GO:0006139	nucleobase-containing compound metabolic process	1.20E-03 (50)
GO:0009451	RNA modification	1.90E-03 (9)
GO:0046483	heterocycle metabolic process	3.00-03 (51)
GO:0006725	cellular aromatic compound metabolic process	3.00-03 (51)
GO:0032259	methylation	3.30E-03 (8)
GO:0006399	tRNA metabolic process	3.30E-03 (11)
GO:1901360	organic cyclic compound metabolic process	4.60E-03 (51)
GO:0001522	pseudouridine synthesis	9.70E-03 (6)
GO:0043414	macromolecule methylation	1.30E-02 (6)
GO:0008033	tRNA processing	1.60E-02 (7)
GO:0016741	transferase activity, transferring one-carbon groups	1.40E-04 (20)
GO:0003676	nucleic acid binding	3.90E-04 (50)
GO:0008168	methyltransferase activity	4.00E-04 (18)
GO:0016866	intramolecular transferase activity	4.70E-02 (6)
GO:0034062	RNA polymerase activity	4.70E-02 (6)
GO:0005488	binding	4.70E-02 (123)
GO:0003723	RNA binding	4.70E-02 (17)
GO:0003899	DNA-directed RNA polymerase activity	4.70E-02 (6)
GO:0009982	pseudouridine synthase activity	4.70E-02 (5)
GO:0030684	preribosome	8.30E-03 (5)
GO:0032040	small-subunit processome	2.50E-02 (4)

Table 4.7 GO terms identified in Cluster 8. The probability of being statistically overrepresented is shown for each GO term. Numbers in parentheses indicate the numbers of genes represented by each GO term.

Clusters 2, 3, 6 and 7 (Figure 4.4 B, C, F and G) may be the most informative regarding copper adaptation as these clusters show significant changes in *C. acidophila* under different copper stress conditions in comparison to *C. reinhardtii*. In Cluster 2 there is a huge increase in gene expression for the *C. acidophila* short term stress conditions whilst all other conditions show lower relative expression levels. This is also the second largest cluster identified (n=736), which includes 153 potential paralogues. What is perhaps even more intriguing is that none of the genes showed a significant enrichment of particular GO terms within this cluster, suggesting there is a wide array of genes with many different functions involved in the immediate response to copper. A full list of these genes can be found in supplementary table 4.1. In contrast Cluster 6 shows almost the opposite effect. Under short term copper stress *C. acidophila* showed much lower expression of this set of genes in comparison to all other treatments. All these GO terms were associated with photosynthetic processes and the energy generation system of a cell. Cluster 3 appears to be an interesting group. This set of genes showed higher expression in both short- and long-term copper stress for *C. acidophila*. Interestingly, whilst there seems to be little change in relative expression for the *C. reinhardtii* long term stress, a huge decrease in expression for the short-term stress is seen for this cluster. The GO terms associated with this cluster hint that a lot of these genes are involved with the intracellular transport systems and cytoskeleton reorganisation. Finally, Cluster 7 appears to contain important genes for long term copper stress. Both *C. acidophila* and *C. reinhardtii* show a higher expression in response to long term copper stress. Interestingly, short-term copper stress for *C. reinhardtii* shows a lower relative expression level, whilst the short-term copper stress for *C. acidophila* remains relatively unchanged. This cluster seems to have a wide variety of genes and spans many different clusters regarding GO terms. It shares many of the same GO terms as Clusters 1 and 3 whilst also having many unique GO terms, predominantly associated with organelles (Table 2.2, 2.3 and 2.6).

4.4.3 Oxidative Stress Response

To get a more detailed understanding of what pathways were being altered in response to copper exposure, genes identified from the GO enrichment of the clusters were taken and mapped out into pathways with known functions in oxidative stress response. I also looked at certain genes known to be involved within the oxidative stress response that were not enriched within the cluster. In doing so several key processes were identified and helped widen our understanding of how green microalgae can acclimatise to a high copper environment. Due to the diverse nature of the GO terms in Clusters 1 and 7 it was not possible to summarise the genes from these clusters in a single pathway or functional group, while Cluster 2, as previously mentioned, showed no significant enrichment for a specific set of genes.

Figure 4.5 shows genes involved in the ROS stress response mapped from Cluster 4. The genes are identified by the *C. reinhardtii* transcript information with expression data shown in Table 4.8. Interestingly the highest expression for treatments in Cluster 4, was the short-term copper stress for *C. reinhardtii* whilst the same treatment for *C. acidophila* showed unchanged relative expression. Both long term treatments show the lowest expression levels of all four data sets, whilst the short-term copper stress showed baseline expression that was equivalent with the overall mean expression.

Cysteine is a vital amino acid that is central to the oxidative stress response, particularly as it is important for Fe-S cluster proteins. Perhaps most importantly, it is a key amino acid for the synthesis of glutathione (GSH), which plays an important role in governing the ROS stress response. Figure 4.5 shows several genes involve in GSH metabolism including *GSR1* and *BBB1*. *BBB1* is a glutathione-s-transferase kappa (Table 4.8), whilst GSR1 reduces oxidised, dimerised glutathione (GSSG) back to GSH, both of which will be discussed later. There is contrasting evidence for the importance of the glutathione response to cells under metal stress. Sabatini et al. (2009) and Li et al. (2006) both reported an increase in GSH levels after 7 and 13-15 days respectively of copper and zinc stress in *Scenedesmus vacuolatus* and *Pavlova viridis*. However, Jamers et al. (2013) reported a decrease in GSH levels after 72 hours of copper exposure. As GSH is a central molecule that can be a precursor to many other antioxidative responses as well as its direct role, it is perhaps unsurprising that there is contrasting evidence in the way different organisms utilise GSH. Due to the vast diversity in nature it is likely different species may adopt different strategies to deal with ROS.

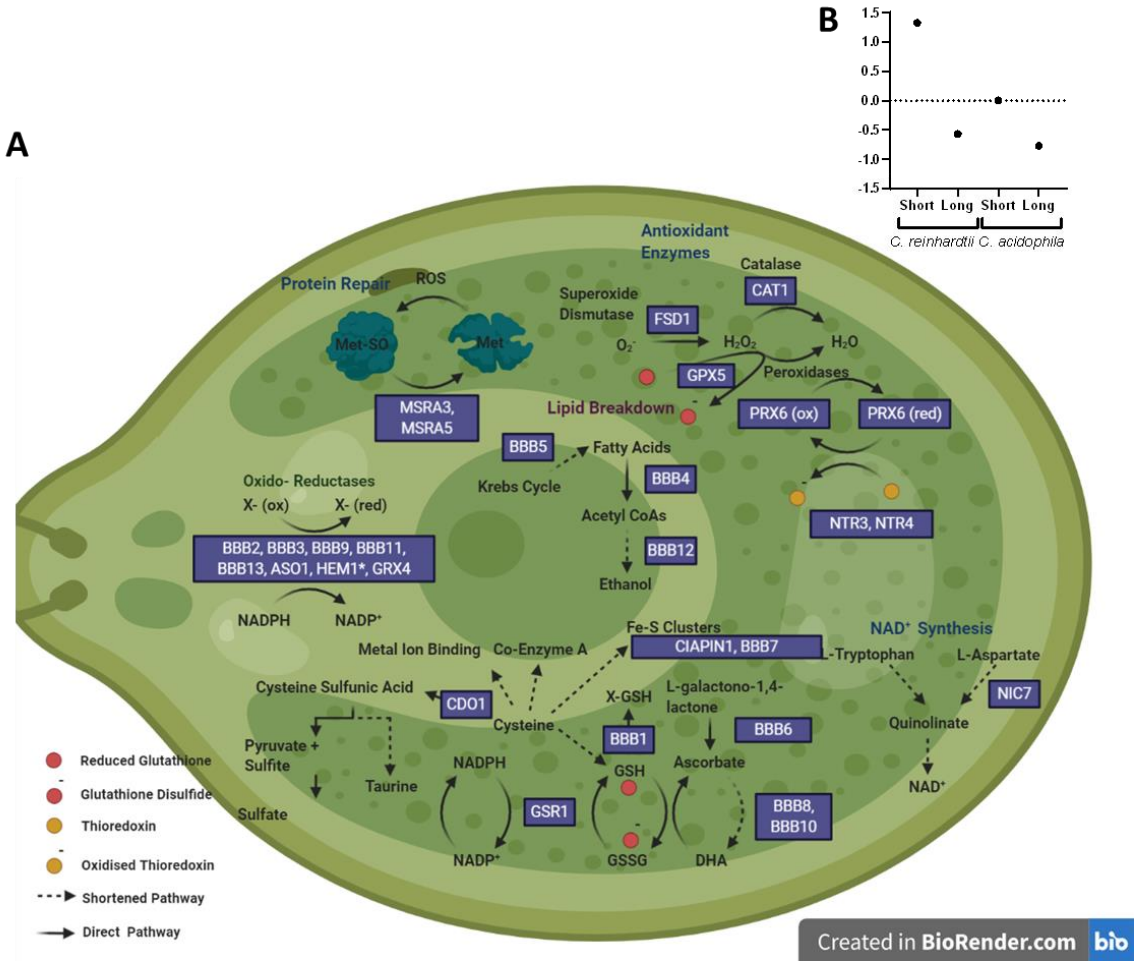

Figure 4.5 (A) Genes involved in the ROS stress response in C. reinhardtii and C. acidophila under copper stress taken from significantly enriched GO terms from Cluster 4 (expression pattern seen in B) of the heatmap data. Only genes with clear annotation were mapped, some putative genes/ genes with a broad range description are indicated with an asterisk. Gene names starting with BBB had to be ascribed a gene name, specific gene info can be found in Table 4.8. DHA: dehydroascorbate; GSH: Glutathione

Gene ID	Transcript	Gene info	PM01			11/32c		
			Control	Long Stress	Short Stress	Control	Long Stress	Short Stres
ASO1	Cre12.g528450	L-aspartate oxidase	2635.3	2450.2	9594.4	1433.0	3683.7	15025.4
BBB1	Cre12.g553700	(1 of 3) PTHR13887 - GLUTATHIONE S-TRANSFERASE KAPPA	1598.6	3818.6	66352.6	295.7	2347.2	48133.7
BBB10	Cre09.g401886	L-ascorbate peroxidase, heme-containing	3361.9	3226.1	3886.0	4775.3	4719.5	16990.9
BBB11	Cre03.g207800	(1 of 2) 1.1.1.195 - Cinnamyl-alcohol dehydrogenase / CAD	726.4	2712.5	23298.1	224.4	1651.7	22721.3
BBB12	Cre01.g033350	(1 of 1) PTHR11699:SF25 - ALDEHYDE DEHYDROGENASE-LIKE PROTEIN YHR039C-RELATED	1676.8	1859.1	7252.9	215.6	296.3	2478.6
BBB14	Cre08.g358538	Putative chloroplast lycopene beta cyclase	999.7	877.0	950.7	1909.2	1813.6	5039.9
BBB15	Cre13.g583050	Pheophorbide a oxygenase, Rieske iron-sulfur cluster protein	361.3	363.7	493.0	42.3	60.7	331.5
BBB16	Cre16.g693202	(1 of 1) K00392 - sulfite reductase (ferredoxin) (sir)	5862.9	6994.8	15564.4	66.6	163.3	2070.1
BBB2	Cre12.g556750	Short-chain dehydrogenase/reductase	6204.4	7285.1	13271.5	14.6	36.9	318.5
BBB3	Cre12.g549852	(1 of 2) KOG1611 - Predicted short chain-type dehydrogenase	1792.4	1835.7	3915.6	218.6	343.0	3442.8
BBB4	Cre16.g687350	(1 of 1) PTHR10909:SF11 - ACYL-COENZYME A OXIDASE-LIKE PROTEIN	1050.7	773.0	1516.4	2392.5	3062.3	16382.5
BBB5	Cre13.g577450	(1 of 1) 1.1.5.3 - Glycerol-3-phosphate dehydrogenase / sn-glycerol-3-phosphate dehydrogenase	1028.1	771.3	2235.2	92.8	236.2	764.9
BBB6	Cre13.g567100	D-arabinono-1,4-lactone oxidase/L-galactono-1,4-lactone dehydrogenase	954.6	1037.6	2361.5	364.7	351.6	4423.2
BBB7	Cre11.g467633	(1 of 2) 2.8.4.3 - tRNA-2-methylthio-N(6)-dimethylallyladenosine synthase / tRNA-i6A37 methylthiotransferase	1715.4	1704.8	3719.4	296.2	745.9	990.0
BBB8	Cre10.g466700	(1 of 2) 1.14.17.4 - Aminocyclopropanecarboxylate oxidase / Ethylene-forming enzyme	336.9	267.0	592.0	274.4	767.3	12907.4
BBB9	Cre10.g424900	(1 of 2) PTHR10869:SF66 - OXIDOREDUCTASE, 2OG-FE(II) OXYGENASE FAMILY PROTEIN-RELATED	906.1	858.0	1495.5	202.5	244.6	810.8
CAT1	Cre09.g417150	Mono-functional catalase	11025.1	10423.1	17522.6	3554.4	2985.2	9767.7
CDO1	Cre03.g174400	Cysteine dioxygenase	541.2	490.4	1649.6	94.1	214.1	556.1

Gene ID	Transcript	Gene info	PM01			11/32c		
			Control	Long Stress	Short Stress	Control	Long Stress	Short Stress
CDO1	Cre03.g174400	Cysteine dioxygenase	541.2	490.4	1649.6	94.1	214.1	556.1
CIAPIN1	Cre11.g475350	(1 of 1) PF05093 - Cytokine-induced anti-apoptosis inhibitor 1, Fe-S biogenesis (CIAPIN1)	1512.8	1502.2	4485.2	559.9	747.5	4107.1
FDX4	Cre07.g334800	Ferredoxin	2472.1	2514.3	6431.4	0.3	0.0	2.7
FSD1	Cre10.g436050	Fe superoxide dismutase	13613.5	11874.8	49489.8	6655.7	5553.6	46408.6
GPX5	Cre10.g458450	Glutathione peroxidase	3071.7	4195.0	8645.0	4848.7	6434.6	179340.8
GRX4	Cre04.g232602	Glutaredoxin, CGFS type	1065.8	1162.2	8302.8	320.1	427.2	6874.8
GSR1	Cre06.g262100	Glutathione reductase	2215.6	3301.2	27338.8	260.0	711.5	14827.6
HDH1	Cre02.g077350	Histidinol dehydrogenase	3348.6	3089.7	8468.1	1663.6	2616.4	40177.4
HEM1	Cre07.g342150	Glutamyl-tRNA reductase	10617.2	11101.8	16336.5	4024.4	5154.0	8177.8
MDH5	Cre09.g410700	NADP-dependent malate dehydrogenase, chloroplastic	2663.1	1971.4	2738.1	12271.1	10778.0	43202.9
MSRA3	Cre08.g380300	Peptide methionine sulfoxide reductase	7267.5	8030.0	33115.5	540.6	891.3	72883.3
MSRA5	Cre10.g464850	Peptide methionine sulfoxide reductase	2333.9	2526.8	8631.1	595.7	838.8	43080.2
NIC7	Cre06.g251450	Quinolinate synthetase A	1202.9	1299.5	2086.7	478.8	742.2	4263.5
NTR3	Cre07.g355600	NADPH dependent thioredoxin reductase	17857.9	18930.8	91973.2	349.9	559.7	15896.4
NTR4	Cre01.g054150	NADPH-dependent thioredoxin reductase	5883.5	5828.2	27330.5	1805.0	3005.0	18706.8
PETC	Cre11.g467689	Rieske iron-sulfur subunit of the cytochrome b6f complex, chloroplast precursor	63733.2	56671.6	77652.1	158239.8	93594.9	282781.0
PRX6	Cre10.g422300	Thioredoxin dependent peroxidase	4113.0	3100.8	9026.7	570.8	920.4	5152.5

Table 4.8 List of genes present in Figure 4.5 Gene ID is the identifier present on Figure 4.5. The transcript is the C. reinhardtii gene which the paralogues were found to be most similar to and the gene info represents the function. Data is expressed as normalised counts as calculated using DEseq2

To get a better idea of the role of GSH in the stress response, genes which involve the antioxidant molecule GSH, were manually pulled out of the RNA-seq data for a more in-depth analysis. These include three sets of genes, GSH-s-transferases (GST), glutathione synthetase and GSH reductase (GSR). Five GST isoforms were identified from *C. acidophila* and four isoforms from *C. reinhardtii*. From Figure 4.6 it is apparent that *GST1* and *GST2* show a similar pattern in both species. The short-term treatments presented significantly higher expression than the control and long term treatments. For both isoforms the *C. reinhardtii* short term expression values were higher than for the *C. acidophila* transcripts. *CrGST1* is most likely a beta class of GST whilst *CrGST2* appears to be closely related to the Pi class of GSTs, although neither of these classes are thought to be found in higher plants (Chatzikonstantinou et al., 2017; Lallement et al., 2014). *GST3* and *GST4* could present interesting candidates for copper adaptation. For both genes the short-term copper stress expression in *C. acidophila* was significantly higher than for all other treatments. This was more pronounced for *GST4* in which all the other treatments were not significantly different from each other, however, the short-term treatment for *CaGST3* (mean expression = 40770.5 NC ±6616) was almost 6 times higher than *CaGST4* (mean expression = 6913 NC ±1159.3). *CrGST3* is thought to be closely related to the sigma class of GST enzymes found in both vertebrates and invertebrates, whilst *CrGST4* is thought to be closely related to the theta class of GSTs (Chatzikonstantinou et al., 2017). Theta GSTs have been found to have high glutathione peroxidase activity, reducing the amount of oxidised lipids in Arabidopsis (Dixon et al., 2000). Additionally, a tobacco plant overexpressing a theta class GST, showed enhanced tolerance to abiotic stresses such as herbicides, mannitol and salt stress, as well as an enhanced oxidative stress response (Stavridou et al., 2019). Sigma class GSTs are thought to have emerged before the split of eukaryotes, meaning functions have had a lot of time to diversify in specific organisms (Hervé et al., 2008). An analysis of two other sigma class GSTs in *C. reinhardtii*, GST7 and GST10 were thought to target isothiocyanates, a cellular antioxidant (Chatzikonstantinou et al., 2017). However, there is no evidence to suggest that CrGST3 will have a similar function, more so for *C. acidophila*, which may have an alternative activity.

GSTx is a *C. acidophila* isoform where a *C. reinhardtii* orthologue could not be found to be expressed in this dataset. Like most of the other *CaGSTs*, under the short-term treatment the transcript is significantly increased when compared to both other treatments. *CaGSTx* could be a product of gene duplication, providing a new function which could confer an enhanced copper tolerance. Another putative GST was also found to be enriched in Cluster4 and is identified as a Glutathione-S-Transferase Kappa, which has been labelled as *BBB1* (Figure 4.5). The kappa class of GSTs are classified as mitochondrial GSTs (Kumar and Trivedi, 2018). GSTs as a class have a wide variety of functions under metal stress, some have been found to bind metals to phytochelatins so that they can be stored in an inert state in the vacuole (Kumar and Trivedi, 2018). Others have been shown to play a vital role in the oxido-reductant cycling of cells (Le Martret et al., 2011). While some have even been shown to have peroxidase activity (Franco et al., 2008). When an endophytic fungus, *Exophiala pisciphila*, was exposed to metal stress, 24 GSTs were found to be increased in expression. The highest GST to be increased was a mitochondrial GST epmetaxin11 (Shen et al., 2015). The kappa

class GSTs seem to be poorly described in the literature for microalgae and even higher plants. One group has

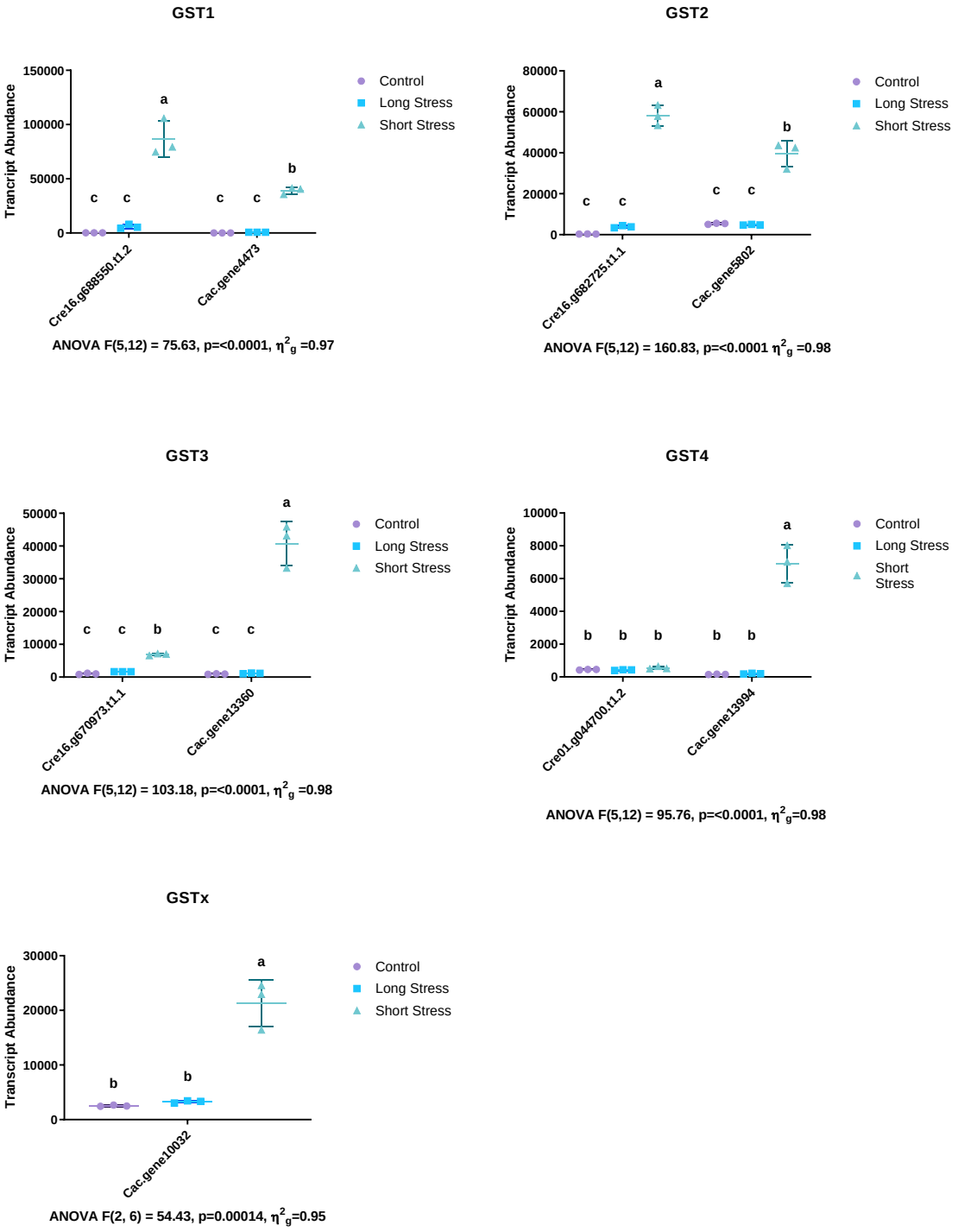

Figure 4.6 transcript abundance shown as normalised counts, calculated using DEseq2, of glutathione- s - transferases for both C. acidophila and C. reinhardtii under a short and long term copper stress. All genes were present in both species apart from GSTx. Treatments were tested for significance across both species and all treatments using a one way ANOVA, Tukey's post-hoc test were used for pairwise comparisons to test for significant differences between treatments. Letters represent different groups of significance.

described a single mitochondrial GST from the brown alga *Ectocarpus siliculosus*, but its function is unknown (Franco et al., 2008). However, due to their location in the mitochondria, a highly oxidised environment, which can be exacerbated under metal stresses, it is likely that they will have an antioxidative role. This would be in agreement with Allocati et al. (2009) who suggested that two mitochondrial GSTs have domains involved in redox catalysis.

The second gene class is GSH, which could also provide interesting insights into the copper adaptation of PM01. For *GSH1* all the control and long-term stress conditions for both species do not significantly differ in transcript level. In contrast, both *GSH1* isoforms were expressed at a significantly higher level in the short term treatments, and the *C. acidophila* transcript (54388.5 NC ±6185.6) was nearly 2.5 times higher than the *C. reinhardtii* transcript (22223.2 NC ±1084.5). *GSH2* is perhaps more intriguing, as there is no significant change for any of the treatments in *C. reinhardtii*, and all three treatments are significantly lower than any of the *C. acidophila* treatments. Additionally, the short-term copper stress for *C. acidophila* gave significantly higher *GSH2* abundance than all other treatments. It is important to note that the transcript abundance of *GSH2* was, overall, much lower than the *GSH1* transcripts. The GSH genes encode for a glutathione synthetase involved in the biosynthesis of glutathione. Glutathione synthetase has been found to be increased in expression in response to both zinc and cadmium in the marine alga *Dunaliella tertiolecta* (Tsuji et al., 2003). Additionally, it has also been shown to play a role in arsenic tolerance of the extremophile *C. eustigma* (Hirooka et al., 2017). It is unsurprising that both isoforms involved in glutathione synthesis are increased in expression in the short-term for the extremophile PM01. Glutathione plays such a prevalent role in the ROS detoxification system, as well as being an important precursor to other metal binding proteins such as phytochelatins. What is interesting is that none of the long-term treatments gave significantly higher GST or GSH expression than the controls for PM01. Unfortunately, due to the negative results in attempting to quantify ROS in section 3 it is unclear whether the short-term and long-term copper stress induce a similar quantity of ROS in the cells. Additionally, we also do not know the time point at which transcript levels may decrease after a copper. From this data we could suggest that while in the short-term copper treatment cells experience high ROS requiring inducement of glutathione metabolism, during long term copper exposure cells quench these ROS by unknown mechanisms to prevent any further damage in the cell, and so do not need to maintain high expression of GST and GSH genes. However, further experiments would need to be conducted to clarify this.

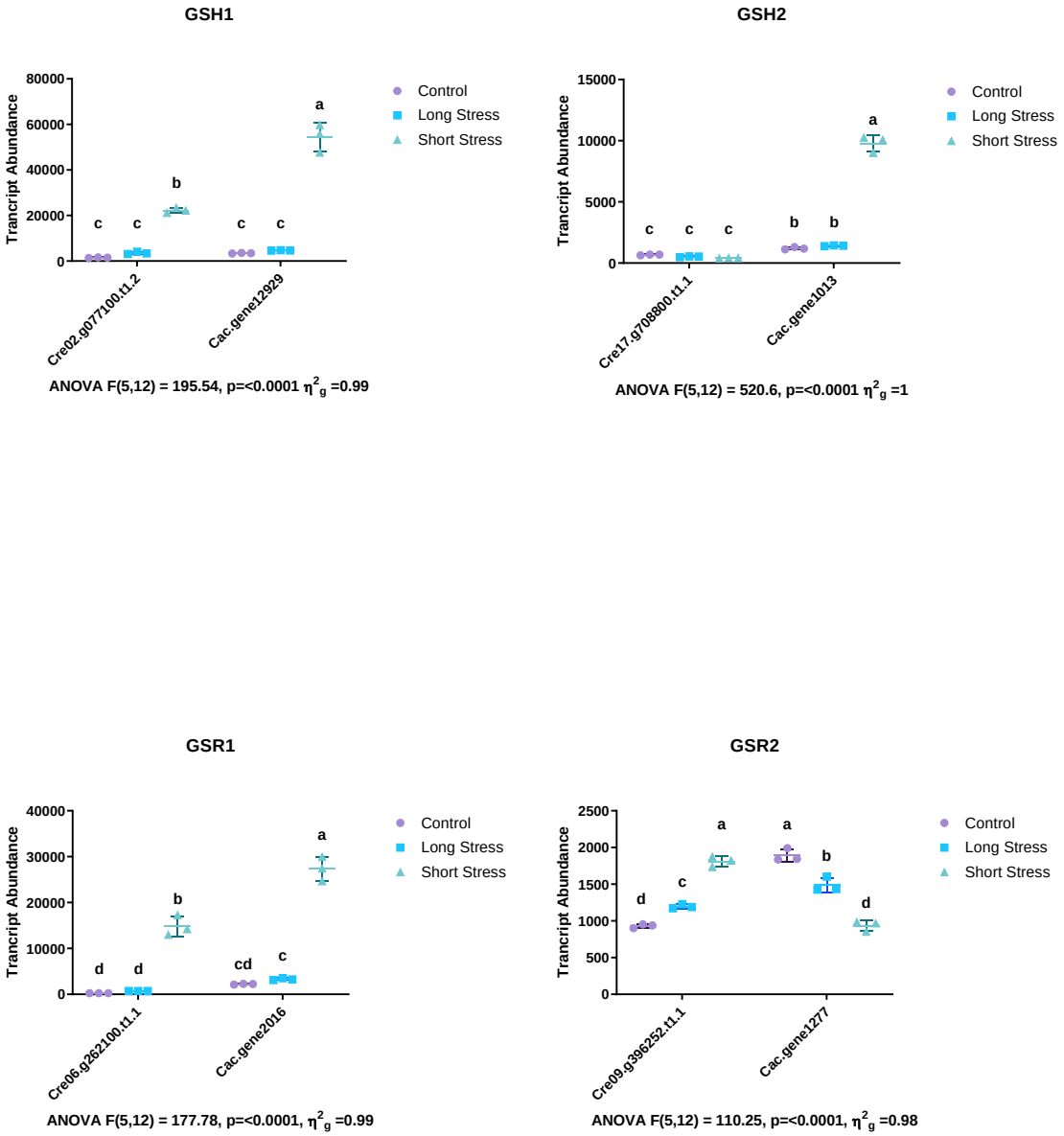

Figure 4.7 Transcript abundance shown as normalised counts, calculated using DEseq2, of genes related to glutathione synthesis and oxidation state for both C. acidophila and C. reinhardtii under a short and long term copper stress. Treatments were tested for significance across both species and all treatments using a one way ANOVA, Tukey's post-hoc test were used for pairwise comparisons to test for significant differences between treatments. Letters represent different groups of significance.

The final set of genes related to glutathione of interest is the GSR genes and there are two isoforms identified in the transcriptomes of both species, which respond to a copper treatments very differently. The *GSR1* isoform was enriched in Cluster 4 (Figure 4.5). GSR1 converts the oxidised GSSG into two molecules of GSH. Study of *gsr-1* knockdown mutants in *Caenorhabditis elegans* has shown that this enzyme is extremely important for nematode survival when exposed to oxidative stress (Lüersen et al., 2013). Likewise Ma et al. (2020), found that *GSR1* is increased in a glutathione peroxidase mutant of *C. reinhardtii* under oxidative stress. Whilst it was observed that *GSR1* increased in expression in response to a copper treatment in *C. reinhardtii*, *CaGSR1* has higher relative expression. The *CaGSR1* transcript (27388.8 NC ±2650.8) was expressed significantly higher than the *C. reinhardtii* transcript (14827.6 NC ±2202.6). Interestingly, the long-term treatment for PM01 gave GSR1 expression that was also significantly higher than both the control and long-term treatment for *C. reinhardtii*. On the other hand, *GSR2* gave a very different gene expression profile. *C. acidophila* and *C. reinhardtii* have an inverse response to copper stress in relation to *GSR2* transcript abundance. Under short term copper stress (1809.9 NC ±70.8). *CrGSR2* abundance was almost 2-fold higher when compared to the control (930.6 NC ±26.6). Conversely, the PM01 control treatment gives a high abundance (1890.8 NC ±87) of *GSR2*, but under short term copper treatment, the transcript is significantly reduced (935.4 NC ±71.8) (Figure 4.7). The PM01 long-term copper treated *GSR2* transcript was slightly more abundant than its *C. reinhardtii* counterpart, and for both species, *GSR2* expression values under long term conditions were in between the short-term and control values.

Having a reduced glutathione pool clearly has many potential benefits, so it is unsurprising that isoforms of the GSR gene are more highly expressed under copper conditions. These results also agreed with Laporte et al. (2016) who showed that a glutathione reductase was increased in expression in *Ulva compressa* under a copper stress. Interestingly, they showed that the expression of glutathione reductase varied greatly over time, such that the expression started to increase on day 3 and reached maximal expression by day 9, then very rapidly declined back to the basal levels by day 12. This is important to note as we are only looking at two brief snapshots for both the algae strains. Following a similar pattern to some of the other genes described here, *GSR1* shows a much higher expression in both short term treatments. Like the other genes noted so far, metal stresses such as Cu and Zn were capable of inducing GSR in *Chlorella sorokiniana* and *Scenedesmus acuminatus* (Hamed et al., 2017). GSR has also been implicated in the arsenic detoxification of the extremophile *C. eustigma* (Hirooka et al., 2017). Other abiotic stresses such as salt, high temperature and nitrogen starvation, also induce an increase is GSR activity (Fan et al., 2018; Gigova and Ivanova, 2015; Singh et al., 2018). This suggests that the broad range glutathione detoxification mechanism is highly useful to oxidative stress-inducing conditions in general. My data also suggests that different glutathione metabolism isoforms could play an important role in more specific applications. *CaGSH2* increased in expression in response to a short-term copper treatment, whilst the *CrGSH2* is not, so this could be one of the potential components to allow *C. acidophila* to be more capable at short-term adaptation to copper. Conversely, whilst both the GSR isoforms for *C. reinhardtii* were increased under the short-term copper treatment, for PM01 *GSR2* was decreased in comparison to both the copper treatments when compared to the control. Interestingly, *CaGSR2* is highly expressed, to similar levels under the short-term copper treatment compared to the *C.*

reinhardtii isoform in control conditions. Lin et al. (2018) have shown that both GSR isoforms play an important role in *C. reinhardtii* dealing with high light stress. In 181 Section 4.4.5 we will see how PM01 reduces its photosynthetic capabilities under the short-term copper stress. This could explain why the *GSR2* isoform reduces its expression, in line with a reduced photosynthetic capability. GSR1 on the other hand may either play other roles within the cell or has adapted a special function within PM01 that is still important in copper stress.

CDO1 expression is differentially affected by the copper treatments and is involved in the transfer of cysteine to cysteine sulphunic acid (Figure 4.5), which can then be incorporated into multiple pathways. These pathways lead to the formation of 3-sulfino-L-alanine (cysteine sulphunic acid), and in turn, the formation of taurine and/or pyruvate and sulphate. Taurine can play multiple roles within stress tolerance. It is a good osmoregulator and has antioxidative properties, and has been suggested to be an important metabolite in microorganisms adapted to an acidic and metal rich environment (Mosier et al., 2013). However, Kim et al. (2020) have found that taurine does not have as strong anti-oxidative powers compared to other sulfur containing amino acids such as cysteine. *CDO1* belongs to Cluster 4, out of all the 4 data sets showed the largest increase in expression in the short term copper treatment for *C. reinhardtii.* It is possible that taurine may play a role under a short-term copper stress in *C. reinhardtii* that has yet to be elucidated. Genes *CIAPIN1* and *BBB7*, encodes for proteins involved in the incorporation of cysteine in Fe-S clusters were also affected by different copper stresses across the organisms. Fe-S clusters play a wide range of roles in the cell. They are perhaps most well known for their role in electron transfer, but can also bind and activate substrates, regulate gene expression and have enzymatic activities (Johnson et al., 2005). Copper is a highly reactive metal and can easily displace other metals in core compounds, inactivating the function of the protein (Magdaleno et al., 1997; Nieboer and Richardson, 1980). As such it is likely that these Fe-S clusters could be a prime target for metal displacement by copper and as such their expression may levels may change. Frey et al. (2016) have suggested that CIAPIN1 can act with glutaredoxins to provide a framework for incorporating 2Fe-2S clusters into proteins in human cells. The last set of genes present in this cluster involved in glutathione cycling is *BBB6*, *BBB8* and *BBB10*. *BBB6* encodes for D-arabinono-1,4-lactone oxidase/L-galactono-1,4-lactone dehydrogenase which is involved the synthesis of ascorbate from L-galactono-1,4- lactone. Ascorbate can then be oxidised into dehydroascorbic acid (DHA) by the proteins encoded by *BBB8* and *BBB10*. DHA is then reduced back into ascorbate through the oxidation of GSH. Ascorbate is a well-known antioxidative molecule, many studies have found that ascorbate is accumulated across multiple algal species under a variety of metal stresses such as zinc, copper, lead, mercury and cadmium (Hamed et al., 2017; Kováčik et al., 2017; Moenne et al., 2016; Piotrowska-Niczyporuk et al., 2012, 2015).

Figure 4.5 also shows that antioxidative enzymes are significantly enriched in Cluster 4. An iron superoxide dismutase (FSD1), which converts the superoxide radical (O_2^-) into hydrogen peroxide (H_2O_2), also shows differential expression in Cluster 4. We have also seen from chapter 3 that the *FeSODs*, showed the largest increase in expression under the short-term copper stress (Figure 2.14). FeSODs are typically located in the chloroplast and are thought to be associated with PSI, where they are able to protect the photosynthetic apparatus from any increases in radicals (Wolfe-Simon et al., 2005). Copper stress has been seen to induce SOD activity 30% in the alga *Gonyaulax polyedra*. Transcript levels were also seen to increase ~3 times under copper stress in *G. polyedra*

(Okamoto et al., 2001a, 2001b). This FeSOD may play a role in mitigating radicals produced by copper. The generated H_2O_2 can have signalling function, however, at high elevated concentrations it can cause damage to the cells (Mittler, 2017). H_2O_2 can be detoxified into water through two classes of antioxidative enzymes. The first, are the catalases, and here we see that only CAT1 is differentially expressed also confirmed in Figure 2.13. A study of *Enterobacter cloacae* found that the only protein consistently increased in all three studied strains when exposed to cadmium was a catalase (Chuanboon et al., 2019). Many studies have found that catalase transcript levels and/or activity are increased in multiple algal species and under various metal stresses (Fazelian et al., 2019; Kováčik et al., 2017; Piotrowska-Niczyporuk et al., 2018; Wang et al., 2020). Both *CAT1* transcripts show a slight decrease in expression in the long-term treatments when compared to the control. Although it is not significant, we see a few patterns across the data relating to antioxidative genes that are highly increased under the short-term copper treatment but seem less important in the long-term treatment. To the best of my knowledge there is only one study that has found a decrease in catalase activity under metal stress. At lower copper concentrations Chen et al. (2016), found that catalase activities did increase, however, when reaching much more toxic concentrations catalase activity decreased, coupled with huge reduction in the efficiency of PSII. Additionally, Esperanza et al. (2017) found that catalase transcript levels did decrease when exposed to the herbicide atrazine, which induces oxidative stress through the breakdown of the electron transport chain in PSII. It is not clear as to whether this decrease in transcript level also leads to a decrease in catalase activity. There appears to be a tight link between catalase activity and efficiency of photosynthesis within the cells (Brisson et al., 1998; Zelitch, 1990). It is possible that there is an increase in catalase activity to mitigate any damage before the photosynthetic apparatus can be damaged. We have already seen in Figure 2.6 and Figure 2.13, that this could be the case as PM01 appears to rapidly shut down photosynthesis and increase *CAT1* transcripts in response to the short term copper stress.

The second class of enzymes capable of detoxifying H_2O_2 is the peroxidases. In Cluster 4 two types of peroxidases were identified. Transcripts for glutathione peroxidase (GPX5), which catalyses the detoxification of H_2O_2 using glutathione as a cofactor, converting it to its oxidised form, GSSG. Peroxidase, PRX6 can also catalyse this reaction by oxidising itself, PRX6 can then be reduced again by NTR3 and NTR4 using thioredoxin, the transcripts for these proteins are also significantly enriched in Cluster 4. Jiang et al. (2016) found that both glutathione peroxidase and peroxidase both increased in a concentration dependent manner with copper stress in *C. reinhardtii*. Specifically, GPX5, is located within the cytoplasm and has been found to be increase in expression by various stresses. Interestingly, it has been found to be increased in expression in response to singlet oxygen, but also cold and high light (Brzezowski et al., 2012; Roach et al., 2017; Zalutskaya et al., 2019). It is likely that this upregulation is largely controlled by abundance of singlet oxygen, in preparation for an increase in H_2O_2 production, which will be produced by various stresses, providing an adaptive mechanism to a wide array of stresses.

During oxidative stress to the cells, proteins and metabolites are inevitably damaged through oxidation. These damaged molecules can be repaired through a variety of proteins, of which a wide array of genes encoding these proteins are present within Cluster 4 (Figure 4.5). The first class are the oxido-reductases. These have a wide array of functions and are represented by many genes in Figure 4.5, but in general, they catalyse the transfer of electrons from a reductant to an oxidant.

These are particularly relevant within photosynthesis and respiration, in which electrons are transported to create energy gradients, creating a highly oxidising environment (Lodeyro et al., 2012). However, they can play other roles, GRX4 has been found to be involved in iron deficiency sensing in multiple organisms (Horianopoulos & Kronstad, 2019; Li & Outten, 2019). It is unknown whether the *C. reinhardtii* GRX4 plays a similar role in iron homeostasis although, it has been seen to be increased under other stresses such as H_2O_2 (Blaby et al., 2015). Copper can compete with lead for a common transporter binding, and it is feasible that copper could also compete with iron for iron transporters which could lead to an iron deficiency (Sánchez-Marín et al., 2014). *HEM1*, another transcript encoding for an oxidoreductase identified in Cluster 4, has been shown to be a crucial protein involved in tetrapyrrole biosynthesis (Agrawal et al., 2020). Finally, oxidoreductases have also been shown to reduce damaged oxidised proteins and metabolites, detoxifying them and preventing further damage within the cell (Mahajan et al., 2014). Several other proteins that have an oxidoreductase capacity were identified. However, as they have a broad range of functions, their role in copper tolerance is difficult to assign. The second class enriched in Cluster 4 have a more specific function. These are the peptide methionine sulfoxide reductases, these have multiple functions that include cell signalling, direct quenching of ROS and the reversal of substrates damaged by oxidation (Tarrago et al., 2009). They have also been shown to help protect the function of Fe-S clusters under aerobic conditions in *S. cerevisiae* (Sideri et al., 2009). Of the two MSRAs identified in this cluster, *MSRA3* and *MSRA5*, have been predicted that the proteins they encode are localised to the mitochondria and plastids respectively (Tarrago et al., 2009).

The final set of genes are potentially linked to oxidative stress as they are involved in lipid synthesis and breakdown. *BBB5* is a glycerol-3-phosphate dehydrogenase, which converts glycerol-3-phosphate (GPD), an output from the Krebs cycle, into the fatty acid synthesis pathway. Lipid oxidation is a common effect of elevated ROS within cells (Gechev et al., 2006). It is possible that GPD is increased under copper stress to mitigate lipid loss due to oxidative stress. These lipids are then broken down into by-products of acetyl CoAs and eventually ethanol by BBB4 and BBB12 respectively. Interestingly, Hirooka et al. (2017) identified that *C. eustigma*, a closely related extremophile alga to *C. acidophila* lacks enzymes involve in the organic acid fermentation pathways and as such is unable to produce metabolites such as lactate. They also found that the C. *eustigma* cellular ethanol levels were higher, possibly due to less fermentation pathways available.

4.4.4 Cell Movement and Intracellular Transport

Figure 4.8 summarises three different clusters, all of which focus around intracellular transport and cell movement. All gene descriptions and expression data can be found in Table 4.9. Clusters 3 and 7 are dominated by intracellular transport and cellular movement gene functions, whilst Cluster 5 is represented by only one transcript, which is involved in endoplasmic reticulum (ER) to Golgi transport. Microtubules are critical structural molecules for defining cell shape whilst also providing routes for internal transport of organelles, proteins and other important metabolites (Geitmann and Nebenfähr, 2015). Microtubule polymerisation is the first step for these structures to be put in place. As the unassembled microtubule components are unstable, accessory proteins are needed for microtubule polymerisation to occur. Genes encoding for proteins involved in microtubule polymerisation (*GCP2*, *GCP4*, *AAA9* and *ARPC4*) are found to be enriched in Cluster 7 (Figure 4.8). Once started, polymerisation can occur rapidly, however, this needs to be controlled and stabilised

by other proteins. echinoderm microtubule-associated protein-like 6 (*EML6*), elongator complex protein 2 (*ELP2*) and targeting protein for Xklp2 (*TPX2*) are likely candidates in this process and were found to be enriched within Cluster 3 (Table 4.9). Once microtubules are formed, they are polarised having a plus end and a minus end. Cargo can be transported towards either end using transport proteins called dyneins or kinesin. Dyneins transport cargo towards the minus end, and genes encoding for dyneins were significantly enriched in Cluster 3 (Figure 4.8). Kinesins transport cargo in the opposite direction towards the plus end. Genes encoding kinesins were significantly enriched in both Cluster 3 and 7. A proteomic study of an acidic extremophile *Chlamydomonas* sp. also identified an increase in dyneins and kinesins when the strain was grown in a natural metal rich water (Cid et al., 2010). This species was isolated from the Rio Tinto, which is a highly acidic and metal polluted environment, similar to parts of Parys Mountain, so may share similar mechanisms to *C. acidophila* (Cid et al., 2010). When the same species was exposed to cadmium, scanning electron microscopy showed increasing quantities of vacuoles accumulating within the cytoplasm, with many vacuoles locating towards the periphery (Aguilera and Amils, 2005). The cytoskeleton and increase in dyneins and kinesins could indicate an increase in intracellular organelle trafficking. *C. acidophila* has been shown to accumulate lipid bodies towards the cell periphery in response to metal stresses previously (Spijkerman et al., 2007) as well as an increase in vacuolisation (Díaz et al., 2020). Lipid accumulation is a well-known stress response (Driver et al., 2017), one which we do not appear to see in PM01 chapter 4. However, it is well known that vacuoles can act as metal stores in hyper accumulators (Tian et al., 2011). As such an increase in cellular transport mechanisms could be due to a need for cellular reorganisation in response to increased vacuoles.

Finally, proteins can be post-translationally modified to contain localisation signals, determining where they should be trafficked to within the cell. Cluster 7 contains genes, encoding proteins which can apply such post translational modifications (including *FNTB*, *GIT2*, *PIGW* and *PIGS* (Figure 4.8)), which can be involved in the targeting and incorporation into the plasma membrane (Chiyonobu et al., 2014; Lee et al., 2002; Liu et al., 2010; Premont et al., 2000). If copper elicits a similar response it is likely that the increased expression of these genes in *C. acidophila* may be involved in the structural reorganisation of the cell, including an increase in vacuoles. Díaz et al. (2020) observed vacuolisation in a strain of *C. acidophila* from the Rio Tinto upon exposure to arsenite (As(V)), cadmium and arsenate (As(III)). In fact, this appears to be a common response that has been found in other strains of *C. acidophila* and *C. reinhardtii* upon metal exposure (Nishikawa et al., 2003; Samadani and Dewez, 2018). It is already known that PM01 accumulates and internalises copper from the environment (Dean et al., 2019). It could be that some of this copper is stabilised and stored in storage vacuoles within the cell.

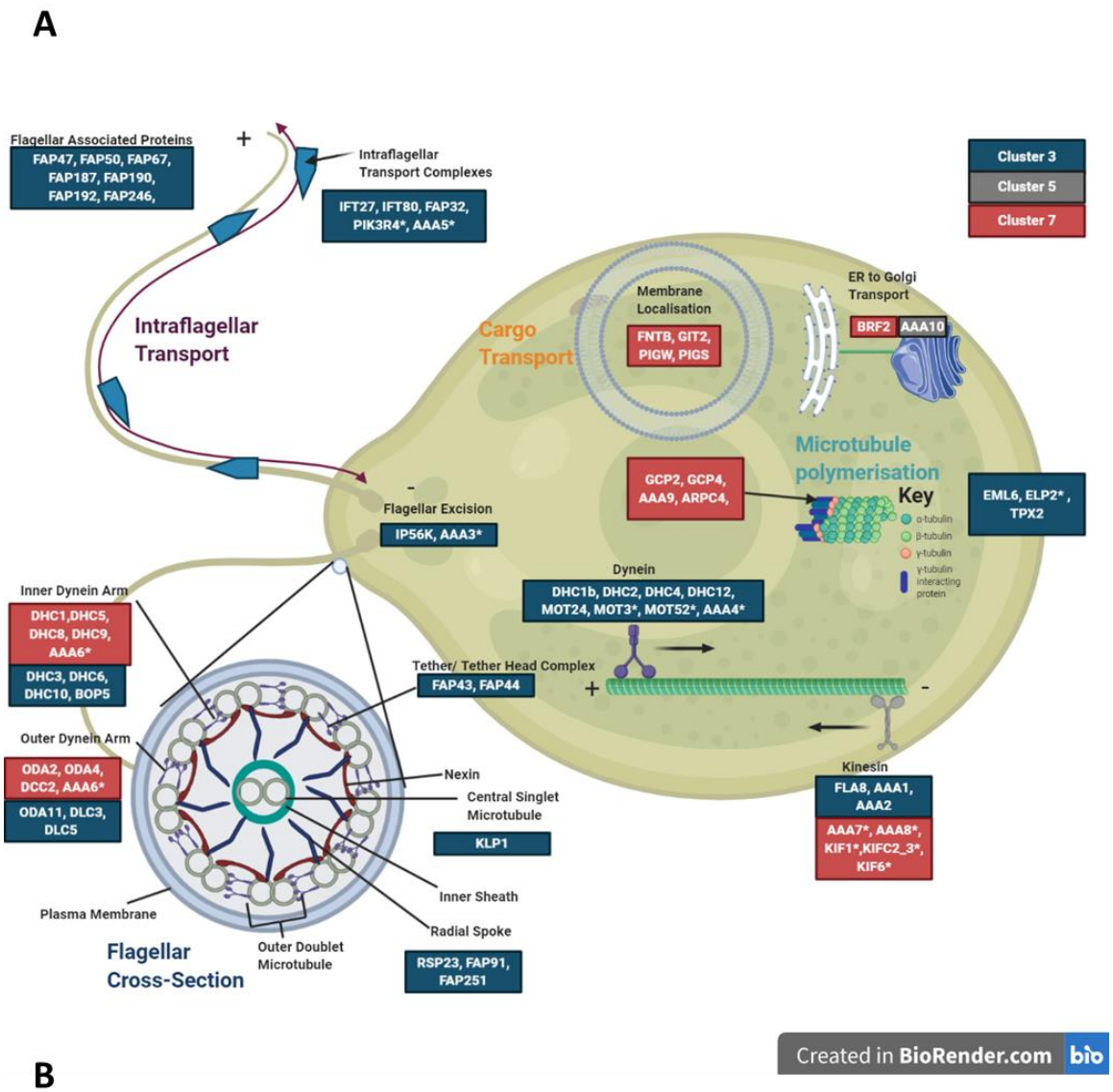

Figure 4.8 (A)Genes involved in the cell movement and intracellular transport of C. reinhardtii and C. acidophila under copper stress taken from significantly enriched GO terms from Cluster 3, 5, and 7 of the heatmap data. Only genes with clear annotation were mapped, some putative genes/ genes with a broad range description are indicated with an asterisk. Gene names starting with AAA had to be ascribed a gene name, specific gene info can be found in supplementary Table 4.9. (B) Average expression plots for each cluster after z-transformation, 0 represents the mean of the 4 treatments and ±1 represents a standard deviation.

			PM01			11/32c		
Gene ID	**Transcript**	**Gene info**	**Control**	**Long Stress**	**Short Stress**	**Control**	**Long Stress**	**Short Stress**
AAA1	Cre19.g750197.t1.1	(1 of 32) 3.6.4.4 - Plus-end-directed kinesin ATPase / Kinesin	447.0	503.8	582.5	407.7	290.4	148.5
AAA10	Cre12.g549950.t1.2	(1 of 2) KOG2887 - Membrane protein involved in ER to `Golgi transport	931.6	787.2	297.2	218.3	290.6	642.8
AAA2	Cre16.g656700.t1.2	(1 of 1) PTHR24115:SF464 - KINESIN-1-RELATED	19.0	32.9	56.1	9.2	21.9	7.0
AAA3	Cre13.g563550.t1.1	(1 of 1) 3.1.3.86 - Phosphatidylinositol-3,4,5-trisphosphate 5-phosphatase / SHIP	229.5	284.0	430.7	417.8	296.1	169.1
AAA4	Cre01.g021950.t1.1	(1 of 1) PF08393//PF12777//PF12781 - Dynein heavy chain, N-terminal region 2 (DHC_N2) // Microtubule-binding stalk of dynein motor (MT) // ATP-binding dynein motor region D5 (AAA_9)	702.1	986.5	968.4	543.9	274.9	87.9
AAA6	Cre14.g627576.t1.1	(1 of 2) PTHR10676:SF136 - DYNEIN HEAVY CHAIN 6, AXONEMAL	1995.1	2454.1	2096.0	1392.0	1220.4	323.5
AAA7	Cre13.g586500.t1.2	(1 of 7) KOG4280 - Kinesin-like protein	355.4	392.1	252.9	244.6	187.4	115.2
AAA8*	Cre13.g568450.t1.1	(1 of 1) PTHR24115:SF535 - KINESIN-RELATED PROTEIN 4	12.3	26.9	25.0	4.7	27.0	2.1
AAA9	Cre07.g345150.t1.2	(1 of 1) 2.3.1.108 - Alpha-tubulin N-acetyltransferase / Tubulin N-acetyltransferase	345.2	343.9	370.9	136.2	140.1	64.9
ARPC4	Cre06.g260800.t1.2	(1 of 1) K05755 - actin related protein 2/3 complex, subunit 4 (ARPC4)	3.4	4.9	2.2	1366.4	743.8	501.8
BFR2	Cre13.g587000.t1.2	(1 of 1) K14782 - protein AATF/BFR2 (AATF, BFR2)	185.6	235.3	152.3	114.0	253.5	47.8
BOP5	Cre12.g520950.t1.1	Flagellar inner dynein arm I1 intermediate chain IC138	413.8	378.8	415.0	842.0	513.9	188.7
DCC2	Cre16.g666150.t1.2	Flagellar outer dynein arm-docking complex protein 2	7113.0	6032.2	5760.1	1725.1	1466.7	477.2
DHC1	Cre12.g484250.t1.1	Flagellar inner arm dynein 1 heavy chain alpha (I1/f alpha)	1041.6	1234.8	1341.6	1873.2	2158.0	495.0
DHC10	Cre14.g624950.t1.1	Flagellar inner arm dynein 1 heavy chain beta	1427.4	1891.5	2384.8	1345.0	1518.7	484.0
DHC12	Cre06.g297850.t1.1	(1 of 1) KOG3595 - Dyneins, heavy chain	1007.8	1756.7	1530.1	825.0	545.7	185.7
DHC1b	Cre06.g250300.t1.2	Cytoplasmic dynein 1b heavy chain (not an inner arm dynein)	904.7	1048.8	2439.0	3034.9	3202.9	701.5

			PM01			11/32c		
Gene ID	**Transcript**	**Gene info**	**Control**	**Long Stress**	**Short Stress**	**Control**	**Long Stress**	**Short Stress**
DHC2	Cre09.g392282.t1.1	Dynein heavy chain 2, inner arm dynein d (monomeric)	1994.2	2327.7	2360.4	1198.8	1240.0	616.8
DHC3	Cre06.g265950.t1.1	Flagellar inner arm dynein heavy chain, novel minor type dynein (monomeric)	970.6	1341.9	1047.6	678.9	534.5	313.3
DHC4	Cre02.g107350.t1.1	Dynein heavy chain 4, novel minor type dynein (monomeric)	1109.0	1568.3	1659.5	872.0	598.1	202.3
DHC5	Cre02.g107050.t1.1	Dynein heavy chain 5, inner arm dynein b (monomeric)	2031.1	2639.7	2179.1	1522.0	1753.3	512.3
DHC6	Cre05.g244250.t1.2	Flagellar inner arm dynein heavy chain, dynein a (monomeric)	2329.3	2871.7	2803.4	960.4	785.6	379.7
DHC8	Cre16.g685450.t1.1	Flagellar inner arm dynein heavy chain, dynein e (monomeric)	1678.0	1798.7	1527.7	1265.6	1338.2	657.2
DHC9	Cre02.g141606.t1.1	Flagellar inner arm dynein heavy chain, dynein c (monomeric)	2570.1	3205.9	3158.2	1418.1	1622.5	687.2
DLC3	Cre12.g528850.t1.1	Flagellar outer dynein arm 16 kDa light chain, LC3	1827.4	1381.2	1633.5	1697.8	1127.0	745.7
DLC5	Cre17.g714250.t1.2	Flagellar outer arm dynein 14 kDa light chain LC5	3782.8	2759.8	4187.1	1227.0	842.1	498.7
ELP2	Cre10.g462750.t1.1	(1 of 1) K11374 - elongator complex protein 2 (ELP2)	354.2	389.4	1747.6	105.4	136.9	45.1
EML6	Cre01.g010880.t1.1	(1 of 2) K18598 - echinoderm microtubule-associated protein-like 6 (EML6)	239.8	280.9	334.5	103.8	89.1	32.1
FAP187	Cre01.g032150.t1.1	Flagellar Associated Protein	481.1	516.5	1001.4	487.1	409.0	108.9
FAP190	Cre01.g004550.t1.2	Flagellar Associated Protein	979.8	1062.9	1110.3	915.0	492.1	431.4
FAP192	Cre10.g440950.t1.2	Flagellar Associated Protein	943.1	1112.3	9749.4	471.5	287.6	106.9
FAP246	Cre14.g618750.t1.1	Flagellar Associated Protein	844.7	998.0	1044.6	480.2	260.3	68.9
FAP251	Cre03.g185650.t1.2	Flagellar Associated Protein	2450.5	2441.3	2446.1	832.0	528.7	172.5
FAP32	Cre05.g241637.t1.1	Intraflagellar transport protein 46	1315.0	1189.7	2056.5	1236.4	1024.3	568.7
FAP43	Cre16.g691440.t1.1	Flagellar Associated Protein (tether, tether head complex)	3509.9	3152.3	3364.0	1003.8	664.3	413.2
FAP44	Cre09.g386736.t1.1	Flagellar Associated Protein (tether, tether head complex)	1394.5	1404.7	1608.9	933.7	701.9	227.8

			PM01			11/32c		
Gene ID	**Transcript**	**Gene info**	**Control**	**Long Stress**	**Short Stress**	**Control**	**Long Stress**	**Short Stress**
FAP44	Cre09.g386736.t1.1	Flagellar Associated Protein (tether, tether head complex)	1394.5	1404.7	1608.9	933.7	701.9	227.8
FAP47	Cre17.g704300.t1.1	Flagellar Associated Protein	1585.7	1797.6	2281.5	1239.2	789.3	208.7
FAP50	Cre14.g612700.t1.2	Flagellar Associated Protein	1843.9	1930.1	1783.1	788.2	543.5	211.4
FAP67	Cre12.g558700.t1.2	Flagellar Associated Protein, nucleoside diphosphate kinase-like	4324.6	3381.7	3841.2	661.5	444.2	202.3
FAP91	Cre07.g330700.t1.2	Flagellar Associated Protein	1579.9	1664.3	1569.3	566.9	436.1	161.7
FBB10	Cre07.g317850.t1.2	Flagellar/basal body protein	1235.8	1229.1	1337.3	200.8	142.7	52.6
FLA8	Cre12.g522550.t1.2	Kinesin motor protein, kinesin-2 (KRP85/95) family	1878.4	1851.7	2488.1	786.2	869.9	189.8
FNTB	Cre14.g612500.t1.2	(1 of 1) K05954 - protein farnesyltransferase subunit beta (FNTB)	208.1	226.9	162.2	544.7	531.8	80.0
GCP2	Cre12.g525500.t1.1	Gamma tubulin interacting protein	124.1	181.5	151.5	53.2	76.3	8.9
GCP4	Cre01.g019150.t1.2	Gamma tubulin interacting protein	76.0	92.8	33.8	55.3	48.8	20.1
GIT2	Cre03.g201664.t1.1	Gaa1-like membrane protein, component of GPI transamidase complex	242.0	208.0	87.3	230.9	169.4	54.4
IFT27	Cre01.g047950.t1.1	Intraflagellar transport protein 27	288.6	197.9	256.1	1619.0	1078.0	401.4
IFT80	Cre03.g204150.t1.2	Intraflagellar transport protein 80	1826.7	1766.4	2698.4	754.1	637.2	304.4
IP56K	Cre16.g681800.t1.1	(1 of 3) 2.7.1.159 - Inositol-1,3,4-trisphosphate 5/6-kinase / IP56K	731.5	697.3	728.6	226.6	66.0	46.4
KIF1,	Cre10.g447500.t1.1	(1 of 1) K10392 - kinesin family member 1 (KIF1)	174.5	172.4	136.5	145.7	101.4	65.5
KIF6	Cre01.g036800.t1.1	(1 of 1) PTHR24115:SF194 - KINESIN-LIKE PROTEIN KIF6	755.3	801.3	458.6	403.1	286.3	158.3
KIFC2_3	Cre05.g233100.t2.1	(1 of 3) K10406 - kinesin family member C2/C3 (KIFC2_3)	36.0	51.2	35.4	6.5	23.2	1.6
KLP1	Cre02.g073750.t1.2	Kinesin motor protein, kinesin-9 (Kif9) family	1240.7	1270.9	1578.3	953.2	729.4	445.7
MOT24	Cre12.g527800.t1.1	Outer dynein light chain, LC10	1408.3	932.0	1090.8	3247.7	1864.1	811.4

			PM01			11/32c		
Gene ID	**Transcript**	**Gene info**	**Control**	**Long Stress**	**Short Stress**	**Control**	**Long Stress**	**Short Stress**
MOT24	Cre12.g527800.t1.1	Outer dynein light chain, LC10	1408.3	932.0	1090.8	3247.7	1864.1	811.4
MOT3	Cre09.g394732.t1.1	Predicted protein	7.2	12.2	133.3	5.9	10.1	0.5
MOT52	Cre05.g237100.t1.2	Predicted protein	15.4	21.1	36.1	42.3	42.0	17.2
ODA11	Cre03.g145127.t1.1	Flagellar outer arm dynein heavy chain alpha	1944.5	2679.2	3616.8	2172.5	2757.4	1083.0
ODA2	Cre11.g476050.t1.2	Flagellar outer arm dynein heavy chain gamma	3815.2	4695.0	4912.9	2677.6	3923.5	1684.0
ODA4	Cre09.g403800.t1.2	Flagellar outer arm dynein heavy chain beta, involved in circadian rhythms	1590.0	2066.8	2400.3	2971.5	4777.8	1744.3
PF20	Cre04.g227900.t1.2	WD-repeat protein of flagellum central pair	2057.2	2144.2	3164.1	415.0	288.9	181.9
PIGS	Cre01.g013400.t1.1	(1 of 1) K05291 - phosphatidylinositol glycan, class S (PIGS)	404.3	372.8	228.2	582.3	349.0	140.7
PIGW	Cre13.g587200.t1.1	(1 of 1) K05283 - phosphatidylinositol glycan, class W (PIGW)	92.5	112.4	74.9	10.7	10.4	0.5
PIK3R4	Cre06.g290500.t1.1	(1 of 1) K08333 - phosphoinositide-3-kinase, regulatory subunit 4 (PIK3R4, VPS15)	470.9	564.6	845.6	406.2	338.2	168.6
RSP23	Cre16.g654300.t1.2	Radial spoke protein 23	1422.5	1504.9	1658.7	2539.9	1477.1	401.1
TPX2	Cre11.g482850.t1.1	(1 of 1) K16812 - targeting protein for Xklp2 (TPX2)	7.8	12.9	32.2	5.6	21.9	8.8

Table 4.9 List of genes present in Figure 4.8 Gene ID is the identifier present on Figure 4.8. The transcript is the C. reinhardtii gene which the paralogues were found to be most similar to and the gene info represents the function. Expression data pulled from the RNA-sea experiment is also shown here. Data is expressed as normalised counts as calculated using DEseq2

Both *C. acidophila* and *C. reinhardtii* have a pair of flagellar used as the main mode of movement. Flagellar are complicated structures (Figure 4.8) and are made up of microtubules spanning the rim of the flagellar, connected by dyneins that allow the microtubules to move over each other, generating movement (Myster et al., 1999). Genes encoding the regulation of both the inner and outer dynein arms connecting the outer microtubules are present in both Cluster 3 and 7. Tether/ tether head complexes allow the attachment of the inner and outer dynein arms to adjacent microtubules (Urbanska et al., 2018). *FAP43* and *FAP44* are both associated with these tether complexes and are enriched in Cluster 3. The radial spokes which extend from the outer microtubules towards the central microtubule pair may also change in response to copper stress as genes involved in their synthesis and regulation appear in Cluster 3. Finally, KLP1, also found enriched in Cluster 3, which is localised at the central singlet microtubule is also differed in expression under the copper treatments.

Beauvais-Flück et al. (2019) also found a small number of motility genes that were differentially expressed under a copper stress in *C. reinhardtii* that, perhaps unsurprisingly, were absent in the macrophyte *Elodea nuttallii*. Toxic metal concentrations have been shown to inhibit motility in many species of diatoms, green algae and bacteria (Gupta and Agrawal, 2007; Ivošević DeNardis et al., 2019; Khare et al., 2020; Pandey and Bergey, 2016). Interestingly, various metal stresses were not found to reduce motility in the extremophile *Euglena gracilis* (Danilov and Ekelund, 2001). It is worth noting that the copper stress used in this study was 65 times weaker than the concentration of copper exposed to PM01. It is possible that at higher concentrations used here we would see a decrease in motility. Mutants in genes involved in flagellar structure such as *ODA2*, *DHC1*, *KLP1*, *FAP43* and *FAP44*, all present in the data set, caused reduction in motility or complete motility loss in *C. reinhardtii* (Liu et al., 2008; Myster et al., 1999; Urbanska et al., 2018; Yokoyama et al., 2004). It is possible that copper could denature proteins such as DHC1, reducing function and inhibiting motility. This could explain why, under copper conditions, these genes are more highly expressed. As PM01 was found in a highly stressful environment, it would be disadvantageous for it to lose all motility under such conditions. Therefore, it may have adapted different mechanisms to maintain flagellar function, without causing any further harm to the cell. Finally, flagellar excision can occur for many reasons, one of them being environmental stresses (Quarmby, 2004). Two genes involved in this process, *IP56K* and *AAA3* were found to be present in Cluster 3. Various stresses, including excess metal are known to induce deflagellation (the excision of the flagellar), which would have a profound effect on motility (Quarmby, 2004). Copper has also been shown to mediate flagellar excision up to 64 µg/L, although no higher treatments were tested, this is 76 times less than the copper treatment that was applied for *C. reinhardtii* (4.87mg/L) (Garvey et al., 1991).

ROS and copper stresses have been seen to induce deflagellation in *C. reinhardtii* (Garvey et al., 1991; Ma et al., 2020), therefore it is not a stretch to imagine PM01 may also be prone to deflagellation upon an immediate copper stress. Any genes involved in flagellar maintenance or regrowth therefore, could increase an organisms fitness under copper stress. Intraflagellar transport complexes move up and down the flagellar transporting cargo for energy, maintenance, and flagellar growth. IFT-A and dynein complexes are linked with retrograde transport whilst IFT-B and kinesin

are linked with anterograde transport (Huet et al., 2014). Five intraflagellar transport complex genes were found to be enriched in Cluster 3: *IFT27, IFT80, FAP32, PIK3R4* and *AAA5*. While the exact role of *IFT27* is unclear, one study has suggested that it is crucial for flagellar maintenance and cell cycle control such that knockdown lines can lead to flagellar excision (Qin et al., 2007). A more recent study showed more robust evidence that IFT27 could play a role in exporting the BBsome, an octameric protein crucial for homeostasis out of the cilia and knockdown mutants gave rise to an increase in signalling molecules accumulating within the flagella (Dong et al., 2017). In contrast, it appears that IFT80 is required for ciliogenesis (Taschner et al., 2018). This could highlight a key adaptation between PM01 and *C. reinhardtii,* as under short term copper stress conditions these genes are more lowly expressed in *C. reinhardtii*, while in PM01 these genes are more highly expressed. This could suggest that although the copper shock may cause PM01 to deflagellate, the cells allow motility to return quickly.

4.4.5 Photosynthetic Response to Copper

Three clusters were found to have significantly enriched genes corresponding to photosynthetic processes that differed in expression under different copper treatments between the two species. Both Clusters 4 and 5 show that relative gene expression is much higher in the short-term copper stress for *C. reinhardtii*, whilst the long-term treatment and both treatments for *C. acidophila* were at the average baseline or under expressed. Cluster 6 shows that all treatments had high relative expression apart from the short-term copper stress for *C. acidophila* which showed very little expression when compared to the other treatments.

When light hits the light harvesting complex (LHC) for PSII the energy capture process begins. Figure 4.9 shows two genes related to the LHC were found in the transcriptomic data set. LHCB7 and LHCB4 were both found in Clusters 5 and 6, respectively. The energy is then transferred from the LHC to the PSII reaction centre where water is split, generating hydrogen and passing an electron onto plastoquinone. The electrons are then passed from plastoquinone to cytochrome b_6f complex (cyt b6f), facilitating two more hydrogen ions to be transferred into the thylakoid. This is the last set of hydrogens to be transferred to the thylakoid in the electron transport chain. ATP synthase can then use this high concentration of hydrogen ions in the thylakoid to drive ATP synthesis by allowing hydrogen ions into the stroma. Cluster 5 contains 3 genes associated with ATP synthase. Copper was found to inhibit activity at the oxidising side of PSII, as seen by a decrease in chlorophyll a fluorescence in the diatom *Phaeodactylum tricornutum*. The authors suggested that this could be due to an inhibition of PSII reaction centres (Cid et al., 1995). Interestingly, Laporte et al. (2020) found that a microalga that grows in copper polluted waters off northern Chile, *Ulva compressa*, increased expression of many genes involved in photosynthesis in response to copper including genes involved in PSII, LHCII and cyt b6f. In my data, these genes seem to be more highly expressed, in respect to their controls, in the *C. reinhardtii* data set. Although Laporte et al. (2020) say that this alga is highly copper tolerant, they suggest that it is only capable of growing up to 50 µM, and for the experiment it was stressed with only 10 µM, a much lower concentration used for even the long-term copper stress used for the *C. reinhardtii* strain in this study. Considering that the short term PM01 treatment had the lowest relative

c

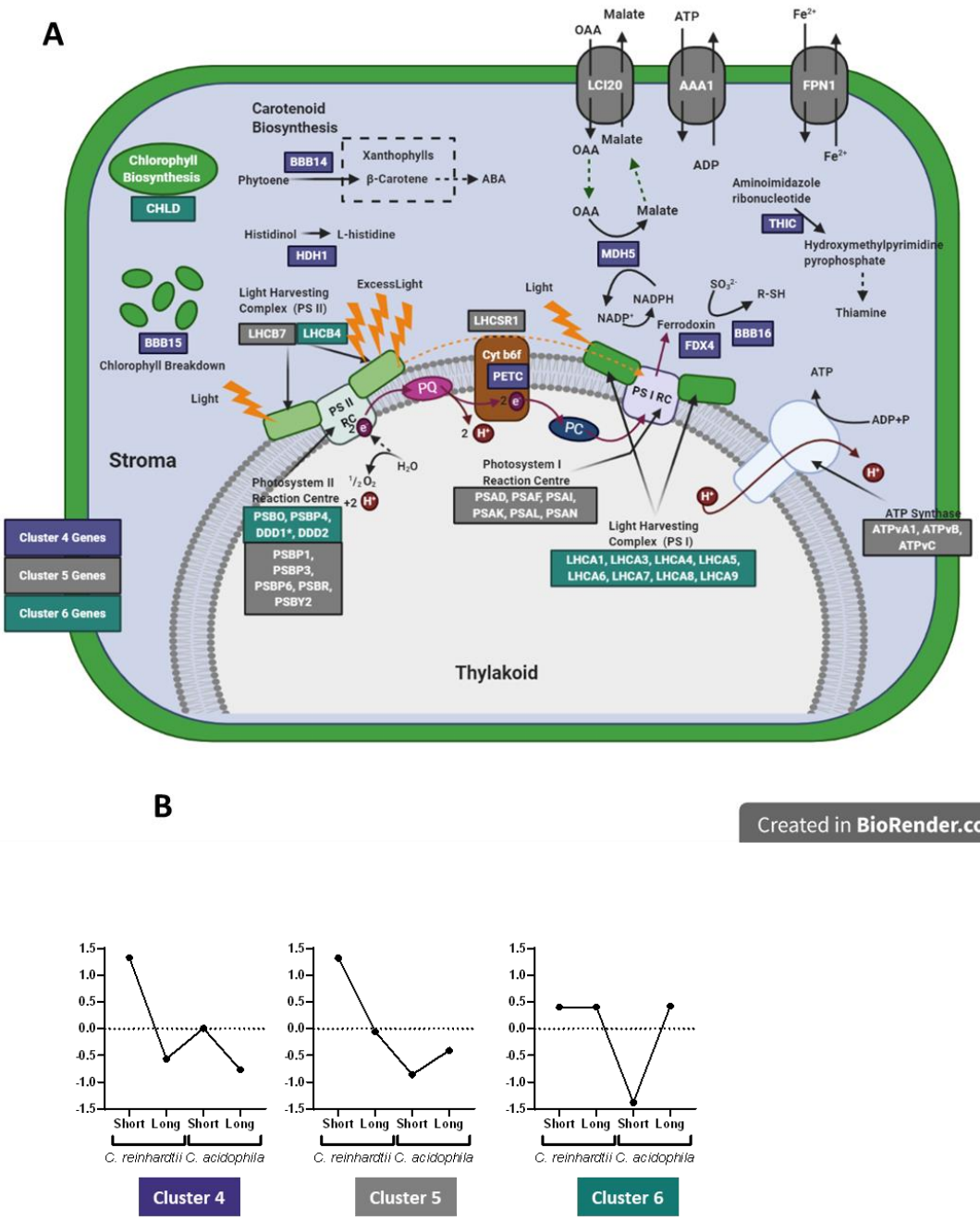

Figure 4.9 Genes involved in photosynthesis of C. reinhardtii and C. acidophila under copper stress taken from significantly enriched GO terms from Cluster 4, 5 and 6 of the heatmap data. Only genes with clear annotation were mapped, some putative genes/ genes with a broad range description are indicated with an asterisk. Gene names starting with DDD had to be ascribed a gene name, specific gene info can be found. ABA: abscisic acid, OAA: oxaloacetate (B) Average expression plots for each cluster after z-transformation, 0 represents the mean of the 4 treatments and ±1 represents a standard deviation.

Gene ID	Transcript	Gene info	PM01 Control	PM01 Long Stress	PM01 Short Stress	11/32c Control	11/32c Long Stress	11/32c Short Stress
BBB14	Cre08.g358538.t1.1	Putative chloroplast lycopene beta cyclase	999.7	877.0	950.7	1909.2	1813.6	5039.9
BBB15	Cre13.g583050.t1.1	Pheophorbide a oxygenase, Rieske iron-sulfur cluster protein	361.3	363.7	493.0	42.3	60.7	331.5
BBB16	Cre16.g693202.t1.1	(1 of 1) K00392 - sulfite reductase (ferredoxin) (sir)	5862.9	6994.8	15564.4	66.6	163.3	2070.1
FDX4	Cre07.g334800.t1.2	Ferredoxin	2472.1	2514.3	6431.4	0.3	0.0	2.7
HDH1	Cre02.g077350.t1.2	Histidinol dehydrogenase	3348.6	3089.7	8468.1	1663.6	2616.4	40177.4
MDH5	Cre09.g410700.t1.2	NADP-dependent malate dehydrogenase, chloroplastic	2663.1	1971.4	2738.1	12271.1	10778.0	43202.9
PETC	Cre11.g467689.t1.1	Rieske iron-sulfur subunit of the cytochrome b6f complex, chloroplast precursor	63733.2	56671.6	77652.1	158239.8	93594.9	282781.0
THIC	Cre05.g240850.t1.2	Hydroxymethylpyrimidine phosphate synthase (thiamine/vitB1 biosynthesis)	1254.3	1100.7	2196.0	1411.7	2452.1	3291.9
AAA1	Cre08.g358526.t1.1	Plastidic ADP/ATP translocase	9277.0	11099.5	10353.3	17019.7	19172.0	39636.8
ATPvA1	Cre10.g461050.t1.2	Vacuolar ATP synthase subunit A	5615.0	5771.7	3392.7	1850.9	3619.9	14713.1
ATPvB	Cre02.g076350.t1.2	Vacuolar ATP synthase subunit B	6088.4	6160.1	4822.7	2917.9	3436.3	5847.2
ATPvC	Cre06.g250250.t1.2	Vacuolar ATP synthase subunit C	4051.4	3959.5	1967.7	446.1	701.1	965.1
FPN1	Cre16.g687000.t1.1	(1 of 1) K14685 - solute carrier family 40 (iron-regulated transporter), member 1 (SLC40A1, FPN1)	436.3	409.2	595.3	131.6	451.0	359.6
LCI20	Cre06.g260450.t1.2	2-oxoglutarate/malate translocator	2892.8	2561.1	3643.7	164.4	562.2	2302.4
LHCB7	Cre02.g110750.t1.2	Chlorophyll a/b binding protein	1325.5	1154.4	568.5	239.8	236.8	467.0
LHCSR1	Cre08.g365900.t1.2	Stress-related chlorophyll a/b binding protein 1	18698.6	15363.2	47783.0	104.3	673.3	1119.1

Gene ID	Transcript	Gene info	PM01 Control	PM01 Long Stress	PM01 Short Stress	11/32c Control	11/32c Long Stress	11/32c Short Stress
PSAL	Cre12.g486300.t1.2	Photosystem I reaction center subunit XI	79316.5	64274.6	37494.7	10646.6	8480.2	20105.7
PSAN	Cre02.g082500.t1.1	Photosystem I reaction center subunit N, chloroplastic	36206.4	31338.3	16192.4	72404.0	48892.4	121471.6
PSBP1	Cre12.g550850.t1.2	Oxygen-evolving enhancer protein 2 of photosystem II	62037.2	54213.5	24647.7	37451.5	25818.7	63997.9
PSBP3	Cre12.g509050.t1.1	OEE2-like protein of thylakoid lumen	7083.4	6421.0	4111.5	2381.3	1533.0	4499.7
PSBP6	Cre07.g328200.t1.2	Lumen targeted protein	1414.0	1042.0	652.9	1069.4	851.9	1550.5
PSBR	Cre06.g261000.t1.2	10 kDa photosystem II polypeptide	49882.4	36783.2	24972.7	186960.6	123565.4	409778.9
PSBY2	Cre10.g452100.t1.1	Ycf32-related polyprotein of photosystem II	31207.9	27107.3	22117.7	6088.1	4049.3	10114.8
CHLD	Cre05.g242000.t1.2	Magnesium chelatase subunit D	3669.6	3792.5	1751.6	5053.0	5305.2	7592.4
DDD1	Cre13.g564050.t1.1	(1 of 1) PTHR37764:SF1 - MOG1/PSBP/DUF1795-LIKE PHOTOSYSTEM II REACTION CENTER PSBP FAMILY PROTEIN	695.4	641.2	192.0	536.0	369.4	765.9
DDD2	Cre03.g198850.t1.2	(1 of 2) PTHR31407:SF18 - PSBP DOMAIN-CONTAINING PROTEIN 4, CHLOROPLASTIC	4017.6	3199.9	1759.8	1246.1	547.1	632.2
LHCA1	Cre06.g283050.t1.2	Light-harvesting protein of photosystem I	122553.4	108420.6	38592.7	78966.0	69533.8	91260.2
LHCA3	Cre11.g467573.t1.1	Chlorophyll a/b binding protein of photosystem I, type III	57121.5	48079.3	18835.7	67795.1	40320.1	74569.1
LHCA4	Cre10.g452050.t1.2	Light-harvesting protein of photosystem I	3414.7	3044.2	1192.2	14350.7	14287.4	14244.8
LHCA5	Cre10.g425900.t1.2	Light-harvesting protein of photosystem I	80338.6	76957.6	20749.2	28661.8	21439.1	19513.9
LHCA6	Cre06.g278213.t1.1	Light-harvesting protein of photosystem I	36467.0	29323.3	14245.9	16165.6	10729.5	14141.4
LHCA7	Cre16.g687900.t1.2	Light-harvesting protein of photosystem I	75984.7	63887.5	26905.8	56277.4	48176.2	46217.3
LHCA8	Cre06.g272650.t1.2	Light-harvesting protein of photosystem I	77151.7	68693.2	35951.0	33423.6	19690.0	30713.7
LHCA9	Cre07.g344950.t1.2	Light-harvesting protein of photosystem I	35638.4	30902.6	15469.3	72363.6	54500.2	51253.0
LHCB4	Cre17.g720250.t1.2	Chlorophyll a/b binding protein of photosystem II	45942.9	38205.6	9004.3	40246.1	35075.7	55209.5

Table 4.10 list of genes present in Figure 4.9, the Gene ID is the identifier present on Figure 4.9. The transcript is the C. reinhardtii gene which the paralogues were found to be most similar to and the gene info represents the function. Data is expressed as normalised counts as calculated using DEseq2

expression, it is likely that copper exerts an excess strain on the cells which could be exacerbated by photosynthesis. The oxidative stress caused by copper could be further impacted if the photosynthetic apparatus is inhibited and/or malfunctioning. Copper has been shown to displace Fe^{2+} from the primary quinone acceptor in PSII, leading to the formation of radicals (Jegerschold et al., 1995). A short-term copper adaptation of PM01 could be to temporarily reduce its photosynthetic capabilities, allowing ample time for the cell to neutralise any excess ROS and free ionic copper causing damage to the cell before it can resume to a more normal growth condition.

However, this is not all the energy that chloroplasts are able to extract from photosynthesis. PETC is a gene associated to the cyt b6f complex and was found in Cluster 4. The electron is then passed onto plastocyanin (PC) which transfers the electron to the PSI reaction centre. This can then utilise energy captured from the LHCs for PSI to transfer the electron the ferredoxin. In my data set Cluster 5 was significantly enriched with six genes associated with the PSI reaction centre, whilst Cluster 6 was significantly enriched with eight genes associated to the LHC of PSI. Cluster 5 also contained the gene *LHCSR1* which is able to directly transfer excess energy from LHC PSII to the PSI reaction centre. Cabrita et al. (2018) found evidence to suggest that *P. tricornutum* also shifted preference from PSII to PSI under copper stress. Copper has been found to increase the amount of light needed to stimulate PSI (Lysenko et al., 2020). PSI appears to be a more robust system, Prasad & Zeeshan (2005) also found that both UV-B and cadmium treatments had a strong inhibitory effect on PSII whilst PSI was least affected. A switch to PSI could be beneficial in this circumstance as less energy may need to be dissipated, reducing the ROS stress on cells. Additionally, Cluster 4 also contains *FDX4* which encodes ferredoxin. FDX4 has been suggested to play multiple roles within the cell, playing a part in glycolysis, but also may help protect the cell from ROS (Peden et al., 2013). Ferredoxin can reduce $NADP^+$ into NADPH, which can then be used as an energy store. Cluster 4 also contains the transcript *MDH5,* MDH5 converts oxaloacetate into malate by oxidising NADPH. Massoud et al. (2019) found an increase in the activities of similar NADP reducers, such as MDH, in pea shoots exposed to copper. They proposed that the reduced NADPH could be used for other redox reactive enzymes such as glutathione and thioredoxin-reductases to quench other ROS present in cells. In the model proposed here it would seem that under a long-term copper stress, transcripts for these genes are less abundant than the short-term copper stresses. If indeed, MDH is used to create a pool of reduced NADPH for redox reactive enzymes, this would fit in with the earlier data that also showed a reduction in the ROS stress response under a long term copper stress (Figure 4.5). Malate can then be exported out of the chloroplast by LCI20, which was also enriched within Cluster 5. Ferredoxin can also be used to reduce hydrogen sulphide into sulphite utilising the electron transport system (Schmidt and Trebst, 1969). A gene coined BBB16 encodes a ferrodoxin sulphite reductase which can catalyse such a reaction and was enriched within Cluster 4.

Chlorophyll are the green pigments which absorb the light in the light harvesting complexes for photosynthesis to occur. In Cluster 6 the gene CHLD was found enriched in the data set which is involved in chlorophyll biosynthesis. CHLD is one of only a few transcripts involved in chlorophyll biosynthesis, others include CHLG, CHLM and CAO. Several studies have found that chlorophyll biosynthesis genes were found to decrease in comparison to the control under various stresses such as ketoprofen and ZnO nanoparticles (Wang et al., 2020; Wang et al., 2016). When we look at these genes in isolation (Figure 4.10), all genes except CHLM were significantly reduced in the short-term

copper treatment when compared to the control for PM01. In stark contrast, all genes, except for CHLG, were increased under the short-term copper treatment compared to the control for *C. reinhardtii*. Opposingly, in Cluster 4 we saw the gene pheophorbide a oxygenase, which was assigned the ID BBB15, is involved in the breakdown of chlorophyll. In the same theme of pigments, we also see lycopene beta cyclase enriched within Cluster 4. Lycopene beta cyclase is involved in the carotenoid biosynthesis pathway converting phytoene into β-carotene. Cluster 4 also contains two other genes which are located in the chloroplast. HDH1 which converts histidinol into L-histidine and THIC, which is involved in the thiamine biosynthesis pathway. The ability to inhibit photosynthesis in the early stages of a harsh copper stress is an adaptive trait that has allowed PM01 to adapt to elevated copper levels. Genes involved with the light harvesting complexes, reaction centres and chlorophyll synthesis are down regulated under a short-term copper stress in PM01. For *C. reinhardtii*, these gene transcripts remain at a relatively high abundance and are even elevated in some circumstances. It is likely that PM01 is able to reduce its photosynthetic capabilities until it is able to quench the excess free copper and ROS, preventing further damage by impaired photosystems, providing the cell a better capability to deal with the stress. As well as the LCI20 transporter mentioned earlier, Cluster 5 also contains other transporters on the chloroplast membrane. An ADP/ATP translocase, assigned AAA1, facilitates the antiport of ADP and ATP in and out of the chloroplast. We also see an iron transporter FPN1 which transports Fe^{2+} in and out of the chloroplast.

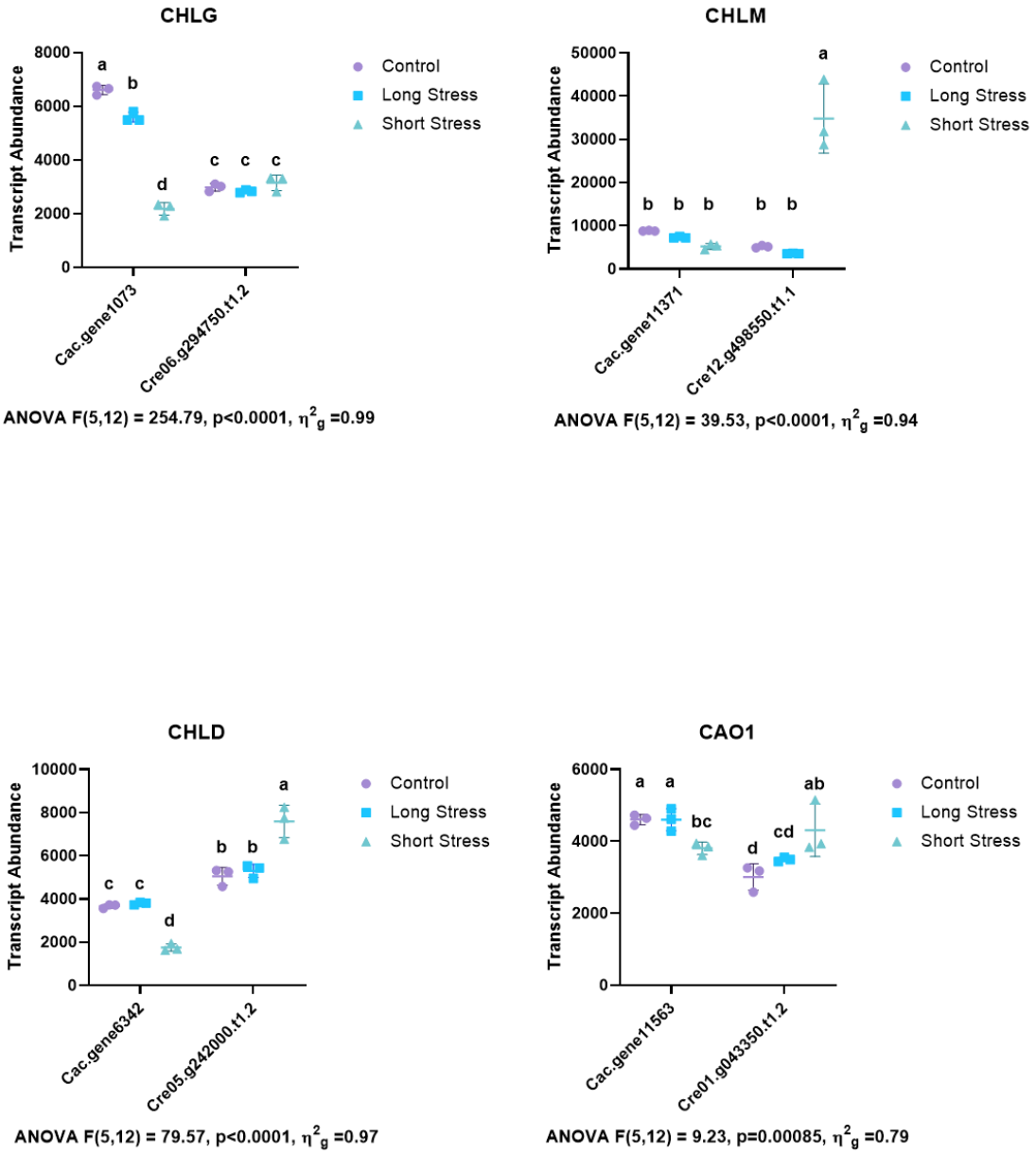

Figure 4.10 transcript abundance shown as normalised counts, calculated using DEseq2, of genes related to chlorophyll synthesis for both C. acidophila and C. reinhardtii under a short and long term copper stress. Treatments were tested for significance across both species and all treatments using a one-way ANOVA, Tukey's post-hoc test were used for pairwise comparisons to test for significant differences between treatments. Letters represent different groups of significance.

4.4.6 Metal Homeostasis and Transport Genes

In addition to examining genes by cluster analysis, well-known genes involved in metal transport and copper homeostasis were also examined individually, with the assumption that they may also play an important role in the copper response. The first set of transporters investigated were the copper transport proteins (CTP), part of the HMA-like (P-type ATPase) class transporters. These are a very interesting set of candidate genes that may explain some of the copper adaptation of PM01. CTP3 standouts out the most of the two transporters identified (Figure 4.11). The lowest *CTP3* transcript abundance of all the PM01 treatments, interestingly the long-term stress (5757.8 NC ±329.1), was still significantly higher than the control (245 NC ±20) long-term (393.9 NC ±16.8) and short-term (2485.5 NC ±845) copper stresses in *C. reinhardtii*. The transcript abundance of *CTP3* for the control in PM01 (7009.8 NC ±286.4) is expressed 28.7 times higher than the control in *C. reinhardtii*. It was even expressed almost 3 times higher than the short-term copper stress in *C. reinhardtii*, which had the highest abundance of the transcript for all its treatments. The potential importance of this gene is even more evident when you look at the short-term copper stress for PM01 where the CTP transcript increased to 14160.5 ±349, 2 times higher than its control and nearly 58 times higher than the *C. reinhardtii* control. The other isoform, CTP1 does not seem to be as important for copper adaptation. The level of transcript abundance for the control treatments for both species and the long-term copper treatment for PM01 did not significantly differ from each other. Moreover, expression levels for both short term copper treatments were significantly higher than their controls (PM01- 2.6 times, *C. reinhardtii*- 3.3 times). The CrCTP3 expression under short term copper stress was only 1.19 times higher than CaCTP1 under the same condition.

CTP3 is predicted to be involved in the efflux pathway to facilitate the removal of Cu^{1+} from the cell (Blaby-Haas and Merchant, 2012). This could explain why we see such high constitutive levels of expression, even in the control, rising significantly under a short-term copper stress for PM01. Although it has been shown previously that copper can accumulate within PM01 (Dean et al., 2019), excreting excess cellular copper will nonetheless be beneficial to the cells. CTP3 therefore, may be an interesting target for future knockout lines, which could improve the copper sequestration and bioremediation potential of PM01, should the cell be able to survive an increase in cellular copper content. CTP1 on the other hand, is thought to be located in the Golgi network, possibly providing copper to FOX1 an iron transporter, but may also be involved in copper secretion (Blaby-Haas and Merchant, 2012). However, if this is the case, my data seems to suggest that this plays a much lesser role in copper homeostasis of the cell. HMA1 presents an interesting comparison between the two species. Neither of the two species show a difference in expression between the control and long-term copper stresses. However, both the control and long-term stress HMA1 abundance were significantly higher in PM01 than the *C. reinhardtii* treatments. Where the species mainly differ is in the short-term treatments. *C. reinhardtii* sees an over 2-fold increase in expression when compared to the control (959.1 NC ±60.9 to 2405.8 NC ±157.9). In contrast, the HMA1 expression levels in the short term copper stress in *C. reinhardtii* actually decrease almost 1.8-fold (1586.7 NC ±80.8 to 890.9 NC ±57.8) from the control. There has been no study of the *C. reinhardtii* HMA1, however, an Arabidopsis HMA1 was found on the chloroplast envelope and thought to facilitate the transport of copper into the chloroplast (Seigneurin-Berny et al., 2006). If the *C. reinhardtii* and PM01 HMA1 isoforms have a similar function to their Arabidopsis orthologue, it could explain why a down

regulation in the short-term copper stress is seen for PM01 as the cell may want to protect the photosynthetic apparatus from excess copper causing further ROS damage.

Another class of copper transporter that was examined were from the CTR family. CTRs are high affinity copper transporters that take up copper into the cell in the Cu^{1+} form. The copper can then be sequestered by other proteins and molecules within the cytoplasm (Blaby-Haas and Merchant, 2012). For the PM01 genes it was unclear which CTR genes were orthologous to the *C. reinhardtii* genes. As such all the CTR genes were grouped together and analysed within the species. *C. reinhardtii* CTR1 and CTR2 (Cre13.g570600.t1.2 and Cre10.g434350.t1.1 respectively) are known to be located at the plasma membrane and involved in copper uptake in response to copper deficiency (Page et al., 2009), however, none of these transcript levels change in response to excess copper, suggesting similar levels of copper uptake may be taking place. Conversely, PM01 sees two CTRs expressed at relatively high levels (Cac.gene5456 and Cac.gene5454). Under both copper stresses these transcript levels drop to a near the baseline level (Cac.gene5456) or roughly a third of the control (Cac.gene5454) (Figure 4.12). That could suggest that these are located at the plasma membrane and are also involved in copper uptake. What is interesting is that although the PM01 transcripts are decreased in expression, they are still equivalent or higher than the *C. reinhardtii* transcripts. This could mean that similar or higher levels of copper are being taken up into the cell, suggesting that similar, or higher levels of copper may be taken up in PM01 compared to *C. reinhardtii* and the cells also have a better capability of dealing with the stress. It is important to note that this is speculative as transcript abundance may not necessarily equate to an increase in protein and especially does not relate to protein activity. Another reason for the PM01 controls being so highly expressed could be that the cell has adapted to high cellular copper levels and that it may be experiencing some form of copper deficiency with no added copper. The remaining CTRs for both species are both relatively lowly expressed and appear relatively unchanged by the copper treatments.

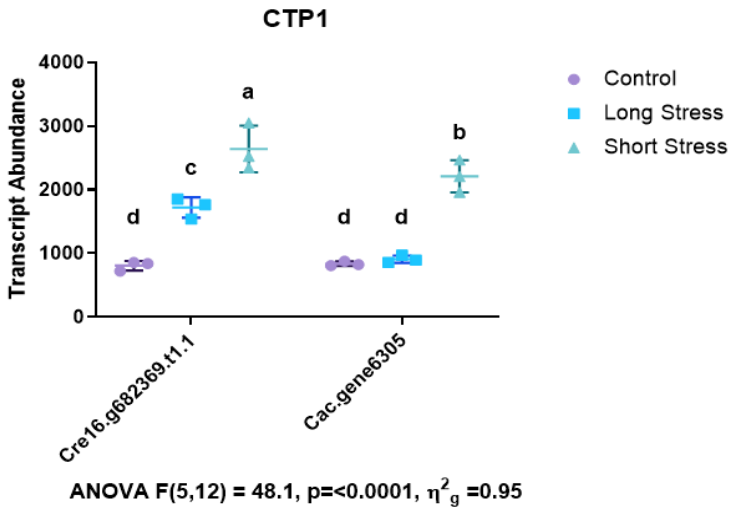

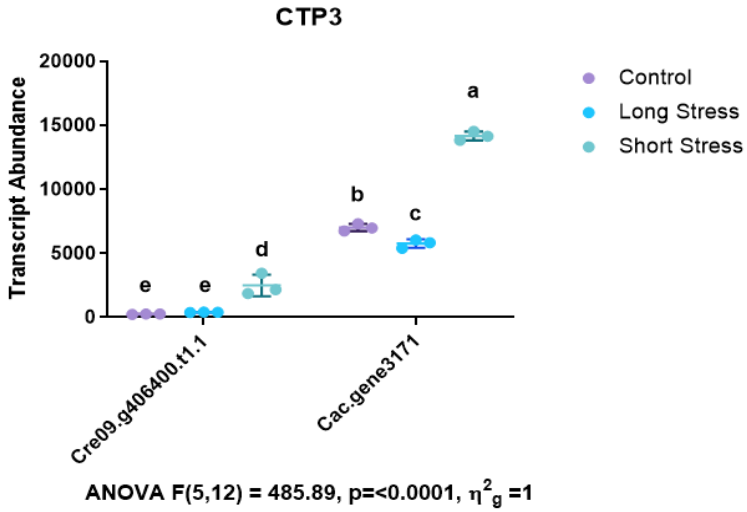

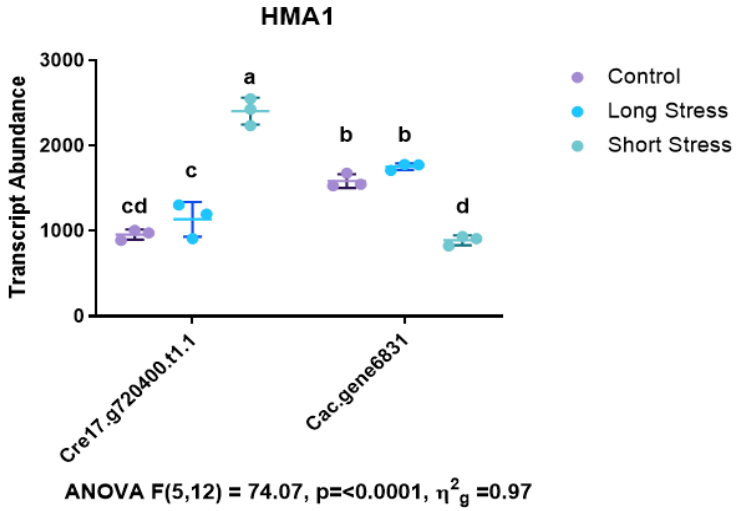

Figure 4.11 transcript abundance shown as normalised counts, calculated using DEseq2, of genes related to metal transporters for both C. acidophila and C. reinhardtii under a short and long term copper stress. Treatments were tested for significance across both species and all treatments using a one way ANOVA, Tukey's post-hoc test were used for pairwise comparisons to test for significant differences between treatments. Letters represent different groups of significance.

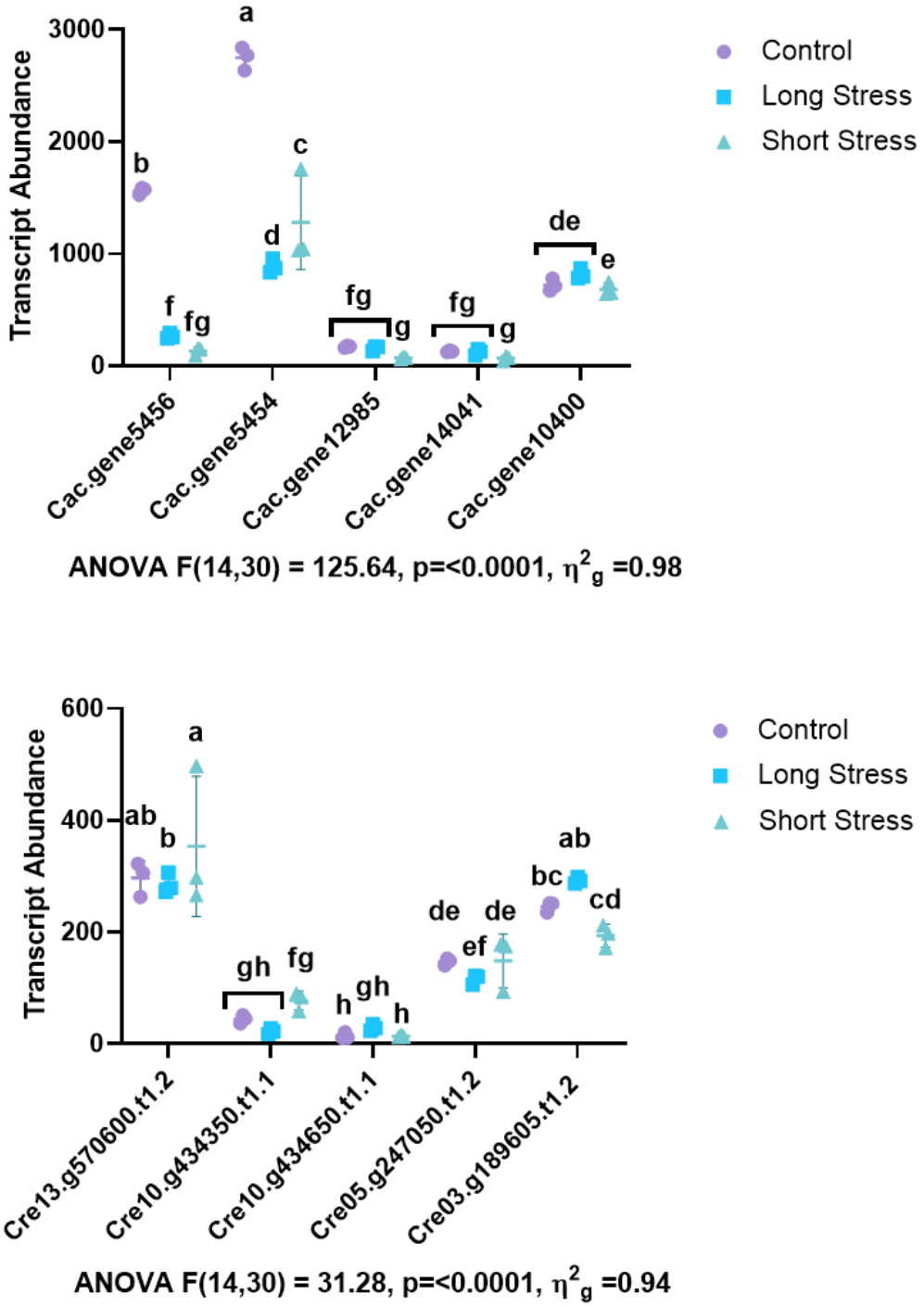

Figure 4.12 transcript abundance shown as normalised counts, calculated using DEseq2, of genes related to CTR genes for both C. acidophila (A) and C. reinhardtii (B) under a short and long term copper stress. Treatments were tested for significance all CTR genes and all treatments using a one way ANOVA, Tukey's post-hoc test were used for pairwise comparisons to test for significant differences between treatments. Letters represent different groups of significance. CTRs had to be compared within species as genes appear to diverged to identify any paralogues across the species.

Excess copper has been shown to cause iron deprivation, possibly through competition of metal transporters (Pätsikkä et al., 2002). For this reason, I decided to look at known iron transporters to see if there were any effects of copper on the expression of iron transporters. The first gene, FTR1 is localised to the plasma membrane and form a complex with FOX1 (also listed) and convert Fe^{2+} to Fe^{3+} for uptake (Blaby-Haas and Merchant, 2012). Both species show a similar expression pattern for both FTR1 and FOX1. PM01 shows the highest expression under a short-term copper stress for both genes, whilst the long-term treatment is slightly *C. reinhardtii* shows the highest expression level under the long-term copper stress for both genes with expression increasing over 5-fold and 12-fold for FTR1 and FOX1 respectively. It would appear that whilst *C. acidophila* may experience a short-term iron deficiency under copper stress, *C. reinhardtii* experiences a much harsher iron deficiency over the long-term when exposed to copper. Terzulli & Kosman (2010) have shown that copper deficiency has also led to iron deficiency in *C. reinhardtii.* To my knowledge there are few studies that have looked at the effects of excess copper on iron deficiency, the only notable exception is a study in which the addition of iron was enough to alleviate phenotypic observations of copper stress (Pätsikkä et al., 2002). Another study has also found that lead and copper both share a common uptake transporter in *C. reinhardtii* suggesting that competition for space in metal transporters and non-specific uptake can occur (Sánchez-Marín et al., 2014). These results would seem to suggest that *C. reinhardtii* experiences some form of iron deficiency under a long-term copper stress. This is further backed up when we look at the iron specific transporters FEA1 and FEA2 (Figure 4.13). Again, we see a similar pattern in that the highest level of expression was seen in the long-term copper stress. FEA1 transcription levels increased from 0.898 ±.915 for the control up to 965.3 ±299.5 for the control and 16.3 ±4.6 for the control to 1737.2 ±407.4 for the long-term stress for FEA2. Unfortunately, no FEA transcripts could be identified for PM01 for comparison. FEA1 and FEA2 are shown to have a high affinity uptake for iron. Additionally, they are not transcriptionally regulated by other metals such as zinc and manganese, and with importance to this study, copper (Allen et al., 2007). This suggests that the difference in regulation we are seeing in the data presented, is not perhaps directly regulated by the copper stress, but perhaps an additional iron deficiency stressed imposed upon the cells. Although trace metals can be toxic at elevated levels, some heavy metals are still more toxic than others. *E. gracilis* has been shown to increase its survivability against cadmium by accumulating zinc (Sánchez-Thomas et al., 2016). As iron is less redox active than copper, accumulating iron could prove a better strategy of surviving copper toxicity, than allowing higher levels of copper into the cell. It is very interesting that PM01 only upregulates genes related to iron deficiency in the short-term and not to a high extent as seen in *C. reinhardtii.* This could suggest that it has either an alternative iron uptake mechanism, due to occurring in naturally high copper concentrations, or alternate mechanisms to deal with iron deficiency. Whatever, the strategy, it could prove an interesting target for further study into alleviating iron deficiency in organisms.

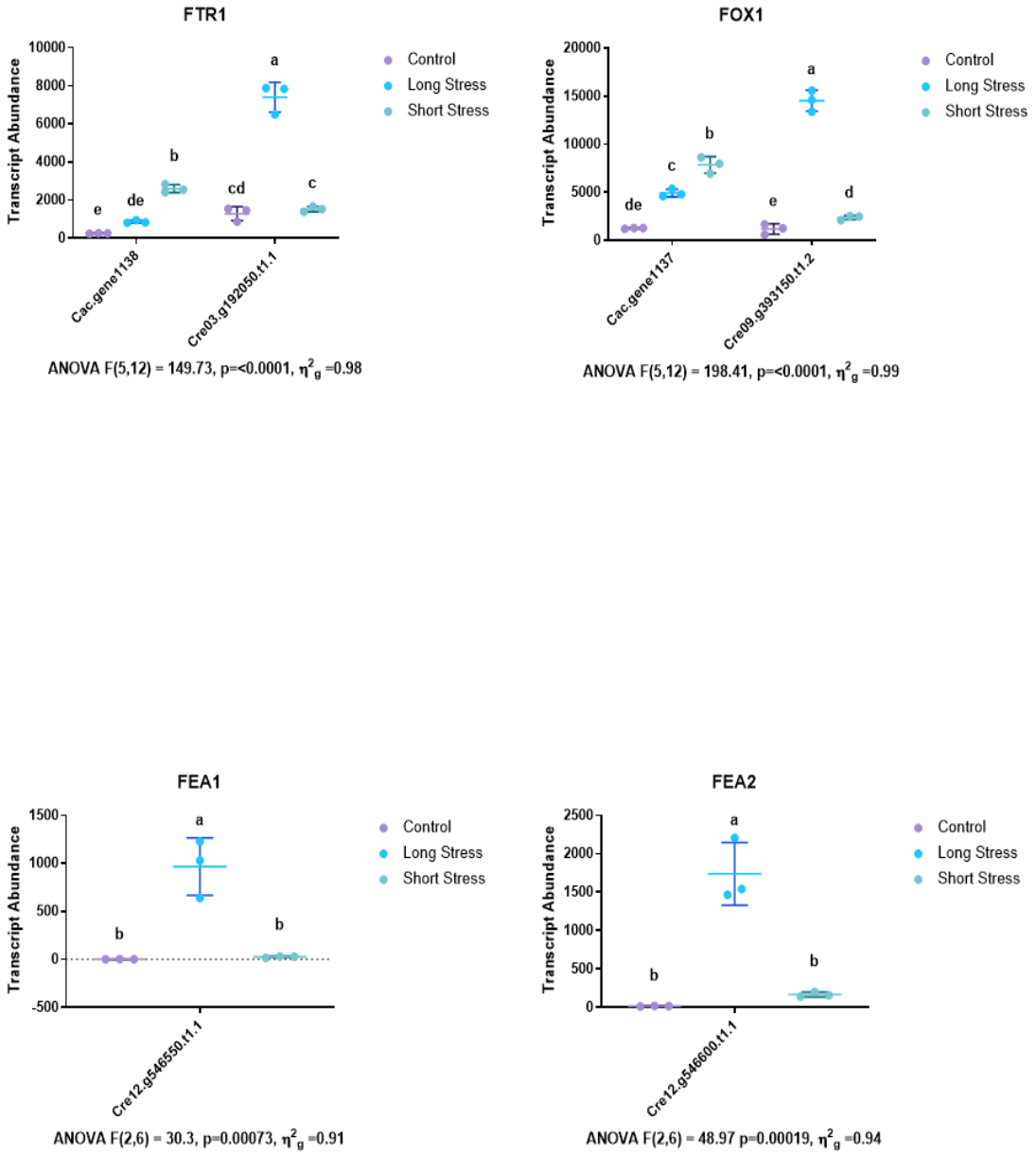

Figure 4.13 transcript abundance shown as normalised counts, calculated using DEseq2, of genes related to metal transporters for both C. acidophila and C. reinhardtii under a short and long term copper stress. Treatments were tested for significance across both species and all treatments using a one-way ANOVA, Tukey's post-hoc test were used for pairwise comparisons to test for significant differences between treatments. Letters represent different groups of significance.

4.5 Conclusion

We have seen how there is no one or two simplistic mechanisms that allow *C. acidophila* to adapt to a high copper environment. From both the PAM (Chapter 2) and RNA-seq data it seems that shutting down photosynthesis is beneficial and likely allows PM01 to neutralise the copper before it can cause excessive damage to the photosystems. Additionally, intracellular transport mechanisms also appear to play large role in the adaptation of PM01, and through the work of other research it is reasonable to deduce that they could be transporting vesicles storing copper to the cell periphery. Finally, if one gene had to be chosen as a candidate to infer a higher copper resistance, CTP3 shows promise. The fact that the basal expression in PM01 is already much higher than any transcript level *C. reinhardtii* showed, plus its likely mechanism of action of exporting copper from the cells, makes it a promising choice for alleviating copper stress in cells. Whilst important processes and genes have almost certainly identified, we can only see a much-reduced sample set. There is a chance that other more important genes could have been lost in this filtering process. Another factor we have not explored in this data, is the pH difference of the media the two strains were cultured in. The organisms were grown in their optimised medias to prevent any unnecessary stress; however, this came at a trade-off between not being able to distinguish genes related in adaption to more acidic conditions for PM01. It could be that some of these differentially expressed genes, especially when comparing the control treatment samples could involve genes related to pH adaption. Finally, the mapping rates for *C. acidophila* suggested that we could still be missing a lot of transcripts from the data set collected in this study. Sequencing the PM01 genome could be of great benefit in the future as it would allow us to map the transcriptome more accurately and could identify further processes that may have been hidden in this study,

4.6 References

Agrawal, S., Karcher, D., Ruf, S., Bock, R., 2020. The functions of chloroplast glutamyl-tRNA in translation and tetrapyrrole biosynthesis1[open]. Plant Physiol. 183, 263–276. https://doi.org/10.1104/pp.20.00009

Aguilera, A., Amils, R., 2005. Tolerance to cadmium in Chlamydomonas sp. (Chlorophyta) strains isolated from an extreme acidic environment, the Tinto River (SW, Spain). Aquat. Toxicol. 75, 316–329. https://doi.org/10.1016/j.aquatox.2005.09.002

Allen, M.D., Del Campo, J.A., Kropat, J., Merchant, S.S., 2007. FEA1, FEA2, and FRE1, encoding two homologous secreted proteins and a candidate ferrireductase, are expressed coordinately with FOX1 and FTR1 in iron-deficient Chlamydomonas reinhardtii. Eukaryot. Cell 6, 1841–1852. https://doi.org/10.1128/EC.00205-07

Allocati, N., Federici, L., Masulli, M., Di Ilio, C., 2009. Glutathione transferases in bacteria. FEBS J. 276, 58-75. https://doi.org/10.1111/j.1742-4658.2008.06743.x

Beauvais-Flück, R., Slaveykova, V.I., Cosio, C., 2019. Comparative study of Cu uptake and early transcriptome responses in the green microalga Chlamydomonas reinhardtii and the macrophyte Elodea nuttallii. Environ. Pollut. 250, 331–337. https://doi.org/10.1016/j.envpol.2019.04.032

Ben Massoud, M., Sakouhi, L., Chaoui, A., 2019. Effect of plant growth regulators, calcium and citric acid on copper toxicity in pea seedlings. J. Plant Nutr. 42, 1230–1242. https://doi.org/10.1080/01904167.2019.1609506

Białkowska, A., Gromek, E., Florczak, T., Krysiak, J., Szulczewska, K., Turkiewicz, M., 2016. Extremophilic Proteases: Developments of Their Special Functions, Potential Resources and Biotechnological Applications, in: Grand Challenges in Biology and Biotechnology. Springer International Publishing Switzerland, pp. 399–444. https://doi.org/10.1007/978-3-319-13521-2_14

Blaby-Haas, C.E., Merchant, S.S., 2012. The ins and outs of algal metal transport. Biochim. Biophys. Acta 1823, 1531–1552. https://doi.org/10.1016/j.bbamcr.2012.04.010

Blaby, I.K., Blaby-Haas, C.E., Pérez-Pérez, M.E., Schmollinger, S., Fitz-Gibbon, S., Lemaire, S.D., Merchant, S.S., 2015. Genome-wide analysis on *Chlamydomonas reinhardtii* reveals the impact of hydrogen peroxide on protein stress responses and overlap with other stress transcriptomes. Plant J. 84, 974–988. https://doi.org/10.1111/tpj.13053

Brisson, L.F., Zelitch, I., Havir, E.A., 1998. Manipulation of catalase levels produces altered photosynthesis in transgenic tobacco plants. Plant Physiol. 116, 259–269. https://doi.org/10.1104/pp.116.1.259

Brzezowski, P., Wilson, K.E., Gray, G.R., 2012. The PSBP2 protein of Chlamydomonas reinhardtii is required for singlet oxygen-dependent signaling. Planta 236, 1289–1303. https://doi.org/10.1007/s00425-012-1683-1

Cabrita, M.T., Duarte, B., Gameiro, C., Godinho, R.M., Caçador, I., 2018. Photochemical features and trace element substituted chlorophylls as early detection biomarkers of metal exposure in the model diatom Phaeodactylum tricornutum. Ecol. Indic. 95, 1038–1052. https://doi.org/10.1016/j.ecolind.2017.07.057

Chatzikonstantinou, M., Vlachakis, D., Chronopoulou, E., Papageorgiou, L., Papageorgiou, A.C., Labrou, N.E., 2017. The glutathione transferase family of Chlamydomonas reinhardtii: Identification and characterization of novel sigma class-like enzymes. Algal Res. 24, 237–250. https://doi.org/10.1016/j.algal.2017.03.010

Chen, Z., Song, S., Wen, Y., Zou, Y., Liu, H., 2016. Toxicity of Cu (II) to the green alga Chlorella vulgaris: a perspective of photosynthesis and oxidant stress. Environ. Sci. Pollut. Res. 23, 17910–17918. https://doi.org/10.1007/s11356-016-6997-2

Chiyonobu, T., Inoue, N., Morimoto, M., Kinoshita, T., Murakami, Y., 2014. Glycosylphosphatidylinositol (GPI) anchor deficiency caused by mutations in PIGW is associated with West syndrome and hyperphosphatasia with mental retardation syndrome. J.

Med. Genet. 51, 203–207. https://doi.org/10.1136/jmedgenet-2013-102156

Chuanboon, K., Nakorn, P.N., Pannengpetch, S., Laengsri, V., Nuchnoi, P., Isarankura-Na-Ayudhya, C., Isarankura-Na-Ayudhya, P., 2019. Proteomics and bioinformatics analysis reveal potential roles of cadmium-binding proteins in cadmium tolerance and accumulation of Enterobacter cloacae. PeerJ 2019, e6904. https://doi.org/10.7717/peerj.6904

Cid, A., Herrero, C., Torres, E., Abalde, J., 1995. Copper toxicity on the marine microalga Phaeodactylum tricornutum: effects on photosynthesis and related parameters. Aquat. Toxicol. 31, 165–174. https://doi.org/10.1016/0166-445X(94)00071-W

Cid, C., Garcia-Descalzo, L., Casado-Lafuente, V., Amils, R., Aguilera, A., 2010. Proteomic analysis of the response of an acidophilic strain of Chlamydomonas sp. (Chlorophyta) to natural metal-rich water. Proteomics 10, 2026–2036. https://doi.org/10.1002/pmic.200900592

Danilov, R.A., Ekelund, N.G.A., 2001. Responses of photosynthetic efficiency, cell shape and motility in Euglena Gracilis (Euglenophyceae) to short-term exposure to heavy metals and pentachlorophenol. Water. Air. Soil Pollut. 132, 61–73. https://doi.org/10.1023/A:1012004607313

Dean, A.P., Hartley, A., McIntosh, O.A., Smith, A., Feord, H.K., Holmberg, N.H., King, T., Yardley, E., White, K.N., Pittman, J.K., 2019. Metabolic adaptation of a Chlamydomonas acidophila strain isolated from acid mine drainage ponds with low eukaryotic diversity. Sci. Total Environ. 647, 75–87. https://doi.org/10.1016/j.scitotenv.2018.07.445

Díaz, S., de Francisco, P., Olsson, S., Aguilera, Á., González-Toril, E., Martín-González, A., 2020. Toxicity, physiological, and ultrastructural effects of arsenic and cadmium on the extremophilic microalga Chlamydomonas acidophila. Int. J. Environ. Res. Public Health 17, 1650. https://doi.org/10.3390/ijerph17051650

Dixon, D.P., Cole, D.J., Edwards, R., 2000. Characterisation of a zeta class glutathione transferase from Arabidopsis thaliana with a putative role in tyrosine catabolism. Arch. Biochem. Biophys. 384, 407–412. https://doi.org/10.1006/abbi.2000.2125

Dong, B., Wu, S., Wang, J., Liu, Y.X., Peng, Z., Meng, D.M., Huang, K., Wu, M., Fan, Z.C., 2017. Chlamydomonas IFT25 is dispensable for flagellar assembly but required to export the BBSome from flagella. Biol. Open 6, 1680–1691. https://doi.org/10.1242/bio.026278

Driver, T., Trivedi, D.K., McIntosh, O.A., Dean, A.P., Goodacre, R., Pittman, J.K., 2017. Two glycerol-3-phosphate dehydrogenases from Chlamydomonas have distinct roles in lipid metabolism. Plant Physiol. 174, 2083–2097. https://doi.org/10.1104/pp.17.00491

Erickson, E., Wakao, S., Niyogi, K.K., 2015. Light stress and photoprotection in Chlamydomonas reinhardtii. Plant J. 82, 449–465. https://doi.org/10.1111/tpj.12825

Esperanza, M., Houde, M., Seoane, M., Cid, Á., Rioboo, C., 2017. Does a short-term exposure to atrazine provoke cellular senescence in Chlamydomonas reinhardtii? Aquat. Toxicol. 189, 184–193. https://doi.org/10.1016/j.aquatox.2017.06.015

Fan, M., Sun, X., Liao, Z., Wang, J., Li, Y., Xu, N., 2018. Comparative proteomic analysis of Ulva prolifera response to high temperature stress. Proteome Sci. 16, 17. https://doi.org/10.1186/s12953-018-0145-5

Fazelian, N., Movafeghi, A., Yousefzadi, M., Rahimzadeh, M., 2019. Cytotoxic impacts of CuO nanoparticles on the marine microalga Nannochloropsis oculata. Environ. Sci. Pollut. Res. 26, 17499–17511. https://doi.org/10.1007/s11356-019-05130-0

Franco, P.O. de, Rousvoal, S., Tonon, T., Boyen, C., 2008. Whole genome survey of the glutathione transferase family in the brown algal model Ectocarpus siliculosus. Mar. Genomics 1, 135–148. https://doi.org/10.1016/j.margen.2009.01.003

Frey, A.G., Palenchar, D.J., Wildemann, J.D., Philpott, C.C., 2016. A glutaredoxin-BolA complex serves as an iron-sulfur cluster chaperone for the cytosolic cluster assembly machinery. J. Biol. Chem. 291, 22344–22356. https://doi.org/10.1074/jbc.M116.744946

Garvey, J.E., Owen, H.A., Winner, R.W., 1991. Toxicity of copper to the green alga, Chlamydomonas

reinhardtii (Chlorophyceae), as affected by humic substances of terrestrial and freshwater origin. Aquat. Toxicol. 19, 89–96. https://doi.org/10.1016/0166-445X(91)90029-9

Gechev, T.S., Van Breusegem, F., Stone, J.M., Denev, I., Laloi, C., 2006. Reactive oxygen species as signals that modulate plant stress responses and programmed cell death. BioEssays 28, 1091–1101. https://doi.org/10.1002/bies.20493

Geitmann, A., Nebenfähr, A., 2015. Navigating the plant cell: Intracellular transport logistics in the green kingdom. Mol. Biol. Cell. 26, 3373-3378. https://doi.org/10.1091/mbc.E14-10-1482

Gigova, L.G., Ivanova, N.J., 2015. Microalgae respond differently to nitrogen availability during culturing. J. Biosci. 40, 365–374. https://doi.org/10.1007/s12038-015-9510-z

Gupta, S., Agrawal, S.C., 2007. Survival and motility of diatoms Navicula grimmei and Nitzschia palea affected by some physical and chemical factors. Folia Microbiol. (Praha). 52, 127–134. https://doi.org/10.1007/BF02932151

Hamed, S.M., Selim, S., Klöck, G., AbdElgawad, H., 2017. Sensitivity of two green microalgae to copper stress: Growth, oxidative and antioxidants analyses. Ecotoxicol. Environ. Saf. 144, 19–25. https://doi.org/10.1016/j.ecoenv.2017.05.048

Hamed, S.M.S.M., Zinta, G., Klöck, G., Asard, H., Selim, S., AbdElgawad, H., 2017. Zinc-induced differential oxidative stress and antioxidant responses in Chlorella sorokiniana and Scenedesmus acuminatus. Ecotoxicol. Environ. Saf. 140, 256–263. https://doi.org/10.1016/j.ecoenv.2017.02.055

Harris, E.H., 2009. The Chlamydomonas Sourcebook. Academic Press, San Diego.

Hervé, C., De Franco, P.O., Groisillier, A., Tonon, T., Boyen, C., 2008. New members of the glutathione transferase family discovered in red and brown algae. Biochem. J. 412, 535–544. https://doi.org/10.1042/BJ20071464

Hirooka, S., Hirose, Y., Kanesaki, Y., Higuchi, S., Fujiwara, T., Onuma, R., Era, A., Ohbayashi, R., Uzuka, A., Nozaki, H., Yoshikawa, H., Miyagishima, S., 2017. Acidophilic green algal genome provides insights into adaptation to an acidic environment. Proc. Natl. Acad. Sci. 114, E8304–E8313. https://doi.org/10.1073/pnas.1707072114

Horianopoulos, L.C., Kronstad, J.W., 2019. Connecting iron regulation and mitochondrial function in Cryptococcus neoformans. Curr. Opin. Microbiol. 52, 7-13. https://doi.org/10.1016/j.mib.2019.04.002

Huet, D., Blisnick, T., Perrot, S., Bastin, P., 2014. The GTPase IFT27 is involved in both anterograde and retrograde intraflagellar transport. Elife 2014. 3, 02419. https://doi.org/10.7554/eLife.02419

Ivošević DeNardis, N., Pečar Ilić, J., Ružić, I., Novosel, N., Mišić Radić, T., Weber, A., Kasum, D., Pavlinska, Z., Balogh, R.K., Hajdu, B., Marček Chorvátová, A., Gyurcsik, B., 2019. Algal cell response to laboratory-induced cadmium stress: a multimethod approach. Eur. Biophys. J. 48, 231–248. https://doi.org/10.1007/s00249-019-01347-6

Jamers, A., Blust, R., De Coen, W., Griffin, J.L., Jones, O.A.H., 2013. Copper toxicity in the microalga Chlamydomonas reinhardtii: An integrated approach. BioMetals 26, 731–740. https://doi.org/10.1007/s10534-013-9648-9

Jamers, A., Van der Ven, K., Moens, L., Robbens, J., Potters, G., Guisez, Y., Blust, R., De Coen, W., 2006. Effect of copper exposure on gene expression profiles in Chlamydomonas reinhardtii based on microarray analysis. Aquat. Toxicol. 80, 249–260. https://doi.org/10.1016/j.aquatox.2006.09.002

Jegerschold, C., Arellano, J.B., Schroder, W.P., van Kan, P.J.M., Barón, M., Styring, S., 1995. Copper(II) Inhibition of Electron Transfer through Photosystem II Studied by EPR Spectroscopy. Biochemistry 34, 12747–12754. https://doi.org/10.1021/bi00039a034

Jiang, Y., Zhu, Y., Hu, Z., Lei, A., Wang, J., 2016. Towards elucidation of the toxic mechanism of copper on the model green alga Chlamydomonas reinhardtii. Ecotoxicology 25, 1417–1425. https://doi.org/10.1007/s10646-016-1692-0

Johnson, D.C., Dean, D.R., Smith, A.D., Johnson, M.K., 2005. Structure, function, and formation of biological iron-sulfur clusters. Annu. Rev. Biochem. 74, 247–281. https://doi.org/10.1146/annurev.biochem.74.082803.133518

Khare, D., Kumar, R., Acharya, C., 2020. Genomic and functional insights into the adaptation and survival of Chryseobacterium sp. strain PMSZPI in uranium enriched environment. Ecotoxicol. Environ. Saf. 191, 110217. https://doi.org/10.1016/j.ecoenv.2020.110217

Kim, J.H., Jang, H.J., Cho, W.Y., Yeon, S.J., Lee, C.H., 2020. In vitro antioxidant actions of sulfur-containing amino acids. Arab. J. Chem. 13, 1678–1684. https://doi.org/10.1016/j.arabjc.2017.12.036

Kováčik, J., Rotková, G., Bujdoš, M., Babula, P., Peterková, V., Matúš, P., 2017. Ascorbic acid protects Coccomyxa subellipsoidea against metal toxicity through modulation of ROS/NO balance and metal uptake. J. Hazard. Mater. 339, 200–207. https://doi.org/10.1016/j.jhazmat.2017.06.035

Kranner, I., Beckett, R., Hochman, A., Nash, T.H., 2008. Desiccation-tolerance in lichens: A review. Bryologist. 111, 576-593. https://doi.org/10.1639/0007-2745-111.4.576

Kumar, S., Trivedi, P.K., 2018. Glutathione S-transferases: Role in combating abiotic stresses including arsenic detoxification in plants. Front. Plant Sci. 9 ,751. https://doi.org/10.3389/fpls.2018.00751

Lallement, P.A., Brouwer, B., Keech, O., Hecker, A., Rouhier, N., 2014. The still mysterious roles of cysteine-containing glutathione transferases in plants. Front. Pharmacol. 5, 192. https://doi.org/10.3389/fphar.2014.00192

Laporte, D., Rodríguez, F., González, A., Zúñiga, A., Castro-Nallar, E., Saéz, C.A., Moenne, A., 2020. Copper-induced concomitant increases in photosynthesis, respiration, and C, N and S assimilation revealed by transcriptomic analyses in Ulva compressa (Chlorophyta). BMC Plant Biol. 20, 25. https://doi.org/10.1186/s12870-019-2229-5

Laporte, D., Valdés, N., González, A., Sáez, C.A., Zúñiga, A., Navarrete, A., Meneses, C., Moenne, A., 2016. Copper-induced overexpression of genes encoding antioxidant system enzymes and metallothioneins involve the activation of CaMs, CDPKs and MEK1/2 in the marine alga Ulva compressa. Aquat. Toxicol. 177, 433–440. https://doi.org/10.1016/j.aquatox.2016.06.017

Le Martret, B., Poage, M., Shiel, K., Nugent, G.D., Dix, P.J., 2011. Tobacco chloroplast transformants expressing genes encoding dehydroascorbate reductase, glutathione reductase, and glutathione-s-transferase, exhibit altered anti-oxidant metabolism and improved abiotic stress tolerance. Plant Biotechnol. J. 9, 661–673. https://doi.org/10.1111/j.1467-7652.2011.00611.x

Lee, K.O., Lee, J.R., Yoo, J.Y., Jang, H.H., Moon, J.C., Jung, B.G., Chi, Y.H., Park, S.K., Lee, S.S., Lim, C.O., Yun, D.J., Cho, M.J., Lee, S.Y., 2002. GSH-dependent peroxidase activity of the rice (Oryza sativa) glutaredoxin, a thioltransferase. Biochem. Biophys. Res. Commun. 296, 1152–1156. https://doi.org/10.1016/S0006-291X(02)02047-8

Li, H., Outten, C.E., 2019. The conserved CDC motif in the yeast iron regulator Aft2 mediates iron–sulfur cluster exchange and protein–protein interactions with Grx3 and Bol2. J. Biol. Inorg. Chem. 24, 809–815. https://doi.org/10.1007/s00775-019-01705-x

Li, M., Hu, C., Zhu, Q., Chen, L., Kong, Z., Liu, Z., 2006. Copper and zinc induction of lipid peroxidation and effects on antioxidant enzyme activities in the microalga Pavlova viridis (Prymnesiophyceae). Chemosphere 62, 565–572. https://doi.org/10.1016/j.chemosphere.2005.06.029

Lin, T.-H., Rao, M.-Y., Lu, H.-W., Chiou, C.-W., Lin, S.-T., Chao, H.-W., Zheng, Z.-L., Cheng, H.-C., Lee, T.-M., 2018. A role for glutathione reductase and glutathione in the tolerance of *Chlamydomonas reinhardtii* to photo-oxidative stress. Physiol. Plant. 162, 35–48. https://doi.org/10.1111/ppl.12622

Liu, M., Sjogren, A.K.M., Karlsson, C., Ibrahim, M.X., Andersson, K.M.E., Olofsson, F.J., Wahlstrom, A.M., Dalin, M., Yu, H., Chen, Z., Yang, S.H., Young, S.G., Bergo, M.O., 2010. Targeting the protein prenyltransferases efficiently reduces tumor development in mice with K-RAS-induced lung cancer. Proc. Natl. Acad. Sci. U. S. A. 107, 6471–6476.

https://doi.org/10.1073/pnas.0908396107

Liu, Z., Takazaki, H., Nakazawa, Y., Sakato, M., Yagi, T., Yasunaga, T., King, S.M., Kamiya, R., 2008. Partially functional outer-arm dynein in a novel Chlamydomonas mutant expressing a truncated γ heavy chain. Eukaryot. Cell 7, 1136–1145. https://doi.org/10.1128/EC.00102-08

Lodeyro, A.F., Ceccoli, R.D., Pierella Karlusich, J.J., Carrillo, N., 2012. The importance of flavodoxin for environmental stress tolerance in photosynthetic microorganisms and transgenic plants. Mechanism, evolution and biotechnological potential. FEBS Lett. 588, 2917-2924. https://doi.org/10.1016/j.febslet.2012.07.026

Lüersen, K., Stegehake, D., Daniel, J., Drescher, M., Ajonina, I., Ajonina, C., Hertel, P., Woltersdorf, C., Liebau, E., 2013. The Glutathione Reductase GSR-1 Determines Stress Tolerance and Longevity in Caenorhabditis elegans. PLoS One 8, 60731. https://doi.org/10.1371/journal.pone.0060731

Lysenko, E.A., Klaus, A.A., Kartashov, A. V., Kusnetsov, V. V., 2020. Specificity of Cd, Cu, and Fe effects on barley growth, metal contents in leaves and chloroplasts, and activities of photosystem I and photosystem II. Plant Physiol. Biochem. 147, 191–204. https://doi.org/10.1016/j.plaphy.2019.12.006

Ma, X., Zhang, B., Miao, R., Deng, X., Duan, Y., Cheng, Y., Zhang, W., Shi, M., Huang, K., Xia, X.Q., 2020. Transcriptomic and physiological responses to oxidative stress in a chlamydomonas reinhardtii glutathione peroxidase mutant. Genes (Basel). 11. https://doi.org/10.3390/genes11040463

Magdaleno, A., Gomez, C.E., Vêlez, C.G., Accorinti, J., 1997. Preliminary toxicity tests using the green alga, Ankistrodesmus falcatus. Environ. Toxicol. Water Qual. 12, 11–14. https://doi.org/10.1002/(SICI)1098-2256(1997)12:1<11::AID-TOX2>3.0.CO;2-B

Mahajan, N.S., Mishra, M., Tamhane, V.A., Gupta, V.S., Giri, A.P., 2014. Stress inducible proteomic changes in Capsicum annuum leaves. Plant Physiol. Biochem. 74, 212–217. https://doi.org/10.1016/j.plaphy.2013.11.017

Maniatsi, S., Farmaki, T., Abatzopoulos, T.J., 2015. The study of fkbp and ubiquitin reveals interesting aspects of Artemia stress history. Comp. Biochem. Physiol. Part - B Biochem. Mol. Biol. 186, 8–19. https://doi.org/10.1016/j.cbpb.2015.04.002

McConnell, E.W., Werth, E.G., Hicks, L.M., 2018. The phosphorylated redox proteome of Chlamydomonas reinhardtii: Revealing novel means for regulation of protein structure and function. Redox Biol. 17, 35–46. https://doi.org/10.1016/j.redox.2018.04.003

Mittler, R., 2017. ROS Are Good. Trends Plant Sci. 22, 11-19. https://doi.org/10.1016/j.tplants.2016.08.002

Moenne, A., González, A., Sáez, C.A., 2016. Mechanisms of metal tolerance in marine macroalgae, with emphasis on copper tolerance in Chlorophyta and Rhodophyta. Aquat. Toxicol. 176, 30-37. https://doi.org/10.1016/j.aquatox.2016.04.015

Mosier, A.C., Justice, N.B., Bowen, B.P., Baran, R., Thomas, B.C., Northen, T.R., Banfield, J.F., 2013. Metabolites associated with adaptation of microorganisms to an acidophilic, metal-rich environment identified by stable-isotope-enabled metabolomics. MBio 4. https://doi.org/10.1128/mBio.00484-12

Myster, S.H., Knott, J.A., Wysocki, K.M., O'Toole, E., Porter, M.E., 1999. Domains in the 1α dynein heavy chain required for inner arm assembly and flagellar motility in Chlamydomonas. J. Cell Biol. 146, 801–818. https://doi.org/10.1083/jcb.146.4.801

Nieboer, E., Richardson, D.H.S., 1980. The replacement of the nondescript term "heavy metals" by a biologically and chemically significant classification of metal ions. Environ. Pollution. Ser. B, Chem. Phys. 1, 3–26. https://doi.org/10.1016/0143-148X(80)90017-8

Nishikawa, K., Yamakoshi, Y., Uemura, I., Tominaga, N., 2003. Ultrastructural changes in Chlamydomonas acidophila (Chlorophyta) induced by heavy metals and polyphosphate metabolism. FEMS Microbiol. Ecol. 44, 253–259. https://doi.org/10.1016/S0168-6496(03)00049-7

Okamoto, O.K., Pinto, E., Latorre, L.R., Bechara, E.J.H., Colepicolo, P., 2001a. Antioxidant modulation in response to metal-induced oxidative stress in algal chloroplasts. Arch. Environ. Contam. Toxicol. 40, 18–24. https://doi.org/10.1007/s002440010144

Okamoto, O.K., Robertson, D.L., Fagan, T.F., Hastings, J.W., Colepicolo, P., 2001b. Different Regulatory Mechanisms Modulate the Expression of a Dinoflagellate Iron-Superoxide Dismutase. J. Biol. Chem. 276, 19989–19993. https://doi.org/10.1074/jbc.M101169200

Olaveson, M.M., Stokes, P.M., 1989. Responses of the acidophilic alga *Euglena mutabilis* (euglenophyceae) to carbon enrichment at ph 3. J. Phycol. 25, 529–539. https://doi.org/10.1111/j.1529-8817.1989.tb00259.x

Olsson, S., Puente-Sánchez, F., Gómez, M.J., Aguilera, A., 2015. Transcriptional response to copper excess and identification of genes involved in heavy metal tolerance in the extremophilic microalga Chlamydomonas acidophila. Extremophiles 19, 657–672. https://doi.org/10.1007/s00792-015-0746-1

Page, M.D., Kropat, J., Hamel, P.P., Merchant, S.S., 2009. Two Chlamydomonas CTR copper transporters with a novel cys-met motif are localized to the plasma membrane and function in copper assimilation. Plant Cell 21, 928–943. https://doi.org/10.1105/tpc.108.064907

Pandey, L.K., Bergey, E.A., 2016. Exploring the status of motility, lipid bodies, deformities and size reduction in periphytic diatom community from chronically metal (Cu, Zn) polluted waterbodies as a biomonitoring tool. Sci. Total Environ. 550, 372–381. https://doi.org/10.1016/j.scitotenv.2015.11.151

Pätsikkä, E., Kairavuo, M., Šeršen, F., Aro, E.M., Tyystjärvi, E., 2002. Excess copper predisposes photosystem II to photoinhibition in vivo by outcompeting iron and causing decrease in leaf chlorophyll. Plant Physiol. 129, 1359–1367. https://doi.org/10.1104/pp.004788

Peden, E.A., Boehm, M., Mulder, D.W., Davis, R., Old, W.M., King, P.W., Ghirardi, M.L., Dubini, A., 2013. Identification of global ferredoxin interaction networks in chlamydomonas reinhardtii. J. Biol. Chem. 288, 35192–35209. https://doi.org/10.1074/jbc.M113.483727

Pena, L.B., Pasquini, L.A., Tomaro, M.L., Gallego, S.M., 2007. 20S proteasome and accumulation of oxidized and ubiquitinated proteins in maize leaves subjected to cadmium stress. Phytochemistry 68, 1139–1146. https://doi.org/10.1016/j.phytochem.2007.02.022

Piotrowska-Niczyporuk, A., Bajguz, A., Talarek, M., Bralska, M., Zambrzycka, E., 2015. The effect of lead on the growth, content of primary metabolites, and antioxidant response of green alga Acutodesmus obliquus (Chlorophyceae). Environ. Sci. Pollut. Res. 22, 19112–19123. https://doi.org/10.1007/s11356-015-5118-y

Piotrowska-Niczyporuk, A., Bajguz, A., Zambrzycka-Szelewa, E., Bralska, M., 2018. Exogenously applied auxins and cytokinins ameliorate lead toxicity by inducing antioxidant defence system in green alga Acutodesmus obliquus. Plant Physiol. Biochem. 132, 535–546. https://doi.org/10.1016/j.plaphy.2018.09.038

Piotrowska-Niczyporuk, A., Bajguz, A., Zambrzycka, E., Godlewska-żyłkiewicz, B., 2012. Phytohormones as regulators of heavy metal biosorption and toxicity in green alga Chlorella vulgaris (Chlorophyceae). Plant Physiol. Biochem. 52, 52–65. https://doi.org/10.1016/j.plaphy.2011.11.009

Prasad, S.M., Zeeshan, M., 2005. UV-B radiation and cadmium induced changes in growth, photosynthesis, and antioxidant enzymes of cyanobacterium Plectonema boryanum. Biol. Plant. 49, 229–236. https://doi.org/10.1007/s10535-005-0236-x

Premont, R.T., Claing, A., Vitale, N., Perry, S.J., Lefkowitz, R.J., 2000. The GIT Family of ADP-ribosylation Factor GTPase-activating Proteins functional diversity of GIT2 through alternative splicing. 275, 22373-22380. https://doi.org/10.1074/jbc.275.29.22373

Puente-Sánchez, F., Díaz, S., Penacho, V., Aguilera, A., Olsson, S., 2018. Basis of genetic adaptation to heavy metal stress in the acidophilic green alga Chlamydomonas acidophila. Aquat. Toxicol. 200, 62–72. https://doi.org/10.1016/j.aquatox.2018.04.020

Qin, H., Wang, Z., Diener, D., Rosenbaum, J., 2007. Intraflagellar Transport Protein 27 Is a Small G

Protein Involved in Cell-Cycle Control. Curr. Biol. 17, 193–202. https://doi.org/10.1016/j.cub.2006.12.040

Quarmby, L.M., 2004. Cellular Deflagellation. Int. Rev. Cytol. 233, 47–91. https://doi.org/10.1016/S0074-7696(04)33002-0

Roach, T., Baur, T., Stöggl, W., Krieger-Liszkay, A., 2017. Chlamydomonas reinhardtii responding to high light: a role for 2-propenal (acrolein). Physiol. Plant. 161, 75–87. https://doi.org/10.1111/ppl.12567

Sabatini, S.E., Juárez, Á.B., Eppis, M.R., Bianchi, L., Luquet, C.M., Ríos de Molina, M. del C., 2009. Oxidative stress and antioxidant defenses in two green microalgae exposed to copper. Ecotoxicol. Environ. Saf. 72, 1200–1206. https://doi.org/10.1016/j.ecoenv.2009.01.003

Samadani, M., Dewez, D., 2018. Cadmium accumulation and toxicity affect the extracytoplasmic polyphosphate level in Chlamydomonas reinhardtii. Ecotoxicol. Environ. Saf. 166, 200–206. https://doi.org/10.1016/j.ecoenv.2018.09.094

Sánchez-Marín, P., Fortin, C., Campbell, P.G.C.C., 2014. Lead (Pb) and copper (Cu) share a common uptake transporter in the unicellular alga Chlamydomonas reinhardtii. BioMetals 27, 173–181. https://doi.org/10.1007/s10534-013-9699-y

Sánchez-Thomas, R., Moreno-Sánchez, R., García-García, J.D., 2016. Accumulation of zinc protects against cadmium stress in photosynthetic Euglena gracilis. Environ. Exp. Bot. 131, 19–31. https://doi.org/10.1016/j.envexpbot.2016.06.009

Schmidt, A., Trebst, A., 1969. The mechanism of photosynthetic sulfate reduction by isolated chloroplasts. BBA - Bioenerg. 180, 529–535. https://doi.org/10.1016/0005-2728(69)90031-0

Seigneurin-Berny, D., Gravot, A., Auroy, P., Mazard, C., Kraut, A., Finazzi, G., Grunwald, D., Rappaport, F., Vavasseur, A., Joyard, J., Richaud, P., Rolland, N., 2006. HMA1, a new Cu-ATPase of the chloroplast envelope, is essential for growth under adverse light conditions. J. Biol. Chem. 281, 2882–2892. https://doi.org/10.1074/jbc.M508333200

Shanmuganathan, A., Avery, S. V., Willetts, S.A., Houghton, J.E., 2004. Copper-induced oxidative stress in Saccharomyces cerevisiae targets enzymes of the glycolytic pathway. FEBS Lett. 556, 253–259. https://doi.org/10.1016/S0014-5793(03)01428-5

Sharaf, A., De Michele, R., Sharma, A., Fakhari, S., Oborník, M., 2019. Transcriptomic analysis reveals the roles of detoxification systems in response to mercury in Chromera velia. Biomolecules 9. https://doi.org/10.3390/biom9110647

Shen, M., Zhao, D.-K., Qiao, Q., Liu, L., Wang, J.-L., Cao, G.-H., Li, T., Zhao, Z.-W., 2015. Identification of Glutathione S-Transferase (GST) Genes from a Dark Septate Endophytic Fungus (Exophiala pisciphila) and Their Expression Patterns under Varied Metals Stress. PLoS One 10, 123418. https://doi.org/10.1371/journal.pone.0123418

Sideri, T.C., Willetts, S.A., Avery, S. V., 2009. Methionine sulphoxide reductases protect iron-sulphur clusters from oxidative inactivation in yeast. Microbiology 155, 612–623. https://doi.org/10.1099/mic.0.022665-0

Singh, R., Upadhyay, A.K., Chandra, P., Singh, D.P., 2018. Sodium chloride incites reactive oxygen species in green algae Chlorococcum humicola and Chlorella vulgaris: Implication on lipid synthesis, mineral nutrients and antioxidant system. Bioresour. Technol. 270, 489–497. https://doi.org/10.1016/j.biortech.2018.09.065

Spijkerman, E., Barua, D., Gerloff-Elias, A., Kern, J., Gaedke, U., Heckathorn, S.A., 2007. Stress responses and metal tolerance of Chlamydomonas acidophila in metal-enriched lake water and artificial medium. Extremophiles 11, 551–562. https://doi.org/10.1007/s00792-007-0067-0

Stamatakis, A., 2006. RAxML-VI-HPC: maximum likelihood-based phylogenetic analyses with thousands of taxa and mixed models. Bioinformatics 22, 2688–2690. https://doi.org/10.1093/bioinformatics/btl446

Stavridou, E., Michailidis, M., Gedeon, S., Ioakeim, A., Kostas, S., Chronopoulou, E., Labrou, N.E., Edwards, R., Day, A., Nianiou-Obeidat, I., Madesis, P., 2019. Tolerance of transplastomic

tobacco plants overexpressing a theta class glutathione transferase to abiotic and oxidative stresses. Front. Plant Sci. 9, 1861. https://doi.org/10.3389/fpls.2018.01861

Tan, K.W.M., Lin, H., Shen, H., Lee, Y.K., 2016. Nitrogen-induced metabolic changes and molecular determinants of carbon allocation in Dunaliella tertiolecta. Sci. Rep. 6, 37235. https://doi.org/10.1038/srep37235

Tarrago, L., Laugier, E., Rey, P., 2009. Protein-repairing methionine sulfoxide reductases in photosynthetic organisms: Gene organization, reduction mechanisms, and physiological roles. Mol. Plant 2, 202–217. https://doi.org/10.1093/mp/ssn067

Taschner, M., Lorentzen, A., Mourão, A., Collins, T., Freke, G.M., Moulding, D., Basquin, J., Jenkins, D., Lorentzen, E., 2018. Crystal structure of intraflagellar transport protein 80 reveals a homodimer required for ciliogenesis. Elife 7, 33067. https://doi.org/10.7554/eLife.33067

Terzulli, A., Kosman, D.J., 2010. Analysis of the high-affinity iron uptake system at the Chlamydomonas reinhardtii plasma membrane. Eukaryot. Cell 9, 815–826. https://doi.org/10.1128/EC.00310-09

Tian, S., Lu, L., Labavitch, J., Yang, X., He, Z., Hu, H., Sarangi, R., Newville, M., Commisso, J., Brown, P., 2011. Cellular sequestration of cadmium in the hyperaccumulator plant species Sedum alfredii. Plant Physiol. 157, 1914–1925. https://doi.org/10.1104/pp.111.183947

Tian, T., Yue, L., Hengyu, Y., You, Q., Yi, X., Du, Z., Xu, W., Su, Z., 2017. agriGO v2.0: a GO analysis toolkit for the agricultural community, 2017 update. Nucleic Acids Res.

Tsuji, N., Hirayanagi, N., Iwabe, O., Namba, T., Tagawa, M., Miyamoto, S., Miyasaka, H., Takagi, M., Hirata, K., Miyamoto, K., 2003. Regulation of phytochelatin synthesis by zinc and cadmium in marine green alga, Dunaliella tertiolecta. Phytochemistry 62, 453–459. https://doi.org/10.1016/S0031-9422(02)00559-9

Urbanska, P., Joachimiak, E., Bazan, R., Fu, G., Poprzeczko, M., Fabczak, H., Nicastro, D., Wloga, D., 2018. Ciliary proteins Fap43 and Fap44 interact with each other and are essential for proper cilia and flagella beating. Cell. Mol. Life Sci. 75, 4479–4493. https://doi.org/10.1007/s00018-018-2819-7

Vallentine, P., Hung, C.Y., Xie, J., Van Hoewyk, D., 2014. The ubiquitin-proteasome pathway protects Chlamydomonas reinhardtii against selenite toxicity, but is impaired as reactive oxygen species accumulate. AoB Plants 6, 1–11. https://doi.org/10.1093/aobpla/plu062

Wang, H., Jin, M., Xu, L., Xi, H., Wang, B., Du, S., Liu, H., Wen, Y., 2020. Effects of ketoprofen on rice seedlings: Insights from photosynthesis, antioxidative stress, gene expression patterns, and integrated biomarker response analysis. Environ. Pollut. 263, 114533. https://doi.org/10.1016/j.envpol.2020.114533

Wang, T., Hu, Y., Zhu, M., Yin, S., 2020. Integrated transcriptome and physiology analysis of Microcystis aeruginosa after exposure to copper sulfate. J. Oceanol. Limnol. 38, 102–113. https://doi.org/10.1007/s00343-019-8357-9

Wang, X., Yang, X., Chen, S., Li, Q., Wang, W., Hou, C., Gao, X., Wang, L., Wang, S., 2016. Zinc oxide nanoparticles affect biomass accumulation and photosynthesis in Arabidopsis. Front. Plant Sci. 6, 1243. https://doi.org/10.3389/fpls.2015.01243

Wolfe-Simon, F., Grzebyk, D., Schofield, O., Falkowski, P.G., 2005. The role and evolution of superoxide dismutases in algae. J. Phycol. https://doi.org/10.1111/j.1529-8817.2005.00086.x

Yokoyama, R., O'Toole, E., Ghosh, S., Mitchell, D.R., 2004. Regulation of flagellar dynein activity by a central pair kinesin. Proc. Natl. Acad. Sci. U. S. A. 101, 17398–17403. https://doi.org/10.1073/pnas.0406817101

Zalutskaya, Z.M., Skryabina, U.S., Ermilova, E. V, 2019. Generation of Hydrogen Peroxide and Transcriptional Regulation of Antioxidant Enzyme Expression in Chlamydomonas reinhardtii under Hypothermia. Russ. J. Plant Physiol. 66, 223–230. https://doi.org/10.1134/S1021443719020171

Zelitch, I., 1990. Physiological investigations of a tobacco mutant with O2-resistant photosynthesis

and enhanced catalase activity. Plant Physiol. 93, 1521–1524. https://doi.org/10.1104/pp.93.4.1521

4.7 Supplementary Tables

Supplementary Table 4.1- Genes Identified in Cluster 2 and Their Likely Function

C. reinhardtii Identifier	C. eustigma Identifier	Gene Info
Cre01.g026100.t1.2	CEUSTIGMA_g13206.t1	NA
Cre07.g355250.t1.2	CEUSTIGMA_g931.t1	CDK inhibitory kinase
Cre06.g281050.t1.2	CEUSTIGMA_g9385.t1	Subunit of Retromer complex
Cre01.g029650.t1.1	CEUSTIGMA_g11449.t1	Subunit of Retromer complex
Cre06.g257550.t1.2	CEUSTIGMA_g13844.t1	Uncoupling protein
Cre12.g549550.t1.2	CEUSTIGMA_g9886.t1	Beta tubulin 2
Cre09.g394850.t1.2	CEUSTIGMA_g1602.t1	LrgB-like protein
Cre02.g118250.t1.1	CEUSTIGMA_g8000.t1	SWIB domain-containing protein
Cre06.g297750.t1.2	CEUSTIGMA_g1111.t1	SF3A3 splicing factor 3a, subunit 3
Cre06.g299700.t1.2	CEUSTIGMA_g10224.t1	SOUL heme-binding protein
Cre12.g525050.t1.1	CEUSTIGMA_g11438.t1	Structural Maintenance of Chromosomes protein
Cre17.g726750.t1.2	CEUSTIGMA_g11025.t1	3-deoxy-D-arabino-heptulosonate 7-phosphate synthetase
Cre01.g035850.t1.2	CEUSTIGMA_g11876.t1	COP-II coat subunit
Cre12.g518000.t2.1	CEUSTIGMA_g9022.t1	Chloroplast-associated SecA protein
Cre03.g166050.t1.2	CEUSTIGMA_g7631.t1	Selenium binding protein
Cre12.g496450.t1.2	CEUSTIGMA_g5280.t1	RNA binding component of exosome complex
Cre10.g439150.t1.2	CEUSTIGMA_g4876.t1	26S proteasome regulatory subunit
Cre07.g329700.t1.2	CEUSTIGMA_g6068.t1	26S proteasome regulatory subunit
Cre01.g039250.t2.1	CEUSTIGMA_g9333.t1	NA
Cre09.g411100.t2.1	CEUSTIGMA_g6496.t1	NA
Cre03.g194950.t1.1	CEUSTIGMA_g2915.t1	Chloroplast RNA polymerase sigma factor, c
Cre13.g581450.t1.2	CEUSTIGMA_g3795.t1	NA
Cre06.g275650.t1.2	CEUSTIGMA_g3616.t1	26S proteasome regulatory subunit
Cre17.g727950.t1.1	CEUSTIGMA_g4337.t1	26S proteasome regulatory subunit
Cre09.g397697.t1.1	CEUSTIGMA_g7696.t1	Ribosomal protein L4, component of cytosolic 80S ribosome and 60S large subunit
Cre09.g391097.t1.1	CEUSTIGMA_g2196.t1	NA
Cre12.g491050.t1.2	CEUSTIGMA_g4452.t1	Ribonucleoside-diphosphate reductase R2 subunit
Cre01.g025250.t1.1	CEUSTIGMA_g1264.t1	Riboflavin kinase
Cre03.g145527.t1.1	CEUSTIGMA_g6060.t1	Rhomboid-like protein
Cre06.g278097.t1.1	CEUSTIGMA_g474.t1	mRNA export protein
Cre03.g172500.t1.1	CEUSTIGMA_g5798.t1	Plastid terminal oxidase
Cre02.g078858.t1.1	CEUSTIGMA_g10315.t1	Presenilin protease
Cre07.g332550.t1.2	CEUSTIGMA_g5014.t1	Signal peptide peptidase, eukaryotic-type
Cre02.g114600.t1.2	CEUSTIGMA_g568.t1	2-cys peroxiredoxin
Cre10.g429150.t1.2	CEUSTIGMA_g4436.t1	Anthranilate phosphoribosyltransferase
Cre09.g394750.t1.2	CEUSTIGMA_g8254.t1	Plastid ribosomal protein S1, polyribonucleotide nucleotidyltransferase
Cre16.g673617.t1.1	CEUSTIGMA_g4998.t1	Peptide chain release factor
Cre01.g050500.t1.1	CEUSTIGMA_g11183.t1	Pentatrichopeptide repeat protein
Cre14.g619550.t1.2	CEUSTIGMA_g972.t1	NA
Cre05.g232550.t1.2	CEUSTIGMA_g5917.t1	Phosphoglycerate mutase
Cre06.g272050.t1.2	CEUSTIGMA_g8628.t1	Phosphoglycerate mutase, 2,3-bisphosphoglycerate-independent
Cre12.g523150.t1.2	CEUSTIGMA_g8017.t1	Prefoldin molecular chaperone, subunit 5
Cre07.g328150.t2.1	CEUSTIGMA_g513.t1	NA
Cre03.g204689.t1.1	CEUSTIGMA_g10438.t1	3',5'-cyclic-nucleotide phosphodiesterase

Cre07.g342350.t1.2	CEUSTIGMA_g2690.t1	3',5'-cyclic-nucleotide phosphodiesterase
Cre02.g141400.t1.2	CEUSTIGMA_g7360.t1	Phosphoenolpyruvate carboxykinase
Cre16.g668900.t1.1	CEUSTIGMA_g1395.t1	Hypothetical protein
Cre05.g235750.t1.2	CEUSTIGMA_g3355.t1	DNA mismatch repair protein, MutS homolog
Cre17.g722800.t1.2	CEUSTIGMA_g4651.t1	Mitochondrial processing peptidase alpha subunit
Cre17.g739850.t1.2	CEUSTIGMA_g5974.t1	Predicted protein
Cre17.g722400.t1.2	CEUSTIGMA_g5893.t1	Predicted protein
Cre14.g629700.t1.1	CEUSTIGMA_g2528.t1	NADP malic enzyme
Cre01.g036050.t1.1	CEUSTIGMA_g1297.t1	DNA mismatch repair protein
Cre17.g720350.t1.1	CEUSTIGMA_g7291.t1	Chloroplast division site-determinant MinE
Cre09.g415750.t1.2	CEUSTIGMA_g1558.t1	General substrate transporter, major facilitator superfamily
Cre10.g455850.t1.2	CEUSTIGMA_g10025.t1	Minichromosome maintenance protein
Cre06.g295700.t1.1	CEUSTIGMA_g2771.t1	Minichromosome maintenance protein
Cre07.g325400.t1.2	CEUSTIGMA_g3067.t1	3-Isopropylmalate dehydrogenase, splicing variant a; 3-Isopropylmalate dehydrogenase, splicing variant b
Cre12.g530550.t1.1	CEUSTIGMA_g10433.t1	Diacylglycerol kinase
Cre06.g311650.t1.1	CEUSTIGMA_g476.t1	Inwardly-rectifying potassium channel
Cre01.g027950.t1.2	CEUSTIGMA_g9851.t1	Intraflagellar transport protein 74/72
Cre04.g219250.t1.2	CEUSTIGMA_g8894.t1	Intraflagellar transport protein 52
Cre12.g514850.t1.2	CEUSTIGMA_g2100.t1	Heat shock protein 90C
Cre12.g535700.t1.1	CEUSTIGMA_g11011.t1	Heat shock protein 70D
Cre07.g354500.t1.1	CEUSTIGMA_g12411.t1	Heat shock transcription factor
Cre12.g507559.t1.1	CEUSTIGMA_g3372.t1	NA
Cre17.g708800.t1.1	CEUSTIGMA_g1014.t1	Glutathione synthetase
Cre02.g142186.t1.1	CEUSTIGMA_g11709.t1	Plastid division protein FtsZ2
Cre17.g730950.t1.2	CEUSTIGMA_g5164.t1	Kinesin motor protein, kinesin-2 (KRP85/95) family
Cre12.g543350.t2.1	CEUSTIGMA_g6583.t1	NA
Cre09.g403293.t1.1	CEUSTIGMA_g3818.t1	5-Formyltetrahydrofolate cycloligase
Cre16.g652150.t1.2	CEUSTIGMA_g4467.t1	Fructose-2,6-bisphosphate 2-phosphatase/6-phosphofructo-2-kinase
Cre16.g688450.t1.2	CEUSTIGMA_g7758.t1	Flagellar Basal Body protein
Cre16.g679445.t1.1	CEUSTIGMA_g3362.t1	Fasciclin-like protein
Cre16.g654150.t1.1	CEUSTIGMA_g3982.t1	Flagellar Associated Protein
Cre09.g395250.t1.1	CEUSTIGMA_g13440.t1	Flagellar Associated Protein
Cre01.g025350.t1.2	CEUSTIGMA_g7896.t1	Flagellar Associated Protein
Cre02.g095072.t1.1	CEUSTIGMA_g13863.t1	Flagellar Associated Protein
Cre16.g650550.t1.2	CEUSTIGMA_g4490.t1	NA
Cre10.g435350.t2.1	CEUSTIGMA_g9047.t1	NA
Cre08.g360400.t1.1	CEUSTIGMA_g440.t1	ERD4-related membrane protein
Cre12.g515650.t1.2	CEUSTIGMA_g7114.t1	Eukaryotic translation initiation factor 3, subunit K
Cre03.g159650.t1.2	CEUSTIGMA_g3163.t1	GTP binding protein
Cre06.g279100.t1.2	CEUSTIGMA_g10201.t1	Subunit of chromatin modifying protein
Cre01.g032500.t1.2	CEUSTIGMA_g9772.t1	DnaJ-like protein
Cre09.g416100.t1.2	CEUSTIGMA_g12450.t1	DnaJ-like protein
Cre03.g180650.t1.1	CEUSTIGMA_g4948.t1	DegP-type protease
Cre02.g088400.t2.1	CEUSTIGMA_g605.t1	NA
Cre05.g237400.t1.2	CEUSTIGMA_g10236.t1	Diaminopimelate epimerase
Cre02.g114700.t1.2	CEUSTIGMA_g7997.t1	Peptidyl-prolyl cis-trans isomerase, cyclophilin-type, Radial spoke protein 12
Cre02.g093550.t1.1	CEUSTIGMA_g2634.t1	Adenylate/guanylate cyclase

Cre07.g322000.t1.2	CEUSTIGMA_g2796.t1	Cysteine desulfurase
Cre07.g339150.t1.1	CEUSTIGMA_g6383.t1	Chaperonin 60B2
Cre12.g505850.t1.2	CEUSTIGMA_g4399.t1	Chaperonin 23
Cre08.g358562.t1.1	CEUSTIGMA_g1816.t1	Chaperonin 20
Cre10.g429800.t1.2	CEUSTIGMA_g4477.t1	Ubiquinone biosynthesis protein
Cre02.g112850.t1.1	CEUSTIGMA_g5503.t1	Flavin-dependent monoxygenase
Cre12.g560350.t2.1	CEUSTIGMA_g7854.t1	NA
Cre12.g514750.t1.2	CEUSTIGMA_g3497.t1	Citrate synthase
Cre16.g674890.t2.1	CEUSTIGMA_g1705.t1	NA
Cre03.g151200.t1.2	CEUSTIGMA_g13053.t1	Predicted protein
Cre12.g554103.t1.1	CEUSTIGMA_g1752.t1	Predicted protein
Cre03.g148250.t1.1	CEUSTIGMA_g6054.t1	Conserved expressed zinc-finger protein
Cre16.g692650.t1.2	CEUSTIGMA_g6287.t1	Predicted protein
Cre12.g536500.t1.2	CEUSTIGMA_g111.t1	Conserved Sel1 repeat protein
Cre14.g632000.t1.1	CEUSTIGMA_g3868.t1	GrpE nucleotide release factor
Cre07.g341600.t1.2	CEUSTIGMA_g8495.t1	NA
Cre02.g119900.t1.2	CEUSTIGMA_g8038.t1	Cysteine endopeptidase
Cre17.g705350.t1.1	CEUSTIGMA_g5125.t1	Calcium-dependent protein kinase kinase
Cre12.g507650.t2.1	CEUSTIGMA_g12234.t1	NA
Cre10.g443250.t1.2	CEUSTIGMA_g11507.t1	T-complex protein 1, gamma subunit
Cre04.g227350.t1.1	CEUSTIGMA_g11704.t1	NOT-complex component
Cre02.g096300.t1.1	CEUSTIGMA_g5295.t1	NA
Cre10.g444850.t1.1	CEUSTIGMA_g5831.t1	Voltage-gated Ca2+ channel, alpha subunit
Cre06.g261150.t1.2	CEUSTIGMA_g3599.t1	Biotin synthase
Cre05.g234661.t1.1	CEUSTIGMA_g3819.t1	Ubiquinol:cytochrome c oxidoreductase biogenesis factor
Cre06.g267550.t1.2	CEUSTIGMA_g11480.t1	Bardet-Biedl syndrome-5 associated protein
Cre02.g107450.t1.2	CEUSTIGMA_g997.t1	ATP-sulfurylase
Cre16.g664250.t1.2	CEUSTIGMA_g5117.t1	O-acetylserine (Thiol)-lyase/cysteine synthase
Cre17.g708250.t1.2	CEUSTIGMA_g6254.t1	NA
Cre06.g301050.t1.2	CEUSTIGMA_g1106.t1	ARF-like GTPase
Cre05.g234665.t1.1	CEUSTIGMA_g11611.t1	Beta4-Adaptin
Cre03.g168550.t1.1	CEUSTIGMA_g9654.t1	Amino acid transporter
Cre06.g292350.t1.2	CEUSTIGMA_g8905.t1	Amino acid carrier
Cre01.g000650.t1.1	CEUSTIGMA_g2561.t1	Copper amine oxidase
Cre06.g307150.t1.1	CEUSTIGMA_g7965.t1	Beta-amylase
Cre13.g570350.t1.1	CEUSTIGMA_g12976.t1	NA
Cre06.g307100.t1.1	CEUSTIGMA_g4429.t1	ABC1/COQ8 Ser/Thr kinase
Cre03.g182800.t1.1	CEUSTIGMA_g7154.t1	Alanine-glyoxylate transaminase
Cre10.g435300.t2.1	CEUSTIGMA_g11613.t1	NA
Cre01.g001800.t1.1	CEUSTIGMA_g8618.t1	(1 of 4) PTHR24361//PTHR24361:SF411 - MITOGEN-ACTIVATED KINASE KINASE KINASE // SUBFAMILY NOT NAMED
Cre01.g005813.t1.2	CEUSTIGMA_g8903.t1	NA
Cre01.g006766.t1.1	CEUSTIGMA_g3856.t1	NA
Cre01.g007901.t1.1	CEUSTIGMA_g11265.t1	NA
Cre01.g011100.t2.1	CEUSTIGMA_g2587.t1	NA
Cre01.g012400.t1.2	CEUSTIGMA_g2562.t1	(1 of 2) KOG4510 - Permease of the drug/metabolite transporter (DMT) superfamily
Cre01.g013550.t1.1	CEUSTIGMA_g2086.t1	NA
Cre01.g014100.t1.2	CEUSTIGMA_g6525.t1	(1 of 1) PTHR14614:SF29 - PROTEIN FAM86A

Cre01.g016528.t1.1	CEUSTIGMA_g1740.t1	(1 of 1) 4.2.1.109 - Methylthioribulose 1-phosphate dehydratase / 1-PMT-ribulose dehydratase
Cre01.g017200.t1.2	CEUSTIGMA_g1737.t1	Peptidyl-prolyl cis-trans isomerase, FKBP-type
Cre01.g017400.t2.1	CEUSTIGMA_g1736.t1	NA
Cre01.g019250.t1.2	CEUSTIGMA_g1406.t1	Putative dTDP-glucose 4-6-dehydratase
Cre01.g021600.t1.2	CEUSTIGMA_g2141.t1	(1 of 1) PTHR24031//PTHR24031:SF274 - RNA HELICASE // SUBFAMILY NOT NAMED
Cre01.g021750.t1.2	CEUSTIGMA_g10094.t1	(1 of 1) PTHR13464 - TRANSCRIPTIONAL REGULATOR PROTEIN HCNGP
Cre01.g022550.t1.1	CEUSTIGMA_g2099.t1	(1 of 16) 3.6.5.5 - Dynamin GTPase
Cre01.g023350.t1.1	CEUSTIGMA_g1357.t1	Oligoendopeptidase
Cre01.g025100.t1.1	CEUSTIGMA_g9570.t1	(1 of 1) PTHR18901//PTHR18901:SF22 - 2-DEOXYGLUCOSE-6-PHOSPHATE PHOSPHATASE 2 // SUBFAMILY NOT NAMED
Cre01.g028101.t1.1	CEUSTIGMA_g9848.t1	NA
Cre01.g030250.t1.2	CEUSTIGMA_g11648.t1	(1 of 1) 3.1.3.57 - Inositol-1,4-bisphosphate 1-phosphatase / Inositol polyphosphate 1-phosphatase
Cre01.g030300.t2.1	CEUSTIGMA_g7904.t1	NA
Cre01.g032400.t1.2	CEUSTIGMA_g9621.t1	(1 of 1) PF05118 - Aspartyl/Asparaginyl beta-hydroxylase (Asp_Arg_Hydrox)
Cre01.g033091.t1.1	CEUSTIGMA_g12475.t1	(1 of 1) 6.3.1.14 - Diphthine--ammonia ligase / Diphthamide synthetase
Cre01.g034100.t2.1	CEUSTIGMA_g9363.t1	NA
Cre01.g034400.t1.1	CEUSTIGMA_g13151.t1	(1 of 2) 3.1.1.31 - 6-phosphogluconolactonase
Cre01.g035500.t1.2	CEUSTIGMA_g4789.t1	Phosphatidylinositol-3-kinase, probably vacuolar
Cre01.g037400.t1.1	CEUSTIGMA_g9572.t1	Peptidyl-prolyl cis-trans isomerase, cyclophilin-type, possible splicing factor
Cre01.g038850.t1.1	CEUSTIGMA_g11861.t1	(1 of 1) PTHR24012:SF308 - PROTEIN Y55F3AM.3, ISOFORM A
Cre01.g046237.t1.1	CEUSTIGMA_g11156.t1	NA
Cre01.g047350.t1.1	CEUSTIGMA_g5480.t1	NA
Cre01.g047850.t1.2	CEUSTIGMA_g4515.t1	(1 of 1) 4.2.1.145 - Capreomycidine synthase
Cre01.g048050.t1.2	CEUSTIGMA_g3758.t1	(1 of 1) 6.3.2.5 - Phosphopantothenate--cysteine ligase / Phosphopantothenoylcysteine synthetase
Cre01.g050608.t1.1	CEUSTIGMA_g7697.t1	NA
Cre01.g052000.t1.2	CEUSTIGMA_g3771.t1	(1 of 1) PTHR13748:SF31 - COBW DOMAIN-CONTAINING PROTEIN 1
Cre01.g054650.t1.1	CEUSTIGMA_g9151.t1	NA
Cre01.g054850.t1.2	CEUSTIGMA_g9199.t1	NA
Cre01.g055432.t1.1	CEUSTIGMA_g9745.t1	Protein with mechanosensitive ion channel domain
Cre02.g073250.t1.1	CEUSTIGMA_g6660.t1	(1 of 1) PTHR11477:SF17 - PROTEIN PARTNER OF SNF
Cre02.g074758.t2.1	CEUSTIGMA_g3239.t1	(1 of 72) 4.6.1.2 - Guanylate cyclase / Guanylyl cyclase
Cre02.g074900.t1.1	CEUSTIGMA_g5843.t1	(1 of 1) PTHR10774//PTHR10774:SF82 - EXTENDED SYNAPTOTAGMIN-RELATED // SUBFAMILY NOT NAMED
Cre02.g077401.t1.1	CEUSTIGMA_g6987.t1	NA
Cre02.g077700.t1.1	CEUSTIGMA_g4338.t1	(1 of 2) PTHR22957:SF148 - RE26521P
Cre02.g077951.t1.1	CEUSTIGMA_g4343.t1	(1 of 13) 3.6.3.25 - Sulfate-transporting ATPase
Cre02.g079250.t1.1	CEUSTIGMA_g629.t1	(1 of 1) PTHR16684 - CENTROMERE PROTEIN C
Cre02.g080350.t1.1	CEUSTIGMA_g10029.t1	(1 of 1) K11836 - ubiquitin carboxyl-terminal hydrolase 5/13 [EC:3.4.19.12] (USP5_13, UBP14)
Cre02.g081176.t2.1	CEUSTIGMA_g11501.t1	NA
Cre02.g084650.t1.2	CEUSTIGMA_g10035.t1	(1 of 2) PTHR10997:SF7 - IMPORTIN-11
Cre02.g090600.t1.2	CEUSTIGMA_g9200.t1	(1 of 1) PTHR22652 - NUCLEOPORIN NUP43

Cre02.g090650.t1.1	CEUSTIGMA_g2072.t1	Endoplasmic reticulum Qb-SNARE protein, Sec20-family (Qb.I)
Cre02.g092400.t1.1	CEUSTIGMA_g4786.t1	(1 of 1) PTHR10693 - RAS GTPASE-ACTIVATING PROTEIN-BINDING PROTEIN
Cre02.g092950.t1.2	CEUSTIGMA_g1645.t1	NA
Cre02.g093950.t1.2	CEUSTIGMA_g7481.t1	(1 of 1) 2.7.4.22 - UMP kinase / Uridylate kinase
Cre02.g095082.t1.1	CEUSTIGMA_g11302.t1	(1 of 4) PTHR11875 - TESTIS-SPECIFIC Y-ENCODED PROTEIN
Cre02.g095106.t1.1	CEUSTIGMA_g11283.t1	(1 of 2) 2.7.8.5 - CDP-diacylglycerol--glycerol-3-phosphate 3-phosphatidyltransferase / Phosphatidylglycerophosphate synthase
Cre02.g095150.t1.2	CEUSTIGMA_g9223.t1	(1 of 543) 2.7.11.1 - Non-specific serine/threonine protein kinase / Threonine-specific protein kinase
Cre02.g097550.t1.2	CEUSTIGMA_g5304.t1	(1 of 1) PTHR12532:SF0 - TRANSCRIPTIONAL REGULATORY PROTEIN HAH1-RELATED
Cre02.g098200.t1.1	CEUSTIGMA_g12066.t1	(1 of 1) PTHR15898:SF1 - GLUCOSE-INDUCED DEGRADATION PROTEIN 4 HOMOLOG
Cre02.g098250.t1.2	CEUSTIGMA_g12067.t1	(1 of 1) PTHR13343//PTHR13343:SF4 - CREG1 PROTEIN // SUBFAMILY NOT NAMED
Cre02.g099650.t1.2	CEUSTIGMA_g5299.t1	(1 of 1) PF03661 - Uncharacterised protein family (UPF0121) (UPF0121)
Cre02.g103350.t1.1	CEUSTIGMA_g11707.t1	(1 of 1) 3.5.1.99 - Fatty acid amide hydrolase / Oleamide hydrolase
Cre02.g104600.t1.2	CEUSTIGMA_g11442.t1	(1 of 1) PTHR24148:SF18 - ANKYRIN REPEAT DOMAIN-CONTAINING PROTEIN 39
Cre02.g107700.t1.1	CEUSTIGMA_g4580.t1	(1 of 12) PF00646 - F-box domain (F-box)
Cre02.g108900.t1.2	CEUSTIGMA_g8488.t1	NA
Cre02.g109050.t1.2	CEUSTIGMA_g6378.t1	(1 of 85) PTHR21228 - FAST LEU-RICH DOMAIN-CONTAINING
Cre02.g112200.t1.2	CEUSTIGMA_g2473.t1	(1 of 1) KOG0265//KOG0279//KOG0319 - U5 snRNP-specific protein-like factor and related proteins // G protein beta subunit-like protein // WD40-repeat-containing subunit of the 18S rRNA processing complex
Cre02.g115150.t1.1	CEUSTIGMA_g3348.t1	NA
Cre02.g115850.t1.2	CEUSTIGMA_g1918.t1	(1 of 3) PF01987 - Mitochondrial biogenesis AIM24 (AIM24)
Cre02.g116300.t1.2	CEUSTIGMA_g11963.t1	(1 of 1) K15171 - transcription elongation factor SPT4 (SUPT4H1, SPT4)
Cre02.g117850.t1.2	CEUSTIGMA_g7637.t1	(1 of 1) K11835 - ubiquitin carboxyl-terminal hydrolase 4/11/15 [EC:3.4.19.12] (USP4_11_15, UBP12)
Cre02.g119150.t1.2	CEUSTIGMA_g11299.t1	(1 of 7) PF00169 - PH domain (PH)
Cre02.g120050.t1.2	CEUSTIGMA_g9482.t1	NA
Cre02.g120250.t2.1	CEUSTIGMA_g7636.t1	NA
Cre02.g141406.t1.1	CEUSTIGMA_g5532.t1	(1 of 3) PF05970//PF14214 - PIF1-like helicase (PIF1) // Helitron helicase-like domain at N-terminus (Helitron_like_N)
Cre02.g141500.t1.2	CEUSTIGMA_g13074.t1	NA
Cre02.g142352.t1.1	CEUSTIGMA_g13081.t1	(1 of 1) 6.1.1.21 - Histidine--tRNA ligase / Histidyl-tRNA synthetase
Cre02.g145950.t1.2	CEUSTIGMA_g657.t1	NA
Cre02.g146650.t1.1	CEUSTIGMA_g5732.t1	Tubulin tyrosine ligase
Cre03.g144647.t1.1	CEUSTIGMA_g12674.t1	NA
Cre03.g145107.t1.1	CEUSTIGMA_g8125.t1	(1 of 3) K10406 - kinesin family member C2/C3 (KIFC2_3)
Cre03.g145407.t1.1	CEUSTIGMA_g8083.t1	(1 of 18) PF00642 - Zinc finger C-x8-C-x5-C-x3-H type (and similar) (zf-CCCH)
Cre03.g145507.t1.1	CEUSTIGMA_g8102.t1	NA
Cre03.g146227.t1.1	CEUSTIGMA_g8100.t1	NA
Cre03.g146267.t1.1	CEUSTIGMA_g28.t1	NA

Cre03.g149300.t1.1	CEUSTIGMA_g5341.t1	(1 of 1) 2.8.4.5 - tRNA (N(6)-L-threonylcarbamoyladenosine(37)-C(2))-methylthiotransferase / Methylthio-threonylcarbamoyl-adenosine transferase B
Cre03.g153900.t1.2	CEUSTIGMA_g11562.t1	(1 of 5) 1.14.13.9 - Kynurenine 3-monooxygenase / Kynurenine 3-hydroxylase
Cre03.g155450.t1.1	CEUSTIGMA_g8391.t1	(1 of 4) PTHR16517 - TUBBY-RELATED
Cre03.g157050.t1.1	CEUSTIGMA_g2658.t1	(1 of 4) PF13515 - Fusaric acid resistance protein-like (FUSC_2)
Cre03.g157800.t1.1	CEUSTIGMA_g3184.t1	Thioredoxin-like protein
Cre03.g161050.t1.2	CEUSTIGMA_g2946.t1	(1 of 1) K10732 - GINS complex subunit 1 (GINS1, PSF1)
Cre03.g163300.t1.2	CEUSTIGMA_g3072.t1	DNA replication initiation factor, CDT1-like
Cre03.g164900.t2.1	CEUSTIGMA_g9643.t1	NA
Cre03.g165000.t1.2	CEUSTIGMA_g9641.t1	Translation elongation factor EFG/EF2, LepA-related
Cre03.g165215.t1.1	CEUSTIGMA_g12376.t1	(1 of 1) K08337 - ubiquitin-like modifier-activating enzyme ATG7 (ATG7)
Cre03.g169200.t1.2	CEUSTIGMA_g1575.t1	(1 of 1) 2.7.7.5 - Sulfate adenylyltransferase (ADP) / ADP-sulfurylase
Cre03.g169450.t1.1	CEUSTIGMA_g12171.t1	NA
Cre03.g169650.t1.1	CEUSTIGMA_g4961.t1	NA
Cre03.g171100.t1.1	CEUSTIGMA_g13727.t1	NA
Cre03.g171461.t1.1	CEUSTIGMA_g2870.t1	(1 of 1) 1.3.99.22 - Coproporphyrinogen dehydrogenase / Oxygen-independent coproporphyrinogen-III oxidase
Cre03.g173600.t1.2	CEUSTIGMA_g4943.t1	(1 of 2) KOG0001//KOG0005 - Ubiquitin and ubiquitin-like proteins // Ubiquitin-like protein
Cre03.g174950.t1.1	CEUSTIGMA_g10508.t1	(1 of 3) PTHR21493:SF87 - SN1-SPECIFIC DIACYLGLYCEROL LIPASE BETA
Cre03.g176200.t1.2	CEUSTIGMA_g5777.t1	(1 of 1) PTHR22904//PTHR22904:SF364 - TPR REPEAT CONTAINING PROTEIN // SUBFAMILY NOT NAMED
Cre03.g177053.t1.1	CEUSTIGMA_g5786.t1	(1 of 1) PTHR12696 - TIP120
Cre03.g182750.t1.2	CEUSTIGMA_g2013.t1	(1 of 2) KOG3774 - Uncharacterized conserved protein Lama
Cre03.g185200.t1.2	CEUSTIGMA_g7170.t1	Metallophosphoesterase/metallo-dependent phosphatase
Cre03.g185350.t1.1	CEUSTIGMA_g7146.t1	1,3-beta-D-glucan synthase
Cre03.g187050.t1.2	CEUSTIGMA_g10386.t1	(1 of 1) K12303 - MFS transporter, ACS family, solute carrier family 17 (sodium-dependent inorganic phosphate cotransporter), member 9 (SLC17A9)
Cre03.g188450.t1.2	CEUSTIGMA_g10419.t1	NA
Cre03.g189700.t1.2	CEUSTIGMA_g7185.t1	(1 of 2) K07735 - putative transcriptional regulator (algH)
Cre03.g190900.t1.1	CEUSTIGMA_g236.t1	(1 of 5) PTHR10351:SF42 - LD40663P
Cre03.g195500.t2.1	CEUSTIGMA_g145.t1	NA
Cre03.g196500.t1.1	CEUSTIGMA_g8007.t1	(1 of 1) PTHR12035 - SIALIC ACID BINDING IMMUNOGLOBULIN-LIKE LECTIN
Cre03.g197250.t1.1	CEUSTIGMA_g7905.t1	(1 of 1) PTHR13948//PTHR13948:SF25 - RNA-BINDING PROTEIN // SUBFAMILY NOT NAMED
Cre03.g200095.t1.1	CEUSTIGMA_g185.t1	(1 of 2) K11594 - ATP-dependent RNA helicase DDX3X (DDX3X, bel)
Cre03.g200600.t2.1	CEUSTIGMA_g11866.t1	NA
Cre03.g201750.t1.2	CEUSTIGMA_g13170.t1	NA
Cre03.g202113.t1.1	CEUSTIGMA_g12361.t1	(1 of 1) 6.3.2.6 - Phosphoribosylaminoimidazolesuccinocarboxamide synthase / SAICARs
Cre03.g205697.t1.1	CEUSTIGMA_g3425.t1	(1 of 2) PTHR23155:SF401 - LEUCINE-RICH REPEAT-CONTAINING PROTEIN
Cre03.g205950.t1.1	CEUSTIGMA_g8944.t1	(1 of 6) KOG0198//KOG0583 - MEKK and related serine/threonine protein kinases // Serine/threonine protein kinase

Cre03.g206257.t1.1	CEUSTIGMA_g4320.t1	(1 of 8) KOG0192//KOG1187 - Tyrosine kinase specific for activated (GTP-bound) p21cdc42Hs // Serine/threonine protein kinase
Cre03.g209393.t1.1	CEUSTIGMA_g3.t1	(1 of 2) K05894 - 12-oxophytodienoic acid reductase (OPR)
Cre03.g211745.t1.1	CEUSTIGMA_g9588.t1	(1 of 1) K00666 - fatty-acyl-CoA synthase [EC:6.2.1.-] (K00666)
Cre04.g211600.t1.1	CEUSTIGMA_g10824.t1	(1 of 1) PTHR24343//PTHR24343:SF183 - SERINE/THREONINE KINASE // SUBFAMILY NOT NAMED
Cre04.g214097.t1.1	CEUSTIGMA_g723.t1	(1 of 1) PTHR21419:SF23 - DEFECTIVE IN EXINE FORMATION PROTEIN DEX1
Cre04.g214503.t2.1	CEUSTIGMA_g8209.t1	NA
Cre04.g214900.t1.1	CEUSTIGMA_g4975.t1	NA
Cre04.g215600.t2.1	CEUSTIGMA_g7150.t1	NA
Cre04.g217934.t1.1	CEUSTIGMA_g9362.t1	(1 of 1) K07101 - uncharacterized protein (K07101)
Cre04.g217935.t1.1	CEUSTIGMA_g7007.t1	(1 of 1) K11886 - proteasome component ECM29 (ECM29)
Cre04.g221250.t1.2	CEUSTIGMA_g3416.t1	(1 of 1) PF11378 - Protein of unknown function (DUF3181) (DUF3181)
Cre04.g222500.t1.1	CEUSTIGMA_g520.t1	NA
Cre04.g222700.t1.2	CEUSTIGMA_g10533.t1	(1 of 2) K03235 - elongation factor 3 (EF3, TEF3)
Cre04.g223900.t1.1	CEUSTIGMA_g2721.t1	(1 of 2) K09313 - homeobox protein cut-like (CUTL)
Cre04.g224150.t1.2	CEUSTIGMA_g521.t1	(1 of 1) 2.7.1.30 - Glycerol kinase / Glycerokinase
Cre04.g226500.t1.1	CEUSTIGMA_g512.t1	NA
Cre05.g234500.t1.1	CEUSTIGMA_g9545.t1	(1 of 1) K11801 - WD repeat-containing protein 23 (WDR23)
Cre05.g235102.t1.1	CEUSTIGMA_g7691.t1	NA
Cre05.g235400.t1.2	CEUSTIGMA_g12909.t1	(1 of 2) PTHR24559:SF208 - KRAB-A DOMAIN-CONTAINING PROTEIN 2
Cre05.g239100.t1.1	CEUSTIGMA_g3652.t1	(1 of 1) K01930 - folylpolyglutamate synthase (FPGS)
Cre05.g240150.t1.2	CEUSTIGMA_g12776.t1	(1 of 1) K10689 - peroxin-4 [EC:6.3.2.19] (PEX4)
Cre05.g242650.t1.1	CEUSTIGMA_g6338.t1	NA
Cre05.g243801.t3.1	CEUSTIGMA_g9481.t1	NA
Cre05.g244800.t1.2	CEUSTIGMA_g9885.t1	(1 of 1) PTHR13194:SF19 - NAD(P)-BINDING ROSSMANN-FOLD SUPERFAMILY PROTEIN
Cre05.g246050.t2.1	CEUSTIGMA_g10648.t1	NA
Cre05.g246377.t1.1	CEUSTIGMA_g8106.t1	(1 of 1) 3.5.4.2 - Adenine deaminase / Adenine aminase
Cre05.g246950.t1.1	CEUSTIGMA_g9463.t1	NA
Cre05.g247850.t1.1	CEUSTIGMA_g6485.t1	(1 of 3) 3.6.1.22//3.6.1.55 - NAD(+) diphosphatase / NADP pyrophosphatase // 8-oxo-dGTP diphosphatase / 8-oxo-dGTPase
Cre06.g248750.t1.1	CEUSTIGMA_g200.t1	NA
Cre06.g251250.t1.1	CEUSTIGMA_g1015.t1	(1 of 1) PF00072//PF00512//PF02518 - Response regulator receiver domain (Response_reg) // His Kinase A (phospho-acceptor) domain (HisKA) // Histidine kinase-, DNA gyrase B-, and HSP90-like ATPase (HATPase_c)
Cre06.g255050.t2.1	CEUSTIGMA_g6240.t1	NA
Cre06.g258100.t1.1	CEUSTIGMA_g6461.t1	(1 of 1) PTHR12436:SF4 - LEUKOCYTE RECEPTOR CLUSTER MEMBER 8
Cre06.g258733.t1.1	CEUSTIGMA_g5249.t1	NA
Cre06.g258800.t1.1	CEUSTIGMA_g3356.t1	Hydroxyproline-rich glycoprotein component of the outer cell wall
Cre06.g263289.t1.2	CEUSTIGMA_g3456.t1	(1 of 1) 2.5.1.87 - Ditrans,polycis-polyprenyl diphosphate synthase ((2E,6E)-farnesyl diphosphate specific) / Rer2p Z-prenyltransferase
Cre06.g264250.t1.1	CEUSTIGMA_g1022.t1	(1 of 3) 5.5.1.19 - Lycopene beta-cyclase
Cre06.g265150.t1.1	CEUSTIGMA_g1923.t1	(1 of 1) K11833 - ubiquitin carboxyl-terminal hydrolase 2/21 [EC:3.4.19.12] (USP2_21)
Cre06.g267800.t2.1	CEUSTIGMA_g3460.t1	NA

Cre06.g268550.t2.1	CEUSTIGMA_g2745.t1	NA
Cre06.g269200.t3.1	CEUSTIGMA_g3287.t1	(1 of 2) 2.7.11.1//4.6.1.1 - Non-specific serine/threonine protein kinase / Threonine-specific protein kinase // Adenylate cyclase / ATP pyrophosphate-lyase
Cre06.g269752.t1.2	CEUSTIGMA_g11481.t1	(1 of 2) PTHR10438:SF255 - THIOREDOXIN M4, CHLOROPLASTIC
Cre06.g269865.t2.1	CEUSTIGMA_g8984.t1	NA
Cre06.g270800.t1.2	CEUSTIGMA_g12246.t1	NA
Cre06.g271450.t1.1	CEUSTIGMA_g11469.t1	NA
Cre06.g272000.t1.1	CEUSTIGMA_g8614.t1	(1 of 1) PTHR10281:SF1 - VACUOLE MEMBRANE PROTEIN 1
Cre06.g272350.t1.2	CEUSTIGMA_g8613.t1	NA
Cre06.g272900.t1.2	CEUSTIGMA_g7812.t1	(1 of 2) 5.4.99.9 - UDP-galactopyranose mutase
Cre06.g273300.t1.2	CEUSTIGMA_g12258.t1	(1 of 2) 6.1.1.3 - Threonine--tRNA ligase / Threonyl-tRNA synthetase
Cre06.g275150.t1.2	CEUSTIGMA_g2399.t1	Triacylglycerol lipase
Cre06.g277100.t1.2	CEUSTIGMA_g2407.t1	(1 of 1) KOG2733 - Uncharacterized membrane protein
Cre06.g278126.t1.1	CEUSTIGMA_g6162.t1	NA
Cre06.g278142.t1.1	CEUSTIGMA_g5063.t1	(1 of 1) K14441 - ribosomal protein S12 methylthiotransferase [EC:2.8.4.4] (rimO)
Cre06.g278950.t1.1	CEUSTIGMA_g10198.t1	NA
Cre06.g279000.t1.2	CEUSTIGMA_g10199.t1	20S proteasome beta subunit A1
Cre06.g279400.t1.2	CEUSTIGMA_g10077.t1	(1 of 3) K09645 - vitellogenic carboxypeptidase-like protein [EC:3.4.16.-] (CPVL)
Cre06.g280200.t1.1	CEUSTIGMA_g5699.t1	(1 of 1) PTHR15141 - TRANSCRIPTION ELONGATION FACTOR B POLYPEPTIDE 3
Cre06.g280700.t1.2	CEUSTIGMA_g9384.t1	(1 of 2) PF10197 - N-terminal domain of CBF1 interacting co-repressor CIR (Cir_N)
Cre06.g280900.t2.1	CEUSTIGMA_g9821.t1	NA
Cre06.g282950.t1.2	CEUSTIGMA_g1296.t1	(1 of 1) PTHR12875:SF0 - GOLGI TO ER TRAFFIC PROTEIN 4 HOMOLOG
Cre06.g283634.t2.1	CEUSTIGMA_g12694.t1	(1 of 1) PTHR14304 - P30 DBC PROTEIN
Cre06.g284650.t1.2	CEUSTIGMA_g2677.t1	Dual-specificity protein phosphatase
Cre06.g285200.t1.1	CEUSTIGMA_g912.t1	(1 of 1) 3.6.1.18 - FAD diphosphatase / FAD pyrophosphatase
Cre06.g289500.t1.2	CEUSTIGMA_g135.t1	NA
Cre06.g292650.t1.1	CEUSTIGMA_g10839.t1	(1 of 3) K06236 - collagen, type I/II/III/V/XI/XXIV/XXVII, alpha (COL1AS)
Cre06.g294700.t1.1	CEUSTIGMA_g1116.t1	(1 of 1) KOG1003//KOG2685 - Actin filament-coating protein tropomyosin // Cystoskeletal protein Tektin
Cre06.g295550.t1.2	CEUSTIGMA_g3801.t1	(1 of 7) PF07883 - Cupin domain (Cupin_2)
Cre06.g297650.t2.1	CEUSTIGMA_g1577.t1	NA
Cre06.g299050.t1.2	CEUSTIGMA_g10214.t1	(1 of 4) K14457 - 2-acylglycerol O-acyltransferase 2 (MOGAT2, MGAT2)
Cre06.g301100.t1.1	CEUSTIGMA_g1112.t1	(1 of 4) PF04232 - Stage V sporulation protein S (SpoVS) (SpoVS)
Cre06.g304100.t1.2	CEUSTIGMA_g2489.t1	(1 of 1) K17261 - adenylyl cyclase-associated protein (CAP1_2, SRV2)
Cre06.g307551.t1.1	CEUSTIGMA_g4345.t1	NA
Cre06.g308450.t1.2	CEUSTIGMA_g4356.t1	(1 of 1) PTHR35299:SF2 - RUBISCO ACCUMULATION FACTOR 1, CHLOROPLASTIC-RELATED
Cre07.g320150.t1.2	CEUSTIGMA_g2958.t1	DnaJ-like protein, ER-targeted
Cre07.g320550.t1.2	CEUSTIGMA_g11267.t1	(1 of 3) K15397 - 3-ketoacyl-CoA synthase (KCS)
Cre07.g321100.t1.2	CEUSTIGMA_g2543.t1	(1 of 1) PTHR10196:SF67 - SEDOHEPTULOKINASE
Cre07.g321550.t1.2	CEUSTIGMA_g7985.t1	(1 of 9) PF00170 - bZIP transcription factor (bZIP_1)

Cre07.g321850.t1.2	CEUSTIGMA_g10469.t1	(1 of 1) PTHR13009//PTHR13009:SF5 - HEAT SHOCK PROTEIN 90 HSP90 CO-CHAPERONE AHA-1 // SUBFAMILY NOT NAMED
Cre07.g323100.t1.1	CEUSTIGMA_g10465.t1	Serine/threonine protein kinase
Cre07.g323950.t1.2	CEUSTIGMA_g5656.t1	(1 of 1) PTHR10869//PTHR10869:SF50 - PROLYL 4-HYDROXYLASE ALPHA SUBUNIT // SUBFAMILY NOT NAMED
Cre07.g326600.t1.2	CEUSTIGMA_g4990.t1	(1 of 4) K09584 - protein disulfide-isomerase A6 (PDIA6, TXNDC7)
Cre07.g329250.t1.1	CEUSTIGMA_g12097.t1	(1 of 1) PF02492//PF07683//PF13414 - CobW/HypB/UreG, nucleotide-binding domain (cobW) // Cobalamin synthesis protein cobW C-terminal domain (CobW_C) // TPR repeat (TPR_11)
Cre07.g329350.t1.2	CEUSTIGMA_g8895.t1	(1 of 83) PTHR12203 - KDEL LYS-ASP-GLU-LEU CONTAINING - RELATED
Cre07.g329600.t2.1	CEUSTIGMA_g8148.t1	NA
Cre07.g330500.t1.2	CEUSTIGMA_g11609.t1	(1 of 4) PF04232 - Stage V sporulation protein S (SpoVS) (SpoVS)
Cre07.g334200.t1.2	CEUSTIGMA_g1202.t1	(1 of 1) K13116 - ATP-dependent RNA helicase DDX41 [EC:3.6.4.13] (DDX41, ABS)
Cre07.g336200.t1.1	CEUSTIGMA_g9347.t1	(1 of 1) K11838 - ubiquitin carboxyl-terminal hydrolase 7 (USP7, UBP15)
Cre07.g336350.t1.1	CEUSTIGMA_g8425.t1	(1 of 1) PTHR24012:SF432 - HEPHAESTUS
Cre07.g341300.t1.2	CEUSTIGMA_g8492.t1	(1 of 1) K13119 - protein FAM50 (FAM50, XAP5)
Cre07.g342000.t1.1	CEUSTIGMA_g8494.t1	(1 of 4) 2.1.1.77 - Protein-L-isoaspartate(D-aspartate) O-methyltransferase / Protein L-isoaspartyl methyltransferase
Cre07.g342920.t1.2	CEUSTIGMA_g13495.t1	(1 of 2) 3.4.13.9 - Xaa-Pro dipeptidase / X-Pro dipeptidase
Cre07.g344300.t1.2	CEUSTIGMA_g8648.t1	NA
Cre07.g344400.t1.2	CEUSTIGMA_g8661.t1	(1 of 3) 1.1.1.95 - Phosphoglycerate dehydrogenase / Phosphoglyceric acid dehydrogenase
Cre07.g347100.t1.2	CEUSTIGMA_g10630.t1	(1 of 2) 5.1.3.15 - Glucose-6-phosphate 1-epimerase
Cre07.g348350.t1.2	CEUSTIGMA_g12118.t1	(1 of 15) PF04720 - PDDEXK-like family of unknown function (PDDEXK_6)
Cre07.g350926.t1.1	CEUSTIGMA_g547.t1	NA
Cre07.g351550.t1.1	CEUSTIGMA_g12862.t1	(1 of 1) PTHR31319:SF1 - CCT MOTIF FAMILY PROTEIN
Cre07.g352500.t1.1	CEUSTIGMA_g12407.t1	NA
Cre07.g357157.t1.2	CEUSTIGMA_g12414.t1	(1 of 1) 1.14.13.99 - 24-hydroxycholesterol 7-alpha-hydroxylase / 24-hydroxycholesterol 7-alpha-monooxygenase
Cre07.g357900.t1.2	CEUSTIGMA_g12405.t1	(1 of 1) K08054 - calnexin (CANX)
Cre08.g358525.t1.1	CEUSTIGMA_g10589.t1	(1 of 4) 1.11.1.9 - Glutathione peroxidase
Cre08.g358534.t1.1	CEUSTIGMA_g10620.t1	(1 of 8) PTHR10071 - TRANSCRIPTION FACTOR GATA GATA BINDING FACTOR
Cre08.g361500.t1.2	CEUSTIGMA_g10220.t1	(1 of 1) PF14943 - Mitochondrial ribosome subunit S26 (MRP-S26)
Cre08.g362750.t1.2	CEUSTIGMA_g13656.t1	(1 of 1) K01173 - endonuclease G, mitochondrial (ENDOG)
Cre08.g363874.t2.1	CEUSTIGMA_g2945.t1	NA
Cre08.g366400.t1.2	CEUSTIGMA_g7417.t1	(1 of 1) K10839 - UV excision repair protein RAD23 (RAD23, HR23)
Cre08.g367150.t2.1	CEUSTIGMA_g3484.t1	NA
Cre08.g367750.t1.1	CEUSTIGMA_g5205.t1	(1 of 83) PTHR12203 - KDEL LYS-ASP-GLU-LEU CONTAINING - RELATED
Cre08.g368700.t1.1	CEUSTIGMA_g11069.t1	(1 of 1) PTHR13271//PTHR13271:SF40 - UNCHARACTERIZED PUTATIVE METHYLTRANSFERASE // SUBFAMILY NOT NAMED
Cre08.g370850.t1.1	CEUSTIGMA_g12098.t1	(1 of 1) K10579 - ubiquitin-conjugating enzyme E2 M (UBE2M, UBC12)
Cre08.g371052.t1.1	CEUSTIGMA_g2161.t1	NA
Cre08.g371400.t1.1	CEUSTIGMA_g11764.t1	(1 of 1) PTHR22763//PTHR22763:SF34 - RING ZINC FINGER PROTEIN // SUBFAMILY NOT NAMED

Cre08.g372850.t1.2	CEUSTIGMA_g3883.t1	(1 of 1) PTHR10876 - ZINC FINGER PROTEIN ZPR1
Cre08.g374100.t1.1	CEUSTIGMA_g1848.t1	NA
Cre08.g378100.t1.1	CEUSTIGMA_g1937.t1	(1 of 1) K10745 - ribonuclease H2 subunit C (RNASEH2C)
Cre08.g378200.t1.2	CEUSTIGMA_g12018.t1	(1 of 1) 5.1.99.6 - NAD(P)H-hydrate epimerase / NAD(P)HX epimerase
Cre08.g378800.t1.2	CEUSTIGMA_g1924.t1	(1 of 1) PTHR10071:SF159 - GATA TRANSCRIPTION FACTOR 26-RELATED
Cre08.g379500.t1.1	CEUSTIGMA_g462.t1	(1 of 56) 2.7.12.1 - Dual-specificity kinase
Cre08.g380000.t1.2	CEUSTIGMA_g7390.t1	(1 of 1) PTHR23150 - SULFATASE MODIFYING FACTOR 1, 2
Cre08.g381900.t1.2	CEUSTIGMA_g1796.t1	(1 of 2) PTHR22763:SF71 - PROTEIN Y105C5B.11, ISOFORM B
Cre08.g381950.t1.2	CEUSTIGMA_g1795.t1	(1 of 1) K18670 - dual specificity protein kinase YAK1 [EC:2.7.12.1] (YAK1)
Cre08.g383450.t1.1	CEUSTIGMA_g6509.t1	(1 of 3) PF08495 - FIST N domain (FIST)
Cre08.g384600.t1.2	CEUSTIGMA_g13746.t1	(1 of 2) 3.1.1.81 - Quorum-quenching N-acyl-homoserine lactonase / Quorum-quenching N-acyl homoserine lactone hydrolase
Cre08.g386050.t1.2	CEUSTIGMA_g13121.t1	(1 of 1) PTHR12917:SF11 - RHOMBOID DOMAIN-CONTAINING PROTEIN 2
Cre09.g386350.t1.1	CEUSTIGMA_g13638.t1	(1 of 2) K03145 - transcription elongation factor S-II (TFIIS)
Cre09.g386912.t1.1	CEUSTIGMA_g1974.t1	(1 of 4) K14457 - 2-acylglycerol O-acyltransferase 2 (MOGAT2, MGAT2)
Cre09.g387134.t1.1	CEUSTIGMA_g4211.t1	(1 of 4) PTHR14289 - F-BOX ONLY PROTEIN 3
Cre09.g388615.t1.1	CEUSTIGMA_g8775.t1	(1 of 1) K06965 - protein pelota (PELO, DOM34, pelA)
Cre09.g389430.t1.1	CEUSTIGMA_g8776.t1	(1 of 1) PTHR11538:SF40 - PHENYLALANINE--TRNA LIGASE ALPHA SUBUNIT
Cre09.g389450.t1.2	CEUSTIGMA_g4154.t1	(1 of 2) PF00076//PF04564 - RNA recognition motif. (a.k.a. RRM, RBD, or RNP domain) (RRM_1) // U-box domain (U-box)
Cre09.g389467.t1.1	CEUSTIGMA_g8052.t1	NA
Cre09.g389726.t1.1	CEUSTIGMA_g8051.t1	NA
Cre09.g389912.t1.1	CEUSTIGMA_g9313.t1	(1 of 1) K14018 - phospholipase A-2-activating protein (PLAA, DOA1, UFD3)
Cre09.g390282.t1.1	CEUSTIGMA_g6012.t1	(1 of 1) PTHR21433 - TRANSMEMBRANE PROTEIN INDUCED BY TUMOR NECROSIS FACTOR ALPHA
Cre09.g390319.t1.1	CEUSTIGMA_g8046.t1	(1 of 1) PTHR10663:SF186 - PROTEIN M02B7.5, ISOFORM A
Cre09.g390430.t1.1	CEUSTIGMA_g4116.t1	(1 of 1) K13108 - smad nuclear-interacting protein 1 (SNIP1)
Cre09.g392208.t1.1	CEUSTIGMA_g8022.t1	NA
Cre09.g393550.t1.1	CEUSTIGMA_g8877.t1	(1 of 1) 2.7.11.25//2.7.12.2 - Mitogen-activated protein kinase kinase kinase / MLTK // Mitogen-activated protein kinase kinase / MKK
Cre09.g393913.t1.1	CEUSTIGMA_g5513.t1	(1 of 1) 3.5.4.16 - GTP cyclohydrolase I
Cre09.g394917.t1.1	CEUSTIGMA_g8563.t1	(1 of 4) PTHR16255:SF4 - SPORULATION PROTEIN RMD8
Cre09.g395028.t1.1	CEUSTIGMA_g12033.t1	(1 of 2) PF02470 - MlaD protein (MlaD)
Cre09.g395300.t1.2	CEUSTIGMA_g1214.t1	(1 of 1) PTHR11736 - MELANOMA-ASSOCIATED ANTIGEN MAGE ANTIGEN
Cre09.g396139.t1.1	CEUSTIGMA_g935.t1	(1 of 4) K14326 - regulator of nonsense transcripts 1 (UPF1, RENT1)
Cre09.g398350.t1.2	CEUSTIGMA_g1601.t1	(1 of 1) K10597 - ubiquitin conjugation factor E4 B (UBE4B, UFD2)
Cre09.g398750.t1.2	CEUSTIGMA_g1373.t1	(1 of 26) KOG1187 - Serine/threonine protein kinase
Cre09.g401330.t1.1	CEUSTIGMA_g6437.t1	Phosphoglycolate phosphatase
Cre09.g403034.t1.1	CEUSTIGMA_g3169.t1	(1 of 1) PTHR14119 - HYDROLASE
Cre09.g404650.t1.2	CEUSTIGMA_g5279.t1	(1 of 1) PTHR15954:SF4 - VACUOLAR PROTEIN SORTING-ASSOCIATED PROTEIN 51 HOMOLOG
Cre09.g405350.t1.2	CEUSTIGMA_g2782.t1	NA
Cre09.g407150.t1.1	CEUSTIGMA_g10014.t1	NA

Cre09.g410050.t1.2	CEUSTIGMA_g4516.t1	(1 of 12) 3.6.3.8 - Calcium-transporting ATPase / Calcium-translocating P-type ATPase
Cre09.g413100.t1.1	CEUSTIGMA_g10702.t1	(1 of 30) PF03407 - Nucleotide-diphospho-sugar transferase (Nucleotid_trans)
Cre09.g414800.t2.1	CEUSTIGMA_g7074.t1	NA
Cre09.g415200.t1.1	CEUSTIGMA_g5340.t1	(1 of 1) K17583 - nucleolar MIF4G domain-containing protein 1 (NOM1)
Cre09.g415800.t1.2	CEUSTIGMA_g7055.t1	(1 of 1) K16865 - programmed cell death protein 4 (PDCD4)
Cre10.g417500.t1.2	CEUSTIGMA_g9603.t1	Peptidyl-prolyl cis-trans isomerase, cyclophilin-type
Cre10.g419550.t1.2	CEUSTIGMA_g671.t1	(1 of 2) PTHR28141:SF1 - 2',3'-CYCLIC-NUCLEOTIDE 3'-PHOSPHODIESTERASE
Cre10.g420200.t2.1	CEUSTIGMA_g11378.t1	NA
Cre10.g422150.t1.1	CEUSTIGMA_g10601.t1	(1 of 1) 3.4.16.2 - Lysosomal Pro-Xaa carboxypeptidase / Prolyl carboxypeptidase
Cre10.g429000.t1.1	CEUSTIGMA_g360.t1	NA
Cre10.g429100.t1.2	CEUSTIGMA_g4437.t1	(1 of 1) PTHR11451:SF21 - BIFUNCTIONAL GLUTAMATE/PROLINE--TRNA LIGASE
Cre10.g430750.t1.1	CEUSTIGMA_g4265.t1	(1 of 1) PTHR24078:SF261 - DNAJ (HSP40) HOMOLOG, SUBFAMILY A, MEMBER 3A
Cre10.g430900.t1.1	CEUSTIGMA_g1231.t1	(1 of 5) PTHR19302 - GAMMA TUBULIN COMPLEX PROTEIN
Cre10.g431500.t1.1	CEUSTIGMA_g13123.t1	NA
Cre10.g432100.t1.2	CEUSTIGMA_g8090.t1	(1 of 1) PTHR34687:SF1 - CHAPERONE PROTEIN DNAJ-LIKE PROTEIN
Cre10.g434500.t1.1	CEUSTIGMA_g11589.t1	(1 of 29) PTHR24349:SF79 - NITROGEN NETWORK KINASE 1
Cre10.g439050.t1.2	CEUSTIGMA_g4880.t1	Mitochondrial substrate carrier protein
Cre10.g439550.t2.1	CEUSTIGMA_g387.t1	NA
Cre10.g441000.t1.2	CEUSTIGMA_g12801.t1	(1 of 1) K17498 - transcription factor SPN1 (SPN1, IWS1)
Cre10.g441350.t2.1	CEUSTIGMA_g5700.t1	NA
Cre10.g442450.t1.2	CEUSTIGMA_g11123.t1	(1 of 34) PF13639 - Ring finger domain (zf-RING_2)
Cre10.g443850.t1.1	CEUSTIGMA_g11499.t1	(1 of 1) PTHR11851:SF136 - PROTEIN YHJJ
Cre10.g444950.t1.2	CEUSTIGMA_g10030.t1	NA
Cre10.g446000.t1.1	CEUSTIGMA_g7296.t1	(1 of 3) PF10358 - N-terminal C2 in EEIG1 and EHBP1 proteins (NT-C2)
Cre10.g446400.t1.1	CEUSTIGMA_g4027.t1	Katanin p60 catalytic subunit
Cre10.g446450.t1.2	CEUSTIGMA_g8352.t1	(1 of 1) PTHR26402:SF316 - TRANSCRIPTIONAL REGULATORY PROTEIN CUSR
Cre10.g453807.t2.1	CEUSTIGMA_g4353.t1	NA
Cre10.g454025.t1.1	CEUSTIGMA_g1217.t1	NA
Cre10.g454400.t1.1	CEUSTIGMA_g8267.t1	(1 of 1) K10632 - BRCA1-associated protein (BRAP)
Cre10.g454734.t2.1	CEUSTIGMA_g4246.t1	NA
Cre10.g455650.t1.2	CEUSTIGMA_g7260.t1	(1 of 1) 2.1.1.10 - Homocysteine S-methyltransferase
Cre10.g456800.t1.1	CEUSTIGMA_g12292.t1	(1 of 2) PF09733 - VEFS-Box of polycomb protein (VEFS-Box)
Cre10.g461851.t3.1	CEUSTIGMA_g3683.t1	NA
Cre10.g461950.t1.2	CEUSTIGMA_g2316.t1	20S proteasome beta subunit E, type beta 5
Cre10.g462700.t1.1	CEUSTIGMA_g2387.t1	(1 of 1) K14397 - cleavage and polyadenylation specificity factor subunit 5 (NUDT21, CPSF5, CFIM25)
Cre10.g466000.t1.2	CEUSTIGMA_g2508.t1	(1 of 1) K18179 - cytochrome c oxidase assembly factor 6 (COA6)
Cre10.g466100.t1.2	CEUSTIGMA_g12300.t1	NA
Cre11.g467350.t1.2	CEUSTIGMA_g10309.t1	(1 of 2) PTHR10909:SF317 - ACYL-COENZYME A OXIDASE 2, PEROXISOMAL

Cre11.g467563.t1.1	CEUSTIGMA_g10304.t1	(1 of 10) PTHR10174 - RETINALDEHYDE BINDING PROTEIN-RELATED
Cre11.g467637.t1.1	CEUSTIGMA_g9676.t1	(1 of 11) PF00627 - UBA/TS-N domain (UBA)
Cre11.g467702.t1.1	CEUSTIGMA_g11666.t1	(1 of 2) PF00189 - Ribosomal protein S3, C-terminal domain (Ribosomal_S3_C)
Cre11.g467711.t2.1	CEUSTIGMA_g9021.t1	NA
Cre11.g468900.t1.2	CEUSTIGMA_g10266.t1	NA
Cre11.g469224.t1.1	CEUSTIGMA_g8140.t1	NA
Cre11.g477500.t1.2	CEUSTIGMA_g13195.t1	(1 of 1) KOG2886 - Uncharacterized conserved protein
Cre11.g479250.t1.2	CEUSTIGMA_g8297.t1	(1 of 1) K14319 - Ran GTPase-activating protein 1 (RANGAP1)
Cre11.g480650.t1.2	CEUSTIGMA_g11298.t1	(1 of 11) 1.1.1.300 - NADP-retinol dehydrogenase / Retinol dehydrogenase (NADP(+))
Cre12.g492450.t1.2	CEUSTIGMA_g1510.t1	(1 of 3) PTHR18934:SF145 - ATP-DEPENDENT RNA HELICASE DHX57-RELATED
Cre12.g492850.t1.1	CEUSTIGMA_g473.t1	(1 of 1) PF10595 - Uncharacterised protein family UPF0564 (UPF0564)
Cre12.g493000.t1.2	CEUSTIGMA_g11423.t1	(1 of 3) PTHR16254 - POTASSIUM/PROTON ANTIPORTER-RELATED
Cre12.g493300.t1.2	CEUSTIGMA_g694.t1	(1 of 5) PTHR10582 - TRANSIENT RECEPTOR POTENTIAL ION CHANNEL PROTEIN
Cre12.g497350.t1.1	CEUSTIGMA_g2101.t1	NA
Cre12.g498450.t1.2	CEUSTIGMA_g11671.t1	(1 of 1) K11493 - regulator of chromosome condensation (RCC1)
Cre12.g499750.t1.1	CEUSTIGMA_g5597.t1	(1 of 90) PF00076 - RNA recognition motif. (a.k.a. RRM, RBD, or RNP domain) (RRM_1)
Cre12.g500100.t1.2	CEUSTIGMA_g5661.t1	NA
Cre12.g503250.t1.2	CEUSTIGMA_g10553.t1	NA
Cre12.g503350.t1.2	CEUSTIGMA_g5584.t1	NA
Cre12.g507050.t1.2	CEUSTIGMA_g7558.t1	(1 of 543) 2.7.11.1 - Non-specific serine/threonine protein kinase / Threonine-specific protein kinase
Cre12.g508450.t1.1	CEUSTIGMA_g1833.t1	(1 of 39) PTHR12298 - PCDC2 PROGRAMMED CELL DEATH PROTEIN 2 -RELATED
Cre12.g508850.t1.1	CEUSTIGMA_g4567.t1	(1 of 1) PTHR11260//PTHR11260:SF225 - GLUTATHIONE S-TRANSFERASE, GST, SUPERFAMILY, GST DOMAIN CONTAINING // SUBFAMILY NOT NAMED
Cre12.g513600.t1.2	CEUSTIGMA_g5614.t1	(1 of 1) K12795 - suppressor of G2 allele of SKP1 (SUGT1, SGT1)
Cre12.g516750.t2.1	CEUSTIGMA_g1864.t1	NA
Cre12.g522300.t1.1	CEUSTIGMA_g11435.t1	(1 of 1) KOG1909//KOG4308 - Ran GTPase-activating protein // LRR-containing protein
Cre12.g522650.t1.1	CEUSTIGMA_g13747.t1	(1 of 2) 2.4.1.232 - Initiation-specific alpha-1,6-mannosyltransferase / Glycolipid 6-alpha-mannosyltransferase
Cre12.g524650.t2.1	CEUSTIGMA_g7.t1	NA
Cre12.g527600.t1.1	CEUSTIGMA_g2226.t1	(1 of 1) K12865 - polyglutamine-binding protein 1 (PQBP1, NPW38)
Cre12.g529450.t2.1	CEUSTIGMA_g1464.t1	NA
Cre12.g531100.t2.1	CEUSTIGMA_g96.t1	NA
Cre12.g537100.t1.2	CEUSTIGMA_g1336.t1	(1 of 2) 6.1.1.9 - Valine--tRNA ligase / Valyl-tRNA synthetase
Cre12.g537671.t1.1	CEUSTIGMA_g1325.t1	(1 of 1) PTHR10799//PTHR10799:SF677 - SWI/SNF-RELATED MATRIX-ASSOCIATED ACTIN-DEPENDENT REGULATOR OF CHROMATIN SUBFAMILY-RELATED // SUBFAMILY NOT NAMED
Cre12.g538100.t1.2	CEUSTIGMA_g9211.t1	(1 of 3) K07393 - putative glutathione S-transferase (ECM4)
Cre12.g538150.t1.2	CEUSTIGMA_g12615.t1	(1 of 1) K05019 - chloride channel, nucleotide-sensitive, 1A (CLNS1A)

Cre12.g538200.t1.2	CEUSTIGMA_g12616.t1	(1 of 1) PTHR23305//PTHR23305:SF1 - GTP-BINDING PROTEIN-RELATED // SUBFAMILY NOT NAMED
Cre12.g538700.t1.2	CEUSTIGMA_g1340.t1	(1 of 2) PTHR14009 - LEUCINE ZIPPER-EF-HAND CONTAINING TRANSMEMBRANE PROTEIN
Cre12.g539050.t1.1	CEUSTIGMA_g4140.t1	(1 of 3) PF08700 - Vps51/Vps67 (Vps51)
Cre12.g539150.t1.2	CEUSTIGMA_g11273.t1	NA
Cre12.g542750.t1.1	CEUSTIGMA_g1368.t1	NA
Cre12.g543303.t1.1	CEUSTIGMA_g6734.t1	NA
Cre12.g543902.t1.1	CEUSTIGMA_g2085.t1	(1 of 1) 2.7.1.16 - Ribulokinase / L-ribulokinase
Cre12.g546900.t2.1	CEUSTIGMA_g2279.t1	NA
Cre12.g547400.t1.1	CEUSTIGMA_g6520.t1	(1 of 4) KOG2944 - Glyoxalase
Cre12.g548200.t1.1	CEUSTIGMA_g6648.t1	(1 of 1) PTHR21004 - SERINE PROTEASE-RELATED
Cre12.g557250.t2.1	CEUSTIGMA_g9837.t1	NA
Cre12.g557700.t1.2	CEUSTIGMA_g4859.t1	(1 of 1) K01069 - hydroxyacylglutathione hydrolase (E3.1.2.6, gloB)
Cre12.g558850.t1.2	CEUSTIGMA_g9608.t1	NA
Cre12.g559050.t1.2	CEUSTIGMA_g5476.t1	(1 of 1) PTHR24006:SF22 - BCDNA.LD22910
Cre12.g559200.t1.1	CEUSTIGMA_g5467.t1	NA
Cre13.g561800.t1.1	CEUSTIGMA_g119.t1	(1 of 32) PF00168 - C2 domain (C2)
Cre13.g562750.t1.2	CEUSTIGMA_g5665.t1	(1 of 1) PF14234 - Domain of unknown function (DUF4336) (DUF4336)
Cre13.g566650.t2.1	CEUSTIGMA_g2572.t1	NA
Cre13.g569500.t2.1	CEUSTIGMA_g3056.t1	NA
Cre13.g573150.t1.1	CEUSTIGMA_g3796.t1	(1 of 1) PTHR12103:SF15 - PROTEIN Y71H10B.1, ISOFORM C
Cre13.g574041.t1.1	CEUSTIGMA_g1169.t1	(1 of 6) PTHR10994//PTHR10994:SF72 - RETICULON // SUBFAMILY NOT NAMED
Cre13.g575650.t1.1	CEUSTIGMA_g8382.t1	(1 of 3) KOG0663 - Protein kinase PITSLRE and related kinases
Cre13.g576400.t1.2	CEUSTIGMA_g2467.t1	Branched-chain amino-acid transaminase
Cre13.g579800.t1.2	CEUSTIGMA_g10091.t1	(1 of 1) 2.7.4.26 - Isopentenyl phosphate kinase
Cre13.g580250.t2.1	CEUSTIGMA_g7026.t1	NA
Cre13.g582800.t1.2	CEUSTIGMA_g5408.t1	(1 of 1) 6.3.2.11 - Carnosine synthase / Carnosine synthetase
Cre13.g583100.t1.1	CEUSTIGMA_g1079.t1	(1 of 1) 2.4.99.12 - Lipid IV(A) 3-deoxy-D-manno-octulosonic acid transferase / Lipid IV(A) KDO transferase
Cre13.g583250.t1.1	CEUSTIGMA_g2715.t1	(1 of 1) K15361 - WD repeat-containing protein 48 (WDR48, UAF1)
Cre13.g584750.t1.1	CEUSTIGMA_g2522.t1	(1 of 1) K18162 - NADH dehydrogenase [ubiquinone] 1 alpha subcomplex assembly factor 5 [EC:2.1.1.-] (NDUFAF5)
Cre13.g587150.t1.1	CEUSTIGMA_g1164.t1	(1 of 2) K11308 - histone acetyltransferase MYST1 [EC:2.3.1.48] (MYST1, MOF, KAT8)
Cre13.g591450.t1.2	CEUSTIGMA_g740.t1	(1 of 2) PTHR11767//PTHR11767:SF47 - INWARD RECTIFIER POTASSIUM CHANNEL // SUBFAMILY NOT NAMED
Cre13.g603900.t1.2	CEUSTIGMA_g2128.t1	(1 of 1) K01890 - phenylalanyl-tRNA synthetase beta chain (FARSB, pheT)
Cre13.g605000.t1.1	CEUSTIGMA_g9087.t1	(1 of 1) KOG0580//KOG0610//KOG0658 - Serine/threonine protein kinase // Putative serine/threonine protein kinase // Glycogen synthase kinase-3
Cre14.g608850.t1.2	CEUSTIGMA_g1302.t1	(1 of 3) PF10075 - CSN8/PSMD8/EIF3K family (CSN8_PSD8_EIF3K)
Cre14.g610050.t1.2	CEUSTIGMA_g311.t1	(1 of 1) K15180 - negative elongation factor B (COBRA1, NELFB)
Cre14.g611484.t1.1	CEUSTIGMA_g9977.t1	NA
Cre14.g611650.t1.1	CEUSTIGMA_g6035.t1	(1 of 2) 1.1.3.37 - D-arabinono-1,4-lactone oxidase / D-arabinono-gamma-lactone oxidase
Cre14.g613950.t2.1	CEUSTIGMA_g249.t1	NA

Cre14.g614550.t1.1	CEUSTIGMA_g1500.t1	(1 of 10) PTHR21228//PTHR21228:SF20 - FAST LEU-RICH DOMAIN-CONTAINING // SUBFAMILY NOT NAMED
Cre14.g618250.t1.1	CEUSTIGMA_g13031.t1	NA
Cre14.g621300.t2.1	CEUSTIGMA_g977.t1	NA
Cre14.g622901.t1.1	CEUSTIGMA_g2613.t1	(1 of 9) KOG0617 - Ras suppressor protein (contains leucine-rich repeats)
Cre14.g623650.t1.2	CEUSTIGMA_g54.t1	(1 of 3) 1.1.1.2 - Alcohol dehydrogenase (NADP(+)) / Aldehyde reductase (NADPH)
Cre14.g625200.t2.1	CEUSTIGMA_g5081.t1	NA
Cre14.g626350.t1.2	CEUSTIGMA_g5087.t1	(1 of 1) PF04751 - Protein of unknown function (DUF615) (DUF615)
Cre14.g632050.t1.2	CEUSTIGMA_g9331.t1	(1 of 1) PTHR14240 - RPGR-INTERACTING PROTEIN 1 RELATED
Cre14.g632775.t1.1	CEUSTIGMA_g1235.t1	(1 of 1) K03035 - 26S proteasome regulatory subunit N5 (PSMD12, RPN5)
Cre15.g635067.t1.1	CEUSTIGMA_g10034.t1	(1 of 3) PTHR30570 - PERIPLASMIC PHOSPHATE BINDING COMPONENT OF PHOSPHATE ABC TRANSPORTER
Cre15.g636400.t2.1	CEUSTIGMA_g10892.t1	NA
Cre15.g636500.t1.2	CEUSTIGMA_g11209.t1	NA
Cre15.g637100.t1.2	CEUSTIGMA_g12064.t1	(1 of 1) K04523 - ubiquilin (UBQLN, DSK2)
Cre15.g639150.t2.1	CEUSTIGMA_g9427.t1	NA
Cre15.g639308.t1.2	CEUSTIGMA_g9325.t1	(1 of 30) PF08373 - RAP domain (RAP)
Cre15.g639400.t2.1	CEUSTIGMA_g5941.t1	NA
Cre15.g640250.t2.1	CEUSTIGMA_g10886.t1	NA
Cre15.g641250.t1.2	CEUSTIGMA_g13030.t1	(1 of 1) PTHR23056//PTHR23056:SF48 - CALCINEURIN B // SUBFAMILY NOT NAMED
Cre16.g648050.t1.2	CEUSTIGMA_g8519.t1	NA
Cre16.g649400.t1.2	CEUSTIGMA_g6993.t1	Putative rRNA (guanine-N2-)-methyltransferase
Cre16.g649800.t1.1	CEUSTIGMA_g9032.t1	Cyclin-related pentatrichopeptide repeat protein
Cre16.g649833.t1.1	CEUSTIGMA_g12349.t1	NA
Cre16.g652900.t1.1	CEUSTIGMA_g8840.t1	(1 of 16) KOG0131 - Splicing factor 3b, subunit 4
Cre16.g653150.t1.2	CEUSTIGMA_g11344.t1	NA
Cre16.g655400.t1.1	CEUSTIGMA_g1614.t1	(1 of 1) K17985 - activating molecule in BECN1-regulated autophagy protein 1 (AMBRA1)
Cre16.g655800.t1.1	CEUSTIGMA_g9853.t1	NA
Cre16.g656250.t1.1	CEUSTIGMA_g6895.t1	U1 small nuclear ribonucleoprotein
Cre16.g658000.t1.1	CEUSTIGMA_g4043.t1	(1 of 16) PTHR13748 - COBW-RELATED
Cre16.g659400.t2.1	CEUSTIGMA_g3950.t1	NA
Cre16.g663400.t1.2	CEUSTIGMA_g10610.t1	NA
Cre16.g664050.t1.2	CEUSTIGMA_g6894.t1	NA
Cre16.g664301.t1.1	CEUSTIGMA_g12991.t1	(1 of 2) K02349 - DNA polymerase theta [EC:2.7.7.7] (POLQ)
Cre16.g665550.t2.1	CEUSTIGMA_g4057.t1	NA
Cre16.g666300.t1.1	CEUSTIGMA_g2400.t1	(1 of 105) 2.7.11.25 - Mitogen-activated protein kinase kinase kinase / MLTK
Cre16.g668400.t1.2	CEUSTIGMA_g3528.t1	(1 of 1) PTHR23354:SF72 - PROTEIN LMD-3, ISOFORM A
Cre16.g670500.t1.1	CEUSTIGMA_g12121.t1	(1 of 7) PF02190 - ATP-dependent protease La (LON) substrate-binding domain (LON_substr_bdg)
Cre16.g670900.t1.1	CEUSTIGMA_g10591.t1	(1 of 15) PTHR14614 - HEPATOCELLULAR CARCINOMA-ASSOCIATED ANTIGEN
Cre16.g672850.t1.1	CEUSTIGMA_g7368.t1	NA
Cre16.g673841.t1.1	CEUSTIGMA_g5005.t1	(1 of 1) PF10218 - Uncharacterized conserved protein (DUF2054) (DUF2054)

Cre16.g674964.t1.1	CEUSTIGMA_g10154.t1	(1 of 1) K06911 - uncharacterized protein (K06911)
Cre16.g677050.t1.1	CEUSTIGMA_g203.t1	(1 of 6) PF00211//PF13416 - Adenylate and Guanylate cyclase catalytic domain (Guanylate_cyc) // Bacterial extracellular solute-binding protein (SBP_bac_8)
Cre16.g685200.t1.1	CEUSTIGMA_g6479.t1	(1 of 1) K14787 - multiple RNA-binding domain-containing protein 1 (MRD1, RBM19)
Cre16.g685217.t1.1	CEUSTIGMA_g1419.t1	(1 of 1) K14307 - nucleoporin p58/p45 (NUPL1, NUP49)
Cre16.g686400.t1.2	CEUSTIGMA_g10177.t1	(1 of 1) PTHR10742//PTHR10742:SF307 - AMINE OXIDASE // SUBFAMILY NOT NAMED
Cre16.g687294.t1.1	CEUSTIGMA_g7435.t1	NA
Cre16.g688050.t1.1	CEUSTIGMA_g1648.t1	(1 of 1) PTHR32091:SF0 - EUKARYOTIC INITIATION FACTOR 4B-RELATED
Cre16.g688800.t1.2	CEUSTIGMA_g6233.t1	NA
Cre16.g689647.t1.1	CEUSTIGMA_g3038.t1	Argonaute-like protein
Cre16.g690000.t1.2	CEUSTIGMA_g6311.t1	NA
Cre16.g690431.t2.1	CEUSTIGMA_g10184.t1	(1 of 1) 1.3.99.34 - Transferred entry: 1.3.7.11
Cre16.g691215.t2.1	CEUSTIGMA_g4812.t1	NA
Cre17.g696250.t1.1	CEUSTIGMA_g6836.t1	NA
Cre17.g699100.t1.1	CEUSTIGMA_g5481.t1	(1 of 1) K14674 - TAG lipase / steryl ester hydrolase / phospholipase A2 / LPA acyltransferase (TGL4)
Cre17.g699900.t1.2	CEUSTIGMA_g993.t1	(1 of 2) PTHR11732:SF255 - ARYL-ALCOHOL DEHYDROGENASE YPL088W-RELATED
Cre17.g702700.t1.1	CEUSTIGMA_g6853.t1	(1 of 6) PTHR11132//PTHR11132:SF101 - SOLUTE CARRIER FAMILY 35 // SUBFAMILY NOT NAMED
Cre17.g703550.t1.2	CEUSTIGMA_g6837.t1	NA
Cre17.g706850.t1.1	CEUSTIGMA_g3580.t1	(1 of 1) PTHR13377 - PLACENTAL PROTEIN 6
Cre17.g711050.t1.1	CEUSTIGMA_g2350.t1	(1 of 1) K15456 - protein KTI12 (KTI12)
Cre17.g712400.t1.2	CEUSTIGMA_g2331.t1	(1 of 1) PTHR30238 - MEMBRANE BOUND PREDICTED REDOX MODULATOR
Cre17.g715150.t1.2	CEUSTIGMA_g5129.t1	NA
Cre17.g717350.t1.2	CEUSTIGMA_g2640.t1	(1 of 1) 2.5.1.75 - tRNA dimethylallyltransferase / tRNA prenyltransferase
Cre17.g721950.t1.2	CEUSTIGMA_g7893.t1	(1 of 1) PTHR11685:SF119 - E3 UBIQUITIN-PROTEIN LIGASE ARI2-RELATED
Cre17.g722000.t1.1	CEUSTIGMA_g11614.t1	Major facilitator superfamily transporter
Cre17.g722350.t1.2	CEUSTIGMA_g5894.t1	Small Rab-related GTPase
Cre17.g725050.t2.1	CEUSTIGMA_g51.t1	NA
Cre17.g725650.t1.1	CEUSTIGMA_g682.t1	(1 of 2) K03453 - bile acid:Na+ symporter, BASS family (TC.BASS)
Cre17.g726050.t1.2	CEUSTIGMA_g11008.t1	(1 of 1) K11843 - ubiquitin carboxyl-terminal hydrolase 14 [EC:3.4.19.12] (USP14, UBP6)
Cre17.g727400.t1.1	CEUSTIGMA_g12147.t1	NA
Cre17.g729700.t1.2	CEUSTIGMA_g4370.t1	(1 of 1) PTHR14374 - FOIE GRAS
Cre17.g729750.t1.2	CEUSTIGMA_g7916.t1	(1 of 1) 2.3.1.87 - Aralkylamine N-acetyltransferase / Serotonin N-acetyltransferase
Cre17.g736650.t1.2	CEUSTIGMA_g9004.t1	(1 of 1) K01256 - aminopeptidase N (pepN)
Cre17.g744797.t1.1	CEUSTIGMA_g3977.t1	(1 of 1) PF05623 - Protein of unknown function (DUF789) (DUF789)
Cre17.g746597.t2.1	CEUSTIGMA_g4015.t1	NA
Cre17.g747897.t1.1	CEUSTIGMA_g3973.t1	NA
Cre18.g748847.t1.1	CEUSTIGMA_g3799.t1	NA
Cre24.g755497.t1.1	CEUSTIGMA_g27.t1	(1 of 2) K05770 - benzodiazapine receptor (BZRP)
Cre32.g758597.t1.1	CEUSTIGMA_g13674.t1	NA

5 General Discussion

Acid mine drainage systems present a highly toxic environment that is incredibly damaging to biodiversity (Brake & Hasiotis, 2010; Dean et al., 2019; Zettler et al., 2002). PM01 has managed to colonise such an environment and through its adaptation, generated mechanisms to confer it a much greater copper tolerance to other strains of *Chlamydomonas acidophila* and the model organism *Chlamydomonas reinhardtii* as seen in section 3.4.1. Whilst tolerance ranges of eukaryotic extremophile microalgae have been well understood and studied (Aguilera & Amils, 2005; Amaral-Zettler, 2012; Cantrell & Duval-Perez, 2012; Dean et al., 2019), the mechanisms of these tolerances are only just beginning to be understood ((Khatiwada et al., 2020; Olsson et al., 2015; Puente-Sánchez et al., 2018)). *C. acidophila* offers a fantastic model as a eukaryotic extremophile, due to its relatively close lineage to the model organism *C. reinhardtii*. Additionally, due to the diverse nature of AMD environments, there is likely a lot of diversity in tolerance mechanisms within the species as seen by PM01's high tolerance to copper compared to CCAP 11/136 and CCAP 11/137.

One of the key, and most surprising findings, was the ability of PM01 to completely shut down photosystem II under a short-term copper tress, as shown by both the PAM and transcriptomics experiment (chapter 2 and chapter 4 respectively). What is most interesting is that the Fv/Fm values of dark adapted PM01 cells under a short-term copper stress did not significantly alter from their control. Despite this, upon exposure to an actinic light, the efficiency of photosystem II completely reduced. This suggests that although PM01 has no reduced capacity for photosynthesis, a feedback mechanism is preventing PS II activity to occur, and could and could indicate as switch to cyclic electron flow using PS I. This suggests an interesting copper adaptation mechanism, that has been eluded to in plants and cyanobacteria (Deng et al., 2014; Lysenko et al., 2020), but does not appear to have been shown previously in microalgae, and certainly not in *C. acidophila*. In fact, the opposite was seen in another transcriptomics experiment in a different strain of *C. acidophila* (RT-46), which when exposed to 500 µM copper for 10 days, saw an increase in transcripts related to photosynthesis.

The diversity seen in different *C. acidophila* strains is quite striking, for example, PM01 and RT-46 exhibit a much higher copper tolerance than 11/136 and 11/137 (Dean et al., 2019; Puente-Sánchez et al., 2018). PM01 was isolated from an abandoned copper mine in Wales, whilst RT-46 was isolated from the Rio Tinto, an acidic river which gets its properties from both the local geochemistry and mining activities. Additionally, the environments both strains are found in vary in geochemistry such as metal content (Dean et al., 2019; López-Archilla et al., 2001), other abiotic factors such as temperature and biotic factors such as the local biodiversity. Therefore, seeing different adaptation mechanisms is entirely possible, however, do similar selection pressures force adaptations in similar biological processes? The photosynthetic process produces a large amount of radicals, which can be exacerbated when it is damaged by copper (Jegerschold et al., 1995). Therefore, shutting down photosynthesis in the short-term could minimise any excessive stress to PM01, until the cells can neutralise the copper, buying the cells crucial time. Under the long-term copper stresses minimal differences were seen between the stress and the control for both species in terms of the

photosynthetic efficiency of PS II. This is surprising due to the significant decrease in culture growth shown in section 2.4.1 and that copper arrests cell growth via other methods, such as an increased energy demand of copping copper inert. What is interesting is that the RT-46 strain of *C. acidophila* saw an increase in relative electron transport rate after 24 hours of copper exposure. This study and the RT-46 study were not like for like as a stronger copper stress over a shorter period was applied, but preliminary comparisons could suggest that differential adaption mechanisms could vary in biological processes. However, the prospect of differential adaption mechanisms, even between strains of the same species, gives an exciting insight into the diversity of eukaryotic extremophiles. There is the potential for a wide array of biotechnological applications that could be derived from this diversity. Additionally, this diversity could also be a great source for bioremediation of contaminated lands. This diversity suggests there could be a vast potential for ecological restoration as well as many biotechnological applications to be found within the eukaryotic extremophiles.

Our data looking into the photosynthetic parameters between the two species also yielded other interesting results. Firstly, PM01 exhibits a 2-stage NPQ process depending on the actinic light intensity under a short-term copper stress. At lower actinic light levels very high NPQ was seen, interestingly, this reduced as the actinic light intensity increased to 350 µM before rising again. Furthermore, when compared to 11/32c, all the PMO1 NPQ values were much higher across all actinic light intensities and this is likely the candidate for the complete shutdown of ΦPS II seen. A likely candidate for this high NPQ at lower actinic light intensities is state transitions. State transitions cause the light harvesting complex to dissociate from PS II to PS I and vice versa (Finazzi, 2005). PSI has been shown to drive ATP synthesis and helped to repair photodamage to PSII (Huang et al., 2018). This makes it a very good candidate for the NPQ seen in PM01. Why this NPQ process dips at the intermediate actinic light intensities remains unknown and warrants further investigation into a novel photosynthetic response in *C. acidophila*. The other interesting photosynthetic response found is the apparent diurnal fluctuations of Fv/Fm under the short-term copper stress (PM01 and 11/32c) and long-term copper stress (PM01) section 3.4.2. I stipulate that this could be due to the experimental conditions in which the samples were left exposed to natural light throughout the day of measurements and as such were exposed to the fluctuations of sunlight throughout the day. However, no changes were seen in the control samples throughout the day, so regardless, copper is still having some additional consequence on the Fv/Fm values. However, it is possible that other intrinsic conditions could alter this Fv/Fm such as proteins involved in the biological clock (Yamada & Prosser, 2020). Again, this is another example of the complicated photosynthetic control mechanisms PM01 exhibits, but is also seen in *C. reinhardtii*. It is also interesting that we see this response in both copper stresses for PM01 but only the short-term copper stress in 11/32c. Further investigations into the actual mechanism of this control, whether it be part of the biological clock or external factors such as the light intensity, would give us a greater understanding of photosynthetic control mechanisms and also the copper adaptation of PM01.

PM01 appears to minimise the copper impact through a series of responses identified through both the transcriptomic and metabolomic experiments. In this study, CTP3 has been identified as a key protein in copper detoxification. As a putative copper exporter, it is easy to see how it can play a role in either exporting copper out of the cell or into a storage vacuole (Blaby-Haas & Merchant, 2012). Previous studies performed by our lab have identified that PM01 can accumulate copper inside the

cell (Dean et al., 2019). Whilst other studies have shown that *C. acidophila* accumulates lipid bodies and vacuoles at the cell periphery in response to metal stress (Nishikawa et al., 2003). It is possible that CTP3 could be exporting copper into one of these vacuoles as a form of storage. Whether the accumulation of metals inside *C. acidophila* cells that have been observed recently, is due to the actions of CTP3 or despite of it is currently unknown. Initially I aimed to clone the gene into an overexpression plasmid with a GFP tag into *C. reinhardtii*, unfortunately, due to time restrictions I was unable to do this. It would also have been interesting to transform this into *C. acidophila*, however, to date there is no literature on *C. acidophila* being genetically modified, so we cannot be certain how effective this would be. This could help elucidate both the localisation and the role of copper homeostasis CTP3 plays within the cell. CTP3 is a large protein and thought to export copper in the Cu^{+} form. As this protein showed peaks where would expect to see it should it be doubly charged means it could be donating electrons to Cu^{2+} to facilitate copper export. However, the transcript abundance in PM01 was constitutively much higher than any of the treatments in 11/32c, which is not reflected in the MALDI analysis.

Additionally, a host of metal chelators, radical scavengers and cysteine type residues were found to be increased under a short-term copper stress in PM01 within the metabolomic data set. To compliment this the transcriptomic data set (Chapter 4) showed that both GSH1 (PM01 and 11/32c) and GSH2 (PM01) were increased in the short-term copper stress, with PM01 showing the highest levels of the transcripts. In addition to GSH a host of other enzymes related to glutathione metabolism were increased in response to copper. GSTs are also more highly expressed in the short-term copper treatment with PM01 exhibiting the highest levels of transcripts. GSR1 transcripts were also highly increased in response to copper in the short-term copper treatments, again with PM01 exhibiting the highest level of transcripts. The other isoform of GSR, GSR2 provided interesting differential expression between PM01 and 11/32c where PM01 decreases transcript levels of GSR2 in response to copper and 11/32c increases transcript levels under copper stress. The reasons for this are unknown and provides an interesting avenue for further investigation. Overall, whilst GSH transcripts are increased in both species, a whole host of genes that encode proteins involved in glutathione metabolism are also elevated. This highlights how important glutathione is in the copper response, especially in a short-term copper response. A host of antioxidative enzymes were tested, to observe the antioxidant capabilities between the two organisms (section 3.4.3). The data did not provide quite a clear difference as you would expect between the extremophile and non-extremophile species as one may expect the extremophile species to have a high antioxidant capability under a long- term copper stress. However, it was only possible to test the long-term copper stress conditions and it is possible we may see the largest differences under a short-term copper stress where the oxidative stress is likely to be highest before any excess copper can be quenched and made inert. Based on the prevalence and importance of glutathione and the role it plays in copper detoxification, especially in PM01, other ROS quenching enzymes could be worth investigating also. Another interesting observation seen in both species, is that the long-term copper stressed cells appear to not be under a high oxidative stress. ROS quenching enzyme expression is not increased in the long-term copper stress. Moreover, ROS enzyme activity in the long-term copper stress conditions is not significantly increased in PM01, and CAT activity is significantly reduced. Additionally, Cluster 4 from the transcriptomic data set, which was enriched with enzymes involved in the antioxidant response,

shows that the long-term copper stress has the smallest relative transcript expression in both species chapter 5. This suggests that the cells may quench ROS generation early and that under a long-term copper stress, oxidative stress is not a damaging factor. This is important as it suggests that either another protective mechanism is in place that we have not been able to identify in preventing ROS generation, or that the cells have managed to make the copper inert.

Other than cysteine, other amino acids can differentiate the two species under copper stress. Metabolites involved in the pathways of the amino acid proline synthesis, was found in high concentrations in the control and long-term copper conditions of PM01, but concentrations were vastly reduced under the short-term copper conditions. This could suggest that the proline is being utilised and involved in the detoxification of copper and could be a distinguishing factor between PM01 and 11/32c where these processes are seen. Transgenic *C. reinhardtii* that accumulated higher proline content in the cells were shown to grow more rapidly, and bind more cadmium than wild-type cells under cadmium stressed conditions (Siripornadulsil et al., 2002) In a study of copper stress effects on amino acid accumulation in *Brassica carinata,* proline and histidine were determined to be the most important amino acids in response to copper (Irtelli et al., 2008). Pathways involved in the methionine based amino acid synthesis appeared to be more upregulated in the 11/32c treatment, this could confer that there is a sulphur based amino acid preference between the two species, with PM01 having more of a preference for cysteine and 11/32c showing a higher preference for methionine.

There was a surprising amount of similarities between PM01 and 11/32c when exposed to copper considering their vast differences in tolerance ranges. It was very hard to distinguish their fingerprints based on the FT-IR spectra alone, although PCA analysis did separate both the species and copper treatments. Similarly, the MALDI-TOF spectra showed very similar peaks patterns, however, the peaks did show varying m/z ratios. The data presented here shows that MALDI-TOF may be a better method for fingerprinting species. However, there are caveats to this, as MALDI-TOF methodologies require slightly more sample preparation and take longer to run with more man hours. Additionally, without any protein extraction and digestion pre-processing, the information we can gleam from MALDI-TOF is much lower. Conversely, FT-IR spectroscopy requires very little pre-processing and a high rate of sampling than MALDI-TOF. Additionally, we can gleam broad information from the spectra such as functional groups. The FT-IR spectra show an increase in protein content under copper stress for both organisms (although we see a higher increase in PM01), whilst a reduction in lipids and carbohydrates (section 3.4.1). This suggests that there is an energy burden on the cells under a copper stress, possibly required for the synthesis and activity of the new proteins. Additionally, the reduction in ΦPSII seen in the PAM data set (section 2.4.2), suggests that less energy is being generated in the cell so they must start utilising any lipid and carbohydrate stores to make up for the energy demand. To assess what is happening with the lipids a colorimetric TBARS assay was used to detect levels of lipid oxidation, which yielded surprising results. PM01 showed high lipid oxidation levels under both the copper stresses, whilst 11/32c showed high lipid oxidation under just the short erm copper stress (section 2.5.5). What's more interesting is that none of the other *C. acidophila* species (11/136 and 11/137) show any increased lipid oxidation under copper stress. Whilst lipids are being oxidised in PM01, this does not fully account for the reduction in lipids seen in the FT-IR spectra, as the by product, MDA, also contains the functional groups that vibrate

at the lipid peak wave numbers. In the future it would be of interest to assess the lipid profile in more detail, through LC-MS analysis of the non-polar fraction from the metabolite extraction.

This study presents a unique overview of the physiological, biochemical transcriptomic and metabolomic changes of a eukaryotic extremophile under both a short-term and long-term copper stress. To identify key areas in which PM01 may differ and identify any constitutively high processes that are occurring, PM01 was compared to a non-copper tolerant organism, *C. reinhardtii*. Previous studies have typically only assessed one time point, while ours allows us to identify significant metabolic shifts between a short-term and long-term copper stress. A lot of data was generated from this study, and there is still a lot to be learnt from these data sets. Currently, the *C. acidophila* transcriptome is very poorly annotated, advances in this area would allow us to identify more processes crucial to the copper adaptation of *C. acidophila* as well as any potential novel genes that may have arisen. Finally, the large number of annotations from the metabolomic data set are ones associated to protein interactions. Due to time constraints it was not possible to match this with the RNA-seq data set collected which could give a comprehensive overview of processes occurring. Overall, a lot of potential copper adaptation mechanisms of PM01 have been identified. Firstly, its ability to shut down PSII, possibly through state transitions can prevent photodamage and the production of excess ROS in the cell. Secondly an upregulation of copper transporters, mainly CTP3 can relocate copper ions to where they can be less harmful (either exporting out of the cell or, potentially, into lipid bodies or storage vacuoles). The oxidative stress response appears to be crucial under a short-term copper stress but less important over the long-term. Several oxidative stress responses were identified in this study; through amino acids such as cysteine (PM01) and methionine (11/32c), metabolites such as glutathione and their related processes and ROS quenching enzymes such as CAT and SOD. This study has started to unravel how eukaryotic extremophiles can adapt to high copper environments, and with further study into some of these mechanisms, we could confirm candidate genes, and processes that have great bioremediation and/ or biotechnological applications. Enhancing expression of key genes identified in this study such as CTP3 or GSH could confer a higher copper tolerance to organisms of biotechnological interest. This could provide the added benefit of being able to grow algae for biofuels or as a food source in open ponds containing elevated copper concentrations whilst minimising the risk of contamination and reduced yields. Understanding the apparent switch from PSII to PS I under copper stress could also confer a higher tolerance, and, as long as it does not affect growth rate too severely, could be a further way to minimise contamination of open growth ponds. PM01 has been previously seen to accumulate copper to high concentrations within the cell, it is possible that CTP3 could be a candidate for this accumulation and could be a great candidate for biomining, whilst the increase in proline synthesis pathways likely also plays a large role. Further characterisation would be needed but if true, this could provide a very interesting candidate for crop improvement as we aim to reduce stress in poor quality soils, lacking trace metals such as copper by loading soils with *C. acidophila* grown in the presence of copper. Perhaps most importantly, it could allow us to enhance the bioremediation power of organisms growing in metal contaminated environments and reducing the impact of anthropogenic activities. If we can enhance this bioremediation properties enough, industries such as mining would also be encouraged to contribute to the remediation process as it could increase their yields through

the harvesting of organisms in contaminated environments and confer an almost passive source of metals.

5.1 References

Aguilera, A., & Amils, R. (2005). Tolerance to cadmium in Chlamydomonas sp. (Chlorophyta) strains isolated from an extreme acidic environment, the Tinto River (SW, Spain). *Aquatic Toxicology*, *75*(4), 316–329. https://doi.org/10.1016/j.aquatox.2005.09.002

Amaral-Zettler, L. A. (2012). Eukaryotic diversity at pH extremes. *Frontiers in Microbiology*, *3*, 441. https://doi.org/10.3389/fmicb.2012.00441

Blaby-Haas, C. E., & Merchant, S. S. (2012). The ins and outs of algal metal transport. *Biochimica et Biophysica Acta*, *1823*(9), 1531–1552. https://doi.org/10.1016/j.bbamcr.2012.04.010

Brake, S. S., & Hasiotis, S. T. (2010). Eukaryote-Dominated Biofilms and Their Significance in Acidic Environments. *Geomicrobiology Journal*, *27*(6–7), 534–558. https://doi.org/10.1080/01490451003702966

Cantrell, S. A., & Duval-Perez, L. (2012). Microbial mats: An ecological niche for fungi. In *Frontiers in Microbiology* Frontiers Research Foundation. 3, 424.https://doi.org/10.3389/fmicb.2012.00424

Dean, A. P., Hartley, A., McIntosh, O. A., Smith, A., Feord, H. K., Holmberg, N. H., King, T., Yardley, E., White, K. N., & Pittman, J. K. (2019). Metabolic adaptation of a Chlamydomonas acidophila strain isolated from acid mine drainage ponds with low eukaryotic diversity. *Science of the Total Environment*, *647*, 75–87. https://doi.org/10.1016/j.scitotenv.2018.07.445

Deng, C., Pan, X., Wang, S., & Zhang, D. (2014). Cu2+ inhibits photosystem II activities but enhances photosystem I quantum yield of Microcystis aeruginosa. *Biological Trace Element Research*, *160*(2), 268–275. https://doi.org/10.1007/s12011-014-0039-z

Finazzi, G. (2005). The central role of the green alga Chlamydomonas reinhardtii in revealing the mechanism of state transitions. *Journal of Experimental Botany*, *56*(411), 383–388. https://doi.org/10.1093/jxb/erh230

Huang, W., Yang, Y. J., Zhang, S. B., & Liu, T. (2018). Cyclic electron flow around photosystem i promotes ATP synthesis possibly helping the rapid repair of photodamaged photosystem ii at low light. *Frontiers in Plant Science*, *9*, 239. https://doi.org/10.3389/fpls.2018.00239

Irtelli, B., Petrucci, W. A., & Navari-Izzo, F. (2008). Nicotianamine and histidine/proline are, respectively, the most important copper chelators in xylem sap of Brassica carinata under conditions of copper deficiency and excess. *Journal of Experimental Botany*, *60*(1), 269–277. https://doi.org/10.1093/jxb/ern286

Jegerschold, C., Arellano, J. B., Schroder, W. P., van Kan, P. J. M., Barón, M., & Styring, S. (1995). Copper(II) Inhibition of Electron Transfer through Photosystem II Studied by EPR Spectroscopy. *Biochemistry*, *34*(39), 12747–12754. https://doi.org/10.1021/bi00039a034

Khatiwada, B., Hasan, M. T., Sun, A., Kamath, K. S., Mirzaei, M., Sunna, A., & Nevalainen, H. (2020). Proteomic response of Euglena gracilis to heavy metal exposure – Identification of key proteins involved in heavy metal tolerance and accumulation. *Algal Research*, *45*, 101764. https://doi.org/10.1016/j.algal.2019.101764

López-Archilla, A. I., Marin, I., & Amils, R. (2001). Microbial community composition and ecology of an acidic aquatic environment: The Tinto River, Spain. *Microbial Ecology*, *41*(1), 20–35. https://doi.org/10.1007/s002480000044

Lysenko, E. A., Klaus, A. A., Kartashov, A. V., & Kusnetsov, V. V. (2020). Specificity of Cd, Cu, and Fe effects on barley growth, metal contents in leaves and chloroplasts, and activities of photosystem I and photosystem II. *Plant Physiology and Biochemistry*, *147*(November 2019), 191–204. https://doi.org/10.1016/j.plaphy.2019.12.006

Nishikawa, K., Yamakoshi, Y., Uemura, I., & Tominaga, N. (2003). Ultrastructural changes in Chlamydomonas acidophila (Chlorophyta) induced by heavy metals and polyphosphate metabolism. *FEMS Microbiology Ecology*, *44*(2), 253–259. https://doi.org/10.1016/S0168-6496(03)00049-7

Olsson, S., Puente-Sánchez, F., Gómez, M. J., & Aguilera, A. (2015). Transcriptional response to

copper excess and identification of genes involved in heavy metal tolerance in the extremophilic microalga Chlamydomonas acidophila. *Extremophiles*, *19*(3), 657–672. https://doi.org/10.1007/s00792-015-0746-1

Puente-Sánchez, F., Díaz, S., Penacho, V., Aguilera, A., & Olsson, S. (2018). Basis of genetic adaptation to heavy metal stress in the acidophilic green alga Chlamydomonas acidophila. *Aquatic Toxicology*, *200*, 62–72. https://doi.org/10.1016/j.aquatox.2018.04.020

Siripornadulsil, S., Traina, S., Verma, D. P. S., & Sayre, R. T. (2002). Molecular mechanisms of proline-mediated tolerance to toxic heavy metals in transgenic microalgae. *The Plant Cell*, *14*(11), 2837–2847. https://doi.org/10.1105/tpc.004853

Yamada, Y., & Prosser, R. A. (2020). Copper in the suprachiasmatic circadian clock: A possible link between multiple circadian oscillators. *European Journal of Neuroscience*, *51*(1), 47–70. https://doi.org/10.1111/ejn.14181

Zettler, L. A. A., Gómez, F., Zettler, E., Keenan, B. G., Amils, R., & Sogin, M. L. (2002). Eukaryotic diversity in Spain's River of Fire: This ancient and hostile ecosystem hosts a surprising variety of microbial organisms. *Nature*, *417*(6885), 137. https://doi.org/10.1038/417137a